Oxidative Decolouring of Bloodmeal Using Peracetic Acid

A thesis

submitted in fulfilment

of the requirements for the degree

of

Doctor of Philosophy in Engineering

at

The University of Waikato

by

TALIA MAREE HICKS

THE UNIVERSITY OF
WAIKATO
Te Whare Wānanga o Waikato

2015

Abstract

Bloodmeal is an ancillary product of the agricultural industry, containing 80 – 100 % protein, and has been used to create a bio-based plastic called Novatein Thermoplastic Protein®, with a proprietary blend of sodium sulfite, sodium dodecyl sulfate (SDS), water and triethylene glycol (TEG). Recent investigation has shown that the colour and odour of bloodmeal based thermoplastic can be significantly improved through the pre-treatment of bloodmeal with equilibrium peracetic acid. The resulting decoloured bloodmeal (DBM) no longer relies on the addition of sodium sulfite to be processed in conventional thermoplastic equipment. The purpose of this study was to gain a comprehensive understanding of the role by which peracetic acid decolours bloodmeal and the consequences of oxidation on composition, physico-chemical properties, protein structure and interactions and final polymer mobility.

Oxidative decolouring of haem is straightforward when the haem is freely accessible or in the form of oxyhaemoglobin and most common oxidants lead to cleavage of the porphyrin ring, resulting in a loss of colour saturation. However, after extensive thermal treatment during manufacture, the haem present in bloodmeal has migrated to inaccessible hydrophobic regions of the protein aggregates or has been oxidised to the form of methaemoglobin. Literature revealed that methaemoglobin catalytically removes hydrogen peroxide, lowering decolouring efficacy. Thus, peracetic acid is required when haem is present in the form of methaemoglobin, as is found in bloodmeal. Further, it was confirmed that a minimum of 3% w/w peracetic acid, in a 3:1 ratio to bloodmeal is required to obtain adequate decolouring (> 70% whiteness based on the RGB colour space).

The role of each component in equilibrium peracetic acid was established; water and acetic acid resulted in protein swelling but were found unlikely to influence accessibility of the oxidants to the haem sites and both hydrogen peroxide and peracetic acid were consumed in oxidising reactions. Acidic conditions were found to reduce the consumption of hydrogen peroxide, possibly through the inhibition of hydroxyl radical formation, resulting in less effective decolouring. Acetic acid was observed to have a protective effect on protein recovery as well as the resulting iron content, molecular mass distribution and secondary structure of protein.

Due to the large excess of peracetic acid solution required to facilitate diffusion and subsequent decolouring, a significant quantity remains unreacted in the recovered wastewater. Unreacted peracetic acid was shown to have potential for recycling, although in its immediate state it was insufficient to decolour fresh bloodmeal.

The protein-rich decoloured bloodmeal recovered had undergone a change in secondary structure composition and was found to contain evidence of a diffusion front, consistent with the heterogeneous phase decolouring mechanism. Oxidation with peracetic acid was found to result in less β-sheet aggregation compared to hydrogen peroxide treatment, although all treatments resulted in an increase in the quantity of disordered structures. Oxidation was also found to result in a significantly lowered glass transition temperature and along with an increased enthalpy of relaxation, evidenced a large improvement in polymer chain mobility compared with untreated bloodmeal.

DBM was found to be comprised of 90 – 99% w/w protein (1 – 10% w/w salt), with a significantly higher protein solubility and a similar volume weighted molecular mass compared with untreated bloodmeal. Further, DBM was found to have a greater composition of charged and polar amino acids, along with a large reduction in lysine and small reduction in aromatic and heterocyclic amino acids. Additionally, cystine crosslinks which stabilise bloodmeal were found to be partially oxidised to cysteine sulfonate compounds and cysteic acid (cleavage of the disulfide bond). Such a reduction in the quantity of amino acids which are capable of forming covalent networks (lysine, tyrosine and cysteine) support prior evidence that DBM no longer requires sodium sulfite to produce a thermoplastic.

The influence of SDS and TEG on secondary structure and chain mobility at ambient and elevated temperatures were explored. It was found that heating DBM and DBM with SDS alone is incapable of providing sufficient energy to induce mobility and chain rearrangement. However, the addition of TEG was found to facilitate chain mobility, and beyond 55 ^{o}C significant changes to the secondary structure composition was observed, first through the formation of α-helices and finally through the aggregation of chains into β-sheets. Wide angle X-ray scattering confirmed that the changes in ordered structures composition were reversible in DBM which contained both SDS and TEG.

The ability of TEG to plasticise DBM was more thoroughly explored, and it was found that prior to heating TEG was localised into regions either plasticiser-rich or -poor, and this resulted in the presence of two glass transition temperatures. After heating, the TEG was more homogeneously distributed, which resulted in the presence of one broad glass transition region.

Acknowledgements

Firstly, I would like to thank my mentor and chief supervisor Dr. Johan Verbeek. Thank you for your expert supervision, encouragement and patience throughout these last few years. Your advice both personally and professionally has been invaluable. Thanks also to Dr. Mark Lay, for your endless enthusiasm and exciting tangents, you're a joy to work with. Finally, thank you to Associate Professor Merilyn Manley-Harris for all of your advice and guidance throughout my association with the Chemistry Department.

I would also like to thank my family, particularly my parents Colin and Wendy Hicks, for supporting me throughout yet another exciting and challenging experience. Thank you to my younger brothers Jordan and Devin for providing me with somewhere to crash, a good laugh and cider throughout the last four years. To my sister Briarley and my brother-in-law Mason, thank you for visiting me as often as possible with my wonderful niece Kory.

To my friends, both within university and abroad, thank you so much for the never ending support you have given me and patience towards the end, when my nerves began to fray. I particularly wish to thank Dr. Paul Parish for taking the time to check in on me throughout the final stages and remind me of what is important.

To my wonderful partner in crime, Daniel, thank you for seeing me through the final challenges having this thesis published; ensuring I practice the correct use of semi-colons.

A highlight of my PhD experience was undertaking research at the Australian Synchrotron on the FT-IR microspectroscopy beamline. I would like to thank Dr. Mark Tobin and Dr. Danielle Martin for their technical support. Thanks also to Don Smith at the Royal Society of New Zealand and The New Zealand Synchrotron Group for the travel funding support.

Thank you to my past PhD colleagues Aaron, Rashid, Marcel and Jim; as well as the new arrivals Chanelle, Anu, Safiya, Herman and Tim for sharing with me all of the highs and lows of this experience in a way nobody else could. Best of luck in all your future endeavors.

I would also like to thank the academics and technical support staff within the Faculty of Science and Engineering at the University of Waikato. The time you have spent helping me throughout this research is hugely appreciated. Thank you also to Mary Dalbeth for your kindness and help with administration and Gwenda Pennington for wonderful assistance with scholarship applications.

Thank you to the Postgraduate Students Association, especially Carrie Swanson, for allowing me to partake in unique opportunities throughout the University. I am very appreciative of financial support provided by the University of Waikato Doctoral Scholarship and the Sir Don Llewlyn Fieldays Scholarship. Without this support it would not have been feasible for me to carry out this research.

Finally, thank you to Aduro Biopolymers LP for the opportunity to continue research and development in this field and gain experience in the commissioning of our new facilities. I am very grateful to Darren, Johan and Jim for welcoming me to the team.

Table of Contents

Copyright Information

List of Other Published Work

1. Verbeek, C., Hicks, T. Langdon, A. (2011). Odorous Compounds in Bioplastics Derived from Bloodmeal. Journal of the American Oil Chemists' Society. 88: p. 1-12.

2. Verbeek, C., Hicks, T. Langdon, A. (2012). Biodegradation of Bloodmeal-Based Thermoplastics in Green-Waste Composting. Journal of Polymers and the Environment. 20(1): p. 53-62.

3. Verbeek, C.J.R., Hicks, T. Langdon, A. (2011). Degradation as a Result of Uv Radiation of Bloodmeal-Based Thermoplastics. Polymer Degradation and Stability. 96(4): p. 515-522.

List of Abbreviations

BM	Bloodmeal
BSA	Bovine Serum Albumin
DBM	Decoloured bloodmeal
DMA	Dynamic mechanical analysis
DSC	Differential scanning calorimetry
FTIR	Fourier transform infrared spectroscopy
Hb	Haemoglobin
HP	Hydrogen peroxide
ICP-MS	Inductively coupled plasma – mass spectrometry
metHb	Methaemoglobin
NTP	Novatein Thermoplastic Protein
oxyHb	Oxyhaemoglobin
PAA	Peracetic acid
ROS	Reactive oxygen species
SDS	Sodium dodecyl sulfate
TEG	Triethylene glycol
WAXS	Wide angle X-ray scattering

1

Introduction

Introduction

Global consumption of agricultural products has established an enormous and ever growing industry. The formation of ancillary products during the production and sale of animal products from livestock poses serious environmental concerns if they are not treated properly. All animal products result in similar waste products including carcasses, intestines, feathers, fish bones and scales as well as blood. While these are viewed as waste by the livestock producer, they are much more valuable after rendering; giving rise to a variety of products such as gelatine, meat-and-bone, blood, feather and fish meals.

New Zealand has a large agricultural industry, processing approximately 2.5 million cattle, 25 million sheep and lamb and 7 hundred thousand pigs in 2014 [1]. Approximately 49% of the live weight of cattle, 44% of pigs, 37% of broilers, and 57% of most fish species are classified as inedible by-products [2]. Although the most valuable components have already been removed during processing, other useful elements may remain in the by-products and waste [3]. In their unprocessed state these ancillary products are worth as little as 10 - 20% of the animal's total value [4], however after processing may nearly equal the value of the meat. In some cases, the value of these by-products exceeds the total operating expenses and the margin required to operate profitably [5]. Despite their environmental and health risks, these materials are now recognized for their potential to be converted into value-added products.

Global production of animal by-product meals totals ~13 million metric tonnes, for which New Zealand contributes ~200 thousand metric tonnes [6]. These high protein meals are often used as animal feed ingredients, but due to varying nutritional properties and local legislation, may require additional processing. Further, in light of global trends regarding legislation for the safe handling and disposal of animal by-products, it is becoming apparent that the use of protein-rich by-products for lower value applications such as animal fodder is no longer sensible.

One of the products of the agricultural industry is bloodmeal, derived from drying the inedible blood collected during slaughter. Collectible blood makes up approximately 4 – 6 % of an animal's live weight, which for adult cows and bulls

slaughtered in New Zealand represents around 30 – 40 thousand metric tonnes annually [1, 7-9].

Whole blood is comprised of ~80 wt% water, 17 wt% protein, 0.2 wt% lipid, 0.1 wt% carbohydrate and 0.6 wt% minerals [10]. Due to its high water and nutrient content, it forms an ideal media for bacterial proliferation and must be disposed of carefully. In general, slaughterhouses and rendering plants typically dispose of collected blood via incineration, to produce bloodchar or by drying, to produce bloodmeal.

Bloodmeal is a low value material (approximately $1.30/kg) primarily used as a fertiliser or animal feed additive. Commercial bloodmeal typically contains 5 – 8wt% water, and 80 – 100 wt% crude protein on a dry basis [11-21], and due to its low cost and high protein content has potential to be used as a feedstock for higher value applications.

Bloodmeal is microbiologically stable, relying on its low moisture content and water activity for preservation [22]. The amino acid composition of blood proteins vary between species. Notably, poultry blood has a significantly higher quantity of isoleucine compared to bovine or porcine blood and porcine blood has a lower quantity of lysine [23]. Further, differences in composition between species has been observed for meals produced by spray drying, where avian bloodmeals have higher quantities of arginine, cysteine, isoleucine and tyrosine compared with porcine and bovine bloodmeals [24]. Such variation in amino acid content not only influences the nutritive quality, but potentially higher value applications such as the manufacture of thermoplastics.

Bloodmeal has been used to produce a second generation bioplastic through the addition of urea, sodium sulfite, sodium dodecyl sulfate, water and triethylene glycol followed by extrusion [25-27]. The resulting material is black in colour and has a peculiar odour which limits its potential markets. To improve its range of applications and consumer acceptance, in 2009 an investigation into improving its aesthetic qualities through oxidative decolouring was undertaken [28].

Bloodmeal was contacted with a variety of aqueous oxidant solutions, with varying reduction potentials, including: copper (II) sulfate, sodium hypochlorite, sodium chlorite, sodium chlorate, chlorine dioxide, hydrogen peroxide and

peracetic acid. The best deodourising and decolouring results were obtained upon treatment of bloodmeal with peracetic acid [29].

Unlike bloodmeal, the decoloured counterpart was found to have a reduced glass transition temperature and increased solubility [28]. Further, peracetic acid also led to retention of high molecular mass proteins (compared to hydrogen peroxide and sodium hypochlorite) and no longer required the addition of urea or sodium sulfite in order to be extruded.

Despite an improvement in colour and odour and the ability to form a thermoplastic material, very little was known about the chemistry and final polymer characteristics. For the purpose of optimising the processing and mechanical properties of the resin, additional research is required to understand the relationship between the extent of oxidation that occurs during decolouring and the material properties of the decoloured bloodmeal feedstock.

Oxidative decolouring of haemoglobin is well documented [30-33]. However, in the context of bloodmeal very little is known about the physical and chemical mechanisms by which the oxidant penetrates the bloodmeal particle and reacts with the haem groups and what modification of the proteins occurred. Further, how these changes then influence the material properties of the final product needs to be intensively explored.

The purpose of this work has been to elucidate the mechanism by which decolouring occurs, to investigate the resultant protein structure and interactions and to discover the effect of processing aids on final polymer mobility.

Specifically the study aimed to carry out:

- An investigation of the reaction mechanism and the role peracetic acid plays in the decolouring of bloodmeal.
- Determination of the effect peracetic acid has on protein secondary structure and polymer chain mobility.
- Characterisation of the effect that peracetic acid has on the protein primary structure of bloodmeal proteins and the material's physico-chemical properties.

- Determination of how processing aids influence protein secondary structure and facilitate polymer mobility.
- Determination of the mechanism by which the amphiphilic plasticiser (triethylene glycol) plasticises decoloured bloodmeal.

These objectives are addressed in the following seven chapters, which comprise a literature review, five journal papers and a final concluding chapter. Further supplementary reading has been provided in Appendices 1 and 2, which are published book chapters exploring the incentives and restrictions to waste valorisation of proteins and typical sources and characteristics of animal protein by-products respectively.

In Chapter 2, a full exploration of protein oxidation is covered specifically investigating the effect of peroxide or peroxycarboxylic acid oxidation on protein structure and physico-chemical properties. This chapter examines the mechanism by which haem is degraded in haem-containing proteins, along with the consequences of protein oxidation to primary and secondary structure and final physical properties of proteins.

The role of peracetic acid in bloodmeal decolouring is examined in Chapter 3. Both the necessity of peracetic acid for ensuring adequate decolouring along with a mechanism for decolouring is proposed. The role each component present in equilibrium peracetic acid solutions plays in facilitating decolouring is explored and a comparison with other equilibrium peroxycarboxylic acids is considered with the final consumption of the reactants being established.

Chapter 4 investigates the effect of the heterogeneous phase decolouring reaction on the secondary structure distribution and polymer physics of the proteins in bloodmeal. This chapter considers the how peracetic acid overcomes stabilizing intra- and intermolecular interactions to increase chain mobility and leads to a greater amorphous content in the material.

Changes to the amino acid composition and physical properties after decolouring are explored in Chapter 5. Initially, decolouring is considered in terms of protein recovery, along with protein content in the recovered solids. Changes to the physical properties of the bloodmeal proteins are subsequently explored through changes in solubility and volume average molecular mass.

The effect of sodium dodecyl sulphate (SDS) and triethylene glycol (TEG) on decoloured bloodmeal (DBM) secondary structure and polymer mobility during heating is determined in Chapter 6. Both SDS and TEG are additives required for processing decolouring bloodmeal in conventional thermoplastic equipment and TEG is required to impart sufficient mobility such that the material can be repeatedly processed.

Triethylene glycol is often used to plasticise protein thermoplastics due to its ability to form both hydrophobic and hydrogen bonding interactions. The effect of triethylene glycol and heating in overcoming stabilising hydrogen bonding interactions has been explored in Chapter 7. Changes in hydrogen bonding interactions in pre-extruded DBM plasticised with TEG were monitored throughout heating.

The experimental chapters are followed by a concluding discussion in Chapter 8, presenting the final understanding of decolouring as a method of modifying bloodmeal for use in thermoplastic preparations.

References

1. Statistics New Zealand. (2015). Total Quarterly New Zealand by Kill by Animal Type. Table Reference LSS026AA.
2. Meeker, D.L., Hamilton, C.R. (2006). An Overview of the Rendering Industry, in Essential Rendering: All About the Animal By-Products Industry, Meeker, D.L., Editor. National Renderers Association: Virginia, U.S.. p. 1-16.
3. Jayathilakan, K., Sultana, K., Radhakrishna, K., Bawa, A.S. (2012). Utilization of Byproducts and Waste Materials from Meat, Poultry and Fish Processing Industries: A Review. Journal of Food Science and Technology. 49(3): p. 278-293.
4. Scaria, K.J. (1989). Economics of Animal By-Products Utilization. Issue 77. Food & Agriculture Organization of the United Nations. Rome, Italy. p. 1-68.
5. Swan, J.E. (1999). Animal By-Product Processing, in Wiley Encyclopedia of Food Science and Technology, Francis, F.J., Editor. John Wiley & Sons Inc.: New York, U.S.. p. 35-43.

6. Kaluzny, D. (2013). World Renderers Organization: Rendered Products Worldwide.
7. Jago, J.G., Lasenby, R.R., Trigg, T.E., Claxton, P.D., Matthews, L.R., Bass, J.J. (1995). The Effect of Immunological Castration on Behaviour and Growth of Young Bulls. Proceedings of the New Zealand Society of Animal Production. 55: p. 190-192.
8. Muir, P.D., Thomson, B.C., Askin, D.C. (2008). A Review of Dressing out Percentage in New Zealand Livestock. Ministry of Agriculture: Wellington, New Zealand. p. 1-88.
9. Livestock Improvement Corporation Limited, DairyNZ Limited. (2014). New Zealand Dairy Statistics 2013-14. Hamilton, New Zealand. p. 1-55.
10. Duarte, R.T., Carvalho Simões, M.C., Sgarbieri, V.C. (1999). Bovine Blood Components: Fractionation, Composition, and Nutritive Value. Journal of Agricultural and Food Chemistry. 47(1): p. 231-236.
11. National Research Council, Canadian Department of Agriculture. (1971). Atlas of Nutritional Data on United States and Canadian Feeds. National Academy of Sciences: Washington, D.C., U.S.. p. 68-69.
12. Martínez-Llorens, S., Vidal, A.T., Moñino, A.V., Gómez Ader, J., Torres, M.P., Cerdá, M.J. (2008). Blood and Haemoglobin Meal as Protein Sources in Diets for Gilthead Sea Bream (*Sparus aurata*): Effects on Growth, Nutritive Efficiency and Fillet Sensory Differences. Aquaculture Research. 39(10): p. 1028-1037.
13. Haughey, D.P. (1976). Market Potential and Processing of Blood Products: Some Overseas Observations. MIRINZ: Hamilton, New Zealand. p. 1-55.
14. Preston, R.L. (2014). 2014 Feed Composition Table, in Beef. Penton Media: Minneapolis, U.S.. p. 18-26.
15. Hicks, T.M., Verbeek, C.J.R., Lay, M.C., Manley-Harris, M. (2013). The Role of Peracetic Acid in Bloodmeal Decoloring. Journal of the American Oil Chemists' Society. 90(10): p. 1577-1587.
16. Howie, S.A., Calsamiglia, S., Stern, M.D. (1996). Variation in Ruminal Degradation and Intestinal Digestion of Animal By-Product Proteins. Animal Feed Science and Technology. 63(1–4): p. 1-7.
17. Kamalak, A., Canbolat, O., Gurbuz, Y., Ozay, O. (2005). In Situ Ruminal Dry Matter and Crude Protein Degradability of Plant- and Animal-Derived

Protein Sources in Southern Turkey. Small Ruminant Research. 58(2): p. 135-141.

18. Laining, A., Rachmansyah, Ahmad, T., Williams, K. (2003). Apparent Digestibility of Selected Feed Ingredients for Humpback Grouper, *Cromileptes altivelis*. Aquaculture. 218(1–4): p. 529-538.
19. Marichal, M., Carriquiry, M., Pereda, R., San Martín, R. (2000). Protein Degradability and Intestinal Digestibility of Blood Meals: Comparison of Two Processing Methods. Animal Feed Science and Technology. 88(1–2): p. 91-101.
20. National Research Council. (2001). Nutrient Composition of Feeds, in Nutrient Requirements of Dairy Cattle: Seventh Revised Edition. The National Academies Press: Washington, D.C., U.S.. p. 281-314.
21. Nengas, I., Alexis, M.N., Davies, S.J., Petichakis, G. (1995). Investigation to Determine Digestibility Coefficients of Various Raw Materials in Diets for Gilthead Sea Bream, *Sparus auratus L*. Aquaculture Research. 26(3): p. 185-194.
22. Ockerman, H.W., Hansen, C.L. (1988). Animal By-Product Processing. Ellis Horwood: Chinchester, England.
23. Márquez, E., Bracho, M., Archile, A., Rangel, L., Benítez, B. (2005). Proteins, Isoleucine, Lysine and Methionine Content of Bovine, Porcine and Poultry Blood and Their Fractions. Food Chemistry. 93(3): p. 503-505.
24. Kats, L.J., Nelssen, J.L., Tokach, M.D., Goodband, R.D., Weeden, T.L., Dritz, S.S., Hansen, J.A., Friesen, K.G. (1994). The Effects of Spray-Dried Blood Meal on Growth Performance of the Early-Weaned Pig. Journal of Animal Sciences. 72(11): p. 2860-9.
25. van den Berg, L. (2009). Development of 2nd Generation Proteinous Bioplastics Science and Engineering. MSc: p. 1-134.
26. Verbeek, C.J.R., Viljoen, C., Pickering, K., van den Berg, L. (2010). Plastics Material. NZ (NZ551531).
27. Verbeek, C.R., van den Berg, L. (2011). Development of Proteinous Bioplastics Using Bloodmeal. Journal of Polymers and the Environment. 19(1): p. 1-10.

28. Low, A., Verbeek, C.J.R., Lay, M.C. (2014). Treating Bloodmeal with Peracetic Acid to Produce a Bioplastic Feedstock. Macromolecular Materials and Engineering. 299(1): p. 75-84.
29. Low, A. (2012) Decoloured Bloodmeal Based Bioplastic. Thesis in Materials and Process Engineering, University of Waikato: Hamilton.
30. Maiolo, K., Marin, P.D., Bridges, T.E., Heithersay, G.S. (2007). Evaluation of a Combined Thiourea and Hydrogen Peroxide Regimen to Bleach Bloodstained Teeth. Australian Dental Journal. 52(1): p. 33-40.
31. Nagababu, E., Rifkind, J.M. (2004). Heme Degradation by Reactive Oxygen Species. Antioxidants & Redox Signaling. 6(6): p. 967-978.
32. Zhou, S., Wang, J., Huang, W., Lu, X., Cheng, J. (2007). Monitoring the Reaction of Hemoglobin with Hydrogen Peroxide by Capillary Electrophoresis-Chemiluminescence Detection. Journal of Chromatography B. 850(1-2): p. 343-347.

2

Properties of Proteins after Treatment with Peracetic Acid

A Literature Review

I prepared the draft manuscript of this literature review, which was refined and edited in consultation with my supervisors. This chapter will be edited further to prepare a journal paper, for which my supervisors will be credited as co-authors.

Properties of Proteins after Treatment with Peracetic Acid

Abstract

Peracetic acid has recently found commonplace use in many industrial applications including use as a bleaching agent in the textiles industry and as a disinfectant during sanitization and wastewater treatment. Its extensive use is in part due to growing concerns over the environmental impact of chlorine. Peracetic acid does not form harmful disinfection by-products, decomposes if discharged into the environment and does not result in bioaccumulation. In addition to these advantages, peracetic acid is rapidly becoming known for its efficacy in its own right and is consequently finding greater use.

Contacting proteins with oxidants is known to result in changes to the chemical structure of the protein. Such changes are generally accompanied by changes in the physical and mechanical properties of protein-based materials, limiting their potential use. With the use of peroxycarboxylic acids becoming more commonplace in industry (particularly the C1-C8 aliphatic series) in the areas of food technology and textiles, a thorough investigation of the action of these peroxides on proteins is warranted.

While reviews of the formation and properties of peracetic acid and other peroxycarboxylic acids have been published, no comprehensive account exists that describes the effects of peracetic acid on protein primary and secondary structure, protein interactions or their final physical properties. For a protein to be utilised in the food or pharmaceutical industry, maintaining functionality is of the utmost importance, subsequently making the impact of oxidation on protein structure important. Further, proteins to be used in bio-based materials often require chemical modification to alter their physico-chemical properties before processing, oxidation is only one means by which this can be achieved, and understanding the repercussions for chemical and mechanical properties will greatly impact the development of the material. This review investigates the effect of equilibrium peracetic acid (PAA) oxidation on protein structure and composition.

1 Introduction

1.1 Production of peroxycarboxylic acids

Peroxycarboxylic acids are compounds containing one or more peroxo group (-O-O-) covalently bound to at least one carboxylic acid group. They are derivatives of hydrogen peroxide in which one or both hydrogens are replaced by a group containing a carboxylic acid. Several methods for producing peroxycarboxylic acids exist, the most common of which involves the equilibrium reaction of the parent carboxylic acid with hydrogen peroxide in the presence of a strong mineral acid [1]. For lower aliphatic carboxylic acids, this yields an aqueous mixture of peroxycarboxylic acid, which also contains the parent carboxylic acid, hydrogen peroxide and water [2].

The proportion and concentration of hydrogen peroxide and carboxylic acid used determines the equilibrium composition. Chelating agents are often added during processing to reduce metal-catalysed decomposition reactions. Greater yields of the peroxyacid can be obtained using preparations containing lower water content, typically accomplished through the use of concentrated hydrogen peroxide or excess carboxylic acid. The equilibrium position can also be shifted to the right by removing water azeotropically and/or under vacuum, and pure peroxycarboxylic acids can be obtained by distillation followed by fractional freezing [3].

Alternative methods for producing peroxycarboxylic acids involve either the reaction of carboxylic anhydrides or carboxylic acid chlorides with hydrogen peroxides or the autoxidation of aldehydes [3]. A common method for industrial production of peracetic acid involves the auto-oxidation of acetaldehyde over a metal catalyst and, if the reaction takes place at less than 40 ^{o}C and at about 35 bar, peracetic acid can be isolated [4].

A summary of the common methods for producing peroxycarboxylic acids is given in Table 1.1.

Table 1.1: Common synthesis reactions for organic peracids.

Reaction	Product	Reference
$RCOOH + H_2O_2 \overset{H^+}{\rightleftharpoons} RCOOOH + H_2O$	Performic acid Peracetic acid Perpropionic acid Perbutyric acid	[5, 6]
$(RCO)_2O + 2H_2O_2 \longrightarrow RCOOOH + H_2O$	Peracetic acid Mono-peroxyphthalic acid	[5-7]
$RCOCl + H_2O_2 \xrightarrow{base} RCOOOH + HCl$	*m*-chloroperbenzoic acid	[8]
$RCHO + O_2 \longrightarrow RCOOOH$	Peracetic acid perbenzoic acid	[9, 10]
$RCO_3COR \xrightarrow{hydrolysis} RCOOOH + RCO_2H$	Perbenzoic acid	[11]
$RCO_2COR + H_2O_2 \xrightarrow{base} RCOOOH + RCO_2H$	Perphthalic acid	[12]

1.2 Physico-chemical properties of peroxycarboxylic acids

The low molecular weight aliphatic peroxycarboxylic acids are liquids at room temperature, whereas the aromatic and higher molecular weight diperoxy aliphatic members are solids [2]. Infrared and X-ray studies show that peroxycarboxylic acids are dimeric in the solid state owing to hydrogen-bonding interactions, whereas in the form of a vapour, pure liquid or in aqueous solutions, are monomeric due to the disruption of stabilising dimeric hydrogen bonds [3].

Unlike their parent carboxylic acids, which are capable of existing as hydrogen bonded dimers in liquid form (and consequently have a relatively low vapour pressure and high boiling point), aliphatic peroxycarboxylic acids have higher vapour pressures and lower extrapolated boiling points due to their inability to form dimers in the liquid state. They are also more water soluble and are much weaker acids than the parent carboxylic acids. Like other aliphatic organics, as chain length increases the peroxycarboxylic acids become increasingly insoluble in water and the C6–C16 peroxycarboxylic acids are soluble in hydrocarbon solvents only [2].

The peroxide bond is known for its instability, and easily undergoes thermal or photo-induced homolytic cleavage of the weak oxygen–oxygen bond [3]. The theoretical bond dissociation enthalpy of the peroxide bond ranges from 92 to 213 kJ/mol (22 to 51 kcal/mol) [13]. Peroxycarboxylic acids are among the strongest

organic peroxide oxidising agents and have found extensive use in applications such as epoxidation, hydroxylation and bleaching reactions.

During reactions with proteins, hydrogen peroxide and peracetic acid may be consumed in four classes of reactions:

- decomposition reactions (spontaneous and transition metal ion catalysed degradation/hydrolysis) [14-18],
- protein oxidation (cross-linking, fragmentation, side-chain modifications) [19, 20],
- deodourising by reaction with odour-causing compounds [16, 21], and
- decolouring by reaction with colour-causing compounds [22].

The major products of these reactions include modified proteins, ethanoic acid, carbon dioxide and oxygen [20, 23].

1.3 Peracetic acid

Peracetic acid (PAA) has been used since the early 1940s in a number of roles (Table 1.2); it finds extensive use as a bleaching agent and disinfectant and in wastewater treatment due to growing concerns over the environmental impact of chlorine. PAA is most commonly used in the textile industry for bleaching of wool, and linen, generally giving better brightness and less fibre damage than the alternatives. PAA is also known to be effective in food and surface sanitisation [20, 24-26] and is regarded as superior since it does not form harmful disinfection by-products in quantities greater than allowable, it decomposes if discharged into the environment and bioaccumulation is unlikely to occur [27, 28]. Recently, PAA has found use for bleaching bloodmeal feedstock prior to bioplastic production [29].

Table 1.2: Common uses of peracetic acid in industry.

Industry	Role	Ref
Textiles	Wool bleaching	[19, 30, 31]
	Cotton bleaching	[17, 32, 33]
	Other fibre bleaching	[34-38]
	Chemical modification of fibres and fabrics	[39]
Pulp and Paper	Delignification	[40-44]
	Bleaching	[23, 45, 46]
Organic synthesis	Epoxidation	[47, 48]
	Hydroxylation	[49-51]
Disinfection	Food industry	[20, 24-26]
	Wastewater disinfection	[16, 21, 52-56]
	Disinfection of surgical instruments	[57-59]

Peracetic acid is an equilibrium mixture of PAA, hydrogen peroxide (HP), acetic acid (AA) and water, produced commercially by reacting glacial acetic acid with hydrogen peroxide in the presence of a mineral acid catalyst, such as ~1 wt% sulfuric acid [60]. The catalyst remains once equilibrium is obtained, leading to a pH less than 1. The concentration of PAA can be increased by distillation to produce non-equilibrium mixtures removing a portion of the AA, HP and water, although this is more expensive and raises safety concerns due to the explosive nature of peroxides.

The equilibrium composition of a commercial peracetic acid solution is typically 5 – 6 wt% (where wt% = percentage by mass) peracetic acid (PAA), 21 – 23 wt% hydrogen peroxide (HP), 10 – 11 wt% ethanoic acid and 63 – 65 wt% water [61]. Chelating agents are added to minimise the transition metal ion catalysed decomposition of peracetic acid to acetic acid and oxygen [62, 63].

$$CH_3COOH + H_2O_2 \rightleftharpoons CH_3COOOH + H_2O$$

In an equilibrium mixture, peracetic acid may be consumed as follows [14-17]:

Hydrolysis:

$$CH_3COOOH + H_2O \longrightarrow CH_3COOH + H_2O_2$$

Spontaneous decomposition:

$$2CH_3COOOH \longrightarrow 2CH_3COOH + O_2$$

Transition metal catalysed decomposition:

$$2CH_3COOOH \xrightarrow{M^{n+}} 2CH_3COOH + O_2 + \text{Other products}$$

The equilibrium constant for peracetic acid at 20 ^oC results in an equilibrium mixture containing ~5 wt% PAA and has been calculated as approximately K= 2, indicating that the formation of the products is favoured but the reaction is easily reversed [62]. The rate of reverse reaction is half that of the forward reaction at 20 ^oC, however as temperatures approach 60 ^oC the rates are approximately equal, Table 1.3, this indicates that at higher temperatures hydrolysis of peracetic acid may become significant during exothermic reactions [62].

Table 1.3: Summary of the composition of the reaction mixture, equilibrium state, equilibration time, equilibrium constant and forward and reverse reaction rates for the formation of peracetic acid, at 20, 40 and 60 ^{o}C at pH ~ 1.2. Reaction rate for spontaneous decomposition k_3 of peracetic acid at pH 5.5 [14].

T (^{o}C)	Equilibration Time (h)	Initial concentration (molL-1)		Equilibrium concentration (molL-1)			K	k_1 ($x10^{-5}$ $Lmol^{-1}s^{-1}$)	k_2 ($x10^{-5}$ $Lmol^{-1}s^{-1}$)	k_3 ($x10^{-5}$ $Lmol^{-1}s^{-1}$)
		HP	AA	PAA	HP	AA				
20	36	9.88	2.47	0.84	9.04	1.63	2.10	6.81	3.25	
40	28	9.88	2.47	0.68	9.20	1.80	1.46	8.55	5.85	7.1
60	22	9.88	2.47	0.54	9.33	1.93	1.07	13.82	12.92	

Peracetic acid is also a weak acid, with a pK_a of 8.2 and is able to partially dissociate at higher pH. This enables the peracetic acid molecule to undergo spontaneous decomposition via the nucleophilic attack of the peracetate anion upon another peracetic acid molecule (or hydrogen peroxide), to form two acetate anions and oxygen [64]:

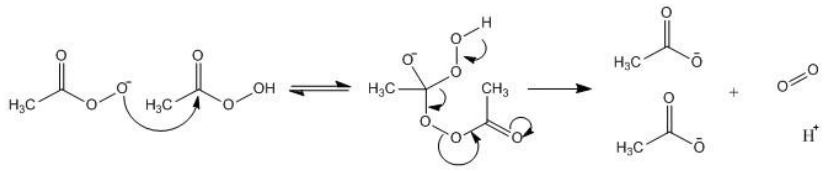

From this scheme the rate of PAA degradation owing to spontaneous decomposition is:

$$-\frac{\partial[\mathrm{PAA}]}{\partial t} = k_3[PAA]^2$$

Due to the high pK_a of peracetic acid (little dissociation at low pH), the rate of spontaneous decomposition of peracetic acid at low pH such as that of commercial PAA (<1) should be small. It was found that the dependence of kinetics of decomposition on total peracetic acid concentration was second-order in PAA, and that at 40 ^{o}C for pH 5.5 k_3 is 7.1 x 10^{-5} $Lmol^{-1}s^{-1}$, comparable with the rate of hydrolysis at the same temperature (Table 1.3), and increases to its maximum observed rate, 7.4 x 10^{-3} $Lmol^{-1}s^{-1}$ at pH 8.2, the pK_a of peracetic acid. This indicates that for an equilibrium mixture at low pH spontaneous decomposition of PAA is unlikely to cause significant changes in the concentration of PAA compared with the rate of formation and hydrolysis, thus giving a stable quantity of PAA over time.

2 Reactive oxygen species from peracetic acid

Reactive Oxygen Species (ROS) is an umbrella term used to describe a number of reactive molecules and free radicals derived from molecular oxygen and hydroperoxides. These molecules have great potential to cause a variety of both useful and sometimes adverse chemical events.

The reactive oxygen species considered in bleaching reactions are generated through the activation or decomposition of hydroperoxides (although radical formation can occur from atomic oxygen). Oxygen has two unpaired electrons in separate orbitals in its outer electron shell, making it susceptible to radical formation. Sequential reduction of oxygen through the addition of electrons leads to the formation of a number of ROS including: superoxide, hydrogen peroxide, hydroxyl and perhydroxyl radicals (Figure 2.1).

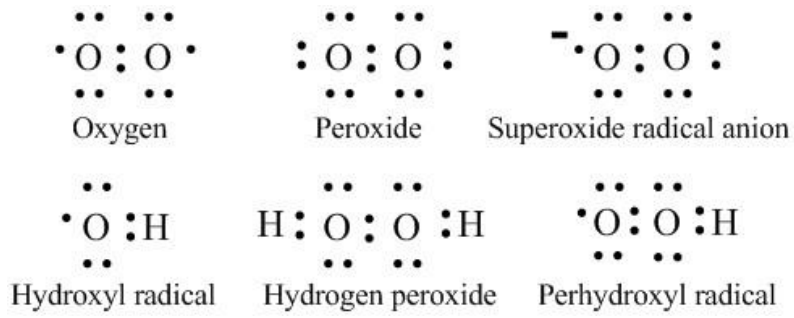

Figure 2.1: Lewis diagrams of common reactive oxygen species generated from molecular oxygen or hydroperoxides.

At the low pH of commercial PAA solutions, peracetic acid and hydrogen peroxide are undissociated and both act as electrophiles. Peroxyacids are ambident electrophiles and are susceptible to nucleophilic attack at either the outer peroxide oxygen or at the carbonyl carbon. Peracetic acid is known for its high reduction potential and its ability to form a variety of free radicals [13, 65] and activation of peracetic acid (and hydrogen peroxide) may occur via light, heat or transition metal catalysis giving rise to homolytic cleavage to yield hydroxyl, acyloxy, perhydroxyl and acetyl radicals [65] as shown below:

1. acyloxy radical + hydroxyl radical

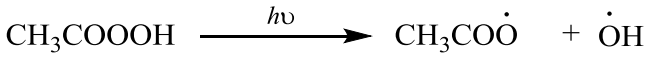

2. acetyl (carbon centred) radical + perhydroxyl radical

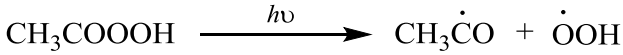

Peracetic acid is able to react with the hydroxyl radical generated in (1) to yield the acetoxy radical (3), acylperoxy radical (4) and the perhydroxy radical (5) [65].

3. acetoxy (oxygen centred) radical + oxygen + water

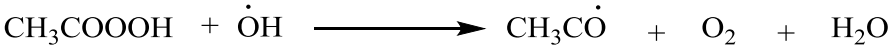

4. acylperoxy radical + water

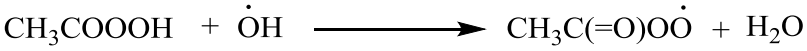

5. acetic acid + perhydroxyl radical

The acyloxy radical formed in (1) is very unstable and tends to dissociate by monomolecular decarboxylation to yield a methyl radical and carbon dioxide [65]:

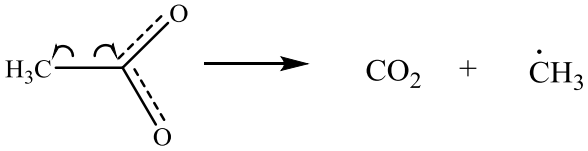

However, in the reactions where the carbon-centred radical is resonance stabilised, the reaction is reversible and is followed by the interaction of methyl radicals with oxygen to produce the methyl peroxy- radical [65].

This reaction is relatively fast in oxygen-saturated environments, and therefore, the amount of methyl radicals in the reaction system is limited [65]. A hydroxyl radical formed as a primary radical simultaneously reacts with $CH_3OO\cdot$ to generate a new PAA molecule, restarting the new oxidation cycle.

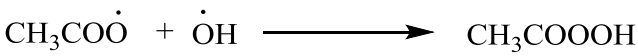

During sterilization processes PAA is considered to be more effective than hydrogen peroxide due to the greater longevity of the radicals it generates compared to the hydroxyl radical generated by hydrogen peroxide [66].

3 Use of PAA to degrade chromophores

Dyes typically have a complex aromatic structure, and are problematic in wastewaters (which may enter surface waters) due to their high attenuation of light, chemical resilience and potential toxicity.

A dye's colour is imparted by the presence of a chromophore; a system of delocalised electrons created by the conjugation of double bonds which absorb specific wavelengths of electromagnetic radiation. These chromophores are typically -C=C-, -C=O, - C=S, -N=N-, -N=O, -NO_2, -C=NH [67].

Not all chromophores absorb visible or ultraviolet light, however the colour of a compound can be further deepened, lightened, intensified or diminished by the addition of electron withdrawing or donating substituents. These substituents change the size of the system of delocalised electrons. These functional groups are known as auxochromes and include: –OH, -NH_2, NH_3, -COOH and -SO_3H groups [67].

The bleaching action of peracetic acid is mainly the result of epoxidation of the double bonds present in unwanted coloured compounds [68]. Peracids, with or without activating compounds (transition metals) have been employed as low temperature oxidants in detergency and other applications for the last two decades.

3.1 PAA degradation of haem

During decolouring the desired function of PAA and HP is to degrade the haem chromogen (Figure 3.1). At low pH both HP and PAA act as electrophiles, attacking regions of high electron density, such as the methene bridges in haem and other chromophores, resulting in a loss of extended conjugation and a consequent loss in colour.

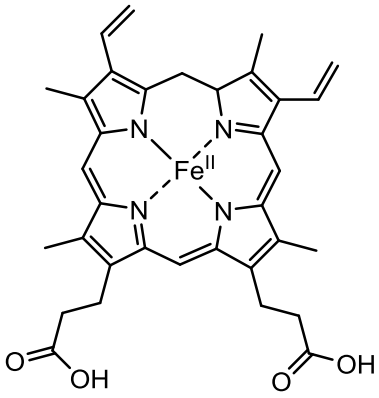

Figure 3.1: Structure of haem tetraporphyrin chelating ferrous iron.

Haem is comprised of a tetraporphyrin ring, which chelates iron II (Fe^{2+}) and is located within the hydrophobic pocket of each of the four globin chains of

haemoglobin. The iron II centre forms a six coordination complex, of which four positions are occupied by the planar nitrogen atoms of the porphyrin ring, a fifth by a covalent bond with a histidine residue of the globin chain, and the sixth position is reversibly occupied by exogenous ligands, such as oxygen, carbon dioxide or water [69].

The iron centre in haem can exist in various oxidation states; in the ferrous oxidation state the haem chelates oxygen, and the haemoglobin is referred to as oxyhaemoglobin (Fe^{2+}, iron II) and is red in colour (Figure 3.2). When the oxygen dissociates it becomes deoxyhaemoglobin (Fe^{2+}, iron II). Exposure to oxygen-rich environments can cause the iron in oxyhaemoglobin to be oxidised to its ferric state resulting in methaemoglobin (Fe^{3+}) where the sixth co-ordination position is occupied by a hydroxide ion or water and the molecule is dark red-brown in colour [38].

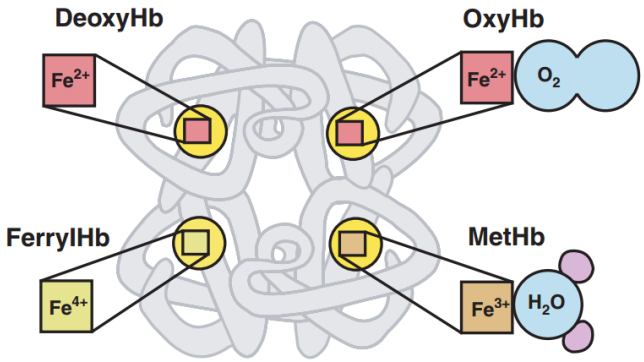

Figure 3.2: Various oxidation states iron present in the haem located within each of the four globin chains of the haemoglobin molecule (Hb). Changes in the iron's oxidation number result in changes to ligand binding as shown. Reproduced from ref. [69], Copyright (2009), with permission from John Wiley and Sons.

Unfortunately, hydrogen peroxide alone is unable to degrade all of the haem present in red blood cells, owing to the catalytic removal of hydrogen peroxide by methaemoglobin ($HbFe^{3+}$) [70]. When the haem iron in haemoglobin is in the ferric state (Fe^{3+}), as in methaemoglobin, and the haem's 6th coordination position is unoccupied, it is able to be accessed by the hydroperoxide group R–O–O–H. This results in the oxidation of ferric haem to the free radical cation oxoferrylHb (Figure 3.3), with the generation of a free radical on either the porphyrin moiety of the haem or on an amino acid; this destruction of hydroperoxide is frequently observed in peroxidases and other haem containing proteins [69, 71, 72].

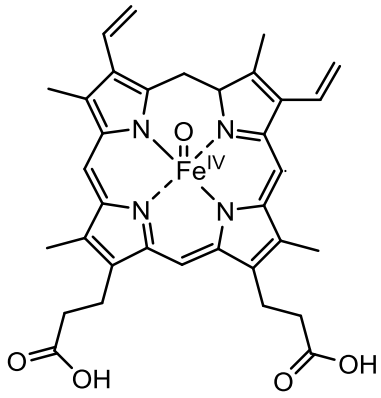

Figure 3.3: Oxoferrylhaemoglobin ($^{\cdot}HbFe^{4+}O$).

The π-radical on the oxoferrylHb is rapidly transferred to a nearby amino acid residue on the protein, and undergoes a cascade of transfers and transformations. The free radicals formed via this oxidation vary depending on the type of proteins and enzymes involved, but are generally formed on tyrosine, tryptophan and sometimes cysteine residues [71].

Thus, unlike free haem which can be directly oxidised by HP, or oxyhaemoglobin ($HbFe^{2+}$) which reacts with HP to form a superoxide radical that degrades the haem moiety, methaemoglobin ($HbFe^{3+}$) reacts with HP to form oxoferrylhaemoglobin ($HbFe^{4+}O$), with a protein radical centred on the globin chain (Hb) [69, 71, 72]. Oxoferrylhaemoglobin can then be reduced by HP, forming molecular oxygen and water, regenerating methaemoglobin, and this chain reaction causes the catalytic removal of HP with a resultant loss of oxidation power [70]:

$$HbFe^{3+} + H_2O_2 \rightarrow {}^{\cdot}HbFe^{4+}O + H_2O$$

$$^{\cdot}HbFe^{4+}O + H_2O_2 \rightarrow HbFe^{3+} + O_2 + H_2O$$

At the acidic pH encountered during peracetic acid decolouring, the oxoferryl species is also able to become protonated to form $[Fe^{4+}OH^{-}]^{3+}$, which has a pK_1 value of ~3.5 [73], and is considered to have a radical-like nature as it is electronically equivalent to the ferric haem species with a radical on either the hydroxyl ligand, the porphyrin or the globin, shown below:

$$[Fe^{4+}O^{2-}]^{2+} + H^{+} \rightleftharpoons [Fe^{4+}OH^{-}]^{3+}$$

Where electronically: $[Fe^{4+}OH^{-}]^{3+} \cong Fe^{3+}OH^{\cdot} \cong {}^{\cdot}PorFe^{3+}OH^{-} \cong {}^{\cdot}HbFe^{3+}OH^{-}$

In addition to reactive oxoferrylHb, free iron species are also able to react with hydrogen peroxide to generate highly reactive hydroxyl radicals [70]:

$$Fe^{2+} + H_2O_2 \rightarrow Fe^{3+} + {\cdot}OH + OH^-$$

Peroxyl radicals can also be generated from the metal ion catalysed decomposition of hydroperoxides [74]:

$$Fe^{3+} + ROOH \rightarrow Fe^{2+} + ROO^{\cdot} + H^+$$

Due to the presence of several reactive species and free radicals, subsequent oxidative damage is likely to occur rapidly as the radicals undergo auto-reduction reactions, by direct intramolecular oxidation of a nearby protein residue, or through protonation linked to oxidation of the substrate molecule [71]. For example, the most likely radical to be formed on a protein chain (from a porphyrin π-cation radical reduction) is a cation radical generated on an amino acid residue with a low oxidation potential such as tryptophan or tyrosine. This cation radical can then oxidise another tryptophan or tyrosine residue on the same protein within a few tens of picoseconds, creating a very fast transfer of the cation radical over a cascade of tryptophan and tyrosine residues, eventually becoming deprotonated to become a neutral radical [71].

4 Protein Oxidation

The radicals described above are able to undergo a variety of reactions with amino acids and proteins, such as hydrogen abstraction, electron transfer (oxidation or reduction of the substrate) or addition. Radicals formed on amino acids may cause them to undergo fragmentation, rearrangement, dimerisation, disproportionation or substitution [74].

For the most part, most oxidative systems result in a general loss of amino acids. Exposure of bovine serum albumin to ·OH, with or without $O_2^{\cdot-}$ resulted in similar dose-dependent losses of most amino acids. Further, the superoxide radical anion alone ($O_2^{\cdot-}$) was not found to significantly damage any of the amino acids in BSA (except cystine); despite the ability of superoxide to undergo dismutation to form hydrogen peroxide. Hydrogen peroxide was only found to cause amino acid modification in the presence of transition metal ions with which it forms hydroxyl radicals [75], it was concluded that all amino acid modifications (except some

related to cystine) originated from reactions involving the hydroxyl radical (not the superoxide radical) [75]. Follow up studies indicated that although the hydroxyl radical initiates protein peroxidation, further reactions with the perhydroxyl anion (HO_2^-) and its conjugate base $O_2^{\cdot-}$ were responsible for the generation of stabilised peroxide end products [76].

4.1 Primary structure

Proteins are heterogeneous polymers derived from the condensation reactions of the 20 L-amino acids shown in Figure 4.1. Protein oxidation can result in changes at several levels. First it may directly alter amino acid residues, resulting in the possibility of hydrolysis, chain scission and crosslinking. Such changes are likely to be influenced by, and themselves influence, the proteins secondary structural components. Further, changes to the primary and secondary structures within proteins are likely to result in a loss of functionality for native proteins, and also impact their physical properties such as isoelectric point, hydrophilicity, swelling, solubility, elasticity, toughness and strength [77, 78]. Complete loss of amino acid side chains is also possible, yielding short chain aldehydes and ketones [77]; this can potentially result in improved chain regularity and greater polymer mobility in protein based materials. Ultimately, alterations to primary structure of a protein are linked with increased proteolysis [75] and potentially change the way in which proteinous materials breakdown during their final use and disposal.

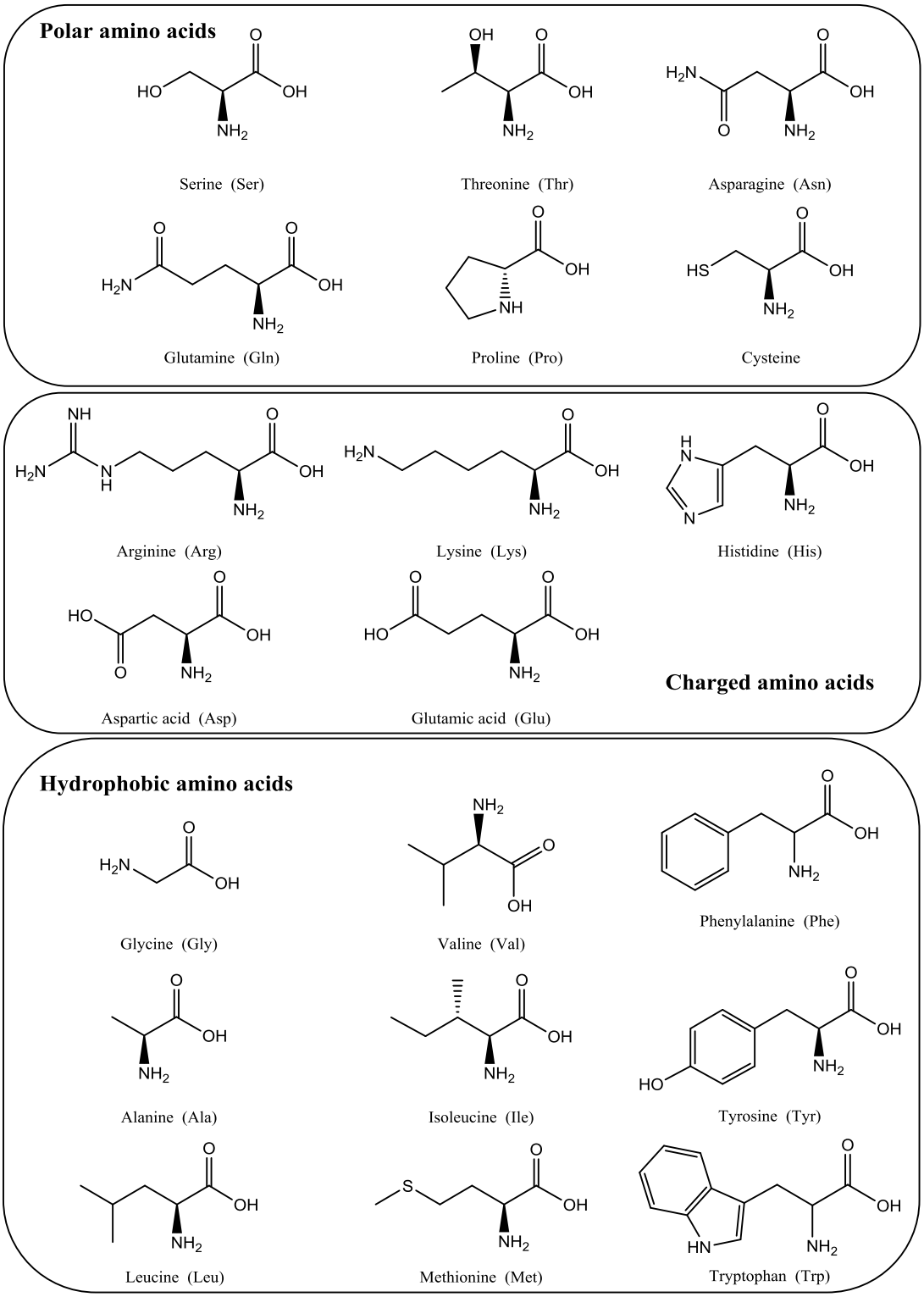

Figure 4.1: Structures of the 20 common L- amino acids.

4.1.1 Peptide cleavage

The α-carbon of amino acids in the polypeptide chain (the site of attachment of the side-chains), and to a lesser extent the β-carbon and other carbons in the side chain of aliphatic amino acid residues are vulnerable to attack by ROS (Figure 4.2). The

most damaging reaction proteins can undergo with reactive oxygen species is hydrogen abstraction from the peptide backbone at the α-carbon position, generating a resonance-stabilised carbon radical. These carbon radicals are able to undergo further reactions, resulting in cleavage of the peptide bond.

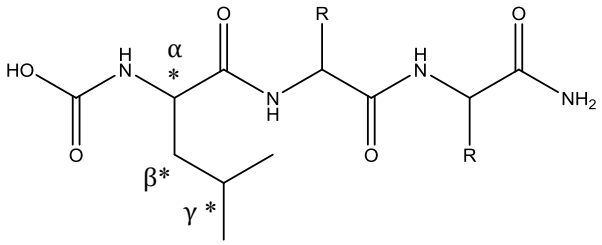

Figure 4.2: Peptide chain indicating the α-, β- and γ- carbon centres where hydrogen atom abstraction may occur.

Exposure of amino acids, peptides and proteins in solution to ionising radiation results in the formation of alkyl peroxide and hydroxyl derivatives, (owing to the generation of the hydroxyl and protonated superoxide radicals from water) [79]. A similar reaction mechanism is purported to occur for amino acids, peptides and proteins exposed to hydrogen peroxide initiated by the formation of the hydroxyl radical (generated via the homolytic cleavage of H_2O_2 by iron or copper ions), shown in Figure 4.3 [80].

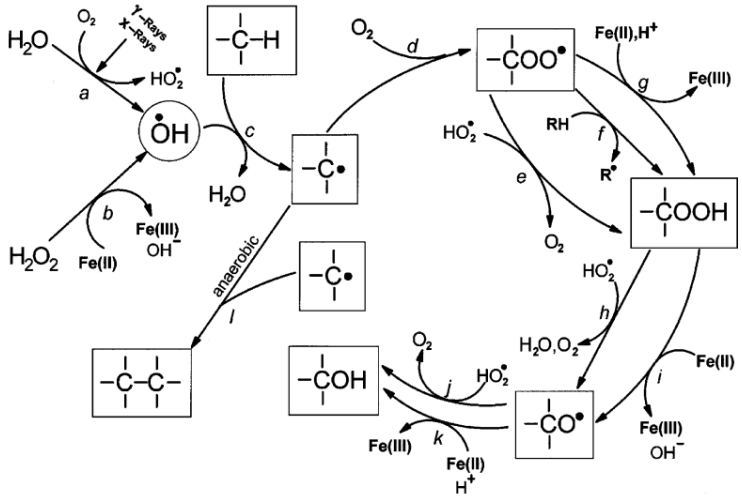

Figure 4.3: Hydroxyl radical formation and oxidation of protein substrate through the formation of a peroxyl radical and hydroperoxy intermediate. Reproduced from E. R. Stadtman and R. L. Levine Free Radical-mediated Oxidation of Free Amino Acids and Amino Acid Residues in Proteins, *Amino Acids* (2003) 25(3) p. 207-218, Figure 1 [80]. Copyright (2003) Springer-Verlag, with kind permission from Springer Science and Business Media.

The hydroxyl radical dependent abstraction of hydrogen generates a carbon-centred radical (reaction c, Figure 4.3), stabilised via electron delocalisation to the neighbouring carbonyl and nitrogen groups, which in aerobic environments is converted to the peroxyl radical (reaction d) [80, 81]. Reaction of this carbon radical with another radical is expected to be limited due to steric hindrance.

The fate of the generated peroxyl radical has yet to be fully elucidated. However, it is known to be converted to an alkyl peroxide via reaction with the protonated superoxide radical (reaction e) or via abstraction of hydrogen from another molecule (reaction f) [82]. Subsequent reactions of the alkyl hydroperoxide with the protonated superoxide radical ($HO_2^{\cdot}$) generates an alkoxyl radical (reaction h), followed by the formation of the hydroxy derivative (reaction j) [80]. Alternatively, in the absence of oxygen the alkyl peroxide may undergo reductive diamidation (Figure 4.4A) via an alkoxyl radical mediated process, resulting in backbone fragmentation with the production of a diamide and an isocyanate derivative [79, 81].

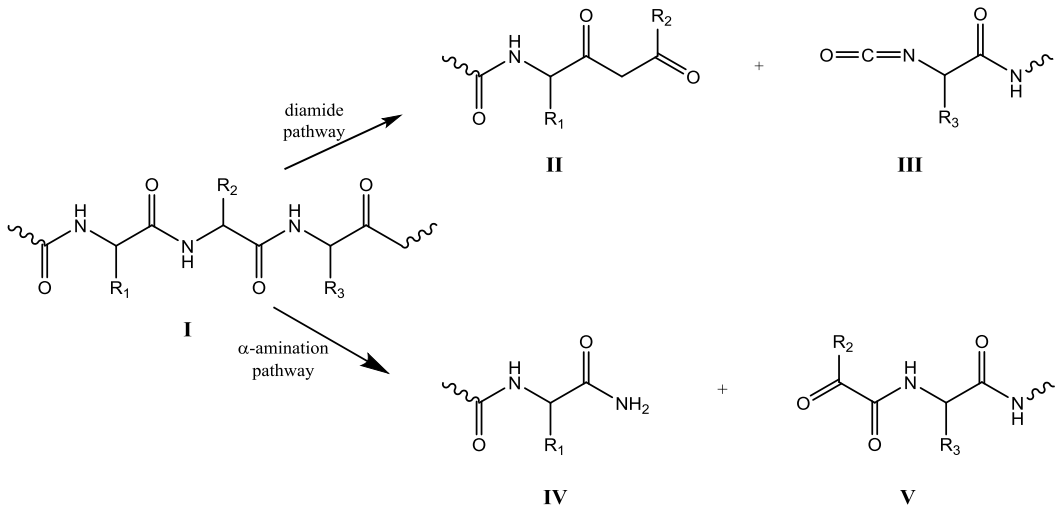

Figure 4.4: Peptide or protein (I) cleavage pathways. A: diamide pathway, generating a diamide (II) and isocyanate derivative (III) and B: α-amidation pathway, generating a terminal amide group (IV) and a keto-acyl derivative (V). Reproduced from E. R. Stadtman and R. L. Levine Free Radical-mediated Oxidation of Free Amino Acids and Amino Acid Residues in Proteins, *Amino Acids* (2003) 25(3) p. 207-218, Figure 2A [80]. Copyright (2003) Springer-Verlag, with kind permission from Springer Science and Business Media.

However, in aerobic environments the peroxyl radical is more likely to undergo an elimination reaction yielding a protonated superoxide radical with the generation of an imine, which undergoes spontaneous hydrolysis (backbone fragmentation) to give a terminal amide group and a keto-acyl derivative (Figure 4.4B) [79, 83].

Another pathway for peptide cleavage involves the oxidation of proline residues to the 2-pyrrolidone derivative via the hydroxyl radical (Figure 4.5) [84].

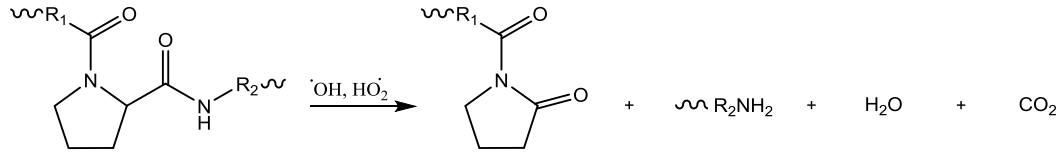

Figure 4.5: Proline oxidation resulting in peptide cleavage [84].

It is fortunate that abstraction of hydrogen atoms from the α- and β- carbons in peptides and proteins by electrophilic free radicals (such as the hydroxyl radical) rarely occurs. Both chlorine and the hydroxyl free radicals have been shown to prefer reacting with C-H groups away from these centres (γ-, δ-, ε- C-H groups) to produce radicals unlikely to result in chain scission [85]. The degradation of peptide bonds may not result in an immediate change in molecular weight as the broken molecule is still held together by hydrogen bonding and electrostatic interactions. Such changes may only be observed in proteins during subsequent heating, when the newly formed fragments are able to link together through new hydrogen bonds, forming aggregates which precipitate (decreasing solubility and increasing viscosity).

There is a variety of amino acid residues present in peptides and proteins which offer many other potential sites for attack in addition to attack on the backbone; free radical reactions lead to the formation of a large array of protein radicals, which depends on the nature of the attacking radical. For example, electrophilic radicals (such as the hydroxyl or alkoxyl radicals) preferentially oxidise electron-rich sites, whereas nucleophilic radicals (such as phenyl and other carbon radicals) attack electron-deficient sites [74]. If two protein radicals come into close proximity they may form a new covalent cross-link with one another, although this is less likely to occur for steric reasons [20].

4.1.2 Carbonyl formation

Oxidation of protein yields an increase in carbonyl content [20, 78], which is often used as a marker of oxidative damage to proteins [86]. Carbonyl functional groups may be a result of oxidative cleavage of the peptide backbone via the α-amidation pathway [79]. However, protein oxidation can also generate carbonyl compounds

through the conversion of tryptophan residues to kynurenine or *N*-formylkynurenine [87-89], histidine to 2-oxohistidine [87, 90], lysine, arginine, and proline residues to other carbonyl derivatives such as semialdehyde [84, 91], methionine residues to methionine sulfoxide or methionine sulfone derivatives [79, 89, 92], cysteine residues to disulfide derivatives [79, 93] and cystine residues to cysteic acid [89]. Common oxidation products of amino acid residues in proteins are given in Table 4.1.

Table 4.1: Amino acid Oxidation products [77, 90, 94].

Amino acid	Oxidation products
Arginine	Glutamic semialdehyde
Cysteine	Cystine, cysteic acid
Glutamate	Oxalic acid, pyruvic acid
Histidine	2-oxo histidine, asparagine, aspartic acid
Lysine	2-aminoadiapic semialdehyde, 3-, 4- and 5- hydroxylysine
Methionine	Methionine sulfoxide, methionine sulfone
Phenylalanine	2,3-Dihydroxyphenylalanine, 2-, 3-, and 4-hydroxyphenylalanine
Proline	2-Pyrrolidone, 4- and 5-hydroxyproline pyroglutamic acid, glutamic semialdehyde
Threonine	2-Amino-3-ketobutyric acid
Tryptophan	2-, 4-, 5-, 6- and 7-hydroxytryptophan, nitrotryptophan, 3-hydroxykynurenine, formylkynurenine
Tyrosine	3,4-Dihidroxyphenylalanine, Tyr-Tyr cross-linkages, Tyr-O-Tyr, cross-linked nitrotyrosine

In systems containing other components, carbonyl derivatives can also be formed as a consequence of secondary reactions of some amino acid side chains with lipid oxidation products or with reducing sugars or their oxidation products [86].

The carbonyl groups of proteins generated by any one of these mechanisms, may then react with the α-amino group of lysine residues to form intra- or inter-molecular protein cross-links by formation of a Schiff base in a Maillard-type mechanism and such secondary reactions, which do not involve radicals, will be accelerated by the heat generated during oxidation [86].

4.1.3 Changes to specific classes of amino acids

There is a large variation in the rates of free radical attack by species such as the hydroxyl radical on free amino acids, ranging from $\sim 1\times10^{7}$ $dm^3mol^{-1}s^{-1}$ for Gly to $\sim 1\times10^{10}$ $dm^3mol^{-1}s^{-1}$ for Trp, His and Cys [74]. Differences in kinetics for each amino acid can be accounted for in terms of preferential attack at positions distant to deactivating groups (electron withdrawing), specifically the protonated amine group on the α-carbon or in the presence of radical stabilising groups (electron

donating) on some side chains. The deactivating effect of the protonated amine group is exerted over several bond lengths, and thus attack on hydrocarbon side chains (such is the case for Val, Leu, Ile) is skewed towards the most remote positions [74].

Presumably, the primary, secondary and tertiary structure of a protein also greatly influences the reactivity of each amino acid residue and any losses would be expected to have a dramatic effect on the final protein structure and function.

Nevertheless, most studies of hydroxyl radical oxidation of amino acids in proteins are in agreement with known rate constants for free amino acids [75]. The most susceptible being tryptophan, histidine, tyrosine and cysteine compared with most other residues. The close agreement between the reaction rates of free amino acids and those within proteins is likely to be due to the small size of the hydroxyl radical, allowing easy penetration through the tertiary and secondary structures of the protein. Alternatively, the presence of haem iron or other transition metals buried within the protein chains may also contribute to the formation of hydroxyl radicals, which react with amino acids in the immediate vicinity as described in Section 3.1 above.

Another determining factor in the selectivity of free radical attack is the presence of functional groups which can stabilise the resulting radical. For example, hydrogen abstraction occurs preferentially at positions adjacent to electron delocalising (stabilising) groups such as the hydroxy groups (in Ser and Thr), carboxyl and amide functions (in Asp, Glu, Asn, Gln), and the guanidine group in Arg [74]. The protonated amine function on the Lys side chain has a similar effect to the amine group on the α-carbon, resulting in hydrogen abstraction at positions remote from both (from the C-4 and C-5 positions) [74].

Unlike aliphatic amino acids, addition to the aromatic rings of Phe, Tyr, Trp, His, and the sulfur atoms of Met and Cyst generally take place in preference to hydrogen atom abstraction from the methylene groups. This is due to the addition reactions occurring faster, as no σ- bond breaking occurs in the rate-determining step [95] and the adduct species is stabilised by electron delocalization about the ring or to the sulfur group resulting in the hydroxy derivatives, discussed below in more detail [74, 96].

4.1.4 Aromatic and heterocyclic amino acids

Oxidation of any of the aromatic amino acids involves the sequential attack of two reactive oxygen species. Most oxidation reactions are initiated through the attack of a hydroxyl radical on any of the aromatic carbons, proceeding through a radical intermediate. For phenylalanine and tyrosine, the first radical attack is an addition to form the radical intermediate, followed by abstraction of a hydrogen atom from the aromatic carbon atom by the second radical, forming the oxidised product [96] (Figure 4.6A). Alternatively but to a lesser extent, the abstraction of a hydrogen atom from the aromatic group on the amino acid may also take place (Figure 4.6B).

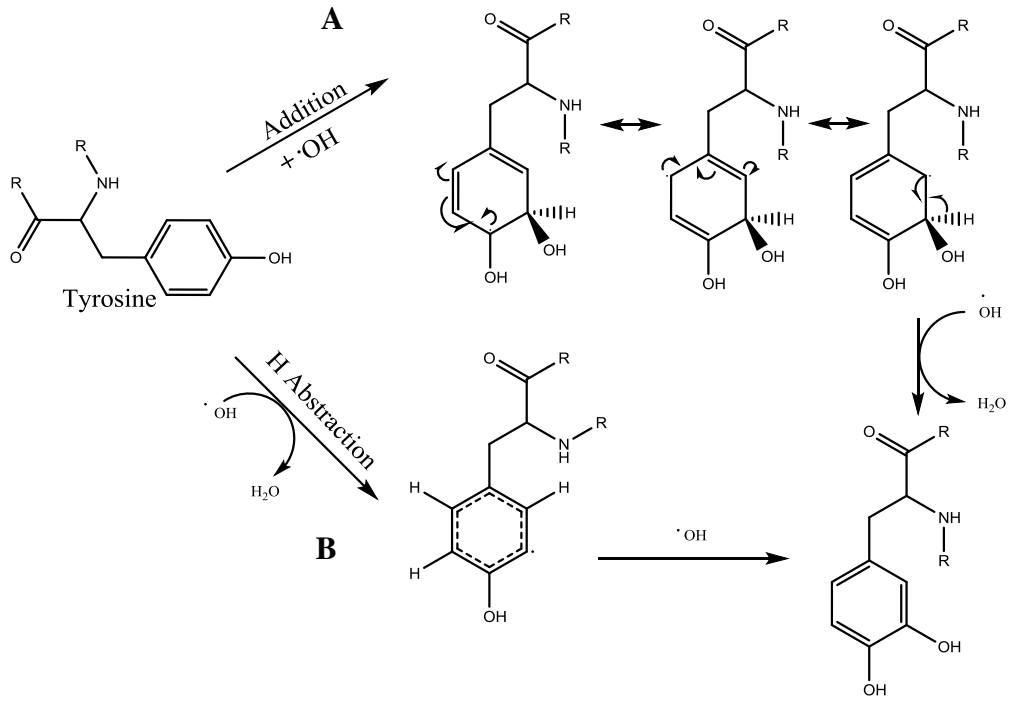

Figure 4.6: Reaction of aromatic amino acid with hydroxyl radicals. A: Hydroxyl addition reaction followed by hydrogen abstraction, B: Hydrogen abstraction followed by hydroxyl addition [96].

A computational study [96] indicates that for phenylalanine and tyrosine, radical intermediates which are formed after the addition of the hydroxyl radical onto any of aromatic positions (Figure 4.6A) are ~12 kcal mol-1 more stable than intermediates formed from hydrogen abstraction (Figure 4.6B); predicting that the first radical attack is an addition, forming the radical intermediate and that the second radical abstracts a hydrogen atom from the carbon atom, forming the oxidised product [96]. This study also indicated that the most stable radical intermediates for Phe and Tyr would form from the abstraction from the aliphatic

β-carbon (not addition to the aromatic ring), owing to the fact that aromaticity is maintained and allowing the radical to be stabilised by its delocalisation over the aromatic ring. However, when the second radical eliminates the hydrogen atom from the intermediate radical adduct, which is shown in Figure 4.6A, the aromaticity in the structure is recovered.

Thus, oxidation at any position on the aromatic ring results in products which are more stable than the oxidation of the aliphatic β-carbon [96], in agreement with the experimentally observed oxidation products for Phe and Tyr [74, 80]. Phenylalanine residues are oxidised to *ortho*- and *meta*-tyrosine derivatives (Figure 4.7) [80], tyrosine residues are converted to the 3,4-dihydroxy derivative and also to bityrosine cross-linked derivatives (Figure 4.8) [75, 89, 97-99].

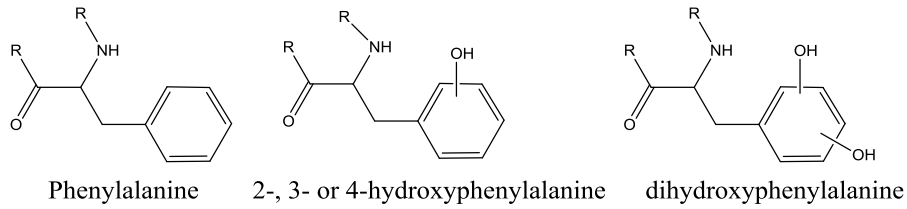

Figure 4.7: Oxidation products of phenylalanine commonly occurring in oxidised proteins 2, 3- or 4-hydroxyphenylalanine and dihydroxyphenylalanine derivatives.

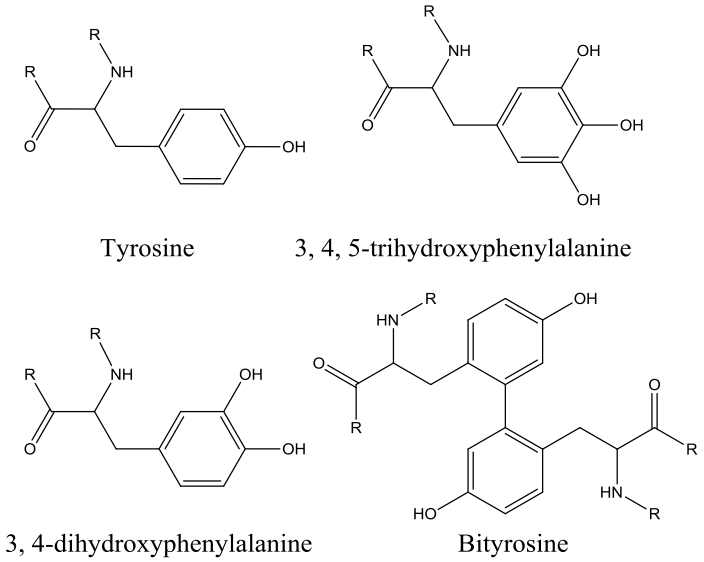

Figure 4.8: Oxidation products of tyrosine commonly occurring in oxidised proteins includes 3,4-dihydroxyphenylalanine, 3,4,5-trihydroxyphenylalanine and bityrosine.

The reaction of a hydroxyl radical with tryptophan is more complex due to the presence of an indole group. However, the reaction involving the addition of the hydroxyl radical to the aromatic group, forming the radical adduct, followed by

hydrogen abstraction is favoured [96]. Further, two additional atoms in the pyrrole ring are also open to radical attack; the C8 atom and abstraction from the N atom which are considered more stable than those that are formed by the addition on to the aromatic ring carbon atoms (Figure 4.9). Typical oxidation products of tryptophan include 2-, 4-, 5-, 6-, or 7- hydroxy derivatives and also *N*-formylkynurenine and kynurenine [87-89].

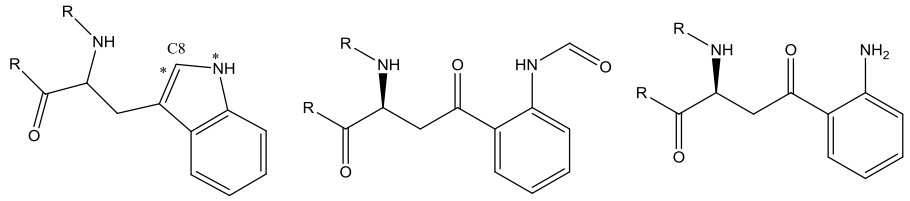

Tryptophan *N*-formylkynurenine Kynurenine

Figure 4.9: Tryptophan residue and positions on indole ring susceptible to radical attack (*), and advanced oxidation products commonly observed in proteins, *N*-formylkynurenine and kynurenine.

It is probable that the accessibility of a radical to the target amino acid is strongly influenced by the bulk of the protein [96], explaining the preference for hydroxyl radical attack at the *meta* positions of tyrosine (as the *ortho* positions are more hindered by the protein backbone). Consequently, the protein backbone is the target of radical attack with small amino acid side chains, whereas in larger residues, the reaction occurs primarily on the side chain [100].

Aromatic and heterocyclic amino acid residues are particularly vulnerable to oxidation by various forms of reactive oxygen species. The most likely radical to be formed on a protein chain is a cation radical generated on an amino acid residue with a low oxidation potential [71, 101]. For haem containing proteins, peroxide reacts with haem to form the oxoferryl ($Fe^{4+}O$) intermediate species with the generation of a radical cation, typically located on the π-system of haem, [$^{\cdot}PorFe^{4+}O$]. This π-radical is rapidly transferred to a nearby amino acid residue which has a low oxidation potential, such as tryptophan or tyrosine [71, 101]. Studies involving PAA and HP have shown that this is often the case, but varies depending on the type of protein involved and the chemical conditions.

For instance, in cytochrome c peroxidase, $PorFe^{4+}O$ coupled with a tryptophan radical cation is formed [102, 103], whereas for other haem proteins and enzymes such as myoglobin [104], bovine catalase [105], turnip peroxidase [106] or catalase peroxidases [107] tyrosyl or tryptophanyl radicals are formed. In the case of

cytochrome c, above pH 7 an oxoferrylHb π-cation radical ($\cdot PorFe^{4+}O$) forms, whereas at acidic pH, $PorFe^{4+}O$ and tyrosyl radical is formed (from the π-cation radical shifting to the tyrosine residue) [101].

Eventually such species become deprotonated and transformed into a neutral radical [71] or are terminated after attacking an electron rich site. Thus, addition of atoms to the aromatic rings of phenylalanine, tyrosine, tryptophan and histidine, and the sulfur atoms of methionine and cystine predominates over abstraction from the methylene (-CH_2-) groups in the protein backbone [74].

Tyrosyl radicals are also produced from hydrogen abstraction on the aromatic ring by the hydroxyl radical. Another common reaction for these tyrosyl radicals involves reacting with nearby tyrosyl radicals (or with tyrosine) to form stable biphenolic compounds. The 2,2'-biphenol, bityrosine, appears to be the major product [75]. Little or no bityrosine is produced by exposure to $O_2^{\cdot-}$ alone or in the presence of hydroxyl radical scavengers [75] and in the case of red blood cells, bityrosine is formed during oxidation with hydrogen peroxide [99], thus it seems that bityrosine formation occurs only during reaction with hydroxyl radicals.

Histidine is particularly good at chelating metal ions, often forming metal binding sites in proteins (such as haemoglobin). This characteristic may explain why histidine is particularly sensitive to metal catalysed oxidation reactions, in which Fenton chemistry can take place resulting in high concentrations of ROS in close proximity to reactive sites [108]. Metal catalysed oxidation of histidine produces 2-oxohistidine (Figure 4.10), which is able to undergo further oxidation to generate open-ring products such as aspartate and asparagine [87, 90].

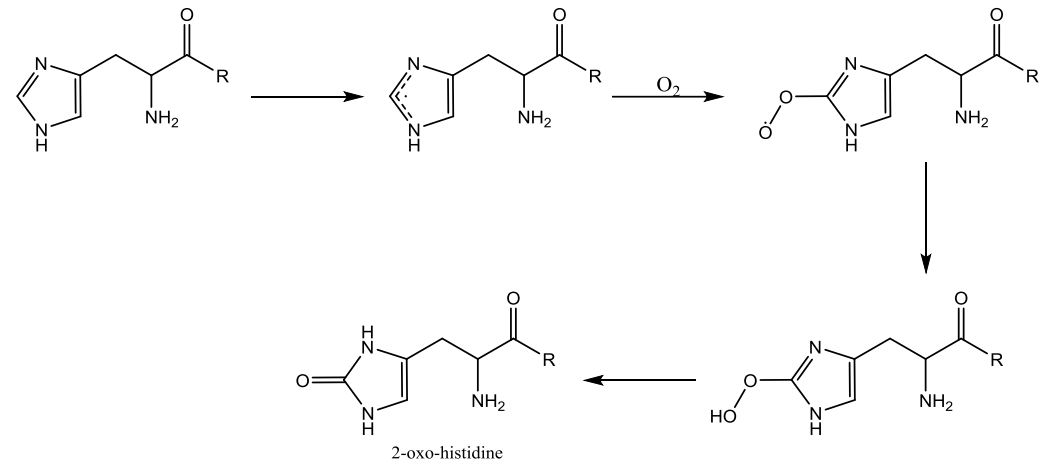

Figure 4.10: Oxidation of histidine to form 2-oxohistidine [87, 90].

4.2 Sulfur containing amino acids

Cysteine, cystine and methionine are particularly sensitive to reactive oxygen species due to their electron rich sulfur atoms. One electron oxidation of cysteine with radical oxidants can generate thiyl radicals.

$$RSH + {}^{\bullet}OH \longrightarrow RS^{\bullet} + H_2O$$

These species have two major pathways: reaction with other thiol/thiolate to form disulfide, or reaction with O_2 to generate thiyl peroxyl radicals ($RSOO^{\cdot}$) [109].

4.2.1 Methionine

Methionine residues are sensitive to oxidation by a large variety of reactive oxygen species. Ozone [89, 110], hydrogen peroxide [111], alkyl peroxides [112], hypochlorous acid [20, 92], metal catalysed reactions [113] and ionising radiations [79] have all been shown to convert methionine residues in proteins to methionine sulfoxide derivatives. The major product from methionine oxidation is sulfoxide, which can be further oxidised to sulfone [92].

4.2.2 Cysteine

The two electron oxidation of cysteine can result in the formation of cysteine sulfenic acid (CysSOH), cysteine sulfinic acid ($CysSO_2H$), and cysteine sulfonic acid ($CysSO_3H$) [79]. These species are unstable and can yield oxyacids by hydrolysis reactions or disulfide bonds by reacting with another thiol group [109].

Hydrogen peroxide oxidation of the protein thiol group forms the sulfenic acid derivative (RSOH) which is considered repairable through the addition of excess cysteine or other thiols:

$$RSOH + 'RSH \longrightarrow RSSR' + H_2O$$
$$RSSR' + "RSH \longrightarrow RSH + "RSSR'$$

Oxidation of the free thiol (SH) groups in cysteine residues can occur, leading to the formation of an inter- or intramolecular disulfide bond, or monomolecular products such as cysteine sulfenic acid, cysteine sulfininc acid and cysteine sulfonic acid [114]. In the absence of metal ions, at low HP concentration the oxidation of cysteine occurs as a two-step nucleophilic reaction generating cystine.

In this reaction the rate determining step is the reaction of the thiolate anion with a neutral HP molecule to form sulfenic acid as an intermediate [115]. At high HP concentration, the percentage of disulfide formation declines as new reaction pathways begin to consume cysteine sulfenic acid, leading to formation of cysteine sulfonic acid [115].

4.2.3 Cystine

Oxidation of cystine bonds also occurs during hydrogen peroxide bleaching of hair. The primary component of hair is the protein keratin, which is highly crosslinked by the amino acid cysteine (forming cystine). Under acidic conditions oxidation results in the formation of several intermediate products, some of which are unstable. Oxidation of wool with hydrogen peroxide or peracetic acid led to no formation of Bunte salt (cysteine-*S*-sulfonate , $RSSO_3^-$) [39].

There are two proposed mechanisms by which cystine disulfide bonds may be broken: S-S scission or C-S scission [116]. In both cases the main end-product is cysteine sulfonic acid (IX, Figure 4.11), more commonly referred to as cysteic acid. The oxidation of the crosslinked cystine groups in protein results in the formation of cystine monoxide ($Cys-SO-S-Cys$, II), cystine dioxide ($Cys-SO_2-S-Cys$ and $Cys-SO-SO-Cys$, III and IV) and cysteine sulfonic acid ($Cys-SO_3H$, IX) as well as cysteine-*S*-sulfonate ($Cys-SO_3M$).

Photooxidation of proteins is associated with the formation of cysteine-*S*-sulfonate ($RSSO_3^-$) [117] which is also formed during alkaline oxidation using permanganate

or hydrogen peroxide [118], as well as hypochlorite and persulfate [39, 116]. Although it has not been reported to occur in wool exposed to hydrogen peroxide or peracetic acid [39], it has been suggested to occur in wool exposed to boiling HP [119] and upon bleaching hair with HP [120]. The generation of cysteine-*S*-sulfonic acid appears to be particularly pH sensitive, and its formation in acidic media may be quickly followed by its interaction with other products [116].

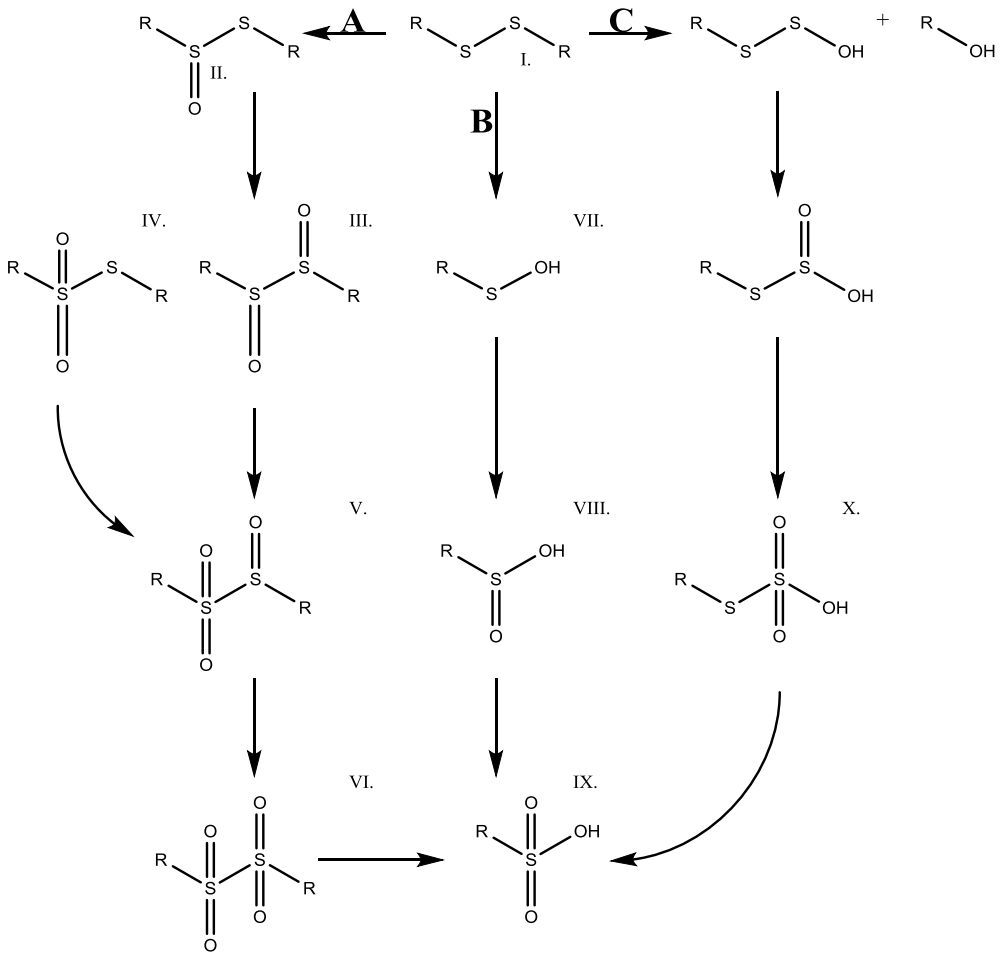

Figure 4.11: Reaction scheme for the oxidation of cysteine. Pathways A and B occur via S–S scission and pathway C through C–S scission. Compound I: Cystine, II: cystine monoxide, III, cystine dioxide, IV: cystine *S*, *S*-dioxide, V: cystine trioxide, VI: cystine tetraoxide, VII: cysteine sulfenic acid, VIII: cysteine sulfinic acid, IX: cysteine sulfonic acid (cysteic acid), X: cysteine-*S*-sulfonic acid. Reprinted from The Chemistry of Organic Sulfur Compounds, H. Tilles, Chapter 15 Oxidation of Disulfides, with Special Reference to Cystine, Pages No. 367-402 ref [116]. Copyright (1966), with permission from Elsevier.

5 Chain architecture, secondary structure and material properties

Proteins behave analogously to conventional synthetic polymers, with the mechanical properties of protein-based materials being defined by the same principles of chain architecture which govern the properties of other polymers [121, 122].

For a polymer to be processed into a thermoplastic, there must be sufficient chain mobility at the applied temperature and pressure for existing chemical interactions to be replaced by new stabilising interactions after processing (e.g. extrusion). Polymer stability is brought about by a combination of van der Waal's, hydrophobic and electrostatic interactions, as well as hydrogen and covalent bonding between nearby chains. Some of these interactions may be reduced through the addition of processing aids, but for the material to be processed the interactions must be overcome through the application of additional thermal energy. For crystalline regions, the temperature must be in excess of its melting point and for amorphous regions, above that of its glass transition temperature (T_g) [121].

5.1 Factors influencing chain mobility

The glass transition temperature is related to the co-operative movement (rotation and vibration) of relatively large chain segments. At temperatures below the T_g (glassy state), the chain segments remain fixed in position with atoms undergoing only low-amplitude vibratory motion about these positions. With increasing temperature, the amplitude of these vibrations becomes greater, overcoming some of the secondary intermolecular bonding forces. At the glass transition temperature, enough of the polymer chains have sufficient energy to undergo rotational and translational motion (large-scale co-operative motion); the position of the T_g being defined by components of chain architecture (any chemical characteristic which affects overall chain mobility) [123]:

- backbone flexibility, branching and symmetry
- inter-polymer attractive forces
- chain regularity and crystallinity
- molecular weight and molecular weight distribution
- Free volume

Flexibility of the polymer backbone greatly influences the overall mobility of the polymer. Free rotation of the σ-bonds comprising the polymer backbone can occur easily provided there are no sterically hindering branching groups or groups within the backbone that impart rigidity (aromatics). However, as sterically hindering groups are positioned further away from the backbone, they have a lesser impact on the glass transition temperature.

Bulky and high mass branching groups result in an increase in T_g as they reduce torsion about the σ-bonds in the polymer backbone. Similarly, the inclusion of aromatic groups within the repeating unit causes chain stiffening [124], typically resulting in brittle materials (materials with a high T_g) [125]. Asymmetric repeating units require a larger sweep volume for rotation about the backbone and accordingly more energy, consequently increasing the T_g [123].

The involvement of inter-chain attractive forces such as van der Waal's, hydrophobic and electrostatic interactions and hydrogen bonding and covalent crosslinking also increase the glass transition temperature.

For polymers with small side groups or regularly repeating units these interactions allow chain segments to pack into crystalline regions, which increase the glass transition temperature of the amorphous regions trapped between crystalline regions (semi-crystalline polymer). Crystalline regions act like a covalent crosslink within the polymer backbone, leading to chain stiffening of the amorphous regions in between, thereby increasing the observed T_g [123].

Molecular weight and molecular weight distribution greatly influence polymer mobility. As larger molecules require more energy to move, a polymer's T_g increases with increasing average molecular weight [126]. Similarly, the distribution of molecular weights present in the considered polymer produces the range of observed glass transition temperatures.

Another factor which influences the glass transition temperature is the polymer's free volume. Polymers with large branching groups attached have variations in density that vary depending on the regularity of the branched group. The regularity of a polymer chain determines the extent to which close packing of inter-polymer chains can occur. Decreased chain regularity would be accompanied by an increase in free volume, facilitating a greater range of motion, with a corresponding lower

glass transition temperature [126]. Further, lower molecular weight polymers have an increased number of chain ends (per volume), also increasing free volume between adjacent chains, consequently reducing T_g.

5.2 Proteins as a feedstock for thermoplastics

Proteins are complex hetero-polymers, comprised of up to 20 different amino acid monomers. The polymer backbone is made up of a repeating unit that contains a nitrogen and two carbons atoms and a differing branched functional group. Historically, proteins have been used to produce thermosetting plastics by shaping the material using a combination of heat and pressure, followed by a crosslinking (curing) process to impart strength to the material. Proteins have many reactive functional groups, and crosslinking can be achieved through the reaction of the protein with tannic acid, chromic acid, or formaldehyde, or by through the covalent bonding of nearby cysteine residues to form a disulfide bridge [127-129]. However, for the purpose of filming or injection moulding parts, thermoplastic behaviour is essential [122].

Protein chain mobility is influenced by its molecular weight, backbone flexibility and secondary structure components. Variation in the branching amino acid side chains leads to a large array of attractive and repulsive forces which influences polymer stability, folding and secondary structure formation. Further, the branched side chains depending on their size (steric hindrance) may prevent torsional movement about the backbone and along with potential covalent crosslinks may result in chain stiffening. The presence of covalent crosslinks, molecular interactions, bulky branching groups and ordered secondary structures would be expected to increase the T_g (Figure 5.1) [130].

In many ways, protein-based thermoplastics are similar in chemical composition and physical properties (and are subject to the same challenges) to synthetic polyamides, particularly nylon 6,6. Due to the high degree of hydrogen bonding interactions between nearby amide groups, proteins exhibit regions containing ordered structures such as α-helices and β-sheets [132]; similarly, the regular spacing of the amide groups in the backbone of nylons allows for multiple hydrogen bonds to form between adjacent strands, observed as stacked sheets of planar hydrogen bonded chain segments and resulting in a high degree of order [133].

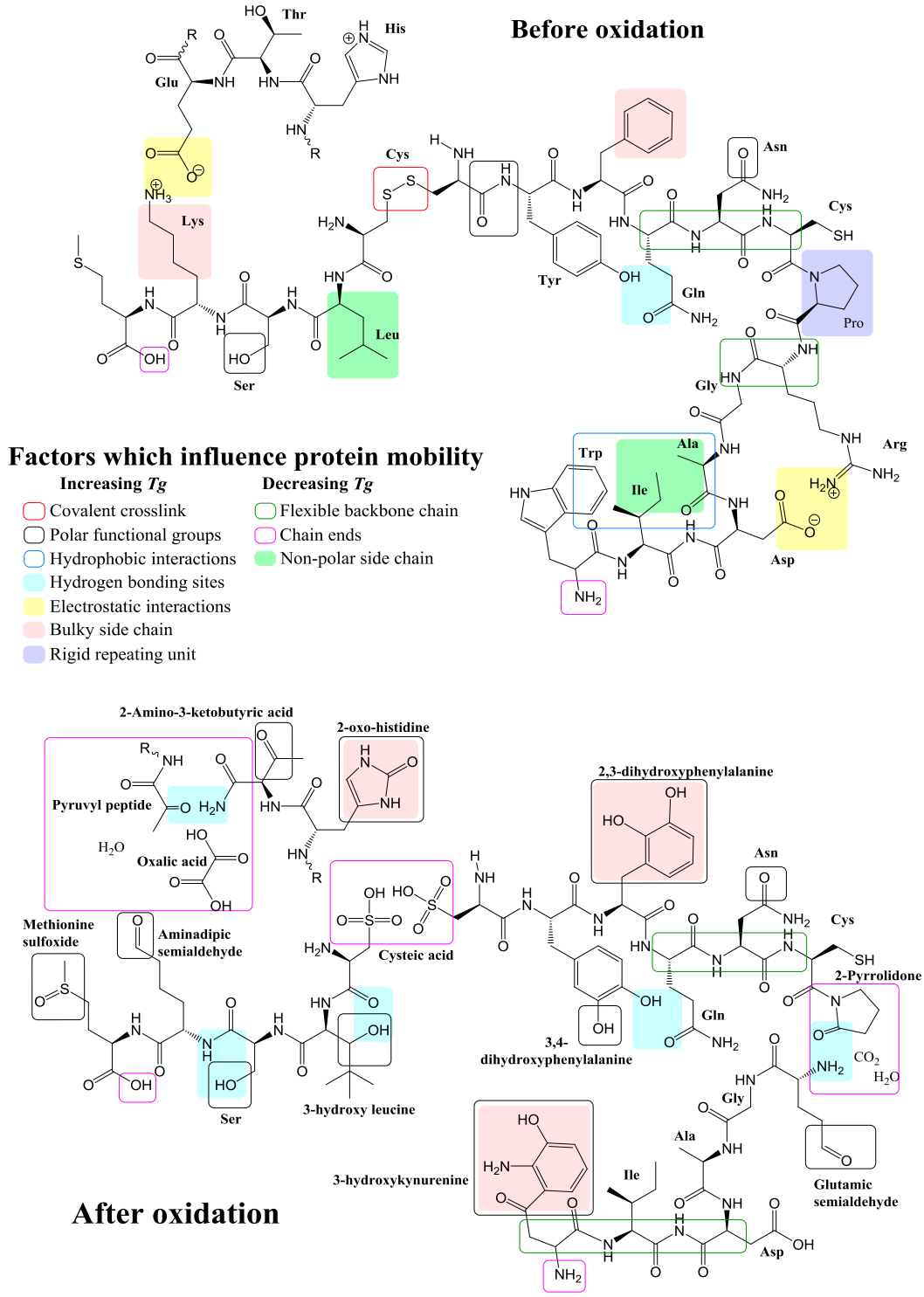

Figure 5.1: Factors which influence glass transition (polymer mobility) and their occurrence in proteins [131]. Top: Prior to oxidation, typical inter- and intramolecular interactions are illustrated between Protein A and B. Only a small segment of Protein A is illustrated, where R_x and R_y are differing polypeptide chains. Protein B is represented by a short sequence of amino acids. In reality, proteins are much larger than those illustrated above, involved in a complex variety of a larger number of interactions. Bottom: After oxidation, proteins may show reduced molecular weight, an increased number of chain ends and a larger number of carbonyl and hydroxyl groups.

In nylon 6,6 the amide groups are orientated in alternating directions, leading to strong hydrogen bonding interactions and the formation of parallel strands, which can form β-pleated sheets (similar to those observed in silk fibroin and β-keratins) [134]. In the case of nylon 6, (resulting from the polymerisation of caprolactam), all of the amide groups are oriented in the same direction along the chain, leading to weaker hydrogen bonding interactions between sheets, and yielding mixed directionalities. The alternating orientation of the amide group in nylon 6,6 allows for better hydrogen bonding, and consequently melts at a higher temperature compared to nylon 6 [135].

Although the mobility of the protein increases with increasing temperature, their glass transition and melting temperatures typically exceed the temperature at which degradation occurs [136]. Consequently, the use of plasticisers or other processing aids to improve chain mobility are required to prevent protein degradation and increase processability [121, 137].

Changes in protein chain mobility would be expected to accompany any modification of the comprising amino acid side chains, molecular weight and molecular weight distribution, as well as secondary structure caused by oxidation. An increase in the number of functional groups which are capable of hydrogen bonding is expected after oxidation, to be accompanied by an increase in T_g. However, oxidation may also increase free volume through the cleavage of the protein backbone and covalent crosslinks between cysteine residues and additionally overcoming hydrophobic interactions, causing a reduction in T_g.

5.3 Secondary structure

The secondary structural components of proteins, helices, sheets, turns and coils are also modified by oxidation [138, 139]. Most amino acids show a propensity to form only one particular type of secondary structure (Table 5.1) [140], however, the periodicity and positioning of polar and non-polar residues in the amino acid sequence has a greater influence on the final secondary structure [141].

The sensitivity of particular amino acid residues to oxidation has been shown to vary between proteins and results from their position and interaction within the protein structure [142]. Selective oxidation of certain amino acids may then

influence the formation of specific secondary structures by changing the ability to form H-bonds between C=O and NH groups.

Table 5.1: Propensity of amino acids for secondary structure types [140, 143-145].

Helical	Sheet	Other
Alanine	Isoleucine	Glycine
Leucine	Phenylalanine	Proline
Methionine	Tryptophan	Asparagine
Glutamine	Valine	Aspartic acid
Glutamic acid	Tyrosine	Serine
Arginine	Threonine	Histidine
Lysine	Cysteine	

Oxidation of amino acids increases in local flexibility or rigidity in the protein chain, leading to an alteration in secondary structure [110, 138], directly influencing its physical and material properties [131, 146-151]. Consequently, protein oxidation may negatively impact the properties and processing characteristics of protein-based thermoplastics.

Modification of the amino acid residues, including complete cleavage of the amino acid side chain from the protein backbone, may result in less participation in stabilising interactions. Although this may increase polymer mobility through the reduction of the T_g, such changes could decrease mechanical properties such as strength, stiffness and elongation. Furthermore, protein hydrolysis/ fragmentation could result in poor consolidation due to reduced chain entanglement, and along with degradation of potential crosslinking sites (through the destruction of cysteine, tyrosine and lysine residues) could result in a material with poor mechanical properties [152].

5.4 Protein Oxidation and Material Properties

Studies of the effects of bleaching on the physical properties of wool found a linear correlation between the extent of disulfide bond oxidation and reduction in work during load extension of fibres (work to extend 20 %) [153]. Similar results have been observed after bleaching of human hair [154].

The disulfide bonds contribute greatly to the wet strength of keratin fibres, however, they do not greatly affect the strength of the dry fibres which is largely dependent on the main chain length and intermolecular hydrogen bonding [155]. After

bleaching, the mechanical properties of hair were changed significantly, observed as a linear decrease in wet-modulus with increased exposure time and virtually no change in either the dry-modulus or ultimate strength of the fibres (owing to negligible chain scission) [155]. The dry extension at break was slightly affected by bleaching, although no evidence of brittleness was observed.

A recent investigation into the oxidation of horn keratin showed that with increasing exposure time to hydrogen peroxide, it underwent a reduction in tensile strength and Young's modulus and had an increased percentage elongation at break [156]. During the oxidation of horn with hydrogen peroxide, degradation of the disulfide bond, peptide bonds or hydrogen bonding interactions led to deterioration of useful mechanical properties in horn keratin [156]. The tensile strength, Young's modulus and elongation at break of untreated samples (9 wt% moisture) were found to be 118 MPa, 1.5 GPa and 24.6% respectively [157]. After prolonged exposure to hydrogen peroxide the tensile strength and Young's modulus of the oxidised horn keratin were moderately reduced, and the elongation at break increased with extent of oxidation [156]. The strength of horn keratin is largely due to the crystalline α-helical structures, with the amorphous regions providing the horn keratin with elasticity and flexibility [158]. The reduction in tensile strength and Young's modulus is attributed to the decrease in α-helical content upon oxidation, while the increase in amorphous content is responsible for the improved elongation at break and increase in toughness (energy to break) [156].

A measure of oxidative damage in the meat industry is the Warner-Bratzler shear force test, used to measure the force required to shear muscle tissue. For fresh oyster muscle, the Warner-Bratzler value (0.43 kgf) was higher than for ozonated samples (0.402 kgf). This is supposedly a result of ozone modification of collagen and elastin, making it more susceptible to proteolysis. The intermolecular cross-links in collagen, which comprises the connective tissue of shellfish, is prone to degradation by ozone, causing undesirable textural changes in the oyster. Hence, the decreased shear strength may have been due to the denaturing and degradation of the protein by ozone [138].

One of the major issues with creating protein-based materials is overcoming some of their original physical and chemical properties in order to make them processable or acceptable to consumers. Skin generated as a by-product of processing squid and

cuttlefish has little market value, although after decolouring with hydrogen peroxide it can be used as raw material for gelatine production [159]. Gelatine film is hydrophilic, has low water vapour barrier properties and poor mechanical properties compared with conventional polymer films. Bleaching with HP resulted in several changes to the bleached gelatine films including increased thickness due to protein aggregation (and resulting inability to align proteins into a compact network), decreased tensile strength, increased elongation at break and decreased water vapour permeability (WVP). Formation of the hydroperoxyl anion, hydroperoxyl and hydroxyl radicals is thought to be responsible for observed changes including fragmentation to form peptides. The consequently reduced intermolecular interactions in the film matrix is likely to have caused the decreased tensile strength and simultaneously increased the elongation at break.

The reduced WVP of the bleached gelatine films suggest that films of gelatine extracted from skin bleached with HP at high concentration had lower hydrophilicity. This is consistent with the observed decrease in free amino and carbonyl groups present in gelatine extracted from bleached squid skin at high HP concentrations. Fewer carbonyl and amino groups would then be present to form hydrogen bonds with water molecules and to a lesser extent, resulting in a decreased hydrophilicity of the resulting films. It is thought that the hydroxyl radicals generated during bleaching might modify amino acids in such a way that it lowers the number of hydrophilic domains present in the final gelatine extracts, lowering the ability of water to migrate through the gelatine films (decreasing WVP) [159].

6 Conclusion

Protein oxidation results in many potential physical and mechanical changes as a result of changes to the primary and secondary structures. Most simply, at a primary structure level oxidation causes changes in the hydrophobic, electrostatic and hydrogen bonding interactions, along with more detrimental changes including carbonylation, hydroxylation, aggregation through the formation of new covalent bonds, crosslink cleavage, hydrolysis and chain scission. Such changes cause loss of functionality in native proteins, but also may lead to changes in solubility, hydrophilicity and susceptibility to proteolysis. Changes to molecular weight and secondary structure characteristics directly influences glass transition temperature

and thermal processing of materials. Moreover, degradation of the protein through crosslink cleavage, chain scission and hydrolysis cause reductions in mechanical properties of protein based materials such as tensile strength, Young's modulus and work during load extension.

These physical parameters often define the usefulness of a material. While efforts can be made to reintroduce structural integrity through the introduction of crosslinking agents or reinforcing fibre composites, understanding the underpinning chemistry and resulting changes to protein primary and secondary structure is the most sensible way to approach future material design for oxidised proteins.

7 References

1. Jones, C.W. (1999). Activation of Hydrogen Peroxide Using Inorganic and Organic Species, in Applications of Hydrogen Peroxide and Derivatives, Clark, J.H., Editor. The Royal Society of Chemistry: Cambridge, U.K.
2. Klenk, H., Götz, P.H., Siegmeier, R., Mayr, W. (2000). Peroxy Compounds, Organic, in Ullmann's Encyclopedia of Industrial Chemistry. Wiley-VCH Verlag GmbH & Co. KGaA: Weinheim, Germany.
3. Sanchez, J., Myers, T.N. (2000). Peroxides and Peroxide Compounds, Organic Peroxides, in Kirk-Othmer Encyclopedia of Chemical Technology. John Wiley & Sons, Inc: New York, U.S..
4. Wittcoff, H.A., Reuben, B.G., Plotkin, J.S. (2013). Industrial Organic Chemicals 3rd ed. Wiley and Sons, Inc:New Jersey, U.S.. p. 187-190.
5. Zhao, X., Zhang, T., Zhou, Y., Liu, D. (2007). Preparation of Peracetic Acid from Hydrogen Peroxide: Part I: Kinetics for Peracetic Acid Synthesis and Hydrolysis. Journal of Molecular Catalysis A: Chemical. 271(1-2): p. 246-252.
6. Goor, G. (1992). Hydrogen Peroxide: Manufacture and Industrial Use for Production of Organic Chemicals, in Catalytic Oxidations with Hydrogen Peroxide as Oxidant, Strukul, G., Editor. Springer: Netherlands. p. 13-43.
7. Heaney, H. (2001). Monoperoxyphthalic Acid, in Encyclopedia of Reagents for Organic Synthesis. John Wiley & Sons, Inc.

8. McDonald, R.N., Steppel, R.N., Dorsey, J.E. (2003). *M*-Chloroperbenzoic Acid, in Organic Syntheses. John Wiley & Sons, Inc.
9. Swern, D., Findley, T.W., Scanlan, J.T. (1944). Epoxidation of Oleic Acid, Methyl Oleate and Oleyl Alcohol with Perbenzoic Acid. Journal of the American Chemical Society. 66(11): p. 1925-1927.
10. Phillips, B., Frostick, F.C., Starcher, P.S. (1957). A New Synthesis of Peracetic Acid. Journal of the American Chemical Society. 79(22): p. 5982-5986.
11. Kolthoff, I.M., Lee, T.S., Mairs, M.A. (1947). Use of Perbenzoic Acid in Analysis of Unsaturated Compounds. I. Preparation and Stability of Solutions of Perbenzoic Acid. Journal of Polymer Science. 2(2): p. 199-205.
12. Adams, R. (1940). Organic Synthesis: An Annual Publication of Satisfactory Methods for the Preparation of Organic Chemicals. Organic Syntheses, ed. Allen, C.F.H. Vol. 20. John Wiley And Sons, Inc: London, U.K.. p 70.
13. Bach, R.D., Ayala, P.Y., Schlegel, H.B. (1996). A Reassessment of the Bond Dissociation Energies of Peroxides. An Ab Initio Study. Journal of the American Chemical Society. 118(50): p. 12758-12765.
14. Yuan, Z., Ni, Y., Van Heiningen, A.R.P. (1997). Kinetics of Peracetic Acid Decomposition: Part I: Spontaneous Decomposition at Typical Pulp Bleaching Conditions. The Canadian Journal of Chemical Engineering. 75(1): p. 37-41.
15. Yuan, Z., Ni, Y., Van Heiningen, A.R.P. (1997). Kinetics of the Peracetic Acid Decomposition: Part II: pH Effect and Alkaline Hydrolysis. The Canadian Journal of Chemical Engineering. 75(1): p. 42-47.
16. Kitis, M. (2004). Disinfection of Wastewater with Peracetic Acid: A Review. Environment International. 30(1): p. 47-55.
17. Križman, P., Kovač, F., Tavčer, P.F. (2005). Bleaching of Cotton Fabric with Peracetic Acid in the Presence of Different Activators. Coloration Technology. 121: p. 304-309.
18. Križman, P., Kovač, F., Tavčer, P.F., Hauser, P., Hinks, D. (2007). Enhanced PAA Bleaching of Cotton by Incorporating a Cationic Bleach Activator. Coloration Technology. 123(4): p. 230-236.

19. Thompson, E.O.P., O'donnell, I.J. (1959). Studies on Oxidised Wool. I. A Comparison of the Completeness of Oxidation with Peracetic and Performic Acid. Australian Journal of Biological Sciences. 12(3): p. 282-293.
20. Kerkaert, B., Mestdagh, F., Cucu, T., Aedo, P.R., Ling, S.Y., De Meulenaer, B. (2011). Hypochlorous and Peracetic Acid Induced Oxidation of Dairy Proteins. Journal of Agricultural and Food Chemistry. 59(3): p. 907-14.
21. Koivunen, J., Heinonen-Tanski, H. (2005). Peracetic Acid (PAA) Disinfection of Primary, Secondary and Tertiary Treated Municipal Wastewaters. Water Research. 39(18): p. 4445-4453.
22. A. Low., J. Verbeek., M. Lay., J. Swan. (2012). Decoloring Hemoglobin as a Feedstock for Second Generation Bioplastics. Preparative Biochemistry and Biotechnology. 42(1): p. 29-43.
23. Yuan, Z., D'Entremont, M., Ni, Y., Van Heiningen, A.R.P. (1998). The Formation of Gaseous Products and Its Relation to Pulp Bleaching During the Peracetic Acid Treatment. Journal of Wood Chemistry and Technology. 18(3): p. 267-288.
24. Bauermeister, L.J., Bowers, J.W.J., Townsend, J.C., McKee, S.R. (2008). The Microbial and Quality Properties of Poultry Carcasses Treated with Peracetic Acid as an Antimicrobial Treatment. Poultry Science. 87(11): p. 2390-2398.
25. Rossoni, E.M.M., Gaylarde, C.C. (2000). Comparison of Sodium Hypochlorite and Peracetic Acid as Sanitising Agents for Stainless Steel Food Processing Surfaces Using Epifluorescence Microscopy. International Journal of Food Microbiology. 61(1): p. 81-85.
26. Silveira, A.C., Conesa, A., Aguayo, E., Artes, F. (2008). Alternative Sanitizers to Chlorine for Use on Fresh-Cut "Galia" (*Cucumis melo var. catalupensis*) Melon. Journal of Food Science. 73(9): p. M405-M411.
27. Dell'Erba, A., Falsanisi, D., Liberti, L., Notarnicola, M., Santoro, D. (2007). Disinfection By-Products Formation During Wastewater Disinfection with Peracetic Acid. Desalination. 215(1–3): p. 177-186.
28. Voukkali, I., Zorpas, A.A. (2014). Disinfection Methods and By-Products Formation. Desalination and Water Treatment. p. 1-12.

29. Verbeek, C.J.R., Lay, M.C., Low, A.W.K. (2013). Methods of Manufacturing Plastic Materials from Decolorized Blood Protein. (US 13/691,438).
30. Stein, H.H., Guarnaccio, J. (1959). Infrared Study of Oxidized Keratin. Textile Research Journal. 29(6): p. 492-496.
31. Weston, G.J. (1955). The Infra-Red Spectrum of Peracetic Acid-Treated Wool. Biochimica et Biophysica Acta. 17(0): p. 462-464.
32. Abdel-Halim, E.S., Al-Deyab, S.S. (2011). Low Temperature Bleaching of Cotton Cellulose Using Peracetic Acid. Carbohydrate Polymers. 86(2): p. 988-994.
33. Shafie, A.E., Fouda, M.M.G., Hashem, M. (2009). One-Step Process for Bio-Scouring and Peracetic Acid Bleaching of Cotton Fabric. Carbohydrate Polymers. 78(2): p. 302-308.
34. Cai, Y., David, S.K. (1997). Low Temperature Bleaching of Jute Fabric Using a Peracetic Acid System. Textile Research Journal. 67(6): p. 459-464.
35. Cardamone, J.M., Marmer, W.N. (1995). The Whitening of Textiles, in Chemistry of the Textiles Industry, Carr, C.M., Editor. Blackie Academic & Professional: Glasgow, Scotland. p. 46-101.
36. Chesner, L., Woodford, G.C. (1958). Some Aspects of Bleaching with Hydrogen Peroxide and with Peracetic Acid. Journal of the Society of Dyers and Colourists. 74(7): p. 531-542.
37. Hickman, W.S. (2002). Peracetic Acid and Its Use in Fibre Bleaching. Review of Progress in Coloration and Related Topics. 32(1): p. 13-27.
38. Karmakar, S.R. (1999). Chemical Technology in the Pre-Treatement Processes of Textiles. Textile Science and Technology. Elsevier: Amsterdam, Netherlands.
39. Denning, R.J., Freeland, G.N., Guise, G.B., Hudson, A.H. (1994). Reaction of Wool with Permonosulfate and Related Oxidants. Textile Research Journal. 64(7): p. 413-422.
40. Kadla, J.F., Chang, H. (2001). The Reactions of Peroxides with Lignin and Lignin Model Compounds, in Oxidative Delignification Chemistry. American Chemical Society. p. 108-129.

41. Kham, L., Le Bigot, Y., Delmas, M., Avignon, G. (2005). Delignification of Wheat Straw Using a Mixture of Carboxylic Acids and Peroxoacids. Industrial Crops and Products. 21(1): p. 9-15.
42. Kumar, R., Hu, F., Hubbell, C.A., Ragauskas, A.J., Wyman, C.E. (2013). Comparison of Laboratory Delignification Methods, Their Selectivity, and Impacts on Physiochemical Characteristics of Cellulosic Biomass. Bioresource Technology. 130(0): p. 372-381.
43. Sun, R.C., Tomkinson, J., Zhu, W., Wang, S.Q. (2000). Delignification of Maize Stems by Peroxymonosulfuric Acid, Peroxyformic Acid, Peracetic Acid, and Hydrogen Peroxide. 1. Physicochemical and Structural Characterization of the Solubilized Lignins. Journal of Agricultural and Food Chemistry. 48(4): p. 1253-62.
44. Zhao, X., Wu, R., Liu, D. (2011). Production of Pulp, Ethanol and Lignin from Sugarcane Bagasse by Alkali-Peracetic Acid Delignification. Biomass and Bioenergy. 35(7): p. 2874-2882.
45. Jiménez, L., Ramos, E., De la Torre, M.J., Pérez, I., Ferrer, J.L. (2008). Bleaching of Soda Pulp of Fibres of *Musa textilis Nee* (Abaca) with Peracetic Acid. Bioresource Technology. 99(5): p. 1474-1480.46. Z. Yuan Peracetic Acid Brightening of Softwood Kraft Pulp, in Chemical Engineering. (1997). New Brunswick: Fredericton.
46. Yuan, Z. (1997). Peracetic Acid Brightening of Softwood Kraft Pulp. Chemical Engineering. PhD. University of New Brunswick: Fredericton, Canada.
47. Findley, T.W., Swern, D., Scanlan, J.T. (1945). Epoxidation of Unsaturated Fatty Materials with Peracetic Acid in Glacial Acetic Acid Solution. Journal of the American Chemical Society. 67(3): p. 412-414.
48. Gelling, I.R. (1985). Modification of Natural Rubber Latex with Peracetic Acid. Rubber Chemistry and Technology. 58(1): p. 86-96.
49. Greenspan, F.P. (1947). Oxidation Reactions with Aliphatic Peracids. Industrial & Engineering Chemistry. 39(7): p. 847-848.
50. Swern, D. (2004). Epoxidation and Hydroxylation of Ethylenic Compounds with Organic Peracids, in Organic Reactions. John Wiley & Sons, Inc: New York, U.S..

51. Swern, D., Billen, G.N., Findley, T.W., Scanlan, J.T. (1945). Hydroxylation of Monounsaturated Fatty Materials with Hydrogen Peroxide. Journal of the American Chemical Society. 67(10): p. 1786-1789.
52. Bianchini, R., Calucci, L., Caretti, C., Lubello, C., Pinzino, C., Piscicelli, M. (2002). An EPR Study on Wastewater Disinfection by Peracetic Acid, Hydrogen Peroxide and UV Irradiation. Annali di Chimica. 92(9): p. 783-93.
53. Caretti, C., Lubello, C. (2003). Wastewater Disinfection with PAA and UV Combined Treatment: A Pilot Plant Study. Water Research. 37(10): p. 2365-2371.
54. Liberti, L., Lopez, A., Notarnicola, M., Barnea, N., Pedahzur, R., Fattal, B. Comparison of Advanced Disinfecting Methods for Municipal Wastewater Reuse in Agriculture. Water Science and Technology, 2000. **42**: p. 215-220.
55. Veschetti, E., Cutilli, D., Bonadonna, L., Briancesco, R., Martini, C., Cecchini, G., Anastasi, P., Ottaviani, M. (2003). Pilot-Plant Comparative Study of Peracetic Acid and Sodium Hypochlorite Wastewater Disinfection. Water Research. 37(1): p. 78-94.
56. Mattle, M.J., Crouzy, B., Brennecke, M., Wigginton, K.R., Perona, P., Kohn, T. (2011). Impact of Virus Aggregation on Inactivation by Peracetic Acid and Implications for Other Disinfectants. Environmental Science & Technology. 45(18): p. 7710-7.
57. Favero, M.S., Bond, W.W. (2001). Chemical Disinfection of Medical and Surgical Materials, in Disinfection, Sterilization and Preservation, Block, S.S., Editor. Lippincott Williams and Wilkins: Philadelphia, U.S.. p. 881-918.
58. Malchesky, P.S. (1993). Peracetic Acid and Its Application to Medical Instrument Sterilization. Artificial Organs. 17(3): p. 147-152.
59. Kampf, G., Bloss, R., Martiny, H. (2004). Surface Fixation of Dried Blood by Glutaraldehyde and Peracetic Acid. Journal of Hospital Infection. 57(2): p. 139-143.
60. Rangarajan, B., Havey, A., Grulke, E., Culnan, P. (1995). Kinetic Parameters of a Two-Phase Model for In Situ Epoxidation of Soybean Oil. Journal of American Oil Chemists' Society. 72(10): p. 1161-1169.

61. FMC Corporation. (2006). Material Safety Data Sheet: Peracetic Acid 5%. FMC Corporation.
62. Dul'neva, L.V., Moskvin, A.V. (2005). Kinetics of Formation of Peroxyacetic Acid. Russian Journal of General Chemistry. 75(7): p. 1125-1130.
63. Peragen Systems (2004). Aq-PAAa™ - Peracetic Acid in Water: Product Information. Peragen Systems, LLC.
64. Zhao, X., Cheng, K., Hao, J., Liu, D. (2008). Preparation of Peracetic Acid from Hydrogen Peroxide, Part II: Kinetics for Spontaneous Decomposition of Peracetic Acid in the Liquid Phase. Journal of Molecular Catalysis A: Chemical. 284(1-2): p. 58-68.
65. Rokhina, E.V., Makarova, K., Golovina, E.A., van As, H., Virkutyte, J. (2010). Free Radical Reaction Pathway, Thermochemistry of Peracetic Acid Homolysis, and Its Application for Phenol Degradation: Spectroscopic Study and Quantum Chemistry Calculations. Environmental Science and Technology. 44(17): p. 6815-6821
66. Block, S.S. (2001). Peroxygen Compounds, in Disinfection, Sterilization and Preservation, Block, S.S., Editor. Lippincott Williams and Wilkins: Philadelphia, U.S.. p. 185-204.
67. Sharma, B.K. (1981). Spectroscopy. Krishna Prakashan Media: Uttar Pradesh, India.
68. Tavcer, P.F., Krizman, P. (2003). Bleaching of Cotton Fibres for Sanitary Products with Peracetic Acid. Tekstil. 52(7): p. 309.
69. Kanias, T., Acker, J.P. (2010). Biopreservation of Red Blood Cells: The Struggle with Hemoglobin Oxidation. FEBS Journal. 277(2): p. 343-356.
70. Nagababu, E., Rifkind, J.M. (2000). Reaction of Hydrogen Peroxide with Ferrylhemoglobin: Superoxide Production and Heme Degradation. Biochemistry. 39(40): p. 12503-12511.
71. Svistunenko, D.A. (2005). Reaction of Haem Containing Proteins and Enzymes with Hydroperoxides: The Radical View. Biochimica et Biophysica Acta (BBA) - Bioenergetics. 1707(1): p. 127-155.
72. Winterbourn, C.C. (1985). Free-Radical Production and Oxidative Reactions of Hemoglobin. Environmental Health Perspectives. 64: p. 321-330.

73. Reeder, B.J., Wilson, M.T. (2001). The Effects of pH on the Mechanism of Hydrogen Peroxide and Lipid Hydroperoxide Consumption by Myoglobin: A Role for the Protonated Ferryl Species. Free Radical Biology and Medicine. 30(11): p. 1311-8.

74. Hawkins, C.L., Davies, M.J. (2001). Generation and Propagation of Radical Reactions on Proteins. Biochimica et Biophysica Acta (BBA) - Bioenergetics. 1504(2-3): p. 196-219.

75. Davies, K.J., Delsignore, M.E. (1987). Protein Damage and Degradation by Oxygen Radicals. III. Modification of Secondary and Tertiary Structure. Journal of Biological Chemistry. 262(20): p. 9908-13.

76. Gebicki, S., Gebicki, J.M. (1993). Formation of Peroxides in Amino Acids and Proteins Exposed to Oxygen Free Radicals. Biochemical Journal. 289 (Pt 3): p. 743-749.

77. Headlam, H.A., Davies, M.J. (2002). Beta-Scission of Side-Chain Alkoxyl Radicals on Peptides and Proteins Results in the Loss of Side-Chains as Aldehydes and Ketones. Free Radical Biology and Medicine. 32(11): p. 1171-1184.

78. Headlam, H.A., Davies, M.J. (2004). Markers of Protein Oxidation: Different Oxidants Give Rise to Variable Yields of Bound and Released Carbonyl Products. Free Radical Biology and Medicine. 36(9): p. 1175-1184.

79. Garrison, W.M. (1987). Reaction Mechanisms in the Radiolysis of Peptides, Polypeptides, and Proteins. Chemical Reviews. 87(2): p. 381-398.

80. Stadtman, E.R., Levine, R.L. (2003). Free Radical-Mediated Oxidation of Free Amino Acids and Amino Acid Residues in Proteins. Amino Acids. 25(3): p. 207-218.

81. Davies, M.J. (2005). The Oxidative Environment and Protein Damage. Biochimica et Biophysica Acta (BBA) - Proteins and Proteomics. 1703(2): p. 93-109.

82. Davies, M.J. (1996). Protein and Peptide Alkoxyl Radicals Can Give Rise to C-Terminal Decarboxylation and Backbone Cleavage. Archives of Biochemistry and Biophysics. 336(1): p. 163-172.

83. Swallow, A.J., Charlesby, A. (2013). Radiation Chemistry of Organic Compounds. International Series of Monographs on Radiation Effects in Materials. Pergamon Press: Oxford, U.K..
84. Uchida, K., Kato, Y., Kawakishi, S. (1990) A Novel Mechanism for Oxidative Cleavage of Prolyl Peptides Induced by the Hydroxyl Radical. Biochemical and Biophysical Research Communications. 169(1): p. 265-271.
85. Chan, B., O'Reilly, R.J., Easton, C.J. Radom, L. (2012). Reactivities of Amino Acid Derivatives toward Hydrogen Abstraction by Cl• and OH•. The Journal of Organic Chemistry. 77(21): p. 9807-9812.
86. Stadtman, E.R., Levine, R.L. (2000). Protein Oxidation. Annals of the New York Academy of Sciences. 899(1): p. 191-208.
87. Uchida, K. (2003). Histidine and Lysine as Targets of Oxidative Modification. Amino Acids. 25(3-4): p. 249-257.
88. Pryor, W.A., Uppu, R.M. (1993). A Kinetic Model for the Competitive Reactions of Ozone with Amino Acid Residues in Proteins in Reverse Micelles. Journal of Biological Chemistry. 268(5): p. 3120-3126.
89. Mudd, J.B., Leavitt, R., Ongun, A., McManus, T.T. (1969). Reaction of Ozone with Amino Acids and Proteins. Atmospheric Environment (1967). 3(6): p. 669-681.
90. Berlett, B.S., Stadtman, E.R. (1997). Protein Oxidation in Aging, Disease and Oxidative Stress. Journal of Biological Chemistry. 272: p. 20313-20316.
91. Requena, J.R., Chao, C., Levine, R.L., Stadtman, E.R. (2001). Glutamic and Aminoadipic Semialdehydes Are the Main Carbonyl Products of Metal-Catalyzed Oxidation of Proteins. Proceedings of the National Academy of Sciences. 98(1): p. 69-74.
92. Vogt, W. (1995). Oxidation of Methionyl Residues in Proteins: Tools, Targets, and Reversal. Free Radical Biology and Medicine. 18(1): p. 93-105.
93. Chalker, J.M., Bernardes, G.J.L., Lin, Y.A., Davis, B.G. (2009). Chemical Modification of Proteins at Cysteine: Opportunities in Chemistry and Biology. Chemistry – An Asian Journal. 4(5): p. 630-640.

94. Stadtman, E. (1992). Protein Oxidation and Aging. Science. 257(5074): p. 1220-1224.
95. Pryor, W.A. (1966). Free Radicals. McGraw-Hill.
96. Mujika, J.I., Uranga, J., Matxain, J.M. (2013). Computational Study on the Attack Of ·OH Radicals on Aromatic Amino Acids. Chemistry. 19(21): p. 6862-73.
97. Huggins, T.G., Wells-Knecht, M.C., Detorie, N.A., Baynes, J.W., Thorpe, S.R. (1993). Formation of *O*-Tyrosine and Dityrosine in Proteins During Radiolytic and Metal-Catalyzed Oxidation. Journal of Biological Chemistry. 268(17): p. 12341-7.
98. Dean, R.T., Gieseg, S., Davies, M.J. (1993). Reactive Species and Their Accumulation on Radical-Damaged Proteins. Trends in Biochemical Sciences. 18(11): p. 437-41.
99. Giulivi, C., Davies, K.J. (1993). Dityrosine and Tyrosine Oxidation Products Are Endogenous Markers for the Selective Proteolysis of Oxidatively Modified Red Blood Cell Hemoglobin by (the 19 S) Proteasome. J of Biological Chemistry. 268(12): p. 8752-9.
100. Stadtman, E.R. (1993). Oxidation of Free Amino Acids and Amino Acid Residues in Proteins by Radiolysis and by Metal-Catalyzed Reactions. Annual Review of Biochemistry. 62(1): p. 797-821.
101. Spolitak, T., Dawson, J.H., Ballou, D.P. (2005). Reaction of Ferric Cytochrome P450cam with Peracids: Kinetic Characterization of Intermediates on the Reaction Pathway. Journal of Biological Chemistry. 280(21): p. 20300-20309..
102. Houseman, A.L., Doan, P.E., Goodin, D.B., Hoffman, B.M. (1993). Comprehensive Explanation of the Anomalous EPR Spectra of Wild-Type and Mutant Cytochrome C Peroxidase Compound ES. Biochemistry. 32(16): p. 4430-43.
103. Wiertz, F.G.M., Richter, O.H., Cherepanov, A.V., MacMillan, F., Ludwig, B., de Vries, S. (2004). An Oxo-Ferryl Tryptophan Radical Catalytic Intermediate in Cytochrome C and Quinol Oxidases Trapped by Microsecond Freeze-Hyperquenching (MHQ). FEBS Letters. 575(1–3): p. 127-130.

104. Gunther, M.R., Sturgeon, B.E., Mason, R.P. (2000). A Long-Lived Tyrosyl Radical from the Reaction between Horse Metmyoglobin and Hydrogen Peroxide. Free Radical Biology and Medicine. 28(5): p. 709-719.

105. Ivancich, A., Jouve, H.M., Sartor, B., Gaillard, J. (1997). EPR Investigation of Compound I in *Proteus mirabilis* and Bovine Liver Catalases: Formation of Porphyrin and Tyrosyl Radical Intermediates. Biochemistry. 36(31): p. 9356-9364.

106. Ivancich, A., Mazza, G., Desbois, A. (2001). Comparative Electron Paramagnetic Resonance Study of Radical Intermediates in Turnip Peroxidase Isozymes. Biochemistry. 40(23): p. 6860-6866.

107. Ranguelova, K., Girotto, S., Gerfen, G.J., Yu, S., Suarez, J., Metlitsky, L., Magliozzo, R.S. (2007). Radical Sites in *Mycobacterium tuberculosis* KatG Identified Using Electron Paramagnetic Resonance Spectroscopy, the Three-Dimensional Crystal Structure, and Electron Transfer Couplings. The Journal of Biological Chemistry. 282(9): p. 6255–6264.

108. McNally, E.J., McNally, E., Hastedt, J.E. (2007). Protein Formulation and Delivery, Second Edition. CRC Press.

109. Zhang, W., Xiao, S., Ahn, D.U. (2013). Protein Oxidation: Basic Principles and Implications for Meat Quality. Critical Reviews in Food Science and Nutrition. 53(11): p. 1191-1201.

110. Cataldo, F. (2003). On the Action of Ozone on Proteins. Polymer Degradation and Stability. 82(1): p. 105-114.

111. Kido, K., Kassell, B. (1975). Oxidation of Methionine Residues of Porcine and Bovine Pepsins. Biochemistry. 14(3): p. 631-5.

112. Chao, C., Ma, Y., Stadtman, E.R. (1997). Modification of Protein Surface Hydrophobicity and Methionine Oxidation by Oxidative Systems. Proceedings of the National Academy of Sciences of the United States of America. 94(7): p. 2969-2974.

113. Schoneich, C., Yang, J. (1996). Oxidation of Methionine Peptides by Fenton Systems: The Importance of Peptide Sequence, Neighbouring Groups and Edta. Journal of the Chemical Society, Perkin Transactions 2. (5): p. 915-924.

114. Li, S., Schoneich, C., Borchardt, R.T. (1995). Chemical Instability of Protein Pharmaceuticals: Mechanisms of Oxidation and Strategies for Stabilization. Biotechnology and Bioengineering. 48(5): p. 490-500.
115. Luo, D., Smith, S.W., Anderson, B.D. (2005). Kinetics and Mechanism of the Reaction of Cysteine and Hydrogen Peroxide in Aqueous Solution. Journal of Pharmaceutical Sciences. 94(2): p. 304-316.
116. Savige, W.E., Maclaren, J.A. (1966). Oxidation of Disulfides, with Special Reference to Cystine, in The Chemistry of Organic Sulfur Compounds, Kharasch, N. and Meyers, C.Y., Editors. Pergamon Press: Oxford, U.K..
117. Carr, C.M., Lewis, D.M. (1993). An FTIR Spectroscopic Study of the Photodegradation and Thermal Degradation of Wool. Journal of the Society of Dyers and Colourists. 109(1): p. 21-24.
118. Torchinskii, Y.M., Dixon, H.B.F. (1974). Oxidation of *S*-*S* Groups: Identification of Cysteine-Containing Peptides, in Sulfhydryl and Disulfide Groups of Proteins. Springer Science & Business Media.
119. Kim, J., Lewis, D.M. (2002). The Effect of Various Anti-Setting Systems in Wool Dyeing. Part 1: Hydrogen Peroxide Based Systems. Coloration Technology. 118(3): p. 121-124.
120. Signori, V., Lewis, D.M. (1997). FTIR Analysis of Cysteic Acid and Cysteine-*S*-Thiosulphate on Untreated and Bleached Human Hair. Macromolecular Symposia. 119(1): p. 235-240.
121. Verbeek, C.J.R., Bier, J.M. (2011). Chapter 7 Synthesis and Characterization of Thermoplastic Agro-Polymers, in A Handbook of Applied Biopolymer Technology: Synthesis, Degradation and Applications. The Royal Society of Chemistry. p. 197-242.
122. Verbeek, C.J.R., van den Berg, L.E. (2010). Extrusion Processing and Properties of Protein-Based Thermoplastics. Macromolecular Materials and Engineering. 295(1): p. 10-21.
123. Ebewele, R.O. (2000). Thermal Transitions in Polymers, in Polymer Science and Technology. CRC Press: Florida, U.S..
124. Gedde, U.W. (1999). The Glassy Amorphous State, in Polymer Physics. Springer: Netherlands.

125. Kunal, K., Robertson, C.G., Pawlus, S., Hahn, S.F., Sokolov, A.P. (2008). Role of Chemical Structure in Fragility of Polymers: A Qualitative Picture. Macromolecules. 41(19): p. 7232-7238.

126. Daniels, C.A. (1989). Polymers Structure and Properties. Technomic Publishing Company, Inc: Pennsylvania, U.S..

127. Peng, W., Riedl, B. (1995). Thermosetting resins. Journal of Chemical Education. 72(7): p. 587-592.

128. Raquez, J.M., Deléglise, M., Lacrampe, M.F., Krawczak, P. (2010). Thermosetting (bio)materials derived from renewable resources: A critical review. Progress in Polymer Science. 35(4): p. 487-509.

129. Seymour, R.B. (1981). History of the Development and Growth of Thermosetting Polymers. Journal of Macromolecular Science: Part A – Chemistry. 15(6): p. 1165-1171.

130. Bengoechea, C., Arrachid, A., Guerrero, A., Hill, S.E., Mitchell, J.R. (2007). Relationship between the Glass Transition Temperature and the Melt Flow Behavior for Gluten, Casein and Soya. Journal of Cereal Science. 45(3): p. 275-284.

131. Bier, J.M., Verbeek, C.J.R., Lay, M.C. (2013). Thermal Transitions and Structural Relaxations in Protein-Based Thermoplastics. Macromolecular Materials and Engineering. 299(5): p. 524-539.

132. Ferrier, D.R. (2013). Protein Structure and Function, in Biochemistry. Wolters Kluwer Health. p. 1-68.

133. Richards, A.F. (2004). Nylon Fibres, in Synthetic Fibres: Nylon, Polyester, Acrylic, Polyolefin, McIntyre, J.E., Editor. Elsevier Science. p. 20-94.

134. Hudson, S.M. (2012). The spinning of silk-like proteins into fibers, in Protein-Based Materials, Kaplan, D., McGrath, K., Editors. Birkhäuser Boston. p. 313-337.

135. Chapman, R.D., Chruma, J.L., (1985). Nylon Plastics, in Engineering Thermoplastics: Properties and Applications, Margolis, J.M., Editor. Taylor & Francis. p. 83-122.

136. Tolstoguzov, V. (1993). Thermoplastic Extrusion – the Mechanism of the Formation of Extrudate Structure and Properties. Journal of the American Oil Chemists' Society. 70(4): p. 417-424.

137. Barone, J.R., Dangaran, K., Schmidt, W.F. (2006). Blends of Cysteine-Containing Proteins. Journal of Agricultural and Food Chemistry. 54(15): p. 5393-5399.

138. Pardio-Sedas, V. (2014). Influence of Ozone Depuration on the Physical Properties of Fresh American Oysters (*Crassostrea virginica*), in Processing and Impact on Active Components in Food, Preedy, V.R., Editor. Elsevier Science.

139. Uzun, H., Ibanoglu, E., Catal, H., Ibanoglu, S. (2012). Effects of Ozone on Functional Properties of Proteins. Food Chemistry. 134(2): p. 647-654.

140. Malkov, S., Živković, M., Beljanski, M., Hall, M., Zarić, S. (2008). A Reexamination of the Propensities of Amino Acids Towards a Particular Secondary Structure: Classification of Amino Acids Based on Their Chemical Structure. Journal of Molecular Modeling. 14(8): p. 769-775.

141. Xiong, H., Buckwalter, B.L., Shieh, H.M., Hecht, M.H. (1995). Periodicity of Polar and Nonpolar Amino Acids Is the Major Determinant of Secondary Structure in Self-Assembling Oligomeric Peptides. Proceedings of the National Academy of Sciences. 92(14): p. 6349-6353.

142. Sharma, V.K., Graham, N.J.D. (2010). Oxidation of Amino Acids, Peptides and Proteins by Ozone: A Review. Ozone: Science & Engineering. 32(2): p. 81-90.

143. Chou, P.Y., Fasman, G.D. (1974). Conformational Parameters for Amino Acids in Helical, Beta-Sheet, and Random Coil Regions Calculated from Proteins. Biochemistry. 13(2): p. 211-222.

144. Costantini, S., Colonna, G., Facchiano, A.M. (2006). Amino Acid Propensities for Secondary Structures Are Influenced by the Protein Structural Class. Biochemical and Biophysical Research Communications. 342: p. 441-451.

145. Levitt, M. (1978). Conformational Preferences of Amino Acids in Globular Proteins. Biochemistry. 17(20): p. 4277-4285.

146. Rabotyagova, O.S., Cebe, P., Kaplan, D.L. (2011). Protein-Based Block Copolymers. Biomacromolecules. 12(2): p. 269-289.

147. Keten, S., Buehler, M.J. (2010). Nanostructure and Molecular Mechanics of Spider Dragline Silk Protein Assemblies. Journal of The Royal Society Interface. Published Online doi:10.1098/rsif.2010.0149

148. Nova, A., Keten, S., Pugno, N.M., Redaelli, A., Buehler, M.J. (2010). Molecular and Nanostructural Mechanisms of Deformation, Strength and Toughness of Spider Silk Fibrils. Nano Letters. 10(7): p. 2626-2634.

149. Qin, G., Hu, X., Cebe, P., Kaplan, D.L. (2012). Mechanism of Resilin Elasticity. Nature Communications. 3: p. 1003.

150. Rauscher, S., Baud, S., Miao, M., Keeley, Fred W., Pomès, R. (2006). Proline and Glycine Control Protein Self-Organization into Elastomeric or Amyloid Fibrils. Structure. 14(11): p. 1667-1676.

151. Nairn, K.M., Lyons, R.E., Mulder, R.J., Mudie, S.T., Cookson, D.J., Lesieur, E., Kim, M., Lau, D., Scholes, F.H., Elvin, C.M. (2008). A Synthetic Resilin Is Largely Unstructured. Biophysical Journal. 95(7): p. 3358-3365.

152. Low, A., Verbeek, C.J.R., Lay, M.C. (2014). Treating Bloodmeal with Peracetic Acid to Produce a Bioplastic Feedstock. Macromolecular Materials and Engineering. 299(1): p. 75-84.

153. Alexander, P., Fox, M., Hudson, R.F. (1951). The Reaction of Oxidising Agents with Wool: 5. The Oxidation Products of the Disulfide Bond and the Formation of a Sulphonamide in the Peptide Chain. Biochemical Journal. 49(129): p. 129 - 138.

154. Robbins, C.R. (2013). The Physical Properties and Cosmetic Behavior of Hair, in Chemical and Physical Behavior of Human Hair. Springer: New York. p. 299- 370.

155. Wolfram, L.J., Hall, K., Hui, I. (1970). The Mechanism of Hair Bleaching. Journal of the Society of Cosmetic Chemists. 21: p. 875-900.

156. Zhang, Q., Shan, G., Cao, P., He, J., Lin, Z., Huang, Y., Ao, N. (2015). Mechanical and Biological Properties of Oxidized Horn Keratin. Materials Science and Engineering C Materials for Biological Applications. 47: p. 123-34.

157. Zhang, Q., Li, C., Pan, Y., Shan, G., Cao, P., He, J., Lin, Z., Ao, N., Huang, Y. (2013). Microstructure and Mechanical Properties of Horns Derived from Three Domestic Bovines. Materials Science and Engineering: C. 33(8): p. 5036-5043.

158. Li, Q., Hurren, C.J., Yu, H., Ding, C., Wang, X. (2012). Thermal and Mechanical Properties of Ultrasonically Treated Wool. Textile Research Journal. 82(2): p. 195-202.

159. Nagarajan, M., Benjakul, S., Prodpran, T., Songtipya, P., Nuthong, P. (2013). Film Forming Ability of Gelatins from Splendid Squid (*Loligo Formosana*) Skin Bleached with Hydrogen Peroxide. Food Chemistry. 138(2–3): p. 1101-1108.

3

The Role of Peracetic Acid in Bloodmeal Decoloring

By

TALIA M. HICKS, C. J. R. VERBEEK, M. C. LAY

AND

M. MANLEY-HARRIS

Published in Journal of American Oil Chemists' Society

I prepared the draft manuscript of this journal paper, which was refined and edited in consultation with my supervisors, whom are credited as co-authors. I was responsible for sample and reagent preparation, experimental design, volumetric analysis to determine consumption of reagents and colour analysis.

J Am Oil Chem Soc (2013) 90:1577–1587
DOI 10.1007/s11746-013-2304-2

ORIGINAL PAPER

The Role of Peracetic Acid in Bloodmeal Decoloring

Talia M. Hicks · C. J. R. Verbeek · M. C. Lay · M. Manley-Harris

Received: 6 March 2013 / Revised: 8 July 2013 / Accepted: 12 July 2013 / Published online: 31 July 2013

Abstract Hydrogen peroxide (HP) can degrade soluble heme, forming yellow or colorless degradation products. Thermal treatment during bloodmeal production changes the conformation of oxyhemoglobin trapping heme in hydrophobic protein regions or forms methemoglobin (metHb) heme which catalytically removes HP. As a result, HP can only degrade a portion of the heme present in bloodmeal leading to poor decoloring. Equilibrium peracetic acid (PAA) solutions can effectively decolor bloodmeal. This work assessed the ability of PAA to decolor bloodmeal and the mechanism by which it occurs. The inability of HP to decolor bloodmeal is determined by the fact that it is unable to permanently degrade metHb heme, or hydrophobically trapped heme. Addition of organic acids to HP led to significant swelling of the protein chains but also to poorer decoloring and lower HP consumption compared to PAA. This suggested that in the case of PAA solutions, where bleaching was facile, the reason PAA solutions are capable of decoloring bloodmeal was due to the action of the PAA molecule against heme, whereas HP and acetic (ethanoic) acid played only minor roles in total bleaching. The decolored protein powder has reduced odor and whiter color, and is suitable for applications such as bioplastics.

Keywords Co-products (Waste) · Biobased products, protein extraction and processing · Processing technology

T. M. Hicks · C. J. R. Verbeek (✉) · M. C. Lay
School of Engineering, Faculty of Science and Engineering, University of Waikato, Private Bag 3105, Hamilton 3240, New Zealand
e-mail: jverbeek@waikato.ac.nz

T. M. Hicks
e-mail: tmh20@waikato.ac.nz

M. Manley-Harris
Department of Chemistry, Faculty of Science and Engineering, University of Waikato, Private Bag 3105, Hamilton 3240, New Zealand

Introduction

Bloodmeal is a dried protein powder of red-brown color, produced from inedible blood collected in meat processing plants. In New Zealand, bloodmeal is currently used as fertilizer, as an additive in animal feed or exported for use in aquaculture. It has also been developed as an inexpensive feedstock for producing protein based bioplastics [1–3].

Bloodmeal can be deodorized and decolored via chemical oxidation and can also be used to produce bioplastics [1]. The heme moiety in hemoglobin is responsible for the dark color and can be degraded with oxidizing agents such as hydrogen peroxide or sodium hypochlorite [1, 4–9]. This can easily occur providing that heme is freely soluble, easily accessible or is in the form of oxyhemoglobin [1, 5, 6, 10].

Heme is a tetraporphyrin that chelates iron II, located within the hydrophobic pocket of each of the four globin chains. Iron II forms a six coordination complex, where four positions are occupied by the planar nitrogen atoms of the porphyrin ring, the fifth by a covalent bond with a histidine residue of the globin chain, and the sixth position is reversibly occupied by exogenous ligands, such as oxygen, carbon dioxide or water [11].

The iron in hemoglobin can exist in various oxidation states. In the ferrous oxidation state the heme chelates

oxygen, and the hemoglobin is referred to as oxyhemoglobin (Fe^{2+}, iron II) and is red in color. When the oxygen dissociates it becomes deoxyhemoglobin (Fe^{2+}, iron II). Exposure to oxygen-rich environments can cause the iron in oxyhemoglobin to be oxidized to its ferric state resulting in methemoglobin (Fe^{3+}) where the sixth co-ordination position is occupied by a hydroxide ion or water and the molecule is dark red-brown in color [11].

In whole blood collected from a healthy animal, the methemoglobin content is <10 % [12, 13]. During destabilizing conditions oxy- and methemoglobin can reversibly form hemochrome (Fe^{2+}) and hemichrome (Fe^{3+}) which readily precipitate, where the sixth coordination position is occupied by another endogenous ligand, such as histidine [11, 14–16]. Dehydration of the hemoglobin at ambient or elevated temperatures leads to a product comprised of approximately 50 wt% methemoglobin [17].

Formation of methemoglobin is expected to occur during bloodmeal production, where whole blood is steam coagulated and decanted prior to rotary drying at 120 °C. During coagulation, thermal denaturation occurs which allows the hydrophobic regions of nearby proteins to interact, resulting in aggregate formation [18–23]. The aggregates are approximately 80 times less soluble than hemoglobin in a native state [24]. Upon drying, bloodmeal is hammer milled, resulting in bloodmeal particles of a uniform size (<1 mm). These are rich in β-sheets at the perimeter with a more randomly structured core and with α-helices evenly distributed throughout the particle [25].

Exposure of hemoglobin to the thermal conditions employed during bloodmeal production leads to significant structural changes to the hemoglobin protein [22, 23] and results in hydrogen peroxide and sodium hypochlorite being no longer effective as decoloring agents [1]. However, aqueous peracetic acid is capable of producing a decolored product.

Aqueous peracetic acid is an equilibrium mixture prepared by reacting hydrogen peroxide with glacial acetic (ethanoic) acid using a mineral acid catalyst such as ~1 wt% sulfuric acid [26]. This catalyst remains in solution, leading to a pH <1.

$$CH_3COOH + H_2O_2 \rightleftharpoons CH_3COOOH + H_2O \quad (1)$$

The equilibrium composition of a commercial peracetic acid solution is typically 5–6 wt% peracetic acid (PAA), 21–23 wt% hydrogen peroxide (HP), 10–11 wt% acetic acid and 63–65 wt% water [27].

Both hydrogen peroxide and peracetic acid participate in decoloring bloodmeal; however the mechanism by which heme is degraded is not well understood. The complex nature of the solution may lead to a variety of mechanisms influencing decoloring. For instance, acetic acid and water can swell protein chains by disrupting intra-molecular hydrogen bonding, analogous to the swelling of collagen during leather tanning which allows chromium to access potential reactive sites [28].

At the low pH of commercial PAA solutions, neither peracetic acid nor hydrogen peroxide are dissociated and both act as electrophiles attacking sites high in electron density [29], such as the carbon methene bridges in heme. During the reaction some activation of the peracetic acid (and hydrogen peroxide) may occur via light, heat or transition metal catalysis resulting in homolytic cleavage which yields hydroxyl, acyloxy, perhydroxyl and acetyl radicals [30]. These can react with peracetic acid components further to yield acetoxy, acylperoxy and perhydroxyl radicals [30]. During sterilization processes PAA is a more effective oxidant than hydrogen peroxide due to the greater longevity of the radicals it generates compared to the hydroxyl radical generated by hydrogen peroxide [31].

Upon treatment with commercial PAA solution, bloodmeal decoloring occurs very rapidly, within 1–2 min. The mixture foams indicative of evolved gases and the reaction is exothermic attaining temperatures up to 100 °C [1]. Any of the radicals described above may be involved during the decoloring of heme as well as in other side reactions. Hydrogen peroxide and peracetic acid may be consumed in four classes of reactions:

- decomposition (spontaneous and transition metal ion catalyzed degradation/hydrolysis) [32–36],
- protein oxidation (cross-linking, fragmentation, side-chain modifications) [37, 38],
- heme degradation [39], and
- deodorizing [34, 40].

The major products of these reactions include modified proteins, acetic acid, carbon dioxide and oxygen [38, 41].

The mechanism responsible for the bleaching action of an oxidizing agent depends upon the type of oxidant while its efficiency is dependent upon its mode of action, concentration and its relative oxidative strength. The objective of this work was to assess the ability of peracetic acid equilibrium mixtures to decolor bloodmeal and to elucidate the mechanism by which decoloring occurs.

Experimental

Reagents

Decoloring Bloodmeal

Agricultural grade bovine bloodmeal was obtained from Wallace Corporation Ltd., Waitoa, New Zealand and sieved to obtain particles under 710 μm for use. Peracetic acid (Proxitane Sanitizer 5 %) was purchased from Solvay

Interox Pty. Ltd., Auckland, New Zealand and 30 and 50 wt% hydrogen peroxide from Sigma Aldrich, Castle Hill, NSW, Australia.

Pre-swelling Bloodmeal

Formic acid, acetic acid, propionic acid (Thermo Fisher Scientific, Auckland, New Zealand) and urea solutions (1.0 mol L^{-1}, Ballance Agri-Nutrients, Taranaki, New Zealand) and sodium dodecyl sulfate (0.26 mol L^{-1}, Thermo Fisher Scientific, Loughborough, UK) were prepared in distilled water.

Volumetric Analysis

Analytic grade reagents ammonium iron (II) sulfate hexahydrate ($\sim$0.1 mol L^{-1}) and ammonium cerium (IV) sulfate ($\sim$0.2 mol L^{-1}, Merck Millipore, Darmstadt, Germany); were prepared in sulfuric acid (0.05 mol L^{-1}, Thermo Fisher Scientific, Auckland, New Zealand). Other chemicals required were Ferroin indicator, Lintner's starch (BDH Chemicals Ltd., Poole, UK), phenolphthalein, analytical grade potassium dichromate ($\sim$0.05 mol L^{-1}), hydrochloric acid, sulfuric acid, potassium iodide (10 wt%, iodate free), sodium hydroxide, sodium thiosulfate ($\sim$0.01–0.02 mol L^{-1}, Thermo Fisher Scientific, Auckland, New Zealand), potassium iodate (May & Baker Ltd., Dagenham, UK) and sodium carbonate decahydrate (Sigma Aldrich, Castle Hill, New South Wales, Australia).

Organic Acids and HP Decoloring

The following—98 % formic acid, 100 % acetic acid, 98 % propionic acid and 98 % sulfuric acid (Thermo Fisher Scientific, Auckland, New Zealand) were used to acidify 26 wt% HP to determine the effect of acids on decoloring.

Analysis

Concentration and Consumption of HP, PAA and Organic Acid

Volumetric analysis was employed to measure the consumption of PAA and HP and was carried out via an iodometric titration using ceric sulfate and sodium thiosulfate [42]. A sample of PAA solution (or supernatant from decoloring) was accurately weighed to five decimal places (0.1–2.0 g) and placed in a 500 mL Erlenmeyer flask containing 5 wt% sulfuric acid (150 mL) and cracked ice to maintain a temperature of 0–10 °C. Three drops of Ferroin indicator were added and the flask contents were titrated with a standardized ceric sulfate solution ($\sim$0.1–0.2 mol L^{-1}) containing 0.05 mol L^{-1} sulfuric acid, giving hydrogen peroxide concentration. Upon completion, 10 wt% potassium iodide solution ($\sim$10 mL) was added and the liberated iodine titrated with standardized sodium thiosulfate ($\sim$0.01–0.02 mol L^{-1}). Starch indicator was added near the end point for the thiosulfate titration to give the peracetic acid concentration. Error limits were based upon the highest experimental error calculated for the series of titrations.

Volumetric analysis of organic acid content was determined via acid–base titration with sodium hydroxide. A sample of PAA solution (or supernatant from decoloring) was accurately weighed to five decimal places (0.1–2.0 g) and placed in a 500-mL Erlenmeyer flask containing two drops of phenolphthalein indicator and the contents titrated against standardized sodium hydroxide ($\sim$0.01–0.02 mol L^{-1}), giving the organic acid concentration.

The effect of the PAA concentration on decoloring and peroxide consumption was investigated by subjecting bloodmeal to solutions of $\sim$1, 2, 3, 4 and 5 wt% PAA prepared by diluting commercial PAA with distilled water. Volumetric analysis was carried out on the PAA solution before and after decoloring. Decoloring was carried out using the method outlined below. Under these conditions bloodmeal was treated using a variable molar ratio of PAA/HP to bloodmeal (BM) as indicated in Table 1. The supernatant was recovered and analyzed via volumetric analysis (three titrations for each treatment type), and the decolored bloodmeal was neutralized, filtered and oven dried overnight (75 °C) for color analysis.

Color Analysis

Decoloring was quantified using a Konica Minolta Chromameter CR-410 (Thermo Fisher Scientific, Auckland, New Zealand) for bloodmeal exposed to solutions of HP or PAA in the concentration range of $\sim$10–30 wt% and PAA $\sim$1–5 wt%. Oven dried samples were ground and sieved to 1 mm, pressed flat, and analyzed. The chromameter utilized diffuse illumination, a D_{65} illuminant and 2^{o}-standard observer with the CR-A33e light projection tube attached, yielding the CIELAB values corresponding to the sample. CIELAB color parameters are indicators of luminosity/lightness (L*), redness (a*) and yellowness (b*) giving a numerical value to an objects color corresponding with human color vision [43]. CIELAB values were converted to red (R), green (G), blue (B) values, to represent the three dimensional color space so that the reader can view the colors using color space software. Percentage whiteness has also been given (the sum of the R G B values as a percentage of total white, 765) and represents the sample RGB color on a continuum where black is 0 and white is 765.

Table 1 Experimental conditions used for preparation of decolored bloodmeal (BM)

Experiment[#]	Actual PAA concentration (wt%)	Quantity PAA (mmol)[#]	Quantity HP (mmol)[#]	Quantity AA (mmol)[#]	Mass PAA solution (g)	Ratio of PAA solution: BM (g/g)
1	1.1	46	455	108	300	3
2	2.5	98	924	216	300	3
3	3.6	143	1,590	324	300	3
4	4.5	177	1,890	425	300	3
5	5.6	221	2,290	539	300	3

[#] The pH of the PAA solutions was 1–2.8. The percentage errors for PAA, HP and AA were <5 %

Methods

Decoloring Bloodmeal

The standard method used to decolor bloodmeal (BM) with equilibrium solutions of peracetic acid was carried out as follows; a constant ratio of PAA solution to bloodmeal (3:1 w/w) was used. Peracetic acid solution (300 g) was added to BM (100 g) and allowed to react with high speed mixing (10 min) to ensure homogenous decoloring before diluting with distilled water (~300 g). This mixture was immediately neutralized with sodium hydroxide and filtered. The decolored bloodmeal was oven dried overnight (75 °C).

Decoloring BM with hydrogen peroxide (HP) solutions was carried out in the same ratio (3:1 w/w) HP solution to BM, under the same reaction conditions. Upon completion the reaction was diluted with distilled water (~300 g), filtered and oven dried overnight (75 °C).

Pre-swelling Bloodmeal

Volumetric swelling was measured by exposing bloodmeal (5 g) to solvent (40 mL) as described earlier, decanting the supernatant and determining volume change by using distilled water and a burette. The decanted supernatant was decolored using 30 % HP (1–3 g). The mass of solvent taken up by the bloodmeal was noted to determine the subsequent concentration of HP used in decoloring. The saturated bloodmeal was decolored using 30 % HP (15 g) and immediately neutralized with sodium hydroxide, filtered, oven dried overnight (75 °C) and subjected to color analysis.

Pre-swelling bloodmeal changes the effective concentration of HP. To account for this, BM was pre-swollen with water to give the same effective concentration. This was carried out by adding water directly to BM (5 g), as required to obtain the concentration observed during pre-swelling with solvents followed by decoloring with 30 wt% HP (15 g). These samples were filtered and oven dried overnight (75 °C) and subjected to color analysis.

Organic Acids and HP Decoloring

The effect of pre-swelling agents on the consumption of HP during decoloring of bloodmeal was determined. Decoloring of bloodmeal (10 g) was carried out using 26 wt% HP (30 g) containing 0.033 mol of formic, acetic or propionic acid and compared to acidification with 0.003 mol sulfuric acid alone. After decoloring, the mixture was diluted two to threefold; volumetric analysis was carried out on the filtered supernatant to determine consumption of HP.

Performic and Perpropionic Acid Decoloring

To investigate the effect of chain length of the peracid on the consumption of oxidants and efficacy of decoloring bloodmeal was also treated with performic and perpropionic acid. Performic acid was prepared by adding 30 % HP (85 g) to 98 % formic acid (14 g) with 98 % sulfuric acid (1 g) and set to mix overnight. The composition of the solution was determined by volumetric analysis to give ~2.5 wt% performic acid. This solution (30 g) was used to decolor bloodmeal (10 g) and the consumption of HP and performic acid was determined by volumetric analysis. The decolored BM was neutralized and air dried overnight and subjected to color analysis.

Perpropionic acid was prepared by adding 30 % HP (85 g) to 98 % propionic acid (14 g) with 98 % sulfuric acid (1 g) and set to mix overnight. The composition of the solution was determined by volumetric analysis to give ~6.0 wt% perpropionic acid. This solution (30 g) was used to decolor bloodmeal (10 g) and the consumption of HP and perpropionic acid was determined by volumetric analysis. The decolored BM was neutralized and air dried overnight and subjected to color analysis.

Statistical Analysis

For the purpose of obtaining data representative of all decoloring treatment types, all samples were prepared in

duplicate before being subjected to volumetric or color analysis.

Volumetric analysis was carried out using three repeat measures for the duplicate samples. The results from volumetric analysis are given as an average with the accumulated percentage error across all steps. The variation between repeated measures as well as the variation between replicates was within the accumulated experimental error.

Color analysis was carried out using ten repeat measures for the triplicate samples. The results are presented as an average with the standard deviation given as an estimate of the experimental error.

Results and Discussion

Decoloring Bloodmeal and the Effect of Pre-swelling

Hydrogen peroxide and sodium hypochlorite are able to degrade various types of heme, such as free heme dissolved in aqueous solvents, and oxyhemoglobin (Fe^{2+}) present in whole blood as well as in isolated lysed red blood cells [1, 44]. However, for bloodmeal, hydrogen peroxide and sodium hypochlorite are not effective as decoloring agents [1].

To establish a baseline for decoloring efficacy bloodmeal was first decolored using hydrogen peroxide at ambient temperature and 40 °C (Table 2).

Decoloring with HP did not lead to a high degree of whiteness or luminosity, and increasing the temperature did not lead to any significant improvements in decoloring. The percentage whiteness and luminosity values obtained for HP decoloring are essentially the same within the margin of error. In contrast, decoloring in the presence of peracetic acid occurred readily and showed an increase with increasing PAA concentration up to 4–5 wt% (Fig. 1).

For decoloring to occur, the oxidant must be able to penetrate into the solid particle of protein and diffuse into the dehydrated hemoglobin molecule to access the four heme moieties that are embedded within their own hydrophobic pockets [45]. Hydrated hemoglobin proteins shrink by approximately 34 % when most or all of the bound water is removed [46], preventing access by HP to the heme moieties. A possible reason PAA solutions give better decoloring is due to its high acetic (ethanoic) acid content, which swells the protein chains, increasing chain mobility, allowing HP greater access to the heme. Pre-swelling the bloodmeal proteins with appropriate solvents might also increase chain mobility, giving greater access of HP to the heme groups, and improve decoloring. The effect of solvent type for pre-swelling bloodmeal on total volumetric swelling of the protein is shown in Table 3.

The presence of sodium dodecyl sulfate (SDS) and short chain carboxylic acids led to the highest volumetric swelling which suggests decoloring might be more effective when pre-treated bloodmeal is exposed to hydrogen peroxide. However, decoloring with HP was less effective for BM pre-swollen with organic acids compared to pre-swelling with water (values shown in parenthesis, Table 3). No significant change in decoloring efficacy was observed when SDS or urea was used (Table 3). This suggests that organic acids inhibit the decoloring process.

The highly pigmented supernatant retained from the pre-swelling experiment was decolored with HP giving a yellow product. The acidic supernatants were expected to contain solubilized heme. The urea and SDS supernatants may also contain small quantities of solubilized hemoglobin. Urea only extracted a very small quantity of heme as evidenced by the pale color of the supernatant,

Table 2 Efficacy of decoloring for bloodmeal treated with only hydrogen peroxide at ambient temperature

Concentration of HP (wt%)	% Whiteness[#]	Luminosity (L^*)[#]	R[#]	G[#]	B[#]	Color
Bloodmeal reference	25 ± 0.5	25 ± 0.5	79	52	64	
19	54 ± 6	62 ± 6	183	141	94	
30	59 ± 8	66 ± 8	193	154	106	
30[a]	63 ± 8	70 ± 8	203	164	117	
50	62 ± 7	69 ± 7	204	161	110	

[a] Decoloring carried out at 40 °C. Bloodmeal without decoloring is listed at the *top* of the table. [#]*R* red, *G* green, *B* blue color space values obtained from chromameter and are also shown as a color swatch

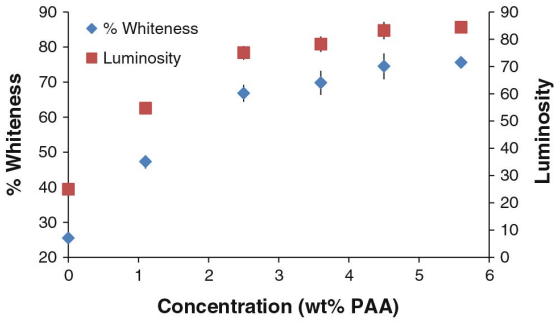

Fig. 1 Decoloring efficacy of ~1–6 wt% peracetic acid (PAA) on bloodmeal expressed as luminosity and % whiteness of final bloodmeal color

which was then decolored by HP. HP consumed during bleaching in formic, acetic and propionic acid solutions was decreased by approximately 10 % compared to water (Table 4).

Not only does the presence of H^+ decrease HP consumption by approximately 10 %, the consumption decreases from ~770 mmol/100 g BM regardless of initial HP concentration to ~450 mmol/100 g BM. This suggests that BM has a finite number of heme/oxidizable groups which are accessible by HP and that acidifying the protein causes a fraction of these oxidizable groups to become unreactive or inaccessible, consistent with a change in structural conformation to the protein or amino acid side chains that would usually react with HP.

Table 3 Effect of pre-swelling bloodmeal on decoloring bloodmeal (BM) with hydrogen peroxide (HP)

Pre-swelling agent	% Swelling	HP concentration wt%	% Whiteness (control)[#]	% Whiteness[#]	Luminosity (L^*) (control)[#]	Luminosity, (L^*)[#]	R[#]	G[#]	B[#]	Color
Bloodmeal reference				25 ± 0.5		25 ± 0.5	79	52	64	
Without swelling		30		59 ± 8		66 ± 8	193	154	106	
Water	260	19	58 ± 7	55 ± 6	67 ± 6	62 ± 6	174	132	84	
Formic acid	420	13	56 ± 4	42 ± 5	64 ± 4	48 ± 6	148	109	70	
Acetic acid	340	14	56 ± 3	46 ± 4	64 ± 3	53 ± 4	161	119	75	
Propionic acid	320	15	57 ± 5	47 ± 4	65 ± 4	54 ± 4	164	121	76	
Urea	240	18	59 ± 4	51 ± 4	67 ± 3	58 ± 4	171	133	89	
Sodium dodecyl sulfate	330	15	57 ± 5	54 ± 3	65 ± 4	62 ± 4	187	141	88	

[#] The control results are those obtained for BM samples pre-swollen with water to the same concentration before decoloring to rule out dilution effects. *R* red, *G* green, *B* blue values color space values obtained from chromameter. The concentration of HP after the uptake of solvent during swelling is listed

Table 4 Consumption of hydrogen peroxide (HP) in the presence of formic (FA), acetic (AA), propionic (PA) or sulfuric acid (H_2SO_4) during decoloring of bloodmeal

Concentration of HP	HP initial (mmol) (±1 %)	HP final (mmol) (±1 %)	HP consumed (mmol) (±2 %)	% HP consumed
50 wt% with water	4,490	3,740	750	17
30 wt% with water	2,680	1,940	740	28
26 wt% with water	2,320	1,550	770	33
26 wt%/FA	2,330	1,880	450	19
26 wt%/AA	2,310	1,860	450	20
26 wt%/PA	2,280	1,810	470	21
26 wt%/1 wt% H_2SO_4	2,270	1,830	440	19

Another reason why HP is unable to fully decolor bloodmeal is related to the high temperature to which hemoglobin is exposed during bloodmeal production (Fig. 2). The thermal conditions convert a fraction of oxyhemoglobin (oxyHb, Fe^{2+}) to methemoglobin (metHb, Fe^{3+}) [18, 22, 23]. MetHb cannot be degraded by HP [10], despite the latter's ability to degrade oxyHb and free heme (Fe^{3+}) such as hemin and hematin [6].

In contrast to oxyHb, where a superoxide radical forms from hydrogen peroxide to degrade the heme moiety; when metHb ($HbFe^{3+}$) is oxidized by HP it forms oxoferrylhemoglobin ($^{*}HbFe^{4+}O$). Oxoferrylhemoglobin is then reduced by HP to form molecular oxygen and water, regenerating metHb and is responsible for the catalytic removal of HP [10]:

$$HbFe^{3+} + H_2O_2 \rightarrow {}^{*}HbFe^{4+}O + H_2O$$

$$^{*}HbFe^{4+}O + H_2O_2 \rightarrow HbFe^{3+} + O_2 + H_2O$$

Additionally, hemoglobin is denatured on heating during drying, and the non-polar heme porphyrin becomes trapped in other hydrophobic regions of the now insoluble hemoglobin protein [24] along with any released iron [24], restricting access by HP.

Finally, to explain the observation that HP is less reactive toward bloodmeal in acidic media the reaction mechanism of HP with ferric iron porphyrins and proteins must be considered. The oxidative power of HP is not affected by H^+ ions as they are required for HP to act as an oxidant. However, lowering the pH of a system has been shown to inhibit nucleophilic oxidation reactions involving hydrogen peroxide [47]. Furthermore the rate of degradation of free ferric heme by hydrogen peroxide has previously been shown to have an inverse linear relationship to hydronium ion concentration between pH 6.5–11, indicating the active species that attacks heme is actually the perhydroxyl anion OH_2^- [8, 48]. Under acidic conditions this reaction mechanism would be expected to have slow kinetics.

While decoloring with HP at low pH is expected to generate hydroxyl radicals from HP, these radicals have been proven not to participate in heme degradation [10]. The lower HP consumption observed in the presence of carboxylic acids may be due to their scavenging effect on the hydroxyl radicals which regenerate hydrogen peroxide, leading to a lower reaction efficacy [49]. Additionally, the sulfate ion in the presence of Fe^{3+} ions (expected to be present from heme) is also known to scavenge hydroxyl radicals leading to poorer oxidation [49]. These effects may only be seen during decoloring of heme bound within a solid protein particle in which HP is unable to diffuse to the heme group faster than it can form radicals which are rapidly removed by scavenging agents.

In conclusion, the ability of HP to act as a bleaching agent on bloodmeal is determined not by the activity of HP or the activity of radicals that it generates against free heme or oxyHb heme, but the fact it is unable to permanently degrade metHb heme or hydrophobically trapped heme in the bloodmeal. Therefore the reason PAA is capable of decoloring bloodmeal is not due to the presence of HP or acetic acid, but is because of how the PAA can access trapped heme and react with metHb.

Decoloring Bloodmeal with Peracetic Acid

Decoloring bloodmeal with peracetic acid led to a high percentage of whiteness and luminosity (Fig. 1). The percentage whiteness improved with increasing PAA, but reached a plateau at about 4–5 wt%. Therefore any further addition of PAA above this point is not appropriate and may cause unnecessary damage to the proteins. It has been

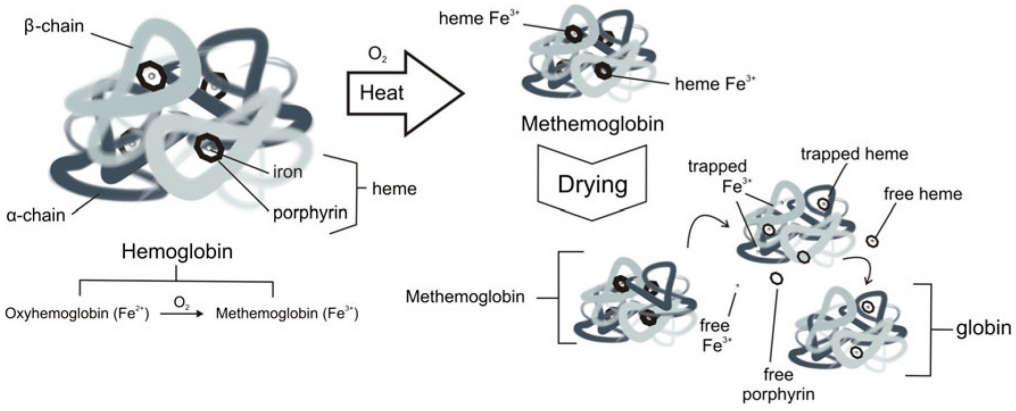

Fig. 2 Distribution of trapped and free heme in hemoglobin species before and after bloodmeal drying

reported elsewhere that competition between oxyHb, ferrylHb, metHb and oxoferrylHb for HP reduced heme degradation and a tenfold excess of HP was required to achieve complete conversion of oxyHb to ferrylHb [10]. This will probably be the case for PAA also since these competitive hemoglobin species are also likely to consume PAA.

HP consumption during decoloring using PAA was significantly lower than when using HP alone, and was comparable to HP consumption in the presence of organic acids (Table 4; Fig. 3a). Therefore HP inhibition by acidification also occurs in PAA solutions. Considering decoloring was poor with HP alone, it can be concluded that it is the PAA molecule and/or its radicals that are responsible for decoloring heme in bloodmeal.

When HP consumption is plotted versus initial quantity of reactant (Fig. 3a) there is an abrupt increase of rate of consumption at an initial quantity of HP about 1,700 mmol/100 g BM (3.6 wt% aqueous PAA, at equilibrium). This change in consumption of HP with concentration was not observed for PAA which exhibits a linear trend up to an initial quantity of PAA of 150 mmol/100 g BM, at which point consumption appears to slow (Fig. 3b). Leaving the reaction to continue overnight (2.5 wt% PAA, ambient temperature) did not improve decoloring. At low concentrations of PAA and HP, PAA is consumed in competing reactions such as protein oxidation, decomposition and hydrolysis. Therefore a large excess of PAA is required to drive diffusion into the particle so sufficient PAA reacts with the metHb and trapped heme. Studies have shown PAA reacts with ferric heme (in both enzymes and hemoglobin) to form a porphyrin radical from the heme group, oxoferryl π-cation radical $[Fe(^{4+})O\ por]^{+}$ which is also formed during oxidation with HP. The advantage of using PAA for metHb is that unlike HP, PAA cannot act as a reducing agent. The interaction of PAA with metHb heme leads to radical formation cleaving the porphyrin structure [39, 50, 51]. The reaction products formed are then able to react with HP, increasing HP consumption rate (Fig. 3a). For higher initial PAA concentrations there was still a significant quantity of unreacted peracetic acid upon completion of decoloring (Fig. 3b), giving rise to the possibility of recycling the PAA solution.

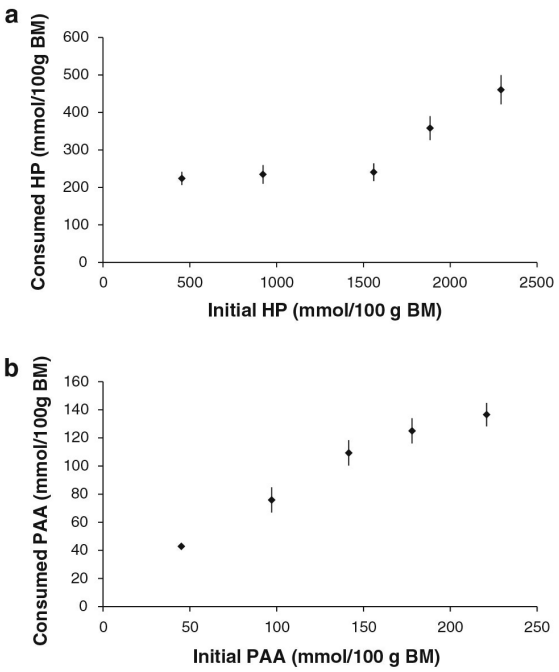

Fig. 3 **a** Consumption of hydrogen peroxide (HP) during decoloring with commercial peracetic acid (PAA). **b** Consumption of PAA during decoloring of bloodmeal with commercial PAA

Decoloring Bloodmeal with Peroxy-Organic Acids

PAA may have an advantage over HP in accessing the hydrophobic regions of the protein due to the presence of a carbon chain, lowering the polarity of the peroxide. To determine the effect of chain size (and consequently hydrophobicity) on decoloring, both performic and perpropionic acid were used to decolor bloodmeal in the same 3:1 mass ratio. Due to difficulties in preparing the equilibrium solutions the performic and perpropionic acid solutions were used at the highest concentrations possible. For comparison, commercial peracetic acid was diluted to similar concentrations using acetic acid and hydrogen peroxide.

Performic acid (PFA) reacted more aggressively and rapidly than PAA, producing foam and heat. This was not surprising as performic is the most powerful peroxy organic acid. The reaction mixture became a very pale yellow color before becoming darker again. Upon neutralizing with sodium hydroxide the protein darkened in color, and after filtering, air drying was required to prevent further browning. Despite the reaction being more vigorous, only ~79 mmol of PFA reacted (per 100 g BM). This was less than expected compared to reactions with similar concentrations of PAA. Despite the higher HP consumption, the extent of decoloring was lower (Table 5). This could be due to performic acid being less able to access trapped heme compared to PAA. Formic acid is used to partially hydrolyze proteins, and has been used with hydrogen peroxide to oxidize the protein due to the formation of performic acid prior to acid hydrolysis [52]. In the case of decoloring bloodmeal, it may be that performic

Table 5 Consumption of performic, peracetic and perpropionic acid and percentage whiteness and luminosity obtained

Peracid	Carboxylic acid (mmol/100 g BM)	HP	Peracid	% Whiteness[#]	Luminosity, (L^*)[#]	R[#]	G[#]	B[#]	Color
2.4 % performic acid									
Initial	4,820	2120	120						
Final	530	1600	40						
Consumed	4,290	520	80						
Expected consumption		415	90	43 ± 2	49 ± 3	149	108	74	
3.0 % peracetic acid									
Initial	490	2,200	120						
Final	230	1,800	30						
Consumed	260	400	90						
Expected consumption		440	90	66 ± 5	75 ± 5	215	180	112	
5.6 % peracetic acid									
Initial	540	2,300	220						
Final	530	1,800	80						
Consumed	10	500	140	76 ± 4	84 ± 3	239	214	140	
6.1 % perpropionic acid									
Initial	330	2,130	200						
Final	390	1,660	12						
Consumed	−60	470	188						
Expected consumption		440	140	50 ± 3	57 ± 4	175	128	81	

[#] *R* red, *G* green, *B* blue color space values obtained from chromameter. Results expressed as mmol/100 g BM. Percentage errors for consumption of carboxylic acid, hydrogen peroxide and peracid are all <5 %

acid reacts rapidly with heme groups and, due to its high reactivity and presence of HP and formic acid, begins hydrolyzing the protein and participating in browning reactions.

Perpropionic acid was consumed in a much higher quantity than expected compared to similar concentrations of PAA, possibly due to a greater uptake into the protein because of accessibility to hydrophobic regions. Despite this, it too led to poor decoloring, possibly because it is too large to react with the heme iron due to steric hindrance by nearby amino acids.

Conclusions

HP is capable of degrading heme, which is freely soluble, easily accessible or part of oxyhemoglobin, to form yellow or colorless degradation products resulting from cleaving the porphyrin ring. However, heme is trapped in the hydrophobic regions of bloodmeal, preventing access by HP. Attempts to improve HP access by pre-swelling the bloodmeal were unsuccessful. Hemoglobin can also form metHb heme which catalytically removes HP. As a result, HP can only degrade free heme or oxyHb heme, which represents a fraction of the heme present in bloodmeal, leading to poor decoloring. Peracetic acid was more effective than HP in decoloring bloodmeal because it can better access hydrophobic regions of bloodmeal and cleave metHb heme.

Performic and perpropionic acids were both inferior to peracetic acid in decoloring bloodmeal. Performic acid caused undesirable browning reactions while perpropionic acid may be too large to react with the heme in the hydrophobic regions due to steric hindrance by surrounding amino acids.

Acknowledgments The authors would like to acknowledge Wallace Corporation Ltd. for their continued support. Talia Hicks was supported by a University of Waikato Doctoral Scholarship and the New Zealand National Agricultural Fieldays Sir Don Llewellyn Scholarship.

References

1. Low A (2012) Decoloured bloodmeal based bioplastic, Ph.D. Thesis, in Materials and Process Engineering. University of Waikato, Hamilton, New Zealand
2. Verbeek C, van den Berg L (2011) Development of proteinous bioplastics using bloodmeal. J Polym Environ 19:1–10
3. Verbeek CJR, Viljoen C, Pickering K, van den Berg L (2010) Plastics material, New Zealand (Patent 551531)
4. Florence TM (1985) The degradation of cytochrome c by hydrogen peroxide. J Inorg Biochem 23:131–141
5. Low A, Verbeek J, Lay M, Swan J (2012) Decoloring hemoglobin as a feedstock for second generation bioplastics. Biochem Biotechnol 42:29–43
6. Nagababu E, Rifkind JM (1998) Formation of fluorescent heme degradation products during the oxidation of hemoglobin by hydrogen peroxide. Biochem Biophys Res Commun 247: 592–596
7. Nagababu E, Rifkind JM (2000) Heme degradation during autoxidation of oxyhemoglobin. Biochem Biophys Res Commun 273:839–845
8. Nagababu E, Rifkind JM (2004) Heme degradation by reactive oxygen species. Antioxid Redox Signal 6:967–978
9. Piot J, Guillochon D, Charet P, Thomas D (1987) Process for decolouring substances colored by tetrapyrrole compounds, USA. (Patent 4650589)
10. Nagababu E, Rifkind JM (2000) Reaction of hydrogen peroxide with ferryl hemoglobin: superoxide production and heme degradation. Biochemistry 39:12503–12511
11. Kanias T, Acker JP (2010) Biopreservation of red blood cells: the struggle with hemoglobin oxidation. FEBS J 277:343–356
12. Salvador P, Toldrà M, Parés D, Carretero C, Saguer E (2009) Color stabilization of porcine hemoglobin during spray-drying and powder storage by combining chelating and reducing agents. Meat Sci 83:328–333
13. Shiono H, Yagi Y, Thongnoon P, Kurabayashi N, Chikayama Y, Miyazaki S, Nakamura I (2001) Acquired methemoglobinemia in anemic cattle infected with *Theileria sergenti*. Vet Parasitol 102:45–51
14. Asghari-Khiavi M, Mechler A, Bambery KR, McNaughton D, Wood BR (2009) A resonance Raman spectroscopic investigation into the effects of fixation and dehydration on heme environment of hemoglobin. J Raman Spectrosc 40:1668–1674
15. Rachmilewitz EA, Peisach J, Blumberg WE (1971) Studies on the stability of oxyhemoglobin: a and its constituent chains and their derivatives. J Biol Chem 246:3356–3366
16. Winterbourn CC (1985) Free-radical production and oxidative reactions of hemoglobin. Environ Health Perspect 64:321–330
17. Labrude P, Chaillot B, Vigneron C (1984) Influence of physical conditions on the oxidation of hemoglobin during freeze-drying. Cryobiology 21:33–38
18. Black JF, Barton JK (2004) Chemical and structural changes in blood undergoing laser photocoagulation. Photochem Photobiol 80:89–97
19. Black JF, Wade N, Barton JK (2005) Mechanistic comparison of blood undergoing laser photocoagulation at 532 and 1,064 nm. Lasers Surg Med 36:155–165
20. Jansson H, Swenson J (2008) Dynamical changes of hemoglobin and its surrounding water during thermal denaturation as studied by quasielastic neutron scattering and temperature modulated differential scanning calorimetry. J Chem Phys 128:245104
21. Liu C, Bo A, Cheng G, Lin X, Dong S (1998) Characterization of the structural and functional changes of hemoglobin in dimethyl sulfoxide by spectroscopic techniques. Biochim Biophys Acta Protein Struct Mol Enzymol 1385:53–60
22. Seto Y, Kataoka M, Tsuge K (2001) Stability of blood carbon monoxide and hemoglobins during heating. Forensic Sci Int 121:144–150
23. Yan Y, Wang Q, He H, Zhou H (2004) Protein thermal aggregation involves distinct regions: sequential events in the heat-induced unfolding and aggregation of hemoglobin. Biophys J 86:1682–1690
24. Bou R, Hanquet N, Codony R, Guardiola F, Decker EA (2010) Effect of heating oxyhemoglobin and methemoglobin on microsomes oxidation. Meat Sci 85:47–53
25. Bier JM, Verbeek CJR, Lay MC (2013) Using synchrotron FTIR spectroscopy to determine secondary structure changes and distribution in thermoplastic protein. J Appl Polym Sci 130: 359–369
26. Rangarajan B, Havey A, Grulke E, Culnan P (1995) Kinetic parameters of a two-phase model for in situ epoxidation of soybean oil. J Am Oil Chem Soc 72:1161–1169
27. FMC Corporation (2006) Material safety data sheet: peracetic acid 5%. FMC Corporation, Philadelphia
28. Covington AD (2009) Pickling. In: Tanning chemistry: the science of leather. RSC Publishing, Cambridge, pp 177–194
29. Unis M (2010) Peroxide reactions of environmental relevance in aqueous solution, Ph.D. Thesis, in School of Applied Sciences. University of Northumbria, Newcastle, UK
30. Rokhina EV, Makarova K, Golovina EA, Van As H, Virkutyte J (2010) Free radical reaction pathway, thermochemistry of peracetic acid homolysis, and its application for phenol degradation: spectroscopic study and quantum chemistry calculations. Environ Sci Technol 44:6815–6821
31. Block SS (2001) Peroxygen compounds. In: Block SS (ed) Disinfection, sterilization and preservation. Lippincott Williams and Wilkins, Philadelphia, pp 185–204
32. Yuan Z, Ni Y, Van Heiningen ARP (1997) Kinetics of peracetic acid decomposition: part I: spontaneous decomposition at typical pulp bleaching conditions. Can J Chem Eng 75:37–41
33. Yuan Z, Ni Y, Van Heiningen ARP (1997) Kinetics of the peracetic acid decomposition: part II: pH effect and alkaline hydrolysis. Can J Chem Eng 75:42–47
34. Kitis M (2004) Disinfection of wastewater with peracetic acid: a review. Environ Int 30:47–55
35. Križman P, Kovač F, Tavčer PF (2005) Bleaching of cotton fabric with peracetic acid in the presence of different activators. Color Technol 121:304–309
36. Križman P, Kovač F, Tavčer PF, Hauser P, Hinks D (2007) Enhanced PAA bleaching of cotton by incorporating a cationic bleach activator. Color Technol 123:230–236
37. Thompson E, O'donnell I (1959) Studies on oxidised wool. I. A comparison of the completeness of oxidation with peracetic and performic acid. Aust J Biol Sci 12:282–293
38. Kerkaert B, Mestdagh F, Cucu T, Aedo PR, Ling SY, De Meulenaer B (2011) Hypochlorous and peracetic acid induced oxidation of dairy proteins. J Agric Food Chem 59:907–914
39. Schünemann V, Jung C, Terner J, Trautwein AX, Weiss R (2002) Spectroscopic studies of peroxyacetic acid reaction intermediates of cytochrome P450cam and chloroperoxidase. J Inorg Biochem 91:586–596
40. Koivunen J, Heinonen-Tanski H (2005) Peracetic acid (PAA) disinfection of primary, secondary and tertiary treated municipal wastewaters. Water Res 39:4445–4453
41. Yuan Z, d'Entremont M, Ni Y, van Heiningen ARP (1998) The formation of gaseous products and its relation to pulp bleaching during the peracetic acid treatment. J Wood Chem Technol 18:267–288
42. Greenspan FP, MacKellar DG (1948) Analysis of aliphatic peracids. Anal Chem 20:1061–1063

43. Stark G, Fawcett JP, Tucker IG, Weatherall IL (1996) Instrumental evaluation of color of solid dosage forms during stability testing. Int J Pharm (Amsterdam, Neth.) 143:93–100
44. Shin H, Kim C, Shin K, Chung H, Heo T (2001) Pretreatment of whole blood for use in immunochromatographic assays for hepatitis B virus surface antigen. Clin Diagn Lab Immunol 8:9–13
45. Lawrance GA (2009) A complex life. In: Introduction to coordination chemistry. John Wiley, Chichester, pp 229–250
46. Bragg L, Howells ER, Perutz MF (1954) The structure of haemoglobin. II. Proc R Soc Lond A 222:33–44
47. Freed AL, Strohmeyer HE, Mahjour M, Sadineni V, Reid DL, Kingsmill CA (2008) pH control of nucleophilic/electrophilic oxidation. Int J Pharm (Amsterdam, Neth.) 357:180–188
48. Brown SB, Hatzikonstantinou H, Herries DG (1978) The role of peroxide in haem degradation. a study of the oxidation of ferrihaems by hydrogen peroxide. J Biochem 174:901–907
49. Petri BG, Watts RJ, Teel AL, Huling SG, Brown RA (2011) Fundamentals of ISCO using hydrogen peroxide. In: Siegrist RL, Crimi M, Simpkin TJ. (eds) In situ chemical oxidation for groundwater remediation. Springer, New York, pp 33–88
50. Jung C, Schünemann V, Lendzian F (2005) Freeze-quenched iron-oxo intermediates in cytochromes P450. Biochem Biophys Res Commun 338:355–364
51. Svistunenko DA (2005) Reaction of haem containing proteins and enzymes with hydroperoxides: the radical view. Biochim Biophys Acta Bioenerg 1707:127–155
52. Rosenburg IM (2005) Identifying and analyzing posttranslational modifications, chap 9. In: Rosenberg IM (ed) Protein analysis and purification: benchtop techniques, BirkHäuser, Boston, pp 259–323

4

Effect of Oxidative Treatment on the Secondary Structure of Decoloured Bloodmeal

By

TALIA M. HICKS, C. J. R. VERBEEK, M. C. LAY

AND

J. M BIER

Published in RSC Advances

As first author for this paper, I prepared the draft manuscript of this journal paper, which was refined and edited in consultation with my supervisors, whom are credited as co-authors. The FT-IR results reported here were collected in collaboration with my supervisors (and Dr. J. Bier) during beamtime at the Australian Synchrotron. In discussion with my co-authors, I designed the experiment and drafted the beamtime proposal. The synchrotron proposal system does not permit students to register as "lead researchers", however, I was registered as co-proposer. I prepared the samples and liaised with the synchrotron regarding import permits to take them to Australia and regarding experimental set up. Together with my co-authors, I travelled to the Australian Synchrotron to conduct the experiments. I then performed the data analysis in OPUS software and Microsoft Excel, along with running the one-way ANOVA in Statistica. I also carried out the DSC and WAXS experiments and analysis.

RSC Advances

PAPER

View Article Online
View Journal | View Issue

Cite this: *RSC Adv.*, 2014, 4, 31201

Effect of oxidative treatment on the secondary structure of decoloured bloodmeal†

Talia Hicks,* Casparus J. R. Verbeek, Mark C. Lay and James M. Bier

Received 28th April 2014
Accepted 27th June 2014

DOI: 10.1039/c4ra03890h

www.rsc.org/advances

Bloodmeal can be decoloured using peracetic acid resulting in a material with a pale-yellow colour which only needs sodium dodecyl sulphate, water and triethylene glycol to extrude into a semi-transparent bioplastic. Fourier-transform infrared (FTIR) spectroscopy using Synchrotron light was used to investigate the effect of peracetic acid treatment at various concentrations on the spatial distribution of secondary structures within particles of bloodmeal. Oxidation caused aggregation of helical structures into sheets and acetic acid suppressed sheet formation. Decolouring with peracetic acid led to particles with a higher degree of disorder at the outer edges and higher proportions of ordered structures at the core, consistent with the expected diffusion controlled heterogeneous phase decolouring reaction. The degradation of stabilizing intra- and intermolecular interactions and the presence of acetate ions results in increased chain mobility and greater amorphous content in the material, as evidenced by reduction in T_g and greater enthalpy of relaxation with increasing PAA concentration.

Introduction

Bloodmeal is a dried protein powder of red-brown colour produced by steam coagulating, decanting and rotary drying whole blood at 120 °C. It contains about 95% protein, mainly haemoglobin and serum albumin and is an ideal feedstock for the production of bio-based plastics.[1] It can also be decoloured *via* chemical oxidation using commercial peracetic acid.[2] Peracetic acid is an equilibrium reaction product of hydrogen peroxide and ethanoic acid (acetic acid, AA) and sulphuric acid as catalyst.[3] The equilibrium composition is typically 5–6 wt% peracetic acid (PAA), 21–23 wt% hydrogen peroxide (HP), 10–11 wt% ethanoic acid and 63–65 wt% water.[4]

Due to the exposure of haemoglobin to the high temperatures employed during bloodmeal production, haem becomes trapped within the protein aggregates. The haem moiety in haemoglobin responsible for the dark colour can usually be degraded with an oxidant such as hydrogen peroxide or sodium hypochlorite[5–11] provided haem is freely soluble, easily accessible or is in the form of oxyhaemoglobin.[6–8,12] However, during bloodmeal production, exposure of haemoglobin to the thermal conditions employed causes significant structural changes to the protein[13,14] including conversion of oxyhaemoglobin to methaemoglobin[15] and aggregation into antiparallel β-sheets.[13,14,16–19] Consequently, hydrogen peroxide and sodium hypochlorite are no longer effective as decolouring agents,[6] and they are either unable to access a portion of the haem, or upon access, are unable to degrade all of the haem species present in bloodmeal.[20] Thus the action of the peracetic acid on haem, specifically on methaemoglobin, is critical for obtaining adequate decolouring.[20]

An earlier model for decolouring bloodmeal proposed peracetic acid solution diffusing into bloodmeal particles leading to haem degradation, where all of the components of PAA play some role in the decolouring process.[20] Water and acetic acid led to swelling of the protein chains making them more mobile, and are thought to facilitate access of the oxidants to sites where they are able to react. In addition to haem degradation, peracetic acid and hydrogen peroxide are also likely to cause structural changes to the bloodmeal proteins during the diffusion process.

During decolouring, peracetic acid and hydrogen peroxide are undissociated due to the low pH of the system, and in their molecular form both act as electrophiles to attack sites high in electron density.[21] In this system, the amino acids most susceptible to oxidation are methionine and cysteine due to their high reactivity with electrophiles, and the aromatic amino acids tyrosine, tryptophan, phenylalanine and histidine due to their high electron density. These amino acids are commonly found in β-sheets and may be significantly changed upon decolouring with peracetic acid.

Oxidation is known to cause structural changes at a primary level including fragmentation, crosslinking and amino acid changes.[22] Upon oxidation with peracetic acid solutions, dairy proteins have been found to contain an increased number of carbonyl groups, reduced thiol (SH) groups, aggregated proteins and showed a reduced solubility at high PAA concentration.[23]

School of Engineering, Faculty of Science and Engineering, University of Waikato, Private Bag 3105, Hamilton 3240, New Zealand. E-mail: tmh20@students.waikato.ac.nz

† Electronic supplementary information (ESI) available: Basic statistics for distribution of secondary structures determined by FTIR microspectroscopy. See DOI: 10.1039/c4ra03890h

Also, in contrast to bloodmeal, peracetic acid decoloured bloodmeal (DBM) has a glass transition temperature of around 50 °C and has a greater solubility in water and SDS solutions.[2] Solubility increased with the strength of PAA treatment, suggesting that hydrophobic interactions are reduced after PAA treatment. To successfully produce a bioplastic from DBM, only TEG and SDS were required, suggesting significant changes to protein structure, protein side groups, and/or protein–protein interactions have occurred during oxidation.[2]

The changes to primary structure caused by oxidation would also be expected to cause changes to the secondary structure of the protein due to the high dependence of secondary structure on the physicochemical and stereo-chemical properties of the amino acids of which they are comprised. Studies of the propensity of amino acids to form particular types of secondary structure indicate that most amino acids show preference for only one type of secondary structure.[24]

Typically, helical structures are comprised of amino acids containing short chain aliphatic side groups (Table 1). With the exception of alanine, all of these amino acids contain an aliphatic group on the Cα carbon with no branching at the Cβ position.[24–27] The amino acids with the highest propensity for β-sheets are most often non-polar or aromatic. Both threonine and cysteine are exceptions, threonine also tends to form bends and cysteine only has a slight propensity for sheets. The remaining amino acids are likely to form coils, bends or turns.[24]

Prior to decolouring thermal drying of blood leads to the unravelling of α-helices followed by the formation of intermolecular anti-parallel β-sheets responsible for aggregation.[14] Understanding the secondary structural composition of bloodmeal and how it is altered by decolouring is important for the development of a useful material, as the physical properties of the polymer will determine how the protein should best be manipulated to obtain the desired material properties in the thermoplastic. Oxidation of native proteins with hydroxyl radicals has previously been found to cause change to the secondary and tertiary structures of bovine serum albumin (BSA), including denaturation and increased hydrophobicity, followed by the formation of intermolecular covalent bonding and increased proteolytic susceptibility.[28] The same study found that BSA oxidized by hydroxyl radicals in the presence of the superoxide anion and molecular oxygen caused denaturation followed by fragmentation at the α-carbon and that the superoxide anion and molecular oxygen alone had no measurable change in secondary or tertiary structure. This suggests that the oxidant type and experimental conditions both determine the extent, if any, of secondary structural modification.

Table 1 Propensity of amino acids for secondary structures types

Helical	Sheet	Other
Alanine	Isoleucine	Glycine
Leucine	Phenylalanine	Proline
Methionine	Tryptophan	Asparagine
Glutamine	Valine	Aspartic acid
Glutamic acid	Tyrosine	Serine
Arginine	Threonine	Histidine
Lysine	Cysteine	

Synchrotron FTIR has recently been used to investigate secondary structure of agricultural proteins using the Amide I region[29,30] and of bloodmeal and its thermoplastic using the Amide III region.[31,32] It was found that although bloodmeal is comprised of denatured proteins, secondary structures such as β-sheets and α-helices remain dispersed throughout random coil, amorphous regions.[32]

The aim of this work was to understand the effect of PAA treatment at various concentrations on protein secondary structure, chain mobility and changes in inter/intra molecular spacing of ordered regions. Secondary structural analysis was done by spatially resolving secondary structures using FTIR Synchrotron microscopy, wide angle X-ray scattering and differential scanning calorimetry.

Experimental

Materials

Agricultural grade bovine bloodmeal was obtained from Wallace Corporation Ltd, New Zealand and sieved to utilize particles under 710 μm. Peracetic acid (Proxitane Sanitizer 5%) was purchased from Solvay Interox Pty Ltd Auckland, New Zealand and 30 wt% hydrogen peroxide from Sigma Aldrich, Castle Hill, NSW, Australia. Acetic and sulphuric acid and sodium hydroxide were purchased from Thermo Fisher Scientific, Auckland, New Zealand.

Sample preparation

Peracetic acid solution (300 g) was added to bloodmeal (100 g) and allowed to react with high speed mixing (10 min) to ensure homogenous decolouring before diluting with distilled water (300 g) a constant ratio of PAA solution to bloodmeal (3 : 1 w/w) was used. This mixture was immediately neutralized with sodium hydroxide and filtered. The decoloured bloodmeal was oven dried overnight (75 °C).

Decolouring BM with hydrogen peroxide (HP) solutions was carried out in the same ratio (3 : 1 w/w) HP solution to BM, under the same reaction conditions. Upon completion the reaction was diluted with distilled water (~300 g), filtered and oven dried overnight (75 °C).

To discern the effect of acetic acid on decolouring, bloodmeal (10 g) was decoloured using 26 wt% HP (30 g) containing 0.033 mol of acetic acid. After decolouring, the mixture was neutralized and oven dried overnight (75 °C). All samples were stored in air-tight polyethylene containers at ambient temperature for a minimum of one week prior to analysis.

Instrumentation

Spatially resolved FTIR experiments were undertaken on the infrared microspectroscopy beamline at the Australian Synchrotron, Victoria, Australia. Bloodmeal and decoloured bloodmeal particles were compressed in a diamond cell then transferred onto a barium fluoride slide. This was placed in a Linkam temperature controlled stage connected to a Bruker Hyperion 3000 with an

MCT collector and XY stage. The stage was set to 24 °C and purged with nitrogen gas. For each sample type, three separate particles were mapped using a 10 × 10 μm spot size chosen on video images. For each point, 32 spectra were collected in transmission mode with a resolution of 4 cm^{-1} between 3900 and 700 cm^{-1} and averaged using Opus 6.5 software (Bruker Optik GmbH 2009).

The spectra with corresponding *xy* coordinates for each point on a particle were combined to give an overall spatial distribution for each particle and sample type. Relative peak height in the amide III region of inverted second derivative spectra was determined according to Bier *et al.*,[31,32] and was used to estimate how relative fractional composition of corresponding secondary structures varied spatially across the particles after different decolouring treatments. Data was filtered for a minimum area under the amide III region to exclude points mapped outside particles from the analysis.

The second derivative of the original spectra (with no baseline correction) was determined using the Savitzky–Golay algorithm in Opus 6.5 using nine point smoothing. The second derivative was inverted by dividing by −1 and peak heights above the zero line were compared. The ratios A'_α/A'_β, A'_t/A'_β and A'_r/A'_β were calculated using Opus 6.5, where A'_x is the maximum height of the inverted second derivative peak within the wavenumber range associated with α-helices, β-sheets, turns and random coils indicated respectively by the subscripts α, β, t and r. The molar fraction for each secondary structure type was calculated using eqn (1)–(5) and spatial maps were drawn based on these compositions using Microsoft Excel. The composition approximates a mole fraction of peptide linkages in each structural conformation, each of which absorbs differently in the amide III region (Table 2).

$$\alpha + \beta + t + r = 1 \quad (1)$$

$$\beta = \frac{1}{A''_\alpha/A''_\beta + A''_t/A''_\beta + A''_r/A''_\beta + 1} \quad (2)$$

$$\alpha = \beta\frac{A''_\alpha}{A''_\beta} \quad (3)$$

$$t = \beta\frac{A''_t}{A''_\beta} \quad (4)$$

$$r = \beta\frac{A''_r}{A''_\beta} \quad (5)$$

Differential Scanning Calorimetry was conducted in a Perkin Elmer DSC 8500 hyper DSC fitted with an autosampler accessory and cooled with liquid nitrogen. Approximately 5–10 mg of sample was weighed into autosampler pans (Perkin Elmer) which were then crimped to provide a seal and placed into the auto sampler. All samples were scanned between 0 and 120 °C at 10 °C min^{-1} and cooled to 0 °C at the same rate prior to performing a second scan. Glass transition temperature (half Cp extrapolated) was determined using Pyris 7 software (Perkin Elmer). Excess enthalpy (ΔH) of relaxation was calculated by integrating the area under the endothermic peak, which occurred at the glass transition region, the reported values are means of two replicates.

Wide angle X-ray scattering of decoloured samples was carried out at ambient temperature using a PANalytical Empyrean X-ray diffractometer with a generator voltage of 45 kV and a current of 40 mA using $CuK_{\alpha 1}$ radiation. The diffraction data was collected in the 2θ range from 4° to 60° with a step size of 0.105°. A soller slit of 0.04 rad was used, with a fixed incident beam mask 15 mm, a fixed 1° anti-scatter silt and fixed 0.5° divergence slit. For the diffracted beam path a fixed 7.5 mm anti-scatter slit was used and detected using a PIXcel3D area detector. Data was smoothed using a cubic function with 7-point convolution in the X'Pert HighScorePlus software. A linear baseline was fitted to the minima between 4 and 60° and subtracted and normalized to the peak occurring at ~19° in Excel. Peak position and *d*-spacing determined according to Bragg's equation were carried out in X'Pert HighScorePlus software.

Table 2 Peak assignment in the amide III region.[33]

Region	Secondary structure	Wavenumber/cm^{-1}
Amide III	α-Helix	1330–1295
	β-Turns	1295–1270
	Random coils	1270–1250
	β-Sheets	1250–1220

Statistical analysis

For FTIR analysis, the average composition of each treatment type was calculated by averaging the secondary structure composition observed for each replicate and an analysis of variance with a two-tail student's *T*-test was performed to identify significant changes (95% confidence) between the mean composition in BM and DBM samples. A summary of basic statistics for the distribution of secondary structures determined by FTIR microspectroscopy is available as supporting information.

Results and discussion

Bloodmeal particles were found to be mostly heterogeneous, with β-sheets and helices randomly dispersed throughout (Table 3). Decolouring bloodmeal with HP or PAA led to changes to the average secondary structure composition of bloodmeal. The effect of PAA concentration on average composition is statistically significant, but relative to inherent structural variation it is only a small effect (partial $\eta 2 < 0.1$), however the spatial distribution of secondary structures throughout the particle is dramatically changed upon PAA treatment.

Decolouring is a two phase reaction involving the diffusion of the oxidizing solution into the solid bloodmeal particle. The ease of diffusion is determined by concentration and also by the relative size and polarity of the diffusing species. PAA concentration was found to have a direct impact on the distribution of secondary structures due to the increasing content of the acetic acid and oxidants (Fig. 1). The diffusion front is clearly observed

Table 3 Average fractional composition of secondary structures and one-way analysis of variance for decoloured bloodmeal, with PAA concentration as the independent variable. Partial η^2 gives the effect size relative to inherent structural variation[a]

Sample	Valid N	α-Helices	β-Turns	Random coils	β-Sheets	Disordered structures
BM	326	0.19 ± 0.04	0.15 ± 0.04	0.20 ± 0.07	0.46 ± 0.06	0.34 ± 0.07
1% PAA	595	0.16 ± 0.05	0.15 ± 0.06	0.20 ± 0.07	0.49 ± 0.09	0.35 ± 0.08
2% PAA	263	0.15 ± 0.04	0.15 ± 0.05	0.21 ± 0.07	0.50 ± 0.08	0.35 ± 0.08
3% PAA	734	0.17 ± 0.03	0.15 ± 0.04	0.19 ± 0.07	0.49 ± 0.06	0.34 ± 0.06
4% PAA	306	0.16 ± 0.04	0.18 ± 0.05	0.20 ± 0.07	0.46 ± 0.08	0.38 ± 0.07
5% PAA	596	0.17 ± 0.04	0.18 ± 0.05	0.22 ± 0.07	0.43 ± 0.06	0.39 ± 0.07
HP	669	0.14 ± 0.06	0.17 ± 0.06	0.17 ± 0.09	0.52 ± 0.11	0.34 ± 0.10
HP/AA	591	0.17 ± 0.04	0.16 ± 0.05	0.23 ± 0.07	0.43 ± 0.06	0.40 ± 0.07
Key results of one way ANOVA *versus* PAA treatment concentration for each structure						
p		<0.001	<0.001	<0.001	<0.001	<0.001
Partial η^2		0.06	0.07	0.02	0.10	0.09

[a] Disordered structures = β-turns + random coils.

as a change in secondary structure from the perimeter to the core of the particles, and is particularly easy to discern in bloodmeal samples treated with solutions of 3–5 wt% PAA.

Upon oxidation, some helical content is converted to other structures. Evaluating each treatment's secondary structure relative to bloodmeal indicated that hydrogen peroxide caused an overall reduction in helices and coils with a subsequent increase in sheets and turns (Fig. 2). A slightly higher quantity of helices and turns were observed at the perimeter of the particle ($p < 0.01$). β-Turns were probably formed in the highest quantity here because the surface of the particle is exposed to the highest concentration of HP; however it is unknown why helical structures remain in a higher concentration at the perimeter. The overall helical content was significantly reduced upon HP decolouring (Fig. 2) and is most likely due to aggregation, leading to the observed increase in β-sheets, a phenomenon commonly observed in proteins exposed to high temperatures. The fact that HP is able to cause aggregation of helices and coils at the core of the bloodmeal particle indicates that HP readily diffuses throughout the particle. HP would presumably carry out the same function in peracetic acid solutions. In the presence of acetic acid, aggregation of helical structures occurred to a lesser extent, suggesting acetic acid may have a protective effect.

Additionally, the formation of β-sheets was suppressed compared with HP alone (Fig. 2). Due to the suppression of helical aggregation and solvation of sheet structures with acetic acid, bloodmeal decoloured using HP and acetic acid mixtures resulted in increased structural disorder. The resulting particles showed regions of homogeneity (random coils and sheets) around the perimeter (Fig. 1). However, as these regions corresponded to both the highest and lowest concentrations observed throughout the sample, they average out and the only conclusion which can be drawn in the case of HP containing acetic acid is that the particles were either agglomerated during decolouring and broke apart, or were affected by drying conditions leading to the observed contrast at the perimeter, compared with the core. Acetic acid therefore influences the resulting secondary structure, and also inhibits hydrogen peroxide consumption.[20]

However, it is uncertain whether the observed secondary structure is a result of the inhibition of oxidation, or the inhibition of oxidation is a result of the modification of the protein secondary structure in such a way that it sterically hinders access of HP to reactive sites. The role of acetic acid in PAA is probably similar, but due to its size may have greater difficulty diffusing through the protein compared with HP.

Decolouring with 1–3 wt% PAA was found to cause aggregation of helices and random coils into sheet structures, with no change to β-turn content ($p > 0.05$). This change in composition was most strongly observed at the core of the particle, which is accessible to hydrogen peroxide (but not acetic acid due to its low concentration and larger size), whereas at the surface where acetic acid concentration would be highest, there was significantly less sheet formation (Fig. 2). This effect became more pronounced at higher concentrations of PAA, until at 5 wt% PAA destruction of sheets at the core is also observed (Fig. 1) with the formation of random coils, which could also be generated by protein chain scission.[2]

The highly reactive nature of both of the oxidants, suggest that it is unlikely the reaction occurs in a selective or systematic way, whereby helices and coils first become aggregated into sheets; that are subsequently degraded into turns and finally back into coils.

The behaviour of the decoloured bloodmeal material as a whole will be defined by the chemical properties of the proteins located throughout the particles. A definite difference in secondary structure composition exists between the perimeter and the core of the particle, caused by concentration gradient limited diffusion of acetic acid (Fig. 3). The difference in the fractional composition of disordered structures (β-turns and coils) between the perimeter and the core is greatest for 1–3 wt% PAA decoloured bloodmeal, and becomes reduced at 4–5 wt% PAA.

At low PAA concentration, with limited diffusion, the properties of DBM are more likely to be representative of the

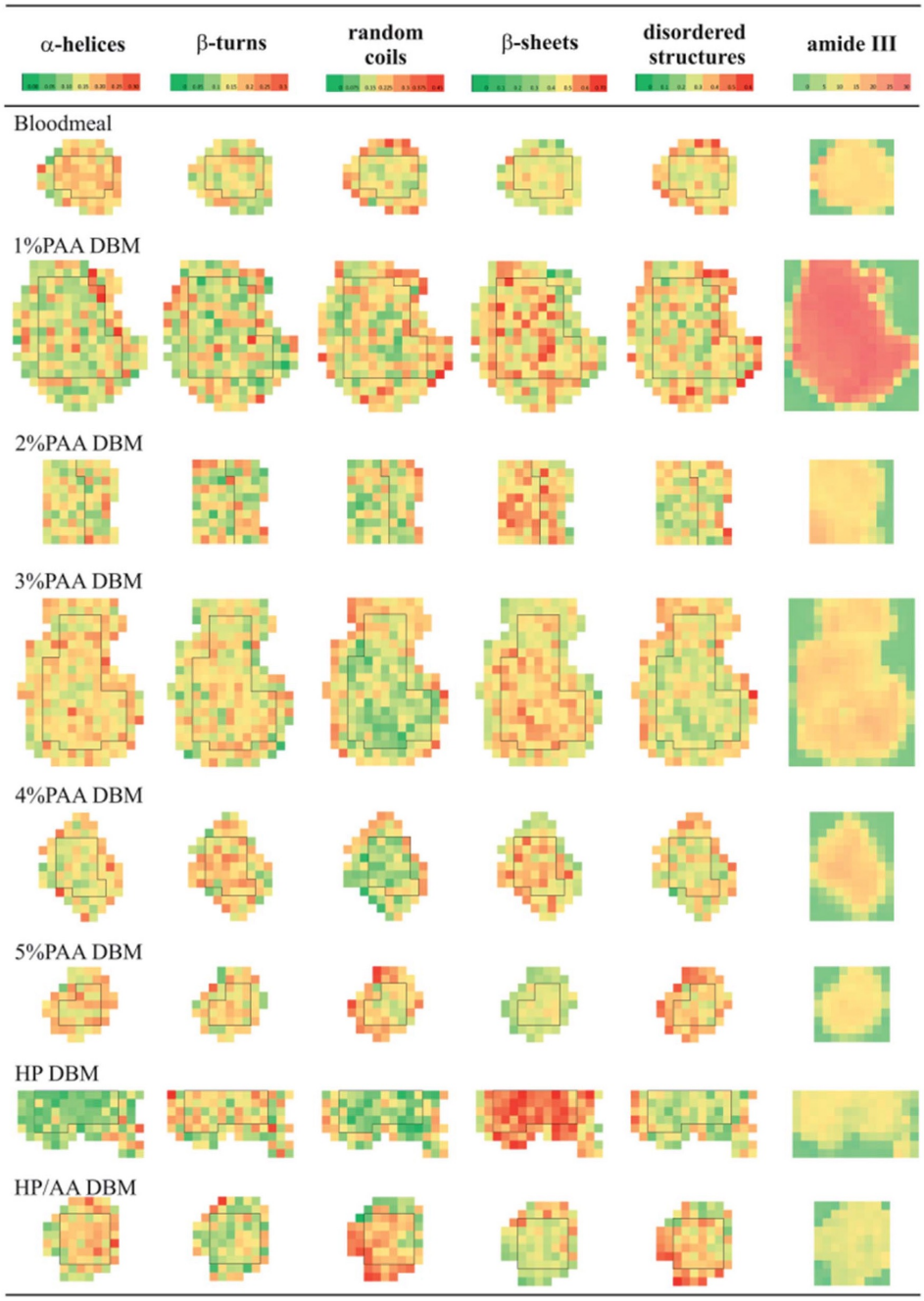

Fig. 1 Secondary structure distribution and total amide III region of bloodmeal and decoloured bloodmeal (DBM) after oxidative decolouring using peracetic acid (PAA), hydrogen peroxide (HP) or HP with acetic acid (HP/AA). Random coils and β-turns have been combined to give proportion of disordered structures. The shape outlined in black within the particle maps represents the boundary between the perimeter and the core of the particle.

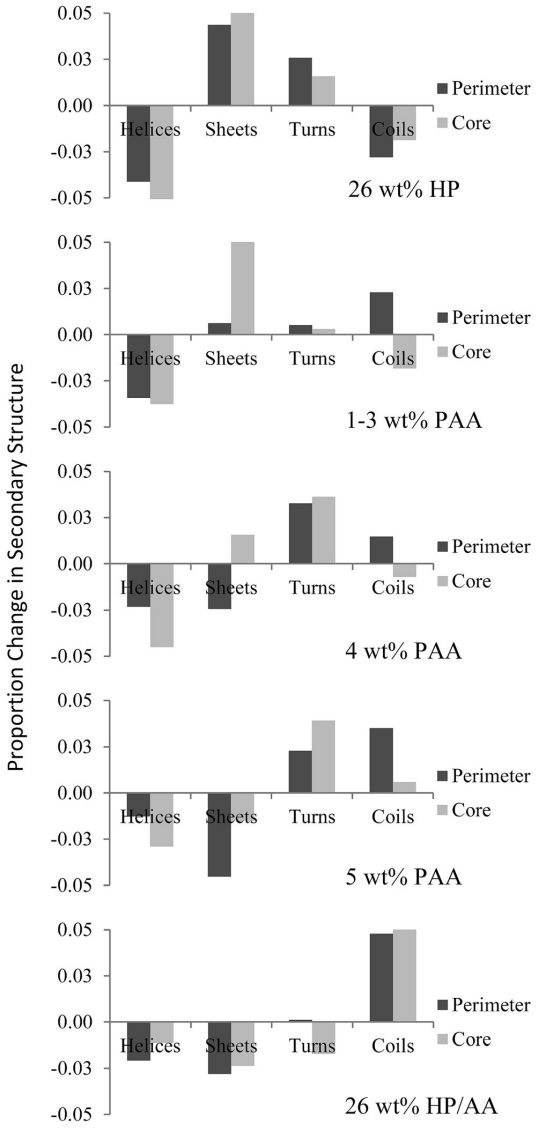

Fig. 2 Change in secondary structure composition at both the perimeter and the core relative to bloodmeal. Top: 26 wt% hydrogen peroxide, 1–3 wt%, 4 wt% and 5 wt% peracetic acid and bottom 26 wt% hydrogen peroxide with 6.6 wt% acetic acid.

structures found at the core of the particle and at higher PAA concentration the material is more likely to resemble the characteristics of the proteins located at the perimeter, as the perimeter would represent the greater mass.

Decolouring of bloodmeal with PAA was found to reduce the glass transition temperature from ~225 °C to ~35 to 45 °C using 3–5 wt% PAA.[2] The glass transition temperature occurs when there is sufficient energy provided to obtain large scale cooperative motion within the amorphous regions of a polymer. In

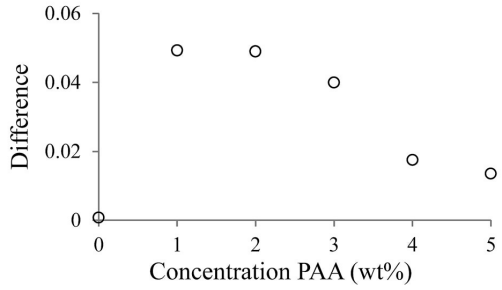

Fig. 3 Change in fractional composition of disordered structures (turns and coils) between the perimeter and the core of the particles after decolouring with PAA.

the case of a semi-crystalline material, both a glass transition temperature (T_g), at which the amorphous regions become mobile, and a higher melting temperature, where crystalline regions melt are observed.[34]

In bloodmeal, the T_g occurs above its degradation temperature (~200 °C) and decolouring with increasing concentrations of PAA resulted in a glass transition that is observed at progressively lower temperatures using DSC (Fig. 4).

The rapid drop in T_g from 225 °C to 80 °C after treatment with 1 wt% PAA indicates that oxidation has the strongest effect on T_g, and its reduction is caused by the disruption of stabilizing interactions, specifically the destruction of crosslinks within the aggregated proteins leading to much higher chain mobility. The destruction of cysteine crosslinks during PAA decolouring allows DBM to be processed into a thermoplastic without the addition of sodium sulphite.[2] Acetic acid also improves chain mobility and can be observed as a continual, but lesser reduction in T_g with treatment of up to 5 wt% PAA. One could therefore conclude that the change in T_g is caused by a change in primary structure *i.e.* chain mobility rather than the observed changes in secondary structure.

Bloodmeal and DBM showed an endothermic peak occurring below the glass transition temperature in the first DSC scans. In proteins, the helical and sheet structures undergo melting at temperatures exceeding ~175 °C at low moisture content,[35,36] indicating the endothermic event observed is not associated with the melting of these crystalline structures. This endothermic peak is reported for numerous proteins and is thought to be caused by physical aging,[37–39] a phenomenon which occurs when an amorphous polymer is maintained below its glass transition temperature.[39] It is able to undergo aging because when it is rapidly cooled to a glassy state from above its T_g, it is unable to physically reorient to an equilibrium conformation, causing the polymer to have a larger free volume, enthalpy and entropy than if it were in an equilibrium conformation.[40] As a result, the non-equilibrium material will undergo slow chain relaxation (through short-range, rotational reorientations) toward an equilibrium conformation.[41] The phenomena is dependent on time and the environment in which the polymer is maintained, where the extent of molecular relaxation is influenced largely by chain mobility and

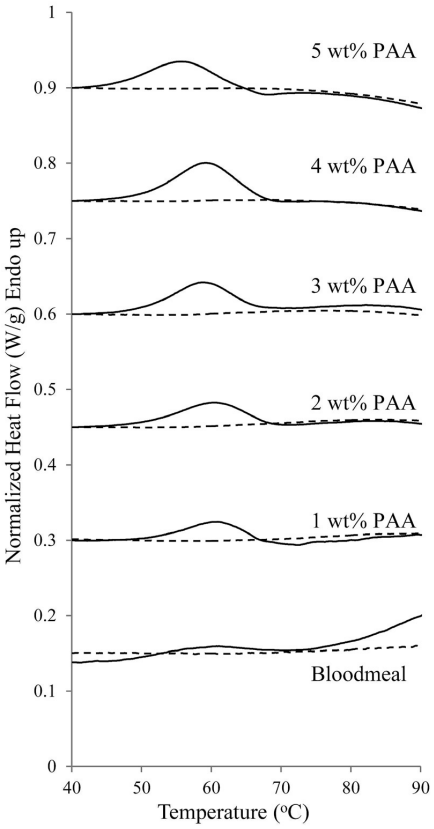

Fig. 4 DSC thermograms of bloodmeal and its decoloured counterparts using a heating rate of 10 °C min^{-1}. First scan solid line (—) and second scan dashed line (- -). Images have been stacked for clarity.

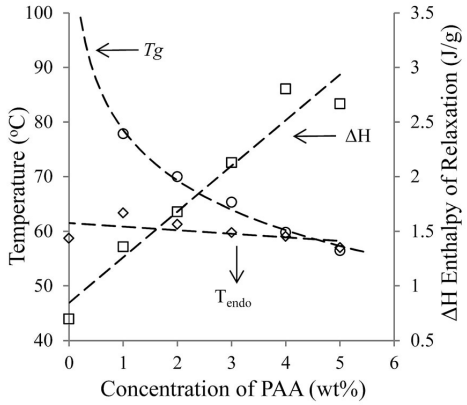

Fig. 5 Thermal transitioning temperatures; glass transition, occurrence of the endothermic peak maximum and specific enthalpy of relaxation (ΔH) after bloodmeal decolouring with peracetic acid during DSC with a heating rate of 10 °C min^{-1}. Results are an average of duplicate samples.

consequently increased temperature and plasticization (moisture content) during storage will cause a higher rate and extent of relaxation.[42]

When an aged polymer is heated above its T_g, it absorbs the heat lost during aging and recovers its lost free volume and is accompanied by the development of an endothermic peak at its glass transition, observed during DSC.[39] In decoloured bloodmeal, the temperature at which this endothermic peak occurred was found to decrease with increasing PAA concentration used (Fig. 5), indicating that less energy is required to mobilize the protein chains and is possibly a result of decreasing intermolecular interactions *via* oxidation and increasing acetic acid content providing plasticization.

The specific enthalpy of relaxation (ΔH) was also found to increase in size from 1–5 wt% PAA. Initially the specific enthalpy for bloodmeal was 0.69 J g^{-1}, and upon treatment with 1 wt% PAA increased to 1.4 J g^{-1}, up to 2.8 J g^{-1} at 4 and 5 wt% PAA, all significantly lower than the heat of fusion associated with melting of helical or sheet crystallites. The increase in peak area reflects a larger degree of "aging" per gram of material taking place during drying and storage.

Oxidation is the primary cause of the increase in ΔH by degrading ordered structures and destroying sterically hindering groups (such as aromatic amino acids) thereby improving chain regularity and allowing the protein chains to pack closer together. Due to their susceptibility to oxidation, it is expected that sulphur and aromatic amino acids, responsible for crosslinking and hydrophobic interactions within a protein chain, would be degraded. Oxidation of casein and whey proteins has been shown to cause formation of carbonyl compounds along with the destruction of tryptophan, methionine, tyrosine, histidine and lysine, and a decrease in free amino groups.[23] Destruction of these amino acids is also likely to occur during bloodmeal decolouring, leading to increased solubility[2] and higher chain mobility as evidenced by the reduction in T_g.

To a smaller extent, increasing acetate content may cause aging to occur more rapidly due to greater chain mobility, also facilitating closer packing. The effect of acetate ions on aging may become important when considering the final material produced from DBM, as aging is generally accompanied by a loss in mechanical properties due to lower reduced molecular mobility.[39]

The shape of the X-ray diffraction curves for PAA treated bloodmeal are similar to that of untreated bloodmeal, with similar diffraction angles observed for each characteristic peak (Fig. 6). For bloodmeal two main peaks were observed, one at 9°, corresponding to *d*-spacing of 9.9 Å, and an additional sharp peak at an angle of 19° with a shoulder appearing at 24°, corresponding to a *d*-spacing of 4.7 Å and 3.8 Å respectively. Peaks that correspond to these distances are often observed in proteins, and are thought to be attributable to α-helix or β-sheet structures.[43,44] A *d*-spacing of 4–5 Å corresponds to interstrand hydrogen bonding in β-sheets or backbone hydrogen bonding in α-helices, while a *d*-spacing of about 10.5 Å corresponds to

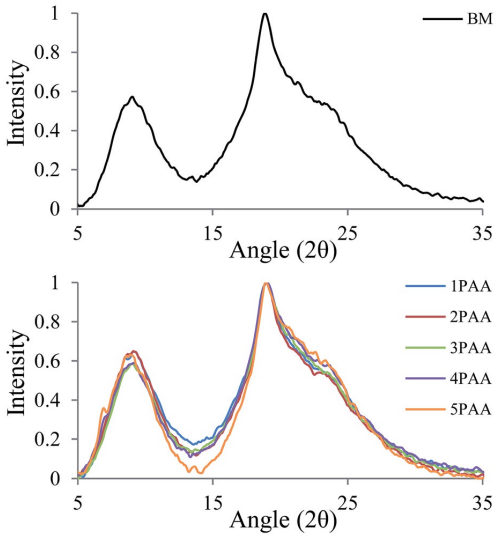

Fig. 6 Normalized WAXS of bloodmeal (top) and 1–5 wt% PAA treated bloodmeal (bottom).

inter-structure packing either intersheet or interhelix spacing for proteins containing β-sheets or α-helices.[45]

The peak observed at 9° was found at a slightly lower angle upon treating with 4–5 wt% PAA. Such a shift could be indicative of larger spacing occurring between adjacent sheets or helices, however, it represents ~0.5 Å difference, and although changes in hydrogen bonding interactions between adjacent ordered structures could explain this shift, it may in fact be variation about a mean. The shoulder appearing at ~24° increased in breadth and height with 4–5 wt% PAA concentration, also suggesting that destruction of ordered structures during oxidative decolouring leads to an increased amorphous content.

Equilibrium peracetic acid oxidants are responsible for breaking up intermolecular interactions between helical and random coil structures. Overcoming strong intermolecular interaction increases the mobility of these structures so that they are capable of rearranging into more highly aggregated sheet structures, most probably during drying (~75 °C). Further to this, acetic acid is largely responsible for disrupting the process of aggregation; during decolouring or drying in the form of the acetate ion. Acetic acid and its conjugate base are both known to strongly hydrogen bond to amino acids found along the backbone of proteins, leading to a lower degree of secondary structural order, and results in a larger quantity of amorphous material being present along with increased chain mobility.

At high PAA concentration an additional peak develops at ~7°, with a *d*-spacing of 12.6 Å. This peak is only observed in bloodmeal exposed to 4 or 5 wt% PAA, and is not present in samples which have been washed with water prior to drying and analysis. This peak may be an artefact of protein–acetate interactions but was not observed in bloodmeal mixed with sodium acetate salt or in bloodmeal pre-soaked in aqueous sodium acetate. However, the peak could originate as a result of separating adjacent sheets or helices apart by a further ~2.7 Å (compared with the main peak observed at 9.9 Å) through the incorporation of sodium or acetate ions between the structures of strongly oxidized structures. The only conclusion that can be drawn is that during decolouring with high concentration PAA, small water soluble compounds are generated, possibly due to salt–protein interaction or peptide chain scission and could influence the processing of DBM material into a thermoplastic in the future.

Conclusions

Bloodmeal decolouring leads to two distinct regions of differing secondary structure composition resulting from diffusion of peracetic acid components into the particle. The innermost region of the particle is found to contain a high portion of β-sheets, owing to exposure to the oxidant species, most probably hydrogen peroxide, while the perimeter region contains much higher random coil content due to the degradation of ordered structures. The disordered structures are most concentrated at the perimeter due to the concentration of acetic acid and oxidant being highest at the surface of the particle.

Therefore PAA decolouring of bloodmeal can be classified into three distinct stages, where the final composition of the protein is dependent on the peracetic acid concentration employed. At low PAA concentration, α-helices and random coils aggregate into β-sheet structures due to the presence of oxidants, at higher concentration the β-sheets begin to degrade into β-turns and at the highest concentration employed, degrade into coils due to increasing acetic acid and oxidant concentration.

Due to their susceptibility to oxidation, sulphur and aromatic amino acids responsible for crosslinking and hydrophobic interactions within a protein chain are degraded and lead to an increased solubility in water and SDS solutions, and higher chain mobility as evidenced by the reduction in T_g and improved mobility observed by the higher degree of aging with increasing PAA concentration.

Acknowledgements

This research was undertaken on the infrared microspectroscopy beamline at the Australian Synchrotron, Victoria, Australia. Proposal number AS132/IRMFI/6636. The authors would especially like to acknowledge the technical assistance of Dr Mark Tobin and Dr Danielle Martin. Travel funding support was received from the New Zealand Synchrotron Group Ltd.

References

1 Waikatolink Limited, *New Zealand Pat.*, 551531, 2010.
2 A. Low, C. J. R. Verbeek and M. C. Lay, *Macromol. Mater. Eng.*, 2014, **299**, 75–84.

3 B. Rangarajan, A. Havey, E. Grulke and P. Culnan, *J. Am. Oil Chem. Soc.*, 1995, **72**, 1161–1169.
4 F. M. C. Corporation, *Material safety data sheet: Peracetic acid 5% 79-21-0-3*, Philadelphia, 2006.
5 T. M. Florence, *J. Inorg. Biochem.*, 1985, **23**, 131–141.
6 A. Low, Ph.D. Thesis, University of Waikato, 2012.
7 A. Low, J. Verbeek, M. Lay and J. Swan, *Biochem. Biotechnol.*, 2012, **42**, 29–43.
8 E. Nagababu and J. M. Rifkind, *Biochem. Biophys. Res. Commun.*, 1998, **247**, 592–596.
9 E. Nagababu and J. M. Rifkind, *Biochem. Biophys. Res. Commun.*, 2000, **273**, 839–845.
10 E. Nagababu and J. M. Rifkind, *Antioxid. Redox Signaling*, 2004, **6**, 967–978.
11 Centre National de la Recherche Scientifique CNRS, Universite des Sciences et Techniques, *USA Pat.*, 4650589, 1987.
12 E. Nagababu and J. M. Rifkind, *Biochemistry*, 2000, **39**, 12503–12511.
13 Y. Seto, M. Kataoka and K. Tsuge, *Forensic Sci. Int.*, 2001, **121**, 144–150.
14 Y. Yan, Q. Wang, H. He and H. Zhou, *Biophys. J.*, 2004, **86**, 1682–1690.
15 P. Labrude, B. Chaillot and C. Vigneron, *Cryobiology*, 1984, **21**, 33–38.
16 J. F. Black and J. K. Barton, *Photochem. Photobiol.*, 2004, **80**, 89–97.
17 J. F. Black, N. Wade and J. K. Barton, *Lasers Surg. Med.*, 2005, **36**, 155–165.
18 H. Jansson and J. Swenson, *J. Chem. Phys.*, 2008, **128**, 245104.
19 C. Liu, A. Bo, G. Cheng, X. Lin and S. Dong, *Biochim. Biophys. Acta, Protein Struct. Mol. Enzymol.*, 1998, **1385**, 53–60.
20 T. M. Hicks, C. J. R. Verbeek, M. C. Lay and M. Manley-Harris, *J. Am. Oil Chem. Soc.*, 2013, 1–11.
21 M. Unis, Ph.D. Thesis, University of Northumbria, 2010.
22 W. Zhang, S. Xiao and D. U. Ahn, *Crit. Rev. Food Sci. Nutr.*, 2013, **53**, 1191–1201.
23 B. Kerkaert, F. Mestdagh, T. Cucu, P. R. Aedo, S. Y. Ling and B. De Meulenaer, *J. Agric. Food Chem.*, 2011, **59**, 907–914.
24 S. Malkov, M. Živković, M. Beljanski, M. Hall and S. Zarić, *J. Mol. Model.*, 2008, **14**, 769–775.
25 P. Y. Chou and G. D. Fasman, *Biochemistry*, 1974, **13**, 211–222.
26 S. Costantini, G. Colonna and A. M. Facchiano, *Biochem. Biophys. Res. Commun.*, 2006, **342**, 441–451.
27 M. Levitt, *Biochemistry*, 1978, **17**, 4277–4285.
28 K. J. Davies and M. E. Delsignore, *J. Biol. Chem.*, 1987, **262**, 9908–9913.
29 P. Yu, *Br. J. Nutr.*, 2004, **92**, 869–885.
30 P. Yu, J. J. McKinnon, C. R. Christensen and D. A. Christensen, *J. Agric. Food Chem.*, 2004, **52**, 7353–7361.
31 J. Bier, C. Verbeek and M. Lay, *J. Therm. Anal. Calorim.*, 2013, 1–9.
32 J. M. Bier, C. J. R. Verbeek and M. C. Lay, *J. Appl. Polym. Sci.*, 2013, **130**, 359–369.
33 S. Cai and B. R. Singh, *Biophys. Chem.*, 1999, **80**, 7–20.
34 J. M. Bier, C. J. R. Verbeek and M. C. Lay, *Macromol. Mater. Eng.*, 2014, **299**, 524–539.
35 J. Cao, *Thermochim. Acta*, 1999, **335**, 5–9.
36 X. Hu, Q. Lu, D. L. Kaplan and P. Cebe, *Macromolecules*, 2009, **42**, 2079–2087.
37 C. Bengoechea, A. Arrachid, A. Guerrero, S. E. Hill and J. R. Mitchell, *J. Cereal Sci.*, 2007, **45**, 275–284.
38 A. Farahnaky, F. Badii, I. A. Farhat, J. R. Mitchell and S. E. Hill, *Biopolymers*, 2005, **78**, 69–77.
39 X. Mo and X. Sun, *J. Polym. Environ.*, 2003, **11**, 15–22.
40 J. W. Lawton and Y. V. Wu, *Cereal Chem.*, 1993, **70**, 471–475.
41 L. C. E. Struik, *Physical aging in amorphous polymers and other materials*, Elsevier, Amsterdam, 1978.
42 F. Badii, W. MacNaughtan and I. A. Farhat, *Int. J. Biol. Macromol.*, 2005, **36**, 263–269.
43 C. S. Thomas, M. J. Glassman and B. D. Olsen, *ACS Nano*, 2011, **5**, 5697–5707.
44 Y. Wang, F. L. Filho, P. Geil and G. W. Padua, *Macromol. Biosci.*, 2005, **5**, 1200–1208.
45 W. Elshemey, A. Elfiky and W. Gawad, *Protein J.*, 2010, **29**, 545–550.

Table 2: Summary of basic statistics for bloodmeal (BM) before and after decolouring (DBM) with peracetic acid (PAA), hydrogen peroxide (HP) or HP with acetic acid (HP/AA). Student T-tests were performed comparing the perimeter and core to the total average and the perimeter and the core to each other. Statistically significant ($p < 0.05$) results are highlighted.

	α-helices			β-turns			random coils			β-sheets			disordered structures		
Sample	Av.	Std. dev.	t-test	Av.	Std. dev.	t-test	Av.	Std. dev.	t-test	Av.	Std. dev.	t-test	Av.	Std. dev.	t-test
Bloodmeal															
Total	0.19	0.04		0.15	0.04		0.20	0.06		0.46	0.06		0.34	0.07	
Perimeter average	0.19	0.05	0.27	0.15	0.05	0.31	0.19	0.08	0.57	0.47	0.07	0.51	0.34	0.09	0.96
Core average	0.20	0.03	0.20	0.15	0.04	0.28	0.19	0.04	0.46	0.47	0.05	0.44	0.34	0.05	0.95
Perimeter vs Core			0.04			0.07			0.29			0.23			0.93
1% PAA															
Total	0.16	0.05		0.15	0.06		0.20	0.07		0.49	0.09		0.35	0.08	
Perimeter average	0.16	0.05	0.26	0.16	0.06	0.08	0.21	0.08	0.00	0.47	0.09	0.00	0.37	0.09	0.00
Core average	0.17	0.05	0.25	0.14	0.05	0.03	0.18	0.06	0.00	0.51	0.07	0.00	0.32	0.07	0.00
Perimeter vs Core			0.00			0.00			0.00			0.00			0.00
2% PAA															
Total	0.15	0.04		0.15	0.05		0.20	0.07		0.49	0.08		0.36	0.08	
Perimeter average	0.15	0.04	0.90	0.15	0.05	0.68	0.24	0.08	0.00	0.47	0.08	0.01	0.38	0.08	0.01
Core average	0.15	0.04	0.73	0.15	0.05	0.92	0.18	0.06	0.00	0.52	0.07	0.00	0.33	0.07	0.00
Perimeter vs Core			0.69			0.75			0.00			0.00			0.00
3% PAA															
Total	0.17	0.03		0.15	0.04		0.19	0.07		0.49	0.06		0.34	0.06	
Perimeter average	0.17	0.04	0.43	0.15	0.04	0.81	0.21	0.08	0.00	0.47	0.06	0.00	0.36	0.07	0.00
Core average	0.17	0.03	0.41	0.15	0.04	0.81	0.17	0.05	0.00	0.51	0.04	0.00	0.32	0.05	0.00
Perimeter vs Core			0.17			0.68			0.00			0.00			0.00
4% PAA															
Total	0.16	0.04		0.18	0.05		0.20	0.07		0.46	0.08		0.38	0.07	
Perimeter average	0.17	0.05	0.04	0.18	0.05	0.76	0.21	0.08	0.18	0.44	0.08	0.02	0.39	0.09	0.33
Core average	0.15	0.03	0.00	0.18	0.05	0.70	0.19	0.06	0.07	0.48	0.06	0.00	0.37	0.07	0.15
Perimeter vs Core			0.00			0.55			0.01			0.00			0.04
5% PAA															
Total	0.17	0.04		0.18	0.05		0.22	0.07		0.43	0.06		0.39	0.07	
Perimeter average	0.18	0.04	0.00	0.17	0.05	0.01	0.23	0.07	0.00	0.42	0.07	0.00	0.40	0.08	0.01
Core average	0.16	0.03	0.00	0.18	0.04	0.01	0.20	0.06	0.09	0.45	0.05	0.13	0.39	0.06	0.83
Perimeter vs Core			0.00			0.00			0.00			0.00			0.01
HP															
Total	0.14	0.06		0.17	0.06		0.17	0.09		0.52	0.11		0.34	0.10	
Perimeter average	0.15	0.06	0.06	0.17	0.06	0.19	0.17	0.09	0.44	0.51	0.12	0.29	0.34	0.11	0.94
Core average	0.14	0.06	0.10	0.16	0.06	0.23	0.18	0.08	0.42	0.52	0.10	0.34	0.34	0.09	1.00
Perimeter vs Core			0.00			0.02			0.17			0.06			0.89
HP /AA															
Total	0.17	0.04		0.13	0.05		0.23	0.09		0.43	0.07		0.39	0.08	
Perimeter average	0.17	0.05	0.94	0.15	0.06	0.60	0.24	0.11	0.02	0.44	0.08	0.02	0.40	0.10	0.00
Core average	0.18	0.03	0.32	0.13	0.04	0.11	0.25	0.07	0.00	0.44	0.05	0.00	0.38	0.06	0.24
Perimeter vs Core			0.15			0.03			0.75			0.48			0.08

5

Changes to Amino Acid Composition of Bloodmeal after Chemical Oxidation

By

TALIA M. HICKS, C. J. R. VERBEEK, M. C. LAY

AND

M. MANLEY-HARRIS

Published in RSC Advances

I prepared the draft manuscript of this journal paper, which was refined and edited in consultation with my supervisors, whom are credited as co-authors. I was responsible for sample preparation, determining yield, solubility and molecular mass distribution. The crude protein, amino acid analysis and ICP-MS were carried out by external parties, however, I was responsible for the data handling and analysis. The FT-IR results reported here were collected in collaboration with my supervisors (and Dr. J. Bier) during beamtime at the Australian Synchrotron. The main experiments from that beamtime are reported in Chapters 4, 6 and 7 but the data reported here considers a different region of the FT-IR spectrum.

RSC Advances

PAPER

View Article Online
View Journal | View Issue

Cite this: *RSC Adv.*, 2015, **5**, 66451

Changes to amino acid composition of bloodmeal after chemical oxidation†

T. M. Hicks,*[a] C. J. R. Verbeek,[a] M. C. Lay[a] and M. Manley-Harris[b]

Received 4th June 2015
Accepted 28th July 2015

DOI: 10.1039/c5ra10587k

www.rsc.org/advances

Bovine-derived bloodmeal can be decoloured using peracetic acid, extruded and injection moulded into a yellow translucent bioplastic. This plastic has different properties to extruded and injection moulded bloodmeal, in that it does not require sodium sulfite or urea to be extrudable. The effect of oxidation on the physical and chemical characteristics of the proteins during bloodmeal decolouring with PAA was studied by assessing changes in the amino acid profile. Polymer interactions, hydrophilicity and the destruction of cysteine crosslinks were measured indirectly by assessing protein solubility, molecular weight distribution and by synchrotron FT-IR analysis. Increasing peracetic acid concentration resulted in an increased loss of iron due to destruction of the porphyrin groups, increased solubility due to destruction or conversion of aromatic amino acids into hydrophilic groups, destruction of lysine, reduced protein content due to increased salt content in the final product, and a larger amount of smaller protein peptides but with a similar average molecular weight to bloodmeal. Amino acid analysis showed an increase in cysteine content in the product, FT-IR of the sulfur groups revealed that these were heavily oxidised, such that some would be unable to participate in disulfide bonds thereby increasing protein solubility.

Introduction

A yellow translucent bioplastic has been produced from bloodmeal by decolouring it using commercial peracetic acid (PAA) followed by extrusion.[1–3] Decolouring bloodmeal using 3–5 wt% PAA has been found to result in the lowering of the glass transition temperature from ~225 °C to ~35–45 °C[2] and also to require different processing aids for extrusion. In contrast to thermoplastic prepared from untreated bloodmeal, once decoloured, bloodmeal no longer required sodium sulfite reduction of the cysteine crosslinks in order to be extruded.[2]

Peracetic acid, which is an equilibrium mixture of peracetic acid, hydrogen peroxide and acetic acid, has been used extensively since the early 1940s due to growing concerns over the environmental impact of chlorine. It is used as a bleaching agent for textiles, as a disinfectant,[4–7] as well as in wastewater treatment. It does not form harmful disinfection by-products and decomposes safely when discharged into the environment.[8,9]

Common oxidants such as hydrogen peroxide are unable to degrade all of the haem present in bloodmeal due to the various oxidation states of haem-iron in haemoglobin.[3,10] However, peracetic acid adequately removed the colour from bloodmeal, with each component of the PAA solution performing a specific function in the overall decolouring and deodorising mechanisms.[10]

The presence of several reactive species and the formation of free radicals, resulted in oxidative damage to the proteins as the radicals underwent auto-reduction reactions.[11] Consequently, treating proteins with oxidising agents leads to undesired side effects, including modification of amino acid residues, protein hydrolysis or chain cleavage and protein aggregation.[7,12] The type of damage and the extent of modification varied depending on the reduction potential and concentration of the oxidant, as well as the presence of other species which exhibited anti-oxidant or free radical scavenging properties.

Bleaching wool with performic or peracetic acid selectively oxidised cystine (disulfide crosslinks), methionine and tryptophan side chains with minimal degradation of the other amino acids.[13] However, a later study indicated that performic acid also degraded serine, threonine, tyrosine, phenylalanine and histidine, while PAA oxidation resulted in the conversion of all cystine to cysteic acid, with only small losses of tyrosine, phenylalanine and histidine.[14] Oxidation of cystine bonds also occurs during hydrogen peroxide bleaching of human hair (keratin is highly crosslinked as a result of disulfide bonds between cysteine residues). As a result, oxidation of hair and wool by hydrogen peroxide or peracetic acid led to a loss in tensile strength proportional to the number of cystine residues degraded.[15–17] Oxidation of bovine serum albumin and aldolase proteins with PAA was found to induce chain fragmentation.[18]

[a]*School of Engineering, Faculty of Science and Engineering, University of Waikato, Private Bag 3105, Hamilton 3240, New Zealand. E-mail: tahicks@waikato.ac.nz*
[b]*School of Science, Faculty of Science and Engineering, University of Waikato, Private Bag 3105, Hamilton 3240, New Zealand*

† Electronic supplementary information (ESI) available. See DOI: 10.1039/c5ra10587k

Oxidation of amino acids in proteins is dependent on oxidant strength, concentration, pH and a range of other chemical conditions. The most recent investigation into the effect of PAA oxidation on dairy proteins, indicated that the amount of carbonyl groups increased while thiol (SH) groups decreased; tryptophan and methionine were most vulnerable to oxidation while lysine was not affected.[7] Neither peptide cleavage, nor protein aggregation occurred to any significant extent.[7] This is probably as a result of the protective effect of short chain carboxylic acids (or their salts) on proteins exposed to hydrogen peroxide, which has been attributed to their action as chelating agents (inhibiting Fenton-type reactions) or as scavengers of reactive oxygen species and free radicals;[19,20] both of the latter cause protein hydrolysis. This concurs with peracetic acid decolouring of bloodmeal, in which the presence of acetic acid (or sulfuric acid) inhibited the reactivity of hydrogen peroxide.[10]

Helices, sheets, turns and coils which define the secondary structure of the protein are modified by oxidation.[21,22] Amino acids show a propensity to form particular types of secondary structures, with most amino acids showing preference for only one type (Table 1),[23] although, the periodicity and positioning of polar and non-polar residues in the amino acid sequence is known to have a greater influence on a peptide's final secondary structure.[24] Selective oxidation of certain amino acids may influence the formation of specific secondary structures by changing the ability to form H bonds between C=O and NH groups.

The sensitivity of particular amino acid residues to oxidation by oxidants has been shown to vary between proteins and results from their position and interaction within the protein structure.[25]

Oxidation of amino acids has been shown to cause increases in local flexibility or rigidity in the protein chain, leading to an alteration in its secondary structure,[21,26] which directly influences its physical and material properties.[27–33]

Protein oxidation may therefore adversely affect the properties and processing characteristics of proteinous bioplastics. Minor modification to amino acid residues may result in less contribution to stabilising interactions, but excessive changes may result in decreased mechanical properties such as strength, stiffness and elongation. Furthermore, protein hydrolysis or fragmentation could result in poor consolidation due to reduced chain entanglement, and along with degradation of potential crosslinking sites (through the destruction of cysteine, tyrosine and lysine residues) could result in a material with poor mechanical properties.[2]

This paper describes the effect of oxidation during bloodmeal decolouring using PAA on the physical and chemical characteristics of the proteins manifested by changes in the amino acid profile. Polymer interactions and hydrophilicity were measured indirectly by assessing protein solubility and molecular weight distribution, while the destruction of cysteine crosslinks was measured *via* synchrotron FT-IR analysis.

Table 1 Propensity of amino acids for α-helical, β-sheet or β-strands and other secondary structures types.[23,34–36] Other secondary structure types include turns, bends, 3-helix and random coils

Helical	Sheet or strand	Other
Alanine	Isoleucine	Glycine
Leucine	Phenylalanine	Proline
Methionine	Tryptophan	Asparagine
Glutamine	Valine	Aspartic acid
Glutamic acid	Tyrosine	Serine
Arginine	Threonine	Histidine
Lysine	Cysteine	

Experimental

Materials

Bovine bloodmeal was obtained from Wallace Corporation Ltd, New Zealand and sieved to utilise particles under 710 μm. Peracetic acid, an equilibrium mixture of peracetic acid, hydrogen peroxide, acetic acid and water (Proxitane Sanitizer 5%) was purchased from Solvay Interox Pty Ltd Auckland, New Zealand and diluted with distilled water to the appropriate concentration for decolouring (Table 2). Hydrogen peroxide (30 wt% EMSURE, ISO) was purchased from Merck, Auckland, New Zealand. Analytical grade glacial acetic acid, sodium hydroxide, sodium dodecyl sulfate, sodium chloride, monosodium phosphate and disodium phosphate were purchased from Thermo-Fisher Scientific, Auckland, New Zealand.

Bloodmeal decolouring

Bloodmeal was decoloured by adding 450 g of a 1–5 wt% peracetic acid solution, or 26 wt% hydrogen peroxide (with or without 6.6 wt% acetic acid) to 150 g bloodmeal and reacting the mixture under constant agitation for 10 min in a Kenwood mixer (KM080) to ensure homogenous decolouring.[37] This mixture was diluted with distilled water (300 g) and immediately neutralised with 1 mol L^{-1} sodium hydroxide and filtered. The decoloured bloodmeal was oven dried overnight (75 °C) and passed through an IKA® MF 10 Basic Microfine Grinder (Sigma-Aldrich, Auckland, New Zealand) fitted with a 1 mm sieve plate at 3000 rpm, with a residence time of less than 10 seconds.

Yield, protein recovery and moisture content

A mass balance before and after the decolouring process (Fig. 1) was used to determine yield and recovery, according to eqn (1) and (2).

$$\text{Yield} = \frac{\text{DBM}_s \times (1 - \text{MC}_{out})}{\text{BM}_s \times (1 - \text{MC}_{in})} \quad (1)$$

$$\text{Protein recovery} = \frac{\text{M(protein)}_{out}}{\text{M(protein)}_{in}} \quad (2)$$

where BM_s is the mass of bloodmeal (g), DBM_s is decoloured bloodmeal mass, MC_{in} and MC_{out} are the moisture content of the solids in and out (wt%) and PC_{in} and PC_{out} are the protein content of the solids in and out on a dry basis (wt%). $M(protein_{in})$ and $M(protein_{out})$ represents the solid mass of protein into and out of the decolouring process, where M

Table 2 Dilution scheme and composition of solutions of equilibrium peracetic acid used for decolouring bloodmeal

Solution	Peracetic acid (wt%)	Hydrogen peroxide (wt%)	Acetic acid (wt%)	Water (wt%)
1 wt% PAA	1.1	5.2	2.2	91.5
2 wt% PAA	2.5	10.4	4.4	82.7
3 wt% PAA	3.6	15.6	6.6	74.2
4 wt% PAA	4.5	20.8	8.8	65.9
5 wt% PAA	5.6	26.0	11.0	5

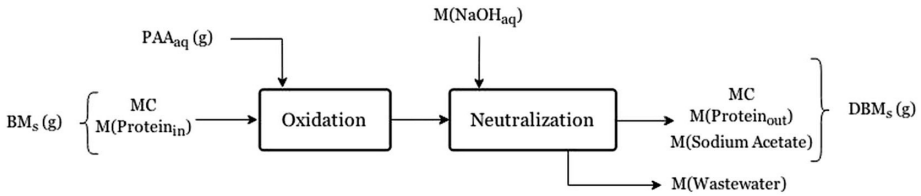

Fig. 1 Schematic of the decolouring process, showing all streams in and out. This was used to determine the yield of solids and protein recovery upon decolouring.

(protein$_{in}$) is equal to $BM_s \times (1 - MC_{in}) \times PC_{in}$ and M(protein$_{out}$) is equal to $DBM_s \times (1 - MC_{out}) \times PC_{out}$.

Moisture content and thermogravimetric analysis. The moisture content obtained for decoloured samples was determined by oven drying of the material (1.00 g) at 100 °C for 12 hours. This moisture content was used for calculating protein recovery, soluble fraction and crude nitrogen.

Mass loss of freeze-dried DBM samples (~10 mg) in a 0.9 g ceramic crucible was recorded during heating in dry air at 10 °C min^{-1} to 800 °C in a Texas Instruments SDT 2960 analyser. Moisture content was determined from the cumulative mass loss up to 120 °C. This moisture content was used to adjust results for amino acid analysis and ICP-MS.

Soluble protein fraction

The soluble fraction of decoloured bloodmeal was determined by boiling a sample (1.00 g) in 2 wt% SDS solution (200 mL) under reflux for 5 min. Samples were centrifuged at 4200 rpm (relative centrifugal force of 4102 × *g*) for 10 min using a Sigma 6-15 Centrifuge fitted with a Sigma swing-out rotor (Nr 11 150) and four Sigma buckets (Nr 13 520) (John Morris Scientific, Auckland, New Zealand). The supernatant was decanted through a filter and any solids retained. The insoluble pellet was washed three times using ~45 mL distilled water (centrifuging and decanting each sequential wash and filtering the supernatant to retain any solids). Washed samples and recovered solids (from each washing stage combined) were oven dried at 100 °C overnight. The soluble protein fraction was calculated using eqn (3).

$$\text{Soluble protein fraction} = 1 - \frac{\text{Total recovered solids}}{\text{Solids}_{in} \times (1 - MC_{in}) \times PC_{in}} \quad (3)$$

where solids$_{in}$ is the mass of solids initially present, MC_{in} is the moisture content of those solids and PC_{in} is the protein content of the solids.

Molecular weight distribution

The soluble fraction of decoloured bloodmeal was obtained using the method described above, however due to solubility limitations, bloodmeal required additional concentration by boiling for a further 10 minutes. Each sample was injected (50 μL) into a Superdex 200 gel filtration column (GE Healthcare) connected to an Akta Explorer 100 FPLC system (GE Healthcare). The column was calibrated using standards from high and low molecular weight gel filtration calibration kits comprised of aprotinin, ribonuclease A, ferritin and thyroglobulin (GE Healthcare Ltd, Auckland, New Zealand), along with bovine serum albumin fraction V, β-lactoglobulin, cytochrome C and vitamin B12 (Sigma-Aldrich, Auckland, New Zealand), see ESI.† Two column volumes of 0.02 mol L^{-1} phosphate running buffer (pH 7, 0.1 wt% SDS, 0.1 mol L^{-1} NaCl) was applied at a flow rate of 0.5 mL min^{-1}. Protein concentration was measured at 215 nm using an inline ultraviolet detector. The volume-average molecular weight ($\bar{M}_v$) was calculated using eqn (4), where V_i is equal to the fractional elution volume of molecules with molecular weight M_i.

$$\overline{M}_v = \frac{\sum_i^{\infty} V_i M_i}{\sum_i^{\infty} V_i} \quad (4)$$

Crude protein (total nitrogen)

Total nitrogen was analysed independently at the Waikato Stable Isotope Unit (University of Waikato, New Zealand) using an Elementar Isoprime 100 analyser, with a precision of ±1%. Each sample type was prepared once, combusted and the resulting gases separated by gas chromatography and analysed using continuous-flow mass spectrometry. All samples were referenced to a urea standard traceable to atmospheric nitrogen. Crude protein content was determined by multiplying

the total weight of nitrogen present in each sample on a dry basis by a factor of 6.25, which has been deemed an accurate Jones' factor for conversion of total nitrogen in bloodmeals.[38]

Amino acid analysis

Amino acid analysis was carried out independently by an accredited laboratory (AgResearch Ltd, Palmerston North, New Zealand), *via* ion-exchange chromatography using post-column derivatisation with ninhydrin. Digestion of the sample to liberate amino acids was carried out according to AOAC 1990 standard methods 982.39 (acid hydrolysis), 988.15 (base hydrolysis to quantify tryptophan) and 985.28 (to quantify cysteine and methionine).[39] Amino acids were quantified on the basis of known amounts of standards and their retention times. Each freeze dried sample was prepared once, and analysed six times for each digestion method. The percentage relative standard deviation (% RSD) reported for each amino acid was obtained over 500 observations. Raw data is given in the ESI.†

Elemental iron and sulfur analysis

Bloodmeal and decoloured bloodmeal (0.25 g) were digested in 50 mL centrifuge tubes containing 65% nitric acid (4 mL) and 30% hydrogen peroxide (2 mL). The tubes were capped and left overnight before heating to 80 °C for 1 hour, obtaining total dissolution. The cooled digest was made up to 200 mL using 17.9 MΩ MilliQ deionised water, and filtered using a 0.45 μm Millipore syringe filter. Analysis was carried out in triplicate on each sample.

Inductively coupled plasma mass spectrometry was carried out independently at the Waikato Mass Spectrometry Facility (University of Waikato, New Zealand) and was used to measure iron and other selected alkali, alkaline earth, heavy and volatile metals of each digest using a Perkin Elmer Elan DRC II ICP-MS equipped with an ASX-320 auto-sampler. Calibration was carried out with five increasing dilutions of ICP multi-element standard solution XXI and IV and 10 000 μg mL^{-1} SCP Science standards (sulfur, sodium, potassium, calcium and iron) diluted to within a working range (similar to sample concentration). Total sulfur was analysed in dynamic reaction cell (DRC) mode with oxygen used as the reacting gas, measuring the SO^+ ion at m/z 49. Similarly, five calibration standards were prepared from a 1000 ppm stock solution of sulfur. Deionised water of 17.9 MΩ resistance was used for all preparation of blanks, standards and for quality assurance.

Synchrotron FT-IR microscopy

Spatially resolved FT-IR experiments were undertaken on the infrared micro-spectroscopy beam line at the Australian Synchrotron, Victoria, Australia. Individual particles of bloodmeal and decoloured bloodmeal were compressed in a diamond cell and then transferred to a barium fluoride slide. This was placed in a Linkam temperature controlled stage connected to a Bruker Hyperion 3000 with an MCT collector and XY stage. The stage was set to 24 °C and purged with nitrogen gas. A grid containing ~130 points was mapped on each particle using a 10 × 10 μm spot size. Thirty-two spectra were collected in transmission mode with a resolution of 4 cm^{-1} between 3900 and 700 cm^{-1} and averaged using Opus 7.2 software (Bruker Optik GmbH 2013) according to Bier *et al.*[40,41]

Data and statistical analysis. Data was filtered for a minimum area under the amide III region to exclude points mapped outside particles from the analysis. Integration of the absorbance bands expected for cystine oxidation (cysteine monoxide, dioxide, thiosulfate and sulfonic acid) was carried out using an Opus type B integral (OPUS 7.2) and divided by the total amide III area from 1330–1180 cm^{-1} (Table 3).

Results and discussion

The primary purpose for bleaching bloodmeal is to degrade the haem chromogen by cleaving some of the conjugated methylene bridges in the haem porphyrin, forming yellow and colourless products known as propentdyopents.[46] The destruction of the ferric haem species results in an overall loss of iron (Fig. 2) as free ferric ions are highly soluble in an acidic environment and are subsequently lost during the neutralisation and filtering stages of decolouring.

Using 1–2 wt% PAA resulted in minimal decolouring,[10] most likely due to insufficient degradation of the haem species present, accompanied by minimal loss of iron (Fig. 2). At least 3 wt% PAA is required for adequate decolouring, and improved haem degradation is evidenced from a significant loss of iron. At 5 wt% PAA a gel-like mixture formed, trapping free iron, which can be removed by washing with distilled water to give an iron content of 1.04 mg g^{-1} BM.

By contrast, decolouring with HP led to no loss of iron, supporting the observation that HP is not an effective oxidant for decolouring bloodmeal.[10] Acetic acid increased iron solubility and is often used to strip iron from solubilised haemin during the preparation of protoporphyin from red blood cells,[47] despite lower HP consumption and an accompanying lower decolouring efficacy.[10]

Both PAA and HP are strong oxidants known to form various reactive oxygen and free radical species. In addition to decolouring, these highly reactive oxidising species are likely to result in oxidative damage to the protein, including modification of amino acid residues, protein hydrolysis, cleavage of covalent crosslinks and protein aggregation.[7] Such modifications to the BM proteins will influence the yield from the bleaching reaction as well as the physical properties of proteins thus obtained.

Yield and protein solubility

Bloodmeal is known to contain 80–100 wt% protein, as well as 1–2 wt% lipids.[48–57] The total nitrogen assay estimated the protein content of bloodmeal to be approximately 100 wt% protein (1 wt% error), and this was reduced to 89 wt% protein after decolouring (Fig. 3).

Low concentrations of PAA led to very low total mass loss in contrast to the use of HP alone (Table 4). Mass loss (or gain) could either be from loss of protein (due to dissolution, or experimental error) or by precipitation of sodium acetate during neutralisation. Considering the mass loss observed, salt precipitation (which would lead to an increase in mass) must be

Table 3 Peak assignment in the amide III region[42] and cystine oxidation products.[43–45] Each oxidation product has been given a roman numeral for ease of reference

Name and number	Structure	Functional group	Wavenumber (cm^{-1})
Amide III region	CHNH	νCN, N–H bending	1330–1180
Cystine dioxide (IV, V, VI)	Cys–SO_2–S–Cys	Cys–SO_2–S–Cys	1135–1120
Cystine monoxide (III)	Cys–SO–S–Cys	Cys–SO–S–Cys	1087–1072
Cysteine sulfonic acid (IX, cysteic acid)	Cys–SO_3H	ν_sS=O sulfonate	1050–1036
Cysteine-*S*-sulfonate (X)	Cys–S–SO_3^-	ν_sSS=O thiosulfonate	1020–1005

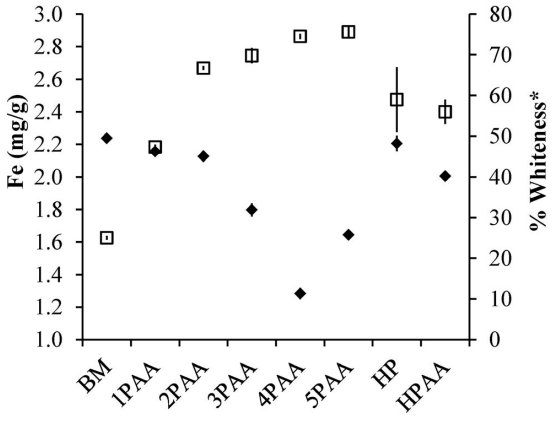

Fig. 2 Concentration of iron (◆) in mg g^{-1} of bloodmeal and decoloured bloodmeal treated with 1–5 wt% PAA or 26 wt% HP with and without 6.6 wt% acetic acid. Washing DBM treated with 5 wt% PAA gives an iron content of 1.04 mg g^{-1} (not shown on graph). Note: percentage whiteness[10] (□) is given for each treatment, in this case HP solutions are 30 wt%.

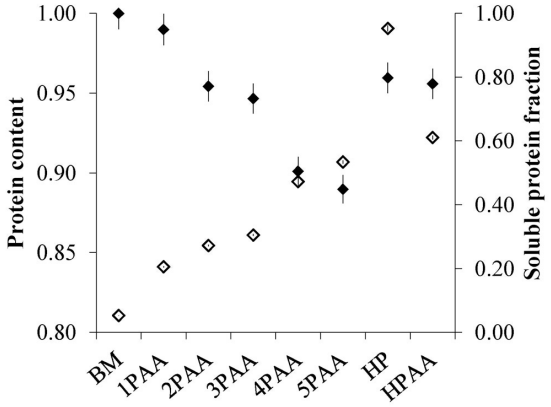

Fig. 3 Fractional protein content (◆) and soluble protein fraction (◇) of bloodmeal and decoloured bloodmeal treated with 1–5 wt% PAA or 26 wt% HP with and without 6.6 wt% acetic acid.

Table 4 Yield and protein recovery (dry mass basis) during decolouring using 1–5 wt% peracetic acid (PAA) or 26 wt% HP with and without 6.6 wt% acetic acid

	1PAA	2PAA	3PAA	4PAA	5PAA	HP	HPAA
Yield (wt%)	98.8	101.7	95.5	97.6	98.8	78.8	92.7
Protein recovery (wt%)	97.6	96.8	90.2	87.8	87.7	75.4	84.5

accompanied by a compensatory loss of solids, probably protein. The loss of protein was probably caused by dissolution and fragmentation, however, evidence is conflicting regarding the occurrence of chain scission.[7,18] In contrast, use of HP alone led to significant loss of protein, which was somewhat inhibited by acetic acid. Acetic acid is known to act as an antioxidant in hydrogen peroxide,[20] preventing the formation of hydroxyl radicals which are purported to cause protein hydrolysis.[58]

The increase in protein solubility undergoes a step change around 3–4 wt% PAA (Fig. 3), and corresponds with the previously observed rates of change for the consumption of oxidants and bleaching efficacy (percentage whiteness).[10] This is an indication that the change in observed solubility is due to the extent of oxidation (molecular weight, structure and chemical interactions within and between the proteins) and not due to the salt content resulting from neutralisation. Increased protein solubility in aqueous buffers is often correlated with a reduction in cysteine crosslinks, increased carbonyl content (and hydrophilicity) as well as hydrolysis/peptide cleavage.[7]

Molecular weight distribution

Two large peaks at 14 mL and 16 mL (~67 kDa and 34 kDa) were detected in the FPLC chromatogram of the soluble fraction of bloodmeal (Fig. 4A). These peaks represent the tetrameric and dimeric forms of haemoglobin, which are known to be in equilibrium in blood.[59,60] After oxidation, a new peak emerged at 18.5 mL, corresponding to a molecular weight of ~8.8 kDa. This could be due to hydrolysis or chain cleavage, as observed by others for BSA or aldolase exposed to PAA.[18] Treatment with high levels of oxidant (5 wt% PAA, HP and HP with acetic acid) also resulted in a loss of resolution, which also indicated fragmentation of protein aggregates present in BM.

However, molecular weight analysis is limited to soluble proteins, and the insoluble fraction could have a completely different average molecular weight and/or distribution. For bloodmeal, the soluble fraction would probably be the smaller size fraction as the larger aggregated proteins formed during the bloodmeal manufacturing would remain insoluble.

The volume-average molecular weight ($\bar{M}_v$), was determined between 9 and 19 mL, excluding the void volume, SDS

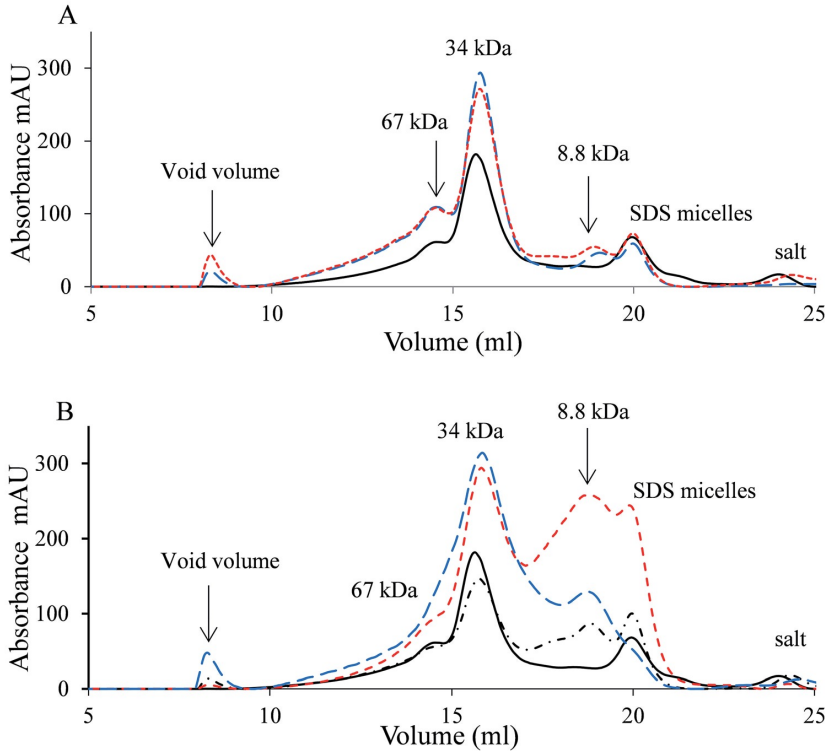

Fig. 4 (A) FPLC chromatogram showing the elution profiles of bloodmeal (——) and decoloured bloodmeal after treatment with 2 (– – – –) and 4 wt% PAA (– – – –), used to determine average molecular weight. Detection at 215 nm. (B) FPLC chromatogram obtained from bloodmeal, BM (——) and bloodmeal decoloured with 5 wt% PAA (— – — –) 26 wt% hydrogen peroxide (– – – –) and hydrogen peroxide with 6.6 wt% acetic acid (— — — —) solutions, used to determine average molecular weight. Detection at 215 nm, peak assignment was predicted from the elution volumes of molecular weight markers.

micelles and salts. The soluble fraction of bloodmeal had a volume-average molecular weight of ~45 kDa. Oxidation led to greater dissolution of protein, for which for samples between 1–4 wt% PAA led to a greater dissolution of larger molecules reflected in an increase in $\bar{M}_v$ (Fig. 5). Oxidation using 5 wt% PAA resulted in a significant quantity of shorter chains, despite not having a significantly greater quantity of total dissolved solids.

The protective effect of acetic acid during oxidation using HP was observed in Fig. 4B. Alone, hydrogen peroxide led to a lower average molecular weight (and 87% soluble fraction), but in the presence of ~6.6 wt% acetic acid, a higher average molecular weight was observed (Fig. 5) and a smaller proportion of lower molecular weight material (Fig. 4B). Alternatively, the presence of acetic acid during decolouring with HP may lead to a larger observed conformation (and lower elution volume) due to volumetric swelling of the proteins.

At 1–2 wt% PAA perhaps there is insufficient oxidant present to significantly change the properties of bloodmeal, which maintains low solubility, similar protein content, high yield and similar molecular weight distribution.

As the concentration of PAA was increased, a larger proportion of high molecular weight proteins become solubilised, and

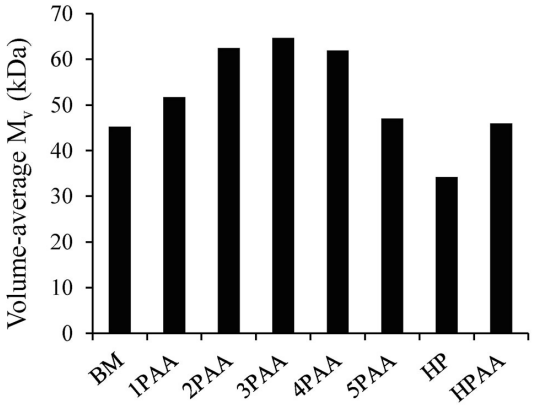

Fig. 5 Volume-average molecular weights (kDa) of bloodmeal (BM) after decolouring with 1–5 wt% PAA, 26 wt% HP and 26 wt% HP containing 6.6 wt% acetic acid.

the formation of lower mass peptides becomes more apparent. Although the presence of acetic acid acts to inhibit extensive degradation, its protective effect is overcome at 5 wt% PAA, and

fragmentation produces a significant quantity of lower molecular weight peptides (Fig. 4B and 5). The increased solubility of DBM proteins between 2–4 wt% PAA must be attributed to changes in the amino acid profile and the stabilising interactions they are involved in, not solely the molecular weight distribution as minimal fragmentation occurred.

Primary structure

Oxidative decolouring of bloodmeal led to a shift in amino acid composition that supports a more hydrophilic material, including an increasing quantity of unidentified species (Fig. 6A), which includes both salts and unidentifiable amino acids. For treatments using 1–4 wt% PAA, the identifiable species corresponds with the salt content of the material (within the error limitations of the experiment) suggesting that any change in amino acid composition is due to the dissolution of modified amino acids, peptides or proteins, (as all of the protein present is accounted for by detectable amino acids). However, treatment with 5 wt% PAA and HP led to the formation of unidentifiable species in excess of the salt content, indicating modification of the amino acids had occurred, and that they remained within the recovered protein.

Overall there is a reduction in aromatic amino acids and lysine with an accordingly greater charged and non-polar content. As oxidation conditions become more stringent many of the amino acids show some decline, however tryptophan, histidine and lysine show losses even under milder oxidation conditions (Fig. 6B).

Aromatic amino acids

Peracetic acid and hydrogen peroxide are both strong oxidants, which at pH 1 (as encountered during decolouring) are both undissociated and act as strong electrophiles, prone to attacking electron dense sites (*i.e.* those with low oxidation potential) such as the carbon methene bridges in haem, as well as sulfur and the aromatic amino acids phenylalanine, tryptophan, and tyrosine and primary and secondary amine containing amino acids lysine and histidine.[61,62]

The selectivity of free radical attack on side chains is affected by the presence of functional groups which can stabilise the resulting radical. For example, hydrogen abstraction occurs preferentially at positions adjacent to electron delocalising (stabilising) groups such as the hydroxy groups (in Ser and Thr), carboxyl and amide functions (in Asp, Glu, Asn, Gln), and the guanidine group in Arg.[63] Comparatively, the protonated amine function on the Lys side chain has a similar effect to the amine group on the α-carbon, resulting in hydrogen abstraction at positions remote from both (from the C-4 and C-5 positions).[63] However, for aromatic, heterocyclic and sulfur containing amino acids (Phe, Tyr, Trp, His, Met and Cys), addition reactions generally take place over hydrogen atom abstraction from the methylene groups. This is due to the addition reactions occurring faster, as no bond breaking occurs in the transition state and the adduct species is stabilised by electron delocalisation about the ring or to the sulfur group.[63]

In light of this, it is interesting to note that phenylalanine content increased slightly with increasing PAA concentration, while hydrogen peroxide treatment led to a reduction (Fig. 6B). This conflicts with other studies which indicate a loss of phenylalanine through oxidation with peracetic acid, however, under these conditions perhaps the presence of acetic acid inhibits hydroxyl radical formation, preventing oxidation of phenylalanine.

Histidine and tyrosine were both reduced by up to 40% and all tryptophan was degraded beyond 3 wt% PAA, consistent with observations of oxidation of dairy proteins.[10] Selective oxidation of the imidazole ring of histidine in the presence of other amino acids has been demonstrated by metal-mediated ascorbic acid oxidation;[64] the product of this oxidation was the imidazolone, which would not significantly change molecular weight but would not be detected as a known amino acid. This type of selectivity is attributed to the generation of reactive oxygen species at specific metal-binding sites, such as that of histidine. From here, the highly reactive oxidants attack labile residues nearby rather than diffusing into the bulk medium.[65]

During peroxide reactions with haem, oxoferryl ($Fe^{4+} = O$) intermediate species are formed, generating a radical cation, typically located on the π-system of haem. The π-radical is rapidly transferred to a nearby amino acid residue, which has a low oxidation potential, such as tryptophan or tyrosine.[66] From there, it is transformed into a variety of oxidation products. For PAA and HP, these radicals are typically formed on tyrosine, tryptophan or cysteine residues.[66–73] Eventually, the free radical is deprotonated into a neutral radical[11] or terminated when it attacks an electron rich site. In the case of bovine cytochrome c oxidase, tyrosinyl and tryptophanyl radicals are formed when hydrogen peroxide binds to the heme unit, followed by migration from the binuclear centre, selectively oxidising surface tryptophan residues to hydroxytryptophan.[74]

Such a reduction in the quantity of non-polar aromatic groups is a result of electrophilic addition reactions (such as hydroxylation and carbonylation)[75] resulting in less hydrophobic interactions.

Polar and charged amino acids

Minimal change to the quantity of polar amino acids (threonine and serine) was observed at low PAA concentration, although an overall relative increase of ~7 wt% serine was observed at high concentration (Fig. 6C). Hydrogen peroxide caused a noticeable increase (a relative increase of ~10%) in the concentration of serine, but made very little difference to threonine. The increase in content is likely an artefact of reducing the content of other amino acids.

By contrast, the overall relative proportion of charged amino acids increased, mostly from the large increase in aspartic acid, and to a lesser extent, glutamic acid (Fig. 6D). It is thought that the increase in aspartic acid may be caused by its formation during histidine oxidation.[76] Arginine content did not appear to change after HP or PAA treatment, which is unusual given that the guanidine group should serve to stabilise the formation of intermediate radicals.

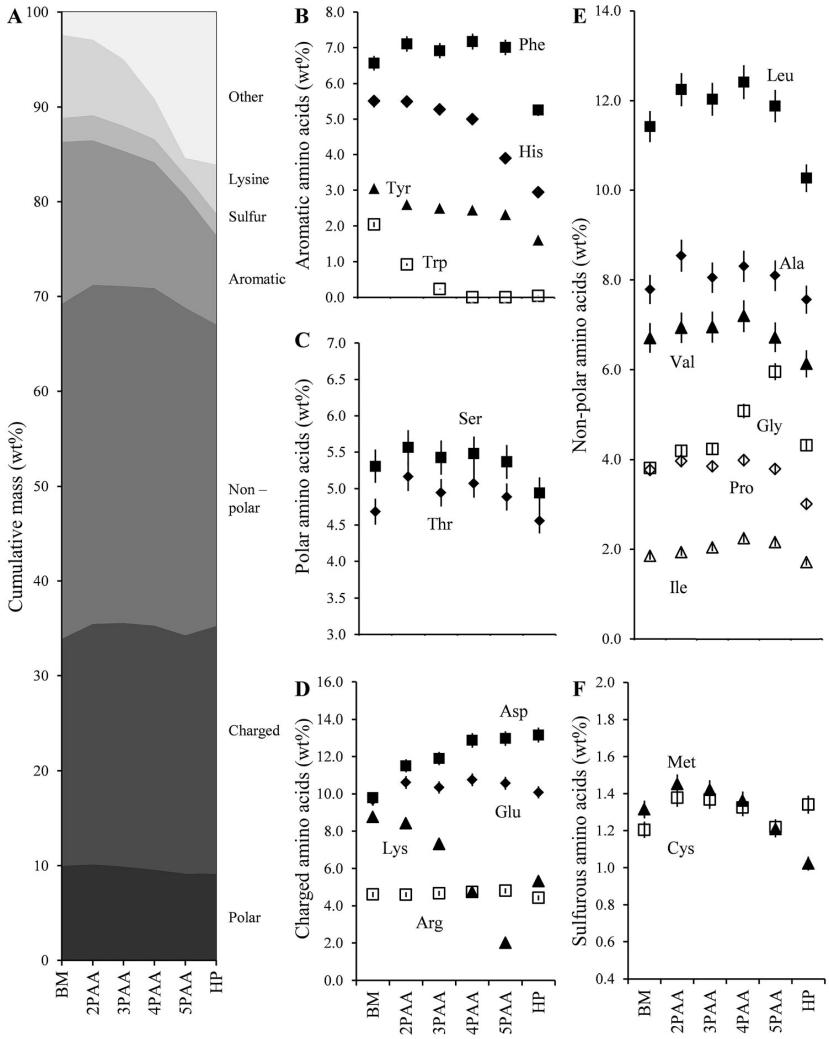

Fig. 6 (A) Amino acid composition of bloodmeal and decoloured bloodmeal expressed as a cumulative mass percentage. Weight percentage of (B) aromatic amino acids phenylalanine (Phe), histidine (His), tyrosine (Tyr) and tryptophan (Trp) (C) polar amino acids serine (Ser) and threonine (Thr) (D) charged amino acids aspartic acid (Asp), glutamic acid (Glu), lysine (Lys) and arginine (Arg) (E) non-polar amino acids leucine (Leu), alanine (Ala), valine (Val), glycine (Gly), proline (Pro) and isoleucine (Ile) (F) sulfurous amino acids methionine (Met) and cysteine (Cys) present in bloodmeal before and after decolouring, expressed as a percentage of crude protein. Error bars are the percentage relative standard deviation for the detection of each amino acid.

Overall DBM contains almost the same amount of hydrophobic amino acids, (sum of glycine, alanine, valine, leucine, isoleucine, proline and methionine) as bloodmeal. However, it contains significantly less of the aromatic amino acids tyrosine, and histidine, but with little change in phenylalanine and notably containing no tryptophan. There is also a relative increase in polar and charged amino acids which are expected to be more hydrophilic (threonine, serine, aspartic and glutamic acid and arginine).

Lysine is an anomaly, in that it would ordinarily be grouped with hydrophilic amino acids, but it undergoes such extensive degradation with PAA treatment (up to 80% relative to the initial concentration in BM) and HP (up to 40% relative to the initial concentration in BM) that it should be considered alone. Bloodmeal is probably best known for its high lysine content compared with other protein meals, and is capable of forming covalent bonds with alanine to form lysinoalanine when exposed to heat.

Both lysine and histidine are known to undergo metal catalysed oxidation forming aminoadipic semi-aldehyde and 2-oxo-hisitidine respectively.[62] The greater reduction in lysine content observed with PAA as compared to HP is unexpected, as acetic

acid is theorised to chelate metal ions which may catalyse lysine oxidation. However, while acetic acid may be capable of chelating all freely dissolved iron present, it may be unable to chelate iron trapped or loosely bound within chains of the protein, allowing the iron to facilitate oxidation much closer to the vulnerable sites. Alternatively, it may simply be due to PAA's higher reduction potential (1.81 V) compared to HP (1.76 V) or due to its greater radical longevity allowing a greater portion of lysine to be accessed.

Non-polar amino acids

Glycine, alanine, valine, leucine, isoleucine and proline are considered non-polar, but only glycine underwent a relative increase above 3 wt% PAA or to a lesser extent with hydrogen peroxide (Fig. 6E). Isoleucine increased about 20% (from 1.9 to 2.3 wt%), with a step change around 3 wt% PAA, while hydrogen peroxide had little effect. PAA had no effect on proline (within the error limits), but decreased by 10% using HP.

Alanine and valine content did not have a clear trend, but increased slightly at high PAA content (Fig. 6E). On the other hand, hydrogen peroxide treatment increased the alanine content to 8.7 wt% (~9% relative increase). Leucine content increased linearly with PAA concentration (from 11.7–12.6 wt%), but remained unaffected by hydrogen peroxide oxidation. It is most likely that the apparent increase in alanine after oxidation with HP is due to a shift in composition caused by the massive loss of aromatic amino acids and dissolution of proteins during decolouring.

Cysteine and methionine

Interestingly, there is a relative increase in sulfur containing amino acids (per gram of protein) during decolouring (Fig. 6F). This suggests that the mass lost during decolouring involves peptides or proteins which contain lower concentrations of sulfur containing amino acids, compared to the overall average (*i.e.* contain less disulfide bridges), resulting in a higher concentration in the remaining insoluble DBM.

However, the HPLC method used to determine the amino acid profile is unable to distinguish between cystine, cysteine or cysteic acid (as formed upon exposure to peracetic acid), as the analysis of this amino acid is achieved after performic acid oxidation in order to convert all species to cysteic acid. In fact, it is likely that despite being richer in sulfur containing components, the material may contain absolutely no cystine or cysteine crosslinks, as they were probably all converted to cysteic acid during decolouring. This is supported by the fact that DBM treated with 4 wt% PAA no longer requires the addition of sodium sulfite as a reducing agent to cleave disulfide bridges when it is used as a feedstock for thermoplastic processing.[2]

Cystine degradation

Some of the intermediate and final products of cystine oxidation are observed in FT-IR between 1150 and 1000 cm^{-1}. Cleavage of the disulfide bond occurs through two major pathways: S–S scission or C–S scission.[77] In both cases, the main end-product is cysteine sulfonic acid (IX), more commonly referred to as cysteic acid (Fig. 7). The oxidation of cystine groups responsible for the crosslinks in protein results in the formation of cysteine monoxide (Cys–SO–S–Cys, II), cysteine dioxide (Cys–SO_2–S–Cys and Cys–SO–SO–Cys, III and IV) and cysteine sulfonic acid (Cys–SO_3H, IX) as well as cysteine-*S*-sulfonate (Cys–SO_3M, X).

The four new peaks, 1150–1000 cm^{-1}, are easily observed after treatment (Fig. 8A). Each has been assigned to oxidation products of cysteine and cysteine, and are labelled as indicated above. Treating bloodmeal with any level of PAA greater than 2 wt% PAA led to subtle changes in the FT-IR spectra (Fig. 8A), generating four new peaks. These peaks increased in intensity and area with increasing PAA concentration.[43–45]

The peak at 1017 cm^{-1} appeared after oxidation with PAA only, and could be assigned to cysteine-*S*-sulfonate (R–S–SO_3^-). This compound has been observed around 1020 cm^{-1} in the FT-IR spectra of other proteins after photooxidation or sulfitolysis[78–80] and is known to be formed during alkaline oxidation using permanganate or hydrogen peroxide,[81] as well as hypochlorite and persulfate.[77,82]

Although it has not been reported to occur in wool exposed to hydrogen peroxide or peracetic acid,[82] it has been suggested to occur in wool exposed to boiling HP,[83] and upon bleaching hair with HP.[44] The generation of cysteine-*S*-sulfonic acid appears to be particularly pH sensitive, and its formation in acidic media may be quickly followed by its interaction with other products.[77] Its presence in bloodmeal decoloured with peracetic acid is evidence that cystine cleavage occurs *via* C–S scission (pathway C in Fig. 7).

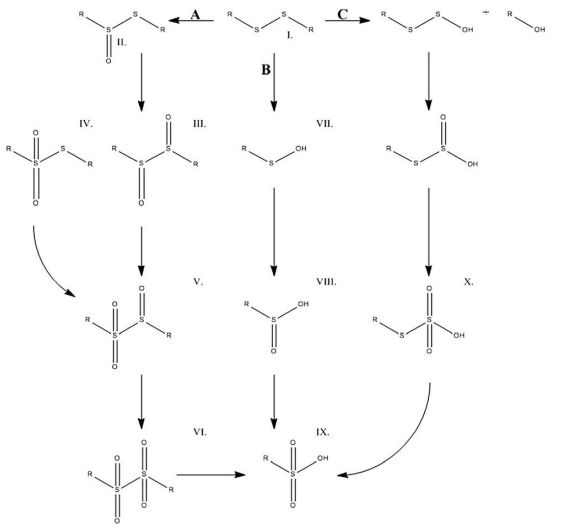

Fig. 7 Reaction scheme for the oxidation of cysteine. Pathways A and B occur *via* S–S scission and pathway C through C–S scission. Compound I: cystine, II: cystine monoxide, III: cystine dioxide, IV: cystine-*S*,*S*-dioxide, V: cystine trioxide, VI: cystine tetraoxide, VII: cysteine sulfenic acid, VIII: cysteine sulfinic acid, IX: cysteine sulfonic acid (cysteic acid), X: cysteine-*S*-sulfonic acid. Reproduced from ref. 77, copyright (1966), with permission from Elsevier.

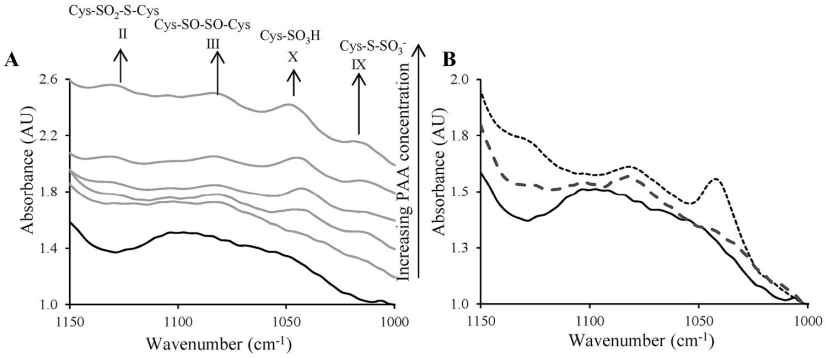

Fig. 8 (A) Average of 10 FT-IR spectra of bloodmeal (——) and 1–5 wt% PAA decoloured bloodmeal (——), normalised at 1000 cm^{-1} and stacked for clarity. (B) Average of 10 FTIR spectra of HP decoloured bloodmeal (- - - -) and HP with acetic acid decoloured bloodmeal (— — — —), normalised at 1000 cm^{-1} (solid line is bloodmeal). Cysteine oxidation products are also assigned.

Sodium acetate is known to have two peaks occurring at ~1017 cm^{-1} and 1050 cm^{-1}, which would also be expected to increase with increasing PAA treatment due to the increase in acetic acid present which would require neutralisation. However, their contribution to the overall spectra has been rejected on the basis that almost no difference is seen in this region in bloodmeal decoloured with HP containing acetic acid, which too would contain sodium acetate salt (Fig. 8B). This indicates that the source of these new peaks is most likely due to oxidation reactions rather than the formation of acetate salt, leaving the designation of the peak at 1017 cm^{-1} to that of cysteine-*S*-sulfonate.

The corresponding area for each peak identified was averaged over the entire area scanned (spatial map) and plotted against the concentration of PAA used (Fig. 9A). While both the cysteine-*S*-sulfonate and cystine dioxide peaks increased with PAA concentration, cystine monoxide appeared to stay almost constant. This indicates that some level of cysteine monoxide is present in BM prior to decolouring, which despite its instability, may be an artefact of the oxidising conditions during the manufacture of bloodmeal.

The ν_sS=O sulfonate absorbance band at 1044 cm^{-1} owing to cysteic acid, had the strongest signal increase, and therefore an increase in its area (relative to the amide III area) could be a good marker of oxidative damage to the protein (Fig. 9B). The strong relative increase would confirm previous observations regarding the effect of PAA on proteins.

Treatment with hydrogen peroxide led to a significantly lower quantity of cystine dioxide formation, with a much higher formation of cysteic acid (the expected end product). Further, the presence of acetic acid appeared to have inhibited the formation of both these oxidation products, perhaps through an anti-oxidant pathway, suppressing the formation of more reactive oxygen species such as the hydroxyl radical.

Overall the composition of decoloured bloodmeal shifted toward a material with improved hydrophilicity, with a higher proportion of charged and non-polar amino acids and a reduced quantity of aromatic amino acids. Decolouring bloodmeal led to an increase in random structures,[37] consistent with an increase in amino acids with a propensity to form turns and coils (glycine, proline, aspartic acid and serine, despite a reduction in histidine). The remaining ordered structures contained a relatively larger proportion of beta sheets compared to alpha helices, most likely caused by the large reduction in lysine and other helix-forming amino acids (leucine, methionine and glutamic acid undergo minimal changes). By contrast, a reduction in the total quantity of sheet forming amino acids (tryptophan, isoleucine, phenylalanine, valine, tyrosine,

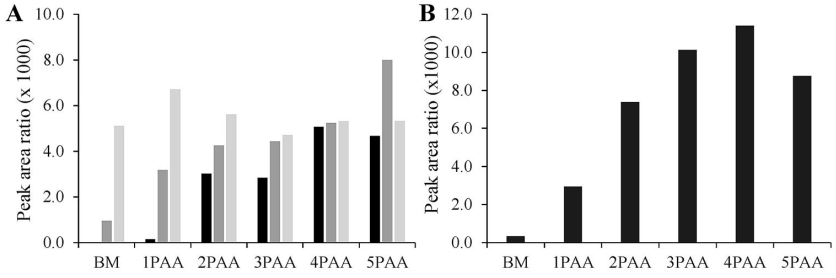

Fig. 9 (A) Peak area ratio of selected peaks to that of the total amide III region. Cystine dioxide ■ (Cys–SO_2–S–Cys), cysteine-*S*-sulfonate ■ (Cys–S–SO_3^-) and cystine monoxide ■ (Cys–SO–S–Cys). (B) Peak area ratio of cysteic acid ■ (Cys–SO_3H) to total amide III region.

threonine and cysteine) was observed, but did not result in a material with fewer β-sheets.[37] This highlights the difficulties of using amino acid composition alone to predict secondary structure.

Conclusion

Solutions containing more than 3 wt% PAA are required for adequately decolouring bloodmeal, as observed by loss of iron. HP and HP containing acetic acid were found to result in only superficial losses of iron during decolouring confirming HP's inability to degrade all of the haem chromogens responsible for the colour of bloodmeal.

HP and PAA cause changes to the physical and chemical properties of bloodmeal proteins. PAA treatment prevented excessive protein loss (higher yield) compared to decolouring with hydrogen peroxide, and this is likely a result of the combination of oxidation mechanisms and the presence of acetate salt enhancing protein precipitation. However, the lower protein content, most noticeable after 4–5 wt% PAA, was due to the dilution with acetate salts.

Oxidation also resulted in an increase in the solubility of the proteins, particularly for those treated with hydrogen peroxide. All treatments resulted in a greater dissolution of protein, and were also responsible for the appearance of a peptide fragment with an approximate mass of 8.8 kDa. Using concentrations of 1–4 wt% PAA gave rise to soluble proteins similar in composition to that of bloodmeal. However, treatment with 5 wt% PAA or HP led to significant fragmentation of the protein chains, inhibited to some extent by the presence of acetic acid.

The protective effect of acetic acid on proteins was observed during HPAA decolouring, resulting in less fragmentation than treatment with HP alone. This has been attributed to the antioxidant properties of acetic acid allowing chelation of free iron which would otherwise facilitate the formation of hydroxyl radical species (to cause protein hydrolysis) through Fenton type reactions. It is expected that acetic acid performs a similar role in PAA solutions.

Due to the minor contribution fragmentation is thought to have in this reaction; the overall increase in hydrophilicity of the proteins upon decolouring is most probably a result of changes to the amino acid residues of which they are comprised. This is most evident from a shift in composition toward more polar and charged amino acids, through the degradation of aromatic residues and also lysine. The most telling feature explaining the improved hydrophilicity is the formation of cysteic acid and cysteine-*S*-sulfonate, indicating that at least to some extent, crosslinking has been overcome. The cleavage of cysteine crosslinks and degradation of lysine may limit the number of new crosslinks which can form during thermoplastic processing.

Acknowledgements

The FTIR research was undertaken on the infra-red microspectroscopy beamline at the Australian Synchrotron, Clayton, VIC, Australia. Proposal number AS132/IRMFI/6636. The authors would especially like to acknowledge the technical assistance of Dr Mark Tobin and Dr Danielle Martin. Travel funding support was received from the New Zealand Synchrotron Group Ltd. The authors also wish to thank Steve Cameron, University of Waikato for carrying out ICP-MS assay and Bryan Treloar from AgResearch for carrying out the amino acid analysis. Further thanks to Anjana Rajendram and Judy Hoult, Waikato Stable Isotope Unit for carrying out the total nitrogen assay for crude protein analysis.

References

1 C. J. R. Verbeek, M. C. Lay and A. W. K. Low, Methods of Manufacturing Plastic Materials from Decolorized Blood Protein, *US Pat.*, 20130139725 13/691, 438, 2013.
2 A. Low, C. J. R. Verbeek and M. C. Lay, *Macromol. Mater. Eng.*, 2014, **299**, 75–84.
3 A. Low, J. Verbeek, M. Lay and J. Swan, *Prep. Biochem. Biotechnol.*, 2012, **42**, 29–43.
4 L. J. Bauermeister, J. W. J. Bowers, J. C. Townsend and S. R. McKee, *Poult. Sci.*, 2008, **87**, 2390–2398.
5 E. M. M. Rossoni and C. C. Gaylarde, *Int. J. Food Microbiol.*, 2000, **61**, 81–85.
6 A. C. Silveira, A. Conesa, E. Aguayo and F. Artes, *J. Food Sci.*, 2008, **73**, 405–411.
7 B. Kerkaert, F. Mestdagh, T. Cucu, P. R. Aedo, S. Y. Ling and B. De Meulenaer, *J. Agric. Food Chem.*, 2011, **59**, 907–914.
8 A. Dell'Erba, D. Falsanisi, L. Liberti, M. Notarnicola and D. Santoro, *Desalination*, 2007, **215**, 177–186.
9 I. Voukkali and A. A. Zorpas, *Desalin. Water Treat.*, 2014, 1–12.
10 T. M. Hicks, C. J. R. Verbeek, M. C. Lay and M. Manley-Harris, *J. Am. Oil Chem. Soc.*, 2013, **90**, 1577–1587.
11 D. A. Svistunenko, *Biochim. Biophys. Acta, Bioenerg.*, 2005, **1707**, 127–155.
12 W. Zhang, S. Xiao and D. U. Ahn, *Crit. Rev. Food Sci. Nutr.*, 2013, **53**, 1191–1201.
13 P. Alexander and D. Gough, *Biochem. J.*, 1951, **48**, 504–511.
14 M. C. Corfield, A. Robson and B. Skinner, *Biochem. J.*, 1958, **68**, 348–352.
15 C. Robbins, in *Chemical and Physical Behavior of Human Hair*, Springer, New York, 1988, ch. 4, pp. 102–121.
16 P. Alexander, M. Fox and R. F. Hudson, *Biochem. J.*, 1951, **49**, 129–138.
17 L. J. Wolfram, K. Hall and I. Hui, *J. Soc. Cosmet. Chem.*, 1970, **21**, 875–900.
18 M. Finnegan, E. Linley, S. P. Denyer, G. McDonnell, C. Simons and J. Y. Maillard, *J. Antimicrob. Chemother.*, 2010, **65**, 2108–2115.
19 O. M. Gecha and J. M. Fagan, *J. Nutr.*, 1992, **122**, 2087–2093.
20 V. M. Zaeska, C. L. Orr, D. L. Prater and J. Lockridge, Stabilized Hydrogen Peroxide Compositions and Methods, European Patent, EP20090767509, 2011.
21 V. Pardio-Sedas, in *Processing and Impact on Active Components in Food*, ed. V. R. Preedy, Elsevier Science, 2014.
22 H. Uzun, E. Ibanoglu, H. Catal and S. Ibanoglu, *Food Chem.*, 2012, **134**, 647–654.

23 S. Malkov, M. Živković, M. Beljanski, M. Hall and S. Zarić, *J. Mol. Model.*, 2008, **14**, 769–775.
24 H. Xiong, B. L. Buckwalter, H. M. Shieh and M. H. Hecht, *Proc. Natl. Acad. Sci. U. S. A.*, 1995, **92**, 6349–6353.
25 V. K. Sharma and N. J. D. Graham, *Ozone: Sci. Eng.*, 2010, **32**, 81–90.
26 F. Cataldo, *Polym. Degrad. Stab.*, 2003, **82**, 105–114.
27 J. M. Bier, C. J. R. Verbeek and M. C. Lay, *Macromol. Mater. Eng.*, 2013, **299**, 524–539.
28 O. S. Rabotyagova, P. Cebe and D. L. Kaplan, *Biomacromolecules*, 2011, **12**, 269–289.
29 S. Keten and M. J. Buehler, *J. R. Soc., Interface*, 2010, 1–13.
30 A. Nova, S. Keten, N. M. Pugno, A. Redaelli and M. J. Buehler, *Nano Lett.*, 2010, **10**, 2626–2634.
31 G. Qin, X. Hu, P. Cebe and D. L. Kaplan, *Nat. Commun.*, 2012, **3**, 1003.
32 S. Rauscher, S. Baud, M. Miao, F. W. Keeley and R. Pomès, *Structure*, 2006, **14**, 1667–1676.
33 K. M. Nairn, R. E. Lyons, R. J. Mulder, S. T. Mudie, D. J. Cookson, E. Lesieur, M. Kim, D. Lau, F. H. Scholes and C. M. Elvin, *Biophys. J.*, 2008, **95**, 3358–3365.
34 P. Y. Chou and G. D. Fasman, *Biochemistry*, 1974, **13**, 211–222.
35 S. Costantini, G. Colonna and A. M. Facchiano, *Biochem. Biophys. Res. Commun.*, 2006, **342**, 441–451.
36 M. Levitt, *Biochemistry*, 1978, **17**, 4277–4285.
37 T. Hicks, C. J. R. Verbeek, M. C. Lay and J. M. Bier, *RSC Adv.*, 2014, **4**, 31201–31209.
38 W. L. Davies, *Analyst*, 1936, **61**, 512–515.
39 AOAC International, *Official Methods of Analysis of AOAC International: Food Composition, Additives, Natural Contaminants*, Association of Official Analytical Chemists, Arlington, VA, 15 edn, 1990.
40 J. Bier, C. Verbeek and M. Lay, *J. Therm. Anal. Calorim.*, 2014, **115**, 433–441.
41 J. M. Bier, C. J. R. Verbeek and M. C. Lay, *J. Appl. Polym. Sci.*, 2013, **130**, 359–369.
42 J. Kong and S. Yu, *Acta Biochim. Biophys. Sin.*, 2007, **39**, 549–559.
43 J. Bantignies, G. L. Carr, D. Lutz, S. Marull, G. P. Williams and G. Fuchs, *J. Cosmet. Sci.*, 2000, **51**, 73–90.
44 V. Signori and D. M. Lewis, *Macromol. Symp.*, 1997, **119**, 235–240.
45 N. Gómez, M. R. Juliá, D. M. Lewis and P. Erra, *J. Soc. Dyers Colour.*, 1995, **111**, 281–284.
46 S. B. Brown, H. Hatzikonstantinou and D. G. Herries, *J. Biochem.*, 1978, **174**, 901–907.
47 M. Grinstein, *J. Biol. Chem.*, 1947, **167**, 515–519.
48 Canadian Department of Agriculture, National Research Council, *Atlas of Nutritional Data on United States and Canadian Feeds*, National Academy of Sciences, Washington, D.C., 1971.
49 S. Martínez-Llorens, A. T. Vidal, A. V. Moñino, J. Gómez Ader, M. P. Torres and M. J. Cerdá, *Aquacult. Res.*, 2008, **39**, 1028–1037.
50 D. P. Haughey, *Market Potential and Processing of Blood Products: Some Overseas Observations*, Meat Industry Research Institute NZ, Hamilton, 1976.
51 R. L. Preston, *BEEF Magazine*, 2014, 18–26.
52 S. A. Howie, S. Calsamiglia and M. D. Stern, *Anim. Feed Sci. Technol.*, 1996, **63**, 1–7.
53 A. Kamalak, O. Canbolat, Y. Gurbuz and O. Ozay, *Small Ruminant Research*, 2005, **58**, 135–141.
54 A. Laining, Rachmansyah, T. Ahmad and K. Williams, *Aquaculture*, 2003, **218**, 529–538.
55 M. d J. Marichal, M. Carriquiry, R. Pereda and R. San Martín, *Anim. Feed Sci. Technol.*, 2000, **88**, 91–101.
56 National Research Council, in *Nutrient Requirements of Dairy Cattle: Seventh Revised Edition*, The National Academies Press, Washington, DC, 7th edn, 2001, ch. 15, pp. 281–314.
57 I. Nengas, M. N. Alexis, S. J. Davies and G. Petichakis, *Aquacult. Res.*, 1995, **26**, 185–194.
58 S. P. Wolff and R. T. Dean, *Biochem. J.*, 1986, **234**, 399–403.
59 S. J. Edelstein, M. J. Rehmar, J. S. Olson and Q. H. Gibson, *J. Biol. Chem.*, 1970, **245**, 4372–4381.
60 W. P. Griffith and I. A. Kaltashov, *Biochemistry*, 2003, **42**, 10024–10033.
61 M. J. Davies, *Biochim. Biophys. Acta, Proteins Proteomics*, 2005, **1703**, 93–109.
62 K. Uchida, *Amino Acids*, 2003, **25**, 249–257.
63 C. L. Hawkins and M. J. Davies, *Biochim. Biophys. Acta, Bioenerg.*, 2001, **1504**, 196–219.
64 K. Uchida and S. Kawakishi, *J. Agric. Food Chem.*, 1990, **38**, 1896–1899.
65 F. Zhao, E. Ghezzo-Schoneich, G. I. Aced, J. Hong, T. Milby and C. Schoneich, *J. Biol. Chem.*, 1997, **272**, 9019–9029.
66 T. Spolitak, J. H. Dawson and D. P. Ballou, *J. Biol. Chem.*, 2005, **280**, 20300–20309.
67 A. L. Houseman, P. E. Doan, D. B. Goodin and B. M. Hoffman, *Biochemistry*, 1993, **32**, 4430–4443.
68 F. G. M. Wiertz, O. M. H. Richter, A. V. Cherepanov, F. MacMillan, B. Ludwig and S. de Vries, *FEBS Lett.*, 2004, **575**, 127–130.
69 M. R. Gunther, B. E. Sturgeon and R. P. Mason, *Free Radicals Biol. Med.*, 2000, **28**, 709–719.
70 A. Ivancich, H. M. Jouve, B. Sartor and J. Gaillard, *Biochemistry*, 1997, **36**, 9356–9364.
71 A. Ivancich, G. Mazza and A. Desbois, *Biochemistry*, 2001, **40**, 6860–6866.
72 K. Ranguelova, S. Girotto, G. J. Gerfen, S. Yu, J. Suarez, L. Metlitsky and R. S. Magliozzo, *J. Biol. Chem.*, 2007, **282**, 6255–6264.
73 A. Ivancich, C. Jakopitsch, M. Auer, S. Un and C. Obinger, *J. Am. Chem. Soc.*, 2003, **125**, 14093–14102.
74 P. Lemma-Gray, S. T. Weintraub, C. A. Carroll, A. Musatov and N. C. Robinson, *FEBS Lett.*, 2007, **581**, 437–442.
75 E. R. Stadtman and R. L. Levine, *Amino Acids*, 2003, **25**, 207–218.
76 B. S. Berlett and E. R. Stadtman, *J. Biol. Chem.*, 1997, **272**, 20313–20316.
77 W. E. Savige and J. A. Maclaren, in *The Chemistry of Organic Sulfur Compounds*, ed. N. Kharasch and C. Y. Meyers, Pergamon Press, 1966, vol. 2.

78 M. Odlyha, C. Theodorakopoulos and R. Campana, *Autex Res. J.*, 2007, **7**, 9–18.
79 C. M. Carr and D. M. Lewis, *J. Soc. Dyers Colour.*, 1993, **109**, 21–24.
80 P. Erra, N. Gómez, L. M. Dolcet, M. R. Juliá, D. M. Lewis and J. H. Willoughby, *Text. Res. J.*, 1997, **67**, 397–401.
81 Y. M. Torchinskii and H. B. F. Dixon, in *Sulfhydryl and Disulfide Groups of Proteins*, Springer Science & Business Media, 1974.
82 R. J. Denning, G. N. Freeland, G. B. Guise and A. H. Hudson, *Text. Res. J.*, 1994, **64**, 413–422.
83 J. Kim and D. M. Lewis, *Color. Technol.*, 2002, **118**, 121–124.

Electronic Supplementary Information

Molecular weight analysis

Table 1. Molecular weight markers used for calibration of the Superdex 200 gel filtration column (void volume, V_o = 8.0 mL). The natural log of the molecular weight was plotted against the elution volume (V_r) divided by the column void volume (V_o) for each marker, generating the graph and equation shown (right).

Molecular Weight Marker	Molecular Weight (Da)	Elution Volume (V_r)	V_r/V_o	$\ln(M_w)$
Thyroglobulin	669000	9.32	1.16	13.41
Ferritin	440000	10.83	1.35	12.99
Bovine serum albumin	67000	13.89	1.74	11.11
β-Lactoglobulin (dimer)	35000	15.29	1.91	10.46
Ribonuclease A	13700	17.13	2.14	9.53
Cytochrome C	13600	18.34	2.29	9.52
Aprotinin	6512	19.87	2.48	8.78
Vitamin B12	1355	21.72	2.72	7.21

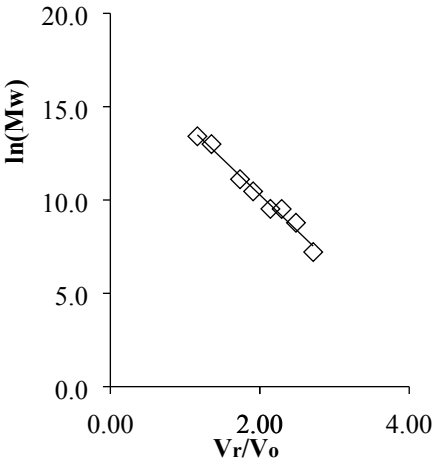

Amino acid analysis

The amino acid composition of each sample as received is shown below (Table 2), along with the percentage relative standard deviation (%RSD) as calculated for standard solutions, over 500 observations. Moisture content of the freeze dried samples was determined via thermogravemetric analysis. From the composition below and the protein content (on a dry basis) as determined by total nitrogen assay, the amino acid composition of the dry protein was determined (Table 3).

Table 2. Absolute amino acid composition of bloodmeal (BM) and decoloured bloodmeal after treating with 2 wt% PAA (2PAA), 3 wt% PAA (3PAA), 4 wt% PAA (4PAA), 5 wt% PAA (5PAA) and 26 wt% HP (HP) solutions. Results expressed in mg/g of sample on an as received basis. NB: Moisture content of the freeze dried powders determined via thermogravemetric analysis and crude protein determined by total nitrogen assay.

Amino acid (mg/g)	**BM**	**2PAA**	**3PAA**	**4PAA**	**5PAA**	**HP**	**%RSD**
Aspartic Acid	95.93	107.11	110.75	113.5	113.13	123.79	3.06
Threonine	52.00	51.80	50.51	48.32	46.80	46.49	3.83
Serine	45.88	48.07	46.02	44.72	42.61	42.87	4.30
Glutamic acid	94.69	98.79	96.21	94.81	92.16	94.79	3.22
Proline	36.90	36.93	35.84	35.12	33.05	28.28	3.46
Glycine	37.39	39.00	39.38	44.84	51.98	40.56	3.19
Alanine	76.30	79.51	74.95	73.24	70.61	71.16	4.19
Valine	65.73	64.56	64.72	63.48	58.66	57.72	4.91
Isoleucine	18.10	18.01	18.98	19.77	18.79	16.08	4.37
Leucine	111.91	114.01	112.01	109.46	103.6	96.58	3.04
Tyrosine	29.80	24.17	23.20	21.57	20.20	15.03	4.29
Phenylalanine	64.28	66.13	64.34	63.22	61.09	49.39	3.11
Lysine	85.78	78.34	68.14	41.84	17.47	50.00	3.05
Histidine	53.94	51.11	49.07	44.08	33.96	27.64	3.22
Arginine	44.09	43.97	43.20	41.87	39.66	36.24	2.96
Cystine	11.80	12.83	12.73	11.69	10.62	12.61	3.65
Methionine	12.88	13.51	13.22	12.01	10.53	9.62	3.65
Tryptophan	20.01	8.54	2.15	0.00	0.00	0.37	3.65
Moisture content*	19.00	15.00	26.00	28.00	25.00	24.00	
Undetected	23.59	28.61	48.58	88.46	150.08	156.78	
Sum of Amino Acids	957.41	956.39	925.42	883.54	824.92	819.22	
Total sum	1000	1000	1000	1000	1000	1000	

6

The Effect of SDS and TEG on Chain Mobility and Secondary Structure of Decolored Bloodmeal

By

TALIA M. HICKS, C. J. R. VERBEEK, M. C. LAY

AND

J. M. BIER

Published in Macromolecular Materials and Engineering

As first author for this paper, I prepared the draft manuscript of this journal paper, which was refined and edited in consultation with my supervisors, whom are credited as co-authors. The FT-IR results reported here were collected in collaboration with my supervisors (and Dr. J. Bier) during beamtime at the Australian Synchrotron. Together with my co-authors, I travelled to the Australian Synchrotron to conduct the experiments. I then performed the data analysis in OPUS software and Microsoft Excel. I also carried out the WAXS and TGA experiments and analysis.

The Effect of SDS and TEG on Chain Mobility and Secondary Structure of Decolored Bloodmeal[a]

Talia M. Hicks,* Casparus J. R. Verbeek, Mark C. Lay, James M. Bier

The effect of sodium dodecyl sulfate (SDS) and triethylene glycol (TEG) on secondary structure of decolored bloodmeal (DBM) during heating was examined via synchrotron-based Fourier transform infra-red spectroscopy (FT-IR) and wide angle X-ray scattering (WAXS). Both additives homogenize secondary structure distribution; SDS increases α-helices and decreases β-sheets and β-turns, while SDS–TEG reduces α-helices and β-sheets and increase random coils. Short heat cycles only change the composition of SDS-TEG treated DBM, implying TEG is responsible for chain mobility. Prolonged heating slowly increases β-sheets and suddenly increases α-helices at 55–75 °C in SDS-TEG treated DBM and 100 °C in SDS-treated DBM. Finally, WAXS shows that structural change due to heating is reversible for SDS-TEG treated DBM.

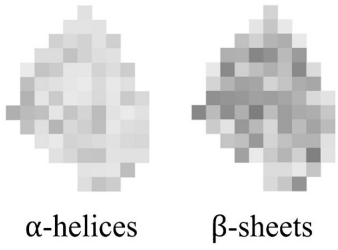

Spatial distribution of secondary structures in decolored bloodmeal

1. Introduction

Recent research into second generation biopolymers from low value co-products of existing agricultural and horticultural processes has been driven by an economic and environmental need to maximize the effective utilization of natural resources.[1] One such co-product is bloodmeal, a protein-rich powder which can be modified to exhibit thermoplastic behavior with the addition of urea, sodium dodecyl sulfate (SDS), sodium sulfite, and triethylene glycol (TEG).[2]

Bloodmeal can also be decolored with equilibrium peracetic acid (PAA),[3] requiring a minimum of 4 wt% PAA to obtain adequate decoloring.[4] The resulting material is pale-yellow in color and requires only SDS, water, and TEG to extrude into a semi-transparent bioplastic.[5] The most significant change observed as a result of decoloring bloodmeal is a major increase in chain mobility, observed as a reduction in glass transition temperature (T_g) from ≈225 °C to around 35–45 °C.[3] Such a drastic drop in T_g is attributed to the effect of oxidation, which has led to improved chain mobility through the reduction in number and strength of stabilizing intermolecular interactions and improved chain regularity.[6]

Thermoplastic processing of proteins involves three steps: heating to overcome stabilizing intermolecular interactions; shaping the melt using pressure; and cooling to reintroduce new chain interactions to stabilize the newly formed shape (fixation).[7] In proteins, covalent crosslinking and secondary structural elements contribute to this fixation.[8]

Inducing sufficient chain mobility is paramount to the formation of new interactions during extrusion. Insoluble proteins are constrained in their mobility by both a lack of solvent to facilitate molecular motion and by strong stabilizing interactions.[9] The addition of processing aids such as plasticizers, are often required to overcome original interactions and to increase free

T. M. Hicks, Dr. C. J. R. Verbeek, Dr. M. C. Lay, Dr. J. M. Bier
Faculty of Science and Engineering, School of Engineering, University of Waikato, Private Bag 3105, Hamilton 3200, New Zealand
E-mail: tmh20@students.waikato.ac.nz

[a]**Supporting Information** is available from the Wiley Online Library or from the author.

DOI: 10.1002/mame.201400290

volume allowing nearby chains to slide past each other more efficiently.[10]

SDS is an anionic surfactant commonly used to denature proteins and is often used during thermoplastic processing of proteins to disrupt hydrophobic interactions in order to facilitate the formation of new interactions during extrusion. Although SDS disrupts some interactions, additional plasticization may also be required. A plasticizer allows more movement between polymer chains by reducing interactions between adjacent chains and increasing its free volume. Plasticization of a polymer is a complex process, first involving wetting and adsorption followed by solvation and/or penetration into the bulk. Absorption and diffusion will occur until the plasticizer is distributed evenly throughout the amorphous regions and structural disruption occurs.[11] The ability of a plasticizer to diffuse through a proteinous material will depend on both the type of plasticizer employed and the amino acids of which the protein is comprised.[11,12]

SDS may also provide plasticization by disrupting hydrogen bonding and increasing charge repulsion between adjacent chains.[13] The extent of this will depend on the quantity added and the type of protein structures involved. SDS initially interacts electrostatically with positively charged groups on the protein surface (via the $-SO_3^-$ groups), later binding hydrophobically to non-polar groups via the dodecyl chain.[14] SDS in whey protein films has been shown to have a small plasticizing effect, which becomes pronounced upon adding ≈0.09–0.12 g of SDS per gram of protein.[13] In the case of decolored bloodmeal (DBM), ≈0.03 g of SDS is used per gram of protein, and may contribute to plasticization of the protein.

TEG is an amphiphilic plasticizer containing both ether and alcohol functional groups; these polar groups are able to hydrogen bond to protein chains. As TEG also contains hydrophobic groups it is able to interact with hydrophobic amino acids in non-polar regions buried within the protein chain.[11] TEG may have a helicogenic effect, where helical secondary structures within polypeptide chains are created, often observed when alcohols are used as solvents for proteins.[15] This occurs firstly through the unfolding of the protein (due to a reduction in hydrophobic stabilizing interactions) followed by refolding into α-helices, which are the most energetically stable conformations.[15] While TEG may cause unfolding of secondary structures in DBM, there may be insufficient solvent present for TEG to diffuse throughout the protein evenly, making refolding into ordered structures difficult without an additional energy input, such as heat and shear.

Secondary structure components within proteins directly influence its physical and material properties. Plastics derived from proteins are typically denatured, long entangled chains and exhibit crystalline regions rich in α-helices and β-sheets.[16] Crystalline regions impart toughness and increase tensile strength (e.g., β-sheets in spider silk[17]), but depending on the type and extent of crystal structure, can also make the plastic brittle. The amorphous regions provide elastomeric properties[18] while β-turns assist in energy storage and release.[18a][19]

Understanding the polymer physics underpinning secondary structural changes of DBM and how it is altered by the addition of processing aids (SDS and TEG) and thermal energy input is important for the development of a useful material. The aim of this research was to determine whether SDS and TEG were capable of inducing sufficient chain mobility in DBM to induce secondary structural changes during preparation, upon heating through its glass transition temperature, and up to a typical extrusion temperature for the material (120 °C). Structural changes were evaluated using synchrotron based Fourier transform infra-red spectroscopy (FT-IR) and compared with wide angle X-ray scattering (WAXS) results over the same temperature range.

2. Experimental Section

2.1. Methodology

2.1.1. Reagents

Bovine bloodmeal was obtained from Wallace Corporation Ltd. (New Zealand) and sieved to utilize particles under 710 μm. PAA (Proxitane Sanitizer 5%) was purchased from Solvay Interox Pty Ltd. Auckland, New Zealand. SDS (Thermo Fisher Scientific, Loughborough, UK) and TEG (Merck Millipore, Auckland, New Zealand) were dissolved in distilled water for addition to DBM.

2.1.2. Sample Preparation

Bloodmeal was decolored using a previously developed method;[6] 4 wt% PAA solution (300 g) was added to bloodmeal (100 g) and allowed to react with high speed mixing (10 min) in a Kenwood Cooking Chef KM080 mixer with the creaming beater attachment to ensure homogenous decoloring before diluting with distilled water (300 g). This mixture was immediately neutralized with ≈1 mol L^{-1} sodium hydroxide and filtered. The DBM was oven dried overnight (75 °C), milled and sieved to 710 μm. Moisture content was determined using thermogravimetric analysis, all samples were found to have a final moisture content of 8 wt%.

Samples were prepared by dissolving SDS (0.6 g) in 10 g distilled water (50 °C), and mixed with DBM (20 g) for 10 min using a hand-held Omni International Tissue Homogenizer set with a hard-tissue plastic generator probe. For samples containing plasticizer, 4 g of TEG was added to the SDS containing blend, followed by an additional 10 min mixing. The resultant mixtures were stored overnight in sealed plastic containers below 4 °C, followed by freeze-drying (48 h) in a Labconco FreeZone 2.5 L Benchtop Freeze Dry System to a final moisture content of ≈8 wt%.

2.1.3. Synchrotron Microscopy

Spatially and thermally resolved FT-IR experiments were undertaken on the infrared microspectroscopy beamline at the Australian Synchrotron, Victoria, Australia. Samples of DBM and DBM with processing aids were compressed in a diamond cell and then transferred onto a barium fluoride slide. This was placed in a Linkam temperature controlled stage connected to a Bruker Hyperion 3000 with an MCT collector and XY stage. The stage was set to 24 °C and purged with nitrogen gas. Two experiments were conducted: i) spatial mapping before and after thermal treatment and ii) spatial mapping throughout thermal treatment using isothermal holds.

For each sample type, three separate particles were mapped and scanned. For each point in the map, 32 spectra were collected in transmission mode with a resolution of 4 cm^{-1} between 3 900 and 700 cm^{-1} and averaged using Opus 7.2 software (Bruker Optik GmbH 2013).

2.1.3.1. Spatial Mapping before and after Thermal Treatment

Each particle was mapped using a 10 × 10 μm spot size chosen on video images at 24 °C and a map containing ≈130 points was obtained. After mapping, the mounted sample was heated at 50 °C min^{-1} in the Linkam stage to 120 °C, held isothermally for 2 min then cooled back to room temperature at 50 °C min^{-1}. A grid with the same *xy* co-ordinates as the original scan was then mapped for a second time.

2.1.3.2. Spatial Mapping Throughout Thermal Treatment Using Isothermal Holds

A particle of DBM with processing aids was mounted and a ≈60 μm × 60 μm grid was chosen using a 10 μm × 10 μm spot size. Grids with the same *xy* co-ordinates were scanned at the following temperatures: ≈24, 45, 55, 75, 100, and 120 °C. Heating was carried out at 50 °C min^{-1} to each successive temperature, and the sample allowed to equilibrate for 10 min before mapping.

2.1.4. Data and Statistical Analysis

Relative peak height in the amide III region of inverted second derivative FT-IR spectra were used to estimate relative fractional composition of corresponding secondary structures according to Bier et al.[7,20] Data was filtered for a minimum area under the amide III region to exclude points mapped outside particles from the analysis.

The second derivative of the raw FT-IR spectra was determined using the Savitzky–Golay algorithm in Opus 7.2 using nine-point smoothing. The second derivative was inverted by dividing by −1 and peak heights above the zero line were obtained for the wavenumber range associated with each secondary structure (Table 1).

The maximum height of the inverted second derivative peak A''_x for the wavenumber range associated with α-helices, β-sheets, turns, and random coils was used to calculate the ratios A''_α/A''_β, A''_t/A''_β, and A''_r/A''_β indicated by the subscripts α, β, t, and r.

Table 1. Peak assignment in the amide III region.[21]

Region	Secondary structure	Wavenumber [cm^{-1}]
Amide III	α-Helix	1 330–1 295
	β-Turns	1 295–1 270
	Random coils	1 270–1 250
	β-Sheets	1 250–1 220

The molar fraction for each secondary structure type was calculated using Equation (1)–(5) and spatial maps were drawn based on these compositions using Microsoft Excel and the respective *xy* coordinates. The composition approximates a mole fraction of peptide linkages in each structural conformation, each of which absorbs differently in the amide III region)

$$\alpha + \beta + t + r = 1 \tag{1}$$

$$\beta = \frac{1}{A''_\alpha/A''_\beta + A''_t/A''_\beta + A''_r/A''_\beta + 1} \tag{2}$$

$$\alpha = \beta\frac{A''_\alpha}{A''_\beta} \tag{3}$$

$$t = \beta\frac{A''_t}{A''_\beta} \tag{4}$$

$$r = \beta\frac{A''_r}{A''_\beta}. \tag{5}$$

The change in secondary structure composition upon addition of SDS and TEG additives was determined for both experiments. For the larger spatial maps, data points obtained from the perimeter and the core of the particles were interpreted separately also. The average composition of DBM with and without additives was calculated by averaging the secondary structure composition observed for each replicate and a two-tail Student's *t*-test was performed to identify significant changes (95% confidence) between the mean composition in DBM and those containing additives.

2.1.5. Wide Angle X-ray Scattering

Thermally resolved WAXS of decolored samples was carried out using a PANalytical Empyrean X-ray diffractometer at 45 kV and 40 mA using Cu $K\alpha_1$ radiation. Samples were mounted in an Anton Paar CHC Plus chamber with air cooling and scanned between 25 and 125 °C in 10 °C increments, controlled by an Anton Paar TCU 110 temperature control unit. The diffraction data was collected in the 2θ range from 4 to 35° with a step size of 0.0263°. A soller slit of 0.04 rad was used, with a fixed incident beam mask of 10 mm and programmable divergence slit set to an irradiated length of 10 mm. For the diffracted beam path, a fixed 5 mm anti-scatter slit (non-ambient and MRD) was used and X-rays detected using a PIXcel3D area detector. Data was smoothed using a 25-point moving average. A linear baseline was fitted to the minima between 5 and 35° and the baseline corrected data was then fitted with a

Gaussian curve to represent the amorphous halo. Removal of the amorphous halo yielded the crystalline peaks, which were then deconvoluted by fitting Gaussian curves. Peak positions were obtained and d-spacing determined using Bragg's law.

2.1.6. Thermogravimetric Analysis

Moisture content was determined from the mass lost at 120 °C during heating at 10 °C min^{-1} in a Texas Instruments SDT 2960 analyzer. Approximately, 10 mg of sample was heated to 800 °C in dry air.

3. Results and Discussion

3.1. Secondary Structure

The ability to form a consolidated material during extrusion requires overcoming the original stabilizing interactions between proteins allowing new intermolecular interactions to form. The purpose of adding SDS and TEG is to impart sufficient chain mobility, and through this impart new interactions, evident from changes in secondary structure. To assess these effects, the secondary structure of large grids across particles were mapped before and after heating. A 2-min isothermal heat treatment at 120 °C followed by cooling to room temperature was chosen to simulate the temperature and residence time encountered during extrusion.

Addition of SDS to DBM caused a small increase in α-helices and random coils at the expense of β-sheets and β-turns (Figure 1). For soluble proteins with cleaved disulphide bridges, SDS often leads to an increase in helical composition,[22] with the helical structure being stabilized through ionic bonding and hydrophobic interaction with the SDS molecule. However, with the inclusion of TEG, a reduction in helical, β-sheet and β-turn structures was observed. This is due to the amphiphilic nature of TEG, which allows it to interact with both non-polar and polar amino acids, further unravelling buried non-polar groups and subsequently leading to a large increase in disordered structures.

The overall composition of both DBM and DBM with SDS were not altered upon heating due to their lack of chain mobility. During thermoplastic processing, chain mobility is paramount for obtaining new stabilizing interactions between proteins, and FT-IR results showed that the addition of SDS alone is insufficient for achieving adequate mobility, and that the addition of TEG plasticizer is required to process DBM thermoplastically. This is evident from samples containing TEG undergoing a structural change upon heating, leading to the recovery of some helical structures resulting in an increase in overall ordered structure. A high helical content may be favored for processes such as film blowing; e.g., for zein, higher α-helical content was favored over those with high β-sheet content.[23]

A clear boundary in composition was observed in the spatial maps as a result of the diffusion controlled decoloring reaction (Figure 2 and Table 2). Particles showed a distinct diffusion front, with a β-sheet rich core and helical and random coil structures remaining

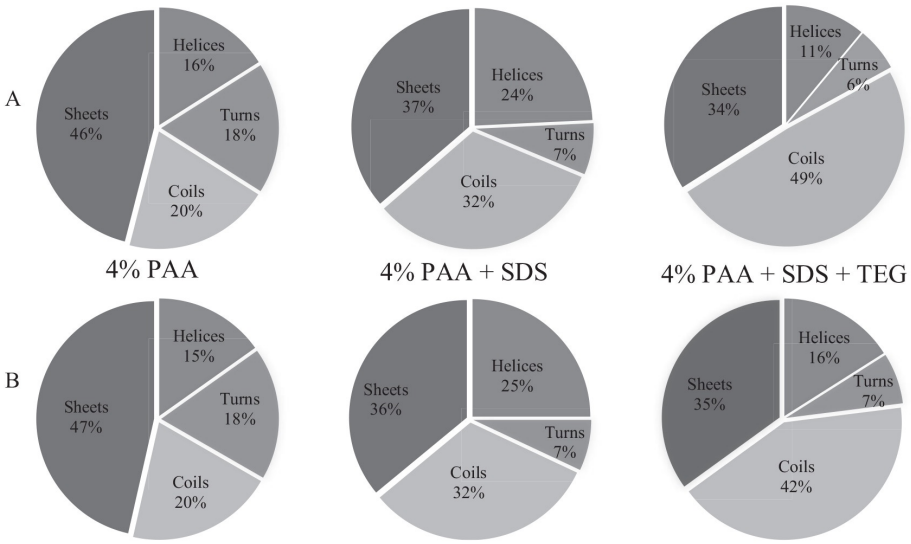

Figure 1. Average fractional composition of secondary structures for left to right: 4 wt% peracetic acid decolored bloodmeal (4% PAA), with sodium dodecyl sulfate (4% PAA SDS) and SDS with triethylene glycol (4% PAA SDS + TEG) (A) before and (B) after heating to 120 °C.

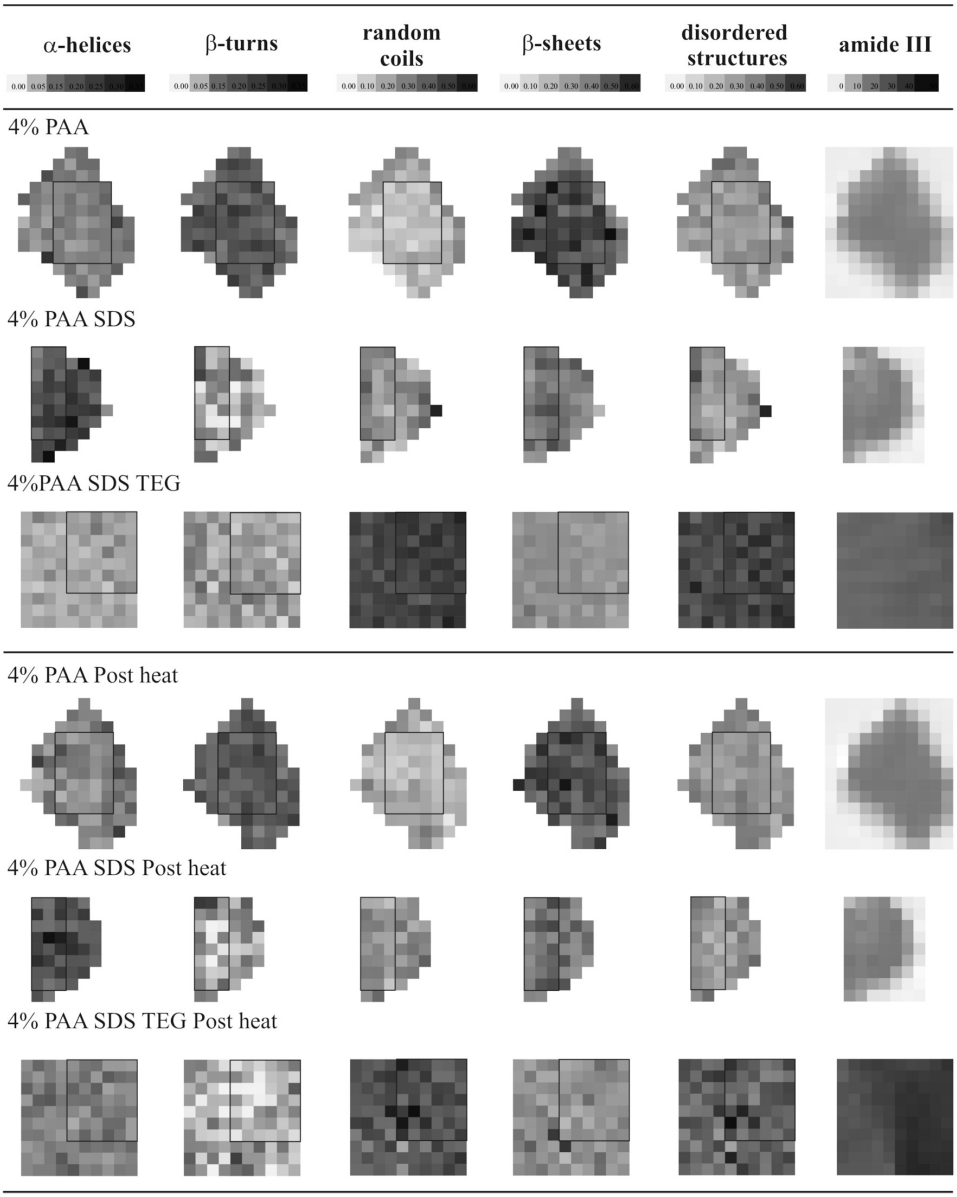

Figure 2. Secondary structure distribution and total amide III region of 4 wt% peracetic acid decolored bloodmeal (4% PAA) with processing aids sodium dodecyl sulfate (SDS) and SDS with triethylene glycol (TEG) at room temperature before and after heating to 120 °C. Random coils and β-turns have been combined to give proportion of disordered structures. The shape outlined in black within the particle maps represents the boundary between the perimeter and the core of the particle.

predominantly at the perimeter, with β-turns distributed evenly throughout.[6]

Although heat is used to provide energy to increase chain mobility, heating DBM led to no overall changes in average secondary structural composition. After plasticizing the DBM with SDS alone or SDS together with TEG, this boundary was much less apparent, with only turns and random coils showing a significant difference between

Table 2. Summary of basic statistics for decolored (DBM) with sodium dodecyl sulfate (SDS) or SDS and triethylene glycol (TEG), from FT-IR experiment 1.

Sample	*N*	α-Helices			β-Turns			Random coils			β-Sheets			Disordered structures		
		Av.	Std. dev.	*t*-Test	Av.	Std. dev.	*t*-Test	Av.	Std. dev.	*t*-Test	Av.	Std. dev.	*t*-Test	Av.	Std. dev.	*t*-Test
4% PAA pre-heat																
Total		0.16	0.04		0.18	0.05		0.20	0.07		0.46	0.08		0.38	0.07	
Perimeter average	174	0.17	0.05		0.18	0.05		0.21	0.08		0.44	0.08		0.39	0.08	
Core average	132	0.15	0.03		0.18	0.05		0.19	0.06		0.48	0.06		0.37	0.07	
Perimeter vs. core				0.00			0.55			0.00			0.00			0.04
4% PAA post-heat																
Total		0.15	0.05		0.18	0.05		0.21	0.07		0.45	0.07		0.39	0.07	
Perimeter average	170	0.16	0.05		0.18	0.06		0.23	0.07		0.43	0.08		0.43	0.08	
Core average	132	0.14	0.04		0.19	0.04		0.19	0.05		0.48	0.06		0.38	0.06	
Perimeter vs. core				0.00			0.20			0.00			0.00			0.00
Perimeter pre vs. post heat				0.08			0.72			0.09			0.50			0.05
Core pre vs. post-heat				0.32			0.31			0.74			1.00			0.29
4%PAA SDS pre-heat																
Total		0.24	0.05		0.07	0.06		0.32	0.12		0.36	0.09		0.40	0.11	
Perimeter average	62	0.24	0.06		0.09	0.06		0.31	0.11		0.36	0.09		0.40	0.12	
Core average	56	0.25	0.06		0.06	0.05		0.33	0.12		0.36	0.09		0.39	0.11	
Perimeter vs. core				0.69			0.01			0.24			1.00			0.85
4%PAA SDS post-heat																
Total		0.25	0.06		0.07	0.06		0.32	0.10		0.36	0.08		0.39	0.10	
Perimeter average	61	0.24	0.05		0.08	0.05		0.32	0.08		0.36	0.08		0.40	0.09	
Core average	52	0.25	0.07		0.06	0.06		0.31	0.11		0.37	0.08		0.37	0.11	
Perimeter vs. core				0.31			0.04			0.69			0.21			0.12
Perimeter pre- vs. post-heat				1.00			0.68			0.54			0.67			0.73
Core pre vs. post-heat				0.49			0.86			0.32			0.44			0.35
4%PAA SDS–TEG pre-heat																
Total		0.11	0.02		0.06	0.03		0.49	0.05		0.34	0.04		0.56	0.04	
Perimeter average	88	0.11	0.02		0.07	0.03		0.48	0.04		0.34	0.04		0.56	0.04	
Core average	212	0.11	0.02		0.06	0.02		0.50	0.05		0.34	0.04		0.55	0.05	
Perimeter vs. core				0.94			0.00			0.01			0.71			0.67

(*Continued*)

Table 2. Continued

Sample	*N*	α-Helices			β-Turns			Random coils			β-Sheets			Disordered structures		
		Av.	Std. dev.	*t*-Test	Av.	Std. dev.	*t*-Test	Av.	Std. dev.	*t*-Test	Av.	Std. dev.	*t*-Test	Av.	Std. dev.	*t*-Test
4%PAA SDS–TEG post-heat																
Total		0.16	0.04		0.07	0.04		0.42	0.08		0.35	0.06		0.49	0.07	
Perimeter average	88	0.16	0.04		0.08	0.04		0.41	0.08		0.35	0.06		0.49	0.08	
Core average	212	0.16	0.08		0.08	0.04		0.40	0.08		0.35	0.07		0.49	0.08	
Perimeter vs. core				0.48			0.37			0.48			0.85			0.83
Perimeter pre- vs. post-heat				0.00			0.62			0.00			0.05			0.00
Core pre- vs. post-heat				0.00			0.00			0.00			0.03			0.00

Statistically significant ($p < 0.05$) results are highlighted. Random coils and β-turns have been combined to give proportion of disordered structures.

the core and perimeter. This indicated that SDS and TEG had a homogenizing effect on secondary structure distribution.

SDS alone led to an increase in helices and random coils (with a corresponding decrease in turns and sheets) and a slight increase in variability of composition, observed as an increase in standard deviation for each structure type (Figure 1 and Table 2). Overall, the change in composition, which occurred at core compared with that of DBM appeared to have been slightly larger than the change occurring at the perimeter, indicating SDS had diffused throughout the particle.

Addition of TEG caused a reduction in both helices and sheets, and a much higher quantity of random coils. In both cases, SDS and SDS with TEG caused a slightly larger reduction in β-sheet content at the core of the particles than they do at the perimeter, suggesting the additives diffused through the particle with ease. Addition of TEG appeared to have reduced variation in secondary structure distribution throughout the particle, reflected by a reduction in the standard deviation (Table 2). The improved homogeneity may be due to the presence of a larger quantity of solvent upon mixing (water and TEG), allowing better dispersion of processing aids throughout the protein.

Upon heat treatment, the secondary structural distribution of the samples containing SDS with TEG appeared more uniformly distributed, showing no significant difference in structural composition between the perimeter and the core ($p > 0.05$). Previous work in blood-based thermoplastics indicated a similar trend, indicating a more even distribution of structures after extrusion,[20] although in this case it is purely a heat treatment cycle excluding the effects of shear and mixing encountered during extrusion.

Heating alone was found to be incapable of providing sufficient chain mobility during the timeframe of this experiment, and led to no significant secondary structural changes in either DBM or with addition of SDS. During preparation of the material, the use of dissolved SDS was found to increase protein chain mobility in DBM leading to the formation of new helical structures. However, without water present as a plasticizer no change in composition was observed during heating. It can be concluded that SDS may support the formation of helical structures and reduce total stabilizing interactions during preparation of DBM feedstock, but does not have a plasticizing effect in DBM. Finally, the addition of TEG caused a major increase in random coil content (at the expense of α-helices) and a reduction in β-sheet content, a result of reducing protein–protein interactions in favor of forming protein–plasticizer interactions. During the heating cycle, this material was found to have sufficient mobility to recover some ordered

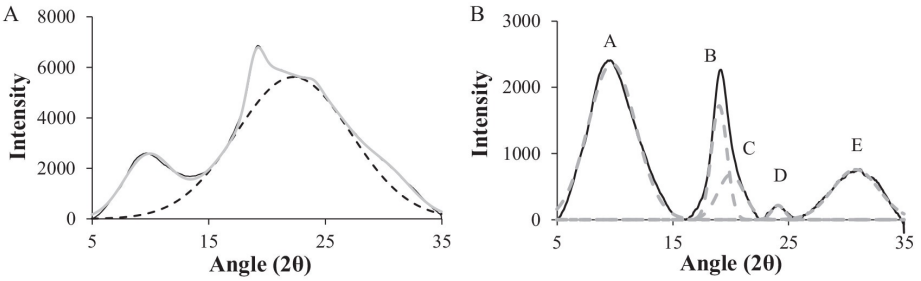

Figure 3. Deconvolution of WAXS diffractogram obtained from 4% PAA decolored bloodmeal at room temperature. A) Fitting of Gaussian amorphous halo and B) deconvolution of crystalline peak area into five peaks. Peak A: Inter-structure spacing, Peaks B and C: Inter-strand spacing between adjacent β-sheets or intra-strand spacing in α-helices. Peaks D and E are caused by interatomic scattering.

structures, an indication of its suitability for thermoplastic processing conditions.

3.2. Ordered Structures

The effect of the additives and thermal input on the crystalline peaks and molecular spacing of DBM was investigated using WAXS. An amorphous halo was fitted between 5 and 35° 2θ that allowed deconvolution of crystalline peaks after the subtraction of the amorphous region from the WAXS curve (Figure 3).

Three main peaks were observed (Peaks A–C), the first at 9.7°, corresponding to d-spacing of 9.1 Å. The second peak occurred at 19.1° with a smaller peak appearing at 20.6°, corresponding to a d-spacing of 4.6 and 4.3 Å, respectively. These peaks are often observed in proteins, and are attributable to α-helix or β-sheet structures.[24] Peaks with a d-spacing ≈10.5 Å correspond to inter-structure packing, either intersheet or interhelix spacing for proteins containing β-sheets or α-helices[25] (Peak A in Figure 3). Peaks B and C with a d-spacing of ≈4–5 Å corresponds to inter-strand hydrogen bonding between adjacent β-sheets or intra-strand hydrogen bonding within the backbone α-helices. Peaks D and E (3.68 and 2.89 Å, respectively) are caused by interatomic scattering not assigned to secondary structure spacing and are redundant in this context.

Addition of processing aids had no discernible effect on the d-spacing of the amorphous halo, although an increase was observed as the sample was heated, caused by thermal expansion, (Figure 4).

The overall diffractograms for DBM and with the addition of SDS revealed an irreversible shape change upon heating, which recovered slightly when TEG was present. An initial increase in the intensity of Peak B (≈19.1°) occurred during heating in the first scan, and is most easily observed for DBM and DBM with SDS. The sharpening of this peak was largely irreversible, as minimal change occurred in the second scan (Figure 5). Furthermore, the shoulder at ≈24° changed shape gradually, but by 75 °C the shoulder virtually smoothed off, and did not appear to have fully recovered upon cooling, as seen in the second scan. The irreversibility of the shape change may be due to the evaporation of water. Initially, the samples contain ≈8 wt% moisture, filling spaces between nearby protein chains, which upon evaporation causes protein chains to come closer together. To prevent the effects of evaporation during processing, plasticizers with low volatility, such as TEG, are chosen.

The sharpening of Peak B (≈19°) occurs as a result of the crystal structures responsible for that scattering increasing in size. For DBM and with SDS, Peak B appears to be sharper initially and sharpen more than the sample containing TEG. This is an indication of a higher degree of relative crystallinity in DBM and in the presence of SDS compared with TEG, known to reduce crystallinity in proteins.

Peak B is associated with intra-structure scattering of X-rays, a result of hydrogen bonding interactions between amino acids within α-helices or β-sheets. The sharpening of Peak B is thought to be caused by the reorienting of β-sheets already present into larger crystals during heating rather than through the formation of new structures. This may be

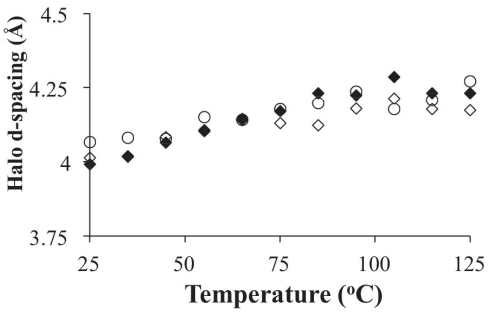

Figure 4. Halo position given as d-spacing (Å) for decolored bloodmeal (◆) with the addition of processing aids SDS (○) and TEG (◇).

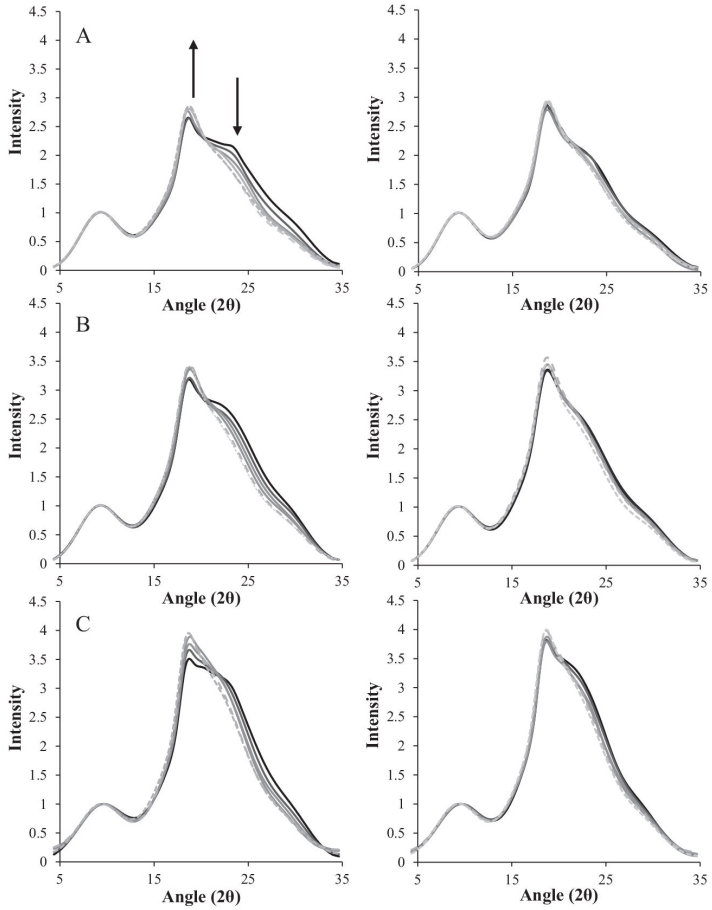

Figure 5. WAXS of decolored bloodmeal with processing aids normalized at $2\theta = 9.65°$. A) 4% PAA decolored bloodmeal (DBM), B) DBM with sodium dodecyl sulfate (SDS), C) DBM with SDS and triethylene glycol. Left: First thermal scan, right: Second thermal scan. Arrow indicates increasing temperature 25 °C (—), 45 °C (—), 65 °C (—), 85 °C (—), 105 °C (- -) and 125 °C (---).

due to the evaporation of solvent, increasing the proximity of nearby β-sheets. For DBM alone Peak B changes significantly, however very little change is observed in FT-IR, indicating no new structures are formed during heating. However, heating may provide β-sheets which are in proximity to one another sufficient energy to reorient into a larger array of sheets, which can be detected during WAXS. The same trend was observed in the presence of SDS and also SDS with TEG, however FT-IR also showed an increase in helical content with only a slight increase in sheets. Although the process appears mostly irreversible, the presence of TEG allowed some recovery, a result of much higher chain mobility, free volume, and competing protein–plasticizer interactions. Thus, the addition of TEG will be important for maintaining processability during multiple heating and cooling cycles.

The intramolecular spacing of Peak B was 4.67 Å for all sample types, and remained constant with heating. However, the area showed a step increase at ≈55–75 °C (Figure 6), occurring at the temperature associated with the formation of helices observed in FT-IR (Figure 7). In these experiments, smaller grids across a number of particles were heated and equilibrated for 10 min at the specified temperature before measuring secondary structure. This means that kinetic effects leading to changes in secondary structure have been accounted for.

Heating DBM in the presence of processing aids led to a gradual increase in β-sheet structures with temperature (Figure 7B), becoming significant between 55 and 75 °C ($p < 0.05$). Although there was a slight increase in β-sheet content for DBM alone, significant from 55 to 75 °C ($p < 0.05$), the larger data set used to obtain the spatial map (Figure 2) shows only a very small difference occurring at the core of the particle occurring upon heating, with no significant change overall. This indicates that DBM does not have enough mobility to reorient to form new β-sheets strongly during a heating cycle, however in the presence of SDS and SDS with TEG sheet formation can occur to a greater extent and appears to be a continual process with no discernible onset temperature.

The formation of helices did not follow a linear trend, appearing to require a temperature of ≈100–120 °C before significant quantities are formed in DBM alone as well as in the presence of SDS. In the case of DBM, the increase of helical content was only observed in the smaller sample set (Figure 7A), accompanied by a loss in β-turns and random coils, and no change in helical content was observed in the larger spatial maps.

Samples containing SDS also showed a variable trend, the smaller data set used to investigate structure at the various temperatures showed that the formation of helices were accompanied by a loss in random coils, whereas the spatial maps (Figure 2) showed no significant change. Like DBM, the difference between the two trends is most likely a kinetic effect, where the large spatial maps were heated quickly and cooled down before remapping, allowing inadequate time for structural rearrangement.

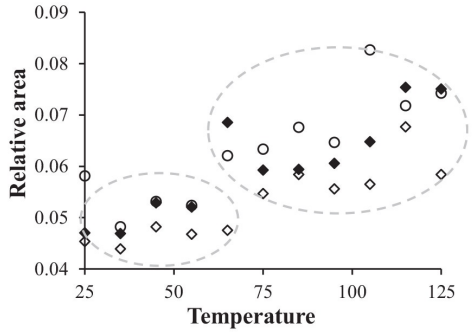

Figure 6. Peak B area relative to amorphous halo for decolored bloodmeal (◆) with the addition of processing aids SDS (○) and TEG (◇).

Finally, samples containing TEG increased in helical content with a reduction in β-turns and random coils, beginning around 55–75 °C. The formation of helices occurred past the glass transition of the material, ≈35–45 °C. An alternative possibility is that the formation of sheets at low temperature is due to the aggregation of helices commonly observed during thermal denaturing of protein, and thus do not appear to increase until higher temperatures.

For structural rearrangement to occur during processing, the raw material must be given adequate chain mobility, thermal energy, and sufficient time to form new stabilizing interactions. Optimization of exposure time and temperature will likely be required for each type of processing, for instance, promoting helical formation for film blowing may require shorter times at elevated temperatures provided there is sufficient plasticization. Storage temperature of the feed may also impact processing, as prolonged exposure of the material at elevated temperature will increase β-sheet content. Formation of β-sheets is known to aid the fixation process of proteins during thermoplastic processing,[8] the premature formation of these structures may inhibit molecular reorientation in the melt, reducing ease of processing and leading to a change in the desired material properties.

In terms of overall order, the addition of SDS caused a small increase in crystallinity relative to DBM, and like DBM increased with increasing temperature. The presence

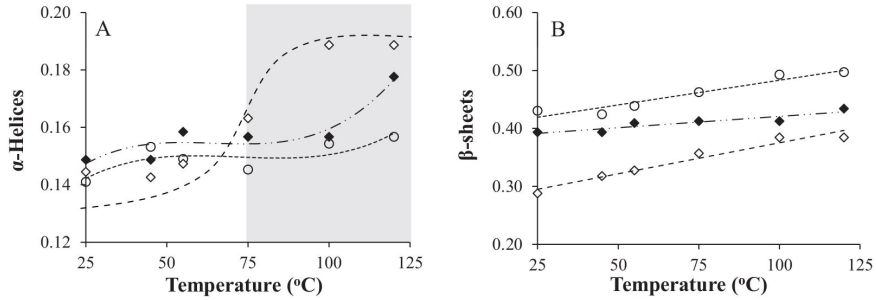

Figure 7. Fractional composition of spatial maps of decolored bloodmeal (◆) with the addition of processing aids SDS (○) and TEG (◇). A) α-Helices, B) β-sheets. Highlighted in gray are the regions in which significant change in ordered structure content is observed. A summary of statistics is available as an electronic Supporting Information Appendix.

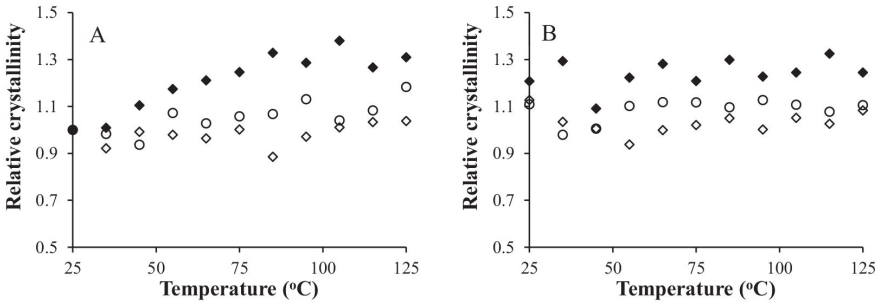

Figure 8. Relative crystallinity of decolored bloodmeal (◆) with the addition of processing aids SDS (○) and TEG (◇), normalized to apparent percentage crystallinity of decolored bloodmeal at room temperature from first scan. A): First scan, B) second scan.

of TEG led to no change in relative crystallinity, even with increasing temperature (Figure 8).

While FT-IR showed a decrease in total ordered structures with increasing temperature for DBM and in the presence of processing aids, it may not directly correspond to an increase in observed crystallinity. For ordered structures to be detected by WAXS, the structures must be in relatively close proximity giving a percentage of "crystalline ordered structures," whereas FT-IR determines the molar content of "total ordered structures." As a result, the same molar number of ordered structures physically rearrange and cause an increase in crystallinity. Relative changes in crystallinity were observed when heating DBM and samples containing SDS in the first scan, however, such changes were no longer observed in the second scan. It would appear that heating DBM materials leads to an irreversible change in structure when exposed for prolonged periods of time, and that plasticization may inhibit the irreversibility of this aggregation by providing space between nearby protein secondary structures.

4. Conclusions

PAA decoloured bloodmeal particles are heterogeneous, with a core containing higher concentrations of β-sheets with the periphery containing higher concentrations of α-helices and coils. SDS addition induced α-helical formation and reduced β-sheets and β-turns, while adding SDS and TEG reduced α-helices and β-sheets and increased random coils. α-Helices are beneficial for protein film forming while random coils increase the elasticity of the material.

There was little or no change in secondary structure for DBM and SDS treated DBM when heated for 2 min and cooled, showing that there was insufficient protein chain mobility to undergo any structural changes within the heat/cool cycle. Heating and cooling SDS and TEG treated DBM increased α-helices at the expense of random coils, showing that TEG addition gave sufficient chain mobility for the random coils to form α-helices.

Treating DBM with SDS alone, or SDS with TEG gave a homogenous feedstock, observed as a more even distribution of secondary structures throughout the DBM particles, which became more uniform again upon heating. This has important implications for extrusion processing, where quick and homogenous blending of crystalline and amorphous structures in the melt is desirable to promote new interactions and prevent thermally induced protein degradation.

Heating over a long period of time showed a gradual increase in β-sheets for all samples, while α-helices showed a dramatic increase around 55–75 °C for SDS and TEG-treated DBM and around 100 °C for SDS-treated DBM, suggesting that with sufficient chain mobility, α-helices will readily form from random coils while β-sheet formation is a slower process. Forming large quantities of β-sheets is often associated with stiffening and embrittlement of the material.

XRD analysis showed that long-term heating causes structural changes that are largely irreversible for DBM and SDS treated DBM, with an increase in crystallinity during heating that did not change upon cooling. This could be detrimental long term for thermoplastic processing as the material would become more difficult to extrude and injection mould if left heated for a long time. DBM treated with both SDS and TEG showed little or no change in crystallinity, suggesting TEG provided sufficient chain mobility to prevent the onset of irreversible change. This is desirable for maintaining processability of the material over multiple heating and cooling cycles.

Acknowledgements: This research was undertaken on the infrared microspectroscopy beamline at the Australian Synchrotron, Clayton, VIC, Australia. Proposal number AS132/IRMFI/6636. The authors would especially like to acknowledge the technical assistance of Dr. Mark Tobin and Dr. Danielle Martin. Travel funding support was received from the New Zealand Synchrotron Group Ltd.

Received: August 15, 2014; Revised: September 30, 2014; Published online: November 18, 2014; Published online: November 18, 2014; DOI: 10.1002/mame.201400290

Keywords: IR spectroscopy; materials science; protein structures

[1] (a) C. R. Álvarez-Chávez, S. Edwards, R. Moure-Eraso, K. Geiser, *J. Clean. Prod.* **2012**, *23*, 47; (b) J. Gonzalez-Gutierrez, P. Partal, M. Garcia-Morales, C. Gallegos, *Bioresource Technol.* **2010**, *101*, 2007.
[2] C. J. R. Verbeek, C. Viljoen, K. Pickering, L. van den Berg, (Waikatolink Limited), *New Zealand 551531*, **2010**.
[3] A. Low, C. J. R. Verbeek, M. C. Lay, *Macromol. Mater. Eng.* **2014**, *299*, 75.
[4] T. M. Hicks, C. J. R. Verbeek, M. C. Lay, M. Manley-Harris, *J. Am. Oil Chem. Soc.* **2013**, *90*, 1577.
[5] C. J. R. Verbeek, M. C. Lay, A. W. K. Low, (Waikatolink Limited) *US20130139725 A1*, **2013**.
[6] T. Hicks, C. J. R. Verbeek, M. C. Lay, J. M. Bier, *RSC Adv.* **2014**, *4*, 31201.
[7] J. Bier, C. Verbeek, M. Lay, *J. Therm. Anal. Calorim.* **2014**, *115*, 433.
[8] L. A. De Graaf, *J. Biotechnol.* **2000**, *79*, 299.
[9] C. J. R. Verbeek, L. E. van den Berg, *Macromol. Mater. Eng.* **2010**, *295*, 10.
[10] V. M. Hernandez-Izquierdo, D. S. Reid, T. H. McHugh, J. De J. Berrios, J. M. Krochta, *J. Food Sci.* **2008**, *73*, E169.
[11] L. di Gioia, S. Guilbert, *J. Agric. Food Chem.* **1999**, *47*, 1254.
[12] T. Bourtoom, M. S. Chinnan, P. Jantawat, R. Sanguandeekul, *Food Sci. Technol. Int.* **2006**, *12*, 119.
[13] P. Fairley, F. J. Monahan, J. B. German, J. M. Krochta, *J. Agric. Food Chem.* **1996**, *44*, 438.
[14] X. Mo, X. Sun, *J. Polym. Environ.* **2000**, *8*, 161.
[15] M. Subirade, I. Kelly, J. Guéguen, M. Pézolet, *Int. J. Biol. Macromol.* **1998**, *23*, 241.

[16] (a) J. M. Bier, C. J. R. Verbeek, M. C. Lay, *Macromol. Mater. Eng.* **2013**, *299*, 524; (b) O. S. Rabotyagova, P. Cebe, D. L. Kaplan, *Biomacromolecules* **2011**, *12*, 269.
[17] (a) S. Keten, M. J. Buehler, *J. R. Soc. Interface* **2010**; (b) A. Nova, S. Keten, N. M. Pugno, A. Redaelli, M. J. Buehler, *Nano Lett.* **2010**, *10*, 2626.
[18] (a) G. Qin, X. Hu, P. Cebe, D. L. Kaplan, *Nat. Commun.* **2012**, *3*, 1003; (b) S. Rauscher, S. Baud, M. Miao, F. W. Keeley, R. Pomès, *Structure* **2006**, *14*, 1667.
[19] K. M. Nairn, R. E. Lyons, R. J. Mulder, S. T. Mudie, D. J. Cookson, E. Lesieur, M. Kim, D. Lau, F. H. Scholes, C. M. Elvin, *Biophys. J.* **2008**, *95*, 3358.
[20] J. M. Bier, C. J. R. Verbeek, M. C. Lay, *J. Appl. Polym. Sci.* **2013**, *130*, 359.
[21] S. Cai, B. R. Singh, *Biophys. Chem.* **1999**, *80*, 7.
[22] (a) K. Takeda, Y. Moriyama, *J. Prot. Chem.* **1990**, *9*, 573; (b) K. Takeda, K. Sasa, K. Kawamoto, A. Wada, K. Aoki, *J. Colloid Interface Sci.* **1988**, *124*, 284.
[23] M. Oliviero, E. Di Maio, S. Iannace, *J. Appl. Polym. Sci.* **2010**, *115*, 277.
[24] (a) C. S. Thomas, M. J. Glassman, B. D. Olsen, *ACS Nano* **2011**, *5*, 5697; (b) Y. Wang, F. L. Filho, P. Geil, G. W. Padua, *Macromol. Biosci.* **2005**, *5*, 1200.
[25] W. Elshemey, A. Elfiky, W. Gawad, *Prot. J.* **2010**, *29*, 545.

7

Changes in Hydrogen Bonding in Protein Plasticized with Triethylene Glycol

By

TALIA M. HICKS, C. J. R. VERBEEK, M. C. LAY

AND

M. MANLEY-HARRIS

Published in Journal of Applied Polymer Science

As first author for this paper, I prepared the draft manuscript of this journal paper, which was refined and edited in consultation with my supervisors, whom are credited as co-authors. The FT-IR results reported here were collected in collaboration with my supervisors (and Dr. J. Bier) during beamtime at the Australian Synchrotron. Together with my co-authors, I travelled to the Australian Synchrotron to conduct the experiments. I then performed the data analysis in OPUS software, Microsoft Excel and MATLAB. I also carried out the TGA, DMA and DSC experiments and analysis.

Journal of Applied Polymer Science

Changes in hydrogen bonding in protein plasticized with triethylene glycol

Talia Maree Hicks,[1] Casparus Johannes Reinhard Verbeek,[1] Mark Christopher Lay,[1] Merilyn Manley-Harris[2]

[1]School of Engineering, Faculty of Science and Engineering, University of Waikato, Hamilton 3240, New Zealand
[2]School of Science, Faculty of Science and Engineering, University of Waikato, Hamilton 3240, New Zealand
Correspondence to: T. M. Hicks (E-mail: tmh20@students.waikato.ac.nz)

ABSTRACT: Bloodmeal decolored with 4 wt % peracetic acid can be extruded into a semi-transparent bio-plastic through the addition of sodium dodecyl sulfate (SDS), water, and triethylene glycol (TEG). TEG is often used to plasticize protein thermoplastic materials because of its ability to form both hydrophobic and hydrogen bonds. Synchrotron-based FT-IR was used to monitor changes in the types of hydrogen bonding occurring in TEG plasticized protein during heating. Heating was found to overcome a portion of the weaker hydrogen bonds found within and between proteins, observed as a blue-shift in the N-H and O-H stretching vibrations occurring at ~3280 cm^{-1}. TEG was shown to be involved in a larger array of hydrogen bonding environments after heating, evidenced by the broadening of the C-OH stretch around 1076 cm^{-1}, suggesting improved plasticizer-protein interactions. Additionally, these bonds were found to be as strong as the original interactions, observed as a shift in the C-OH peak back to its original wavenumber (~1076 cm^{-1}) during cooling. Initially, TEG was spatially distributed into distinct plasticizer-rich and plasticizer-poor domains, giving rise to two glass transitions. Heating allowed the migration and uniform dispersion of TEG throughout the material, and merged the two glass transitions into one broader glass transition region. Heating during DSC removed the peak around 60°C corresponding to the enthalpy of relaxation, which is associated with physical aging of amorphous and semi-crystalline polymers. While physical aging occurred during the storage of DBM, in the presence of TEG it occurred to a lesser extent. © 2015 Wiley Periodicals, Inc. J. Appl. Polym. Sci. **2015**, *132*, 42166.

KEYWORDS: biopolymers & renewable polymers; properties and characterization; proteins; spectroscopy

Received 24 December 2014; accepted 26 February 2015
DOI: 10.1002/app.42166

INTRODUCTION

Bloodmeal, a by-product of the meat industry, can be decolored using 4 wt % peracetic acid. The resulting pale-yellow material can be extruded into a semi-transparent bio-plastic by adding sodium dodecyl sulfate (SDS), water, and triethylene glycol (TEG).[1]

Proteins tend to have a high glass transition and melting temperature, typically higher than the temperature at which degradation occurs. To avoid thermal degradation plasticizers are used to lower the glass transition temperature (Tg).[2]

Oxidative decoloring with peracetic acid breaks disulfide bonds present in bloodmeal and reduces the number of other stabilizing interactions[3] resulting in a more soluble material with a lower Tg.[4] Despite this, the addition of SDS and TEG are also required to impart sufficient mobility of the proteins during extrusion.[5]

In addition to SDS and TEG, the pre-extruded mixture also contains water, which is often used to plasticize protein-based thermoplastics. However, during heating and storage significant evaporation can occur, resulting in embrittlement of the material. To prevent this, less volatile plasticizers are often used alongside or instead of water. Tri-ethylene glycol (TEG) has been shown to be an effective plasticizer in bloodmeal-based thermoplastics[6] and in decolored bloodmeal (DBM).[1,5,7]

During extrusion, creating a homogeneous blend of components in the melt is of paramount importance to obtaining a consolidated product. Adequate dispersion of plasticizer is required, and involves wetting and adsorption followed by solvation and/or penetration into the protein. Absorption and diffusion of the plasticizer may not necessarily result in even distribution and is dependent on both the type of plasticizer used and the amino acids in the protein.[8,9]

In protein-based thermoplastics, polyol plasticizers have been found to be most effective because they contain both polar and nonpolar groups which are able to hydrogen bond and interact hydrophobically with protein chains,[9] which may lead to lower rates of leaching compared to polar plasticizers urea and water.

Plasticizer distribution in the feedstock and melt has implications during processing and on the resulting material properties. For instance, if the plasticizer concentration is too high in the feedstock, it can exceed the compatibility limit and lead to phase separation.[10] Phase separation into regions of high and low plasticizer concentration has been implicated in the presence of two glass transitions in soy protein-based plastics[11] and in bloodmeal protein-based thermoplastic.[12]

The purpose of this article was to investigate how heating disrupted stabilizing hydrogen bonding interactions within and between proteins and facilitated the migration and dispersion of TEG. This would give a greater understanding of how temperature affects hydrogen bonding dynamics which can be used to further optimize processing conditions for extrusion and injection moulding. Synchrotron-based FT-IR was used to monitor changes in hydrogen bonding interactions between proteins and plasticizer during heating. The distribution of TEG throughout the DBM particles before, during and after heating was monitored via peaks corresponding with the alcohol and ether groups in the TEG molecule.

METHODOLOGY

Reagents

Bovine bloodmeal was obtained from Wallace Corporation, New Zealand, and sieved to utilize particles under 710 μm. Peracetic acid (Proxitane Sanitizer 5%) was purchased from Solvay Interox Pty, Auckland, New Zealand. Sodium dodecyl sulfate (Thermo Fisher Scientific, Loughborough, UK) and triethylene glycol (Merck Millipore, Auckland, New Zealand) were dissolved in distilled water for addition to decolored bloodmeal.

Sample Preparation

Bloodmeal was decolored by adding 4 wt % peracetic acid solution (300 g) to bloodmeal (100 g) and reacted during high speed mixing (10 min) in a Kenwood Cooking Chef KM080 mixer with the creaming beater attachment to ensure homogenous decoloring.[3] This mixture was diluted with distilled water (300 g) and immediately neutralized with ~ 1 mol L^{-1} sodium hydroxide and filtered. The decolored bloodmeal was oven dried overnight (75°C) to approximately 2–4 wt % moisture and milled to < 1 mm.

Samples were prepared by dissolving SDS (0.6 g) in 10 g distilled water (50°C), and mixing with decolored bloodmeal (20 g) for 10 minutes using a hand-held Omni International Tissue Homogenizer set with a hard-tissue plastic generator probe. For samples containing plasticizer, 4 g of triethylene glycol was added to the SDS DBM blend, followed by an additional 10 minutes mixing. The resultant mixtures were stored overnight in sealed plastic containers below 4°C, followed by freeze-drying (48 h) in a Labconco FreeZone 2.5 L Benchtop Freeze Dry System. Final moisture content was determined using thermogravimetric analysis. Samples used for synchrotron FT-IR analysis contained ~2–4 wt % moisture. Moisture content was found to have increased to 8 wt % during storage prior to DMA and DSC analysis.

Synchrotron FT-IR Microscopy

Spatially and thermally resolved FT-IR experiments were undertaken on the infrared microspectroscopy beamline at the Australian Synchrotron, Victoria, Australia. Individual particles of decolored bloodmeal (DBM) and DBM with additives were compressed in a diamond cell and then transferred to a barium fluoride slide. This was placed in a Linkam temperature controlled stage connected to a Bruker Hyperion 3000 with an MCT collector and XY stage. The stage was set to 24°C and purged with nitrogen gas. Thirty-two spectra were collected in transmission mode with a resolution of 4 cm^{-1} between 3900 and 700 cm^{-1} and averaged using Opus 7.2 software (Bruker Optik GmbH 2013).

Three types of experiments were performed to determine the effect of thermal treatment on the pre-extruded material: (1) thermally resolved, (2) spatial mapping before and after thermal treatment, and (3) spatial mapping throughout thermal treatment using isothermal holds.

Thermally Resolved FT-IR. A 10 × 10 μm spot within the center of each compressed particle was chosen and spectra collected at 30-s intervals during a constant heating ramp from −60°C to 120°C at 2°C min^{-1}.

Spatial Mapping Before and After Thermal Treatment. Each compressed particle was mapped using a 10 × 10 μm spot size chosen on video images at 24°C and a map containing ~100 points was obtained. After mapping, the mounted sample was heated at 50°C min^{-1} in the Linkam stage to 120°C, held isothermally for 2 min then cooled back to room temperature at 50°C min^{-1}. A grid with the same *xy* co-ordinates as the original scan was then mapped for a second time. For each sample type, three separate particles were mapped and scanned.

Spatial Mapping During Thermal Treatment Using Isothermal Holds. A compressed particle of DBM with processing aids was mounted and a ~60 × 60 μm grid was chosen using a 10 × 10 μm spot size. Grids with the same *xy* co-ordinates were scanned at the following temperatures; ~24°C, 45°C, 55°C, 75°C, 100°C, and 120°C. Heating was carried out at 50°C min^{-1} to each successive temperature, and the sample allowed to equilibrate for 10 minutes before mapping. For each sample type, three separate particles were scanned.

Data and Statistical Analysis

FT-IR spectra for each point were integrated for obtaining the thermally resolved and spatial maps of triethylene glycol to amide III peak area ratios using OPUS 7.2. Opus type B integrals were calculated from 1150 to 1045 cm^{-1} (C-O-C and C-OH functional groups in TEG) and from 1330 to 1180 cm^{-1} (amide III region of proteins), along with the ratio of the first peak over the second,[12] to eliminate the effects of variation in thickness across the sample. These ratios were used to compare TEG distribution relative to protein in spatial maps. A comparison of the C-O-C and C-OH peak areas to each other was determined to discern changes in hydrogen bonding

environment, this was achieved by integrating using an Opus type B integral from 1150 to 1090 cm^{-1} (C-O-C) and from 1090 to 1045 cm^{-1} (C-OH) to obtain the ratio of the second peak over the first. Mean, standard deviation, and corresponding histograms were calculated for the mapped ratios. Two additional peaks unique to triethylene glycol (960–905 and 905–860 cm^{-1}) were also compared to the peak area of the amide III region to determine the accuracy of using the C-O stretches of TEG to determine relative changes in TEG content. Data were filtered for a minimum area under the amide III region to exclude points mapped outside particles from statistical analysis.

Thermogravimetric Analysis

Mass loss of DBM samples (~10 mg) in a 0.9 g ceramic crucible were recorded during heating in dry air at 10°C min^{-1} to 800°C in a Texas Instruments SDT 2960 analyzer. Moisture content was determined from the cumulative mass loss up to 120°C.

Dynamic Mechanical Analysis

DMA was performed using a Perkin Elmer DMA 8000 fitted with a high-temperature furnace and cooled with liquid nitrogen. DBM samples were examined by mounting ~ 50 mg of powder in 1.0 × 7.4 × 28 mm (folded dimensions) material pockets (Perkin Elmer) and tested at 0.1, 0.3, 1, 3, 10, and 30 Hz with a dynamic displacement of 0.05 mm and free length of 12.5 mm. Decolored bloodmeal samples containing TEG were analysed in two ways: (1) heating from −60°C to 250°C and (2) heating from −60°C to 120°C to remove thermal history before heating from −60°C to 250°C.

Differential Scanning Calorimetry

DSC was conducted in a Perkin Elmer DSC 8500 hyper DSC fitted with an autosampler accessory and cooled with liquid nitrogen. Approximately 5–10 mg of sample was weighed into 30 μL aluminium autosampler pans (Perkin Elmer) which were then crimped to provide a seal and placed into the auto sampler. All samples were scanned between 0°C and 120°C at 10°C min^{-1} and cooled to 0°C at the same rate before performing a second scan under the same conditions. Glass transition temperature (half Cp extrapolated) was determined from the second scan using Pyris 7 software (Perkin Elmer).

RESULTS AND DISCUSSION

Triethylene glycol is an aliphatic dihydroxy alcohol containing two ether linkages (Figure 1 insert), which strongly absorbs infrared between 1150–1090 cm^{-1} and 1090–1045 cm^{-1} giving rise to two similar sized peaks (Figure 1). The first peak is assigned to the asymmetric stretching vibration of the aliphatic ether groups, (ν_{as}C–O–C) and the second peak is attributed to the stretch of the primary alcohol groups (νC–OH). Two smaller peaks unique to TEG are also observed, occurring at 960–905 and 905–860 cm^{-1}. Assignment of these peaks is difficult as they are caused by coupling of several vibrational modes such as the ether symmetric stretch (ν_sC–O–C), out of plane C-OH bends, C-C stretches, and C-H out of plane bending within the rest of the molecule. These characteristic peaks were only observed in DBM samples containing TEG and were used to monitor changes in TEG content relative to the amide III region (Figure 1).

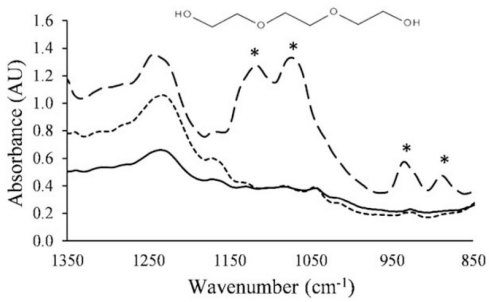

Figure 1. FT-IR absorbance spectrum of decolored bloodmeal (DBM) (—), DBM containing sodium dodecyl sulfate (DBM SDS) (---), and DBM containing SDS and triethylene glycol (DBM TEG) (– –) indicating the absorbance of TEG peaks (*) and the amide III region (1180–1330 cm^{-1}). Insert: structure of triethylene glycol.

The main hydrogen bonding interactions taking place within DBM containing TEG include those formed through intra- and intermolecular protein interactions, TEG–protein interactions and intra- and intermolecular TEG–TEG interactions. A recent frontier orbital study has indicated that the alcohol groups of triethylene glycol are most energetically stable when accepting hydrogen bonds from other molecules such as water, resulting in shorter O---H bond distance, greater interaction energy, and a higher degree of charge transfer compared to when it acted as a hydrogen bond donor.[13] Accordingly, it is most likely that TEG will preferentially act as a hydrogen bond acceptor in the presence of other hydrogen bond donors such as water and protein. Typically, hydrogen bonding is diminished with increasing temperature, but it is possible only some of the weaker bonds are overcome leaving the stronger bonds intact.

Thermally Resolved FT-IR

A single location on a DBM particle was scanned every 30 s using a 10 × 10 μm aperture during a heating cycle (−60°C to 120°C at 2°C min^{-1}). Heating was found to increase the absolute absorbance within each spectra (Figure 2), and were normalized at 2874 cm^{-1} (asymmetric stretching of CH_3) prior to comparison. Heating from room temperature to 120°C led to an increase in intensity in both the amide III region and each of the TEG peaks (Figure 2). In addition to increased absorption, the amide III region changed shape dramatically, gaining intensity around 1306 and 1228 cm^{-1}, and has been attributed to the formation of α-helices and β-sheets during heating.[5]

The peak around 1074.2 cm^{-1} associated with the carbon–oxygen stretch of the TEG primary alcohol groups (νC-OH) red-shifted and broadened with increasing temperature, and by 120°C had shifted to 1070.4 cm^{-1}. As a general rule, hydrogen bonding lowers the frequency of stretching vibrations for the functional group involved because of a reduction in the force constant associated with the X-H covalent bond.[14] However, literature investigating the effects of hydrogen bonding (via solvation and temperature) on the position of the C-O band for

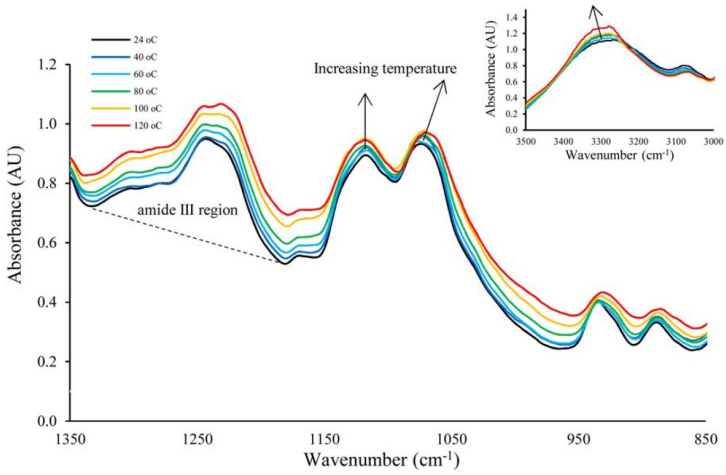

Figure 2. Normalized FT-IR absorbance spectrum of decolored bloodmeal with sodium dodecyl sulfate and triethylene glycol (DBM TEG) with increasing temperature. Insert: Absorbance from 3500 to 3000 cm^{-1} showing the *v*OH peak with increasing temperature. FT-IR Normalized to 1 AU at 2874 cm^{-1}. [Color figure can be viewed in the online issue, which is available at wileyonlinelibrary.com.]

aliphatic alcohols is sparse.[15] The shift in this peak to lower wavenumber with increasing temperature is caused by a reduction in the C-O force constant (increased C-O bond length). The increase in the C-O bond length results from a lower degree of shared electron density between the alcohol oxygen and the hydrogen donor. The broadening of this peak, however, indicates a greater variety of hydrogen bonding interactions are taking place between TEG and other species, perhaps an indication of improved interaction with the protein.

Another indicator of the changing dynamics during heating is the indistinguishable *v*O-H and *v*N-H bands that are also sensitive to their chemical environment. Like N-H, the stretching vibration for O-H generally appears at ~3200 cm^{-1} in a concentrated solution or solid sample (appearing near ~3600 cm^{-1} in dilute or weakly hydrogen bonded samples). Hydrogen bonding (X---O-H) increases the length of the covalent O-H-bond (reducing the force constant and the frequency of IR absorption). In addition, H-bonded hydroxyl groups tend to show reduced absorbance intensity and broadened stretching frequency.

For DBM containing TEG, the *v*OH (and *v*NH) band is situated around 3280 cm^{-1} and was found to become sharper with increasing temperature (Figure 2). The sharpening of this peak reflects a reduction in the overall variety of hydrogen bonds taking place as the temperature increased, a result of thermal energy overcoming weak H-bonds.

Hydrogen bond energies range from 1 to 4 kcal mol^{-1} for weak bonds through to ~15–40 kcal mol^{-1} for strong bonds.[16] Intramolecular H-bonds in ethylene glycol derivatives are comparatively larger (~13.7–15.9 kcal mol^{-1})[17] than intramolecular H-bonding in proteins (~6–8 kcal mol^{-1} for N-H---O=C and ~1.5–1.8 kcal mol^{-1} for C_{α}-H---O=C interactions[18]). The observed blue-shift from ~3280 to 3290 cm^{-1} upon heating suggests that the N-H and O-H groups in the sample are located within weaker or non H-bonded environments.[19]

Considering both the observed shifts (*v*N-H and *v*O-H and that of *v*C-OH) the overall number of hydrogen bonds within the sample was reduced during heating, observed as the narrowing of the *v*N-H and *v*O-H band which also shifted to higher frequency. Estimated values of the hydrogen bonding energies for proteins and ethylene glycol derivatives suggest this change predominantly involves bonding within and between the proteins. Although TEG hydrogen bonding interactions were also weakened overall, TEG was found to take part in a larger variety of interactions during heating, observed as broadening of the *v*C-OH peak.

The hydrogen bonding environment in a material is strongly affected by temperature and concentration of molecules capable of forming hydrogen bonding interactions. FT-IR has revealed the hydrogen bonding environment of TEG changes during heating, which may be in part because of the evaporation of TEG. The area associated with TEG specific peaks relative to the area of the amide III region was monitored throughout heating, and decreased, despite the increase in overall intensity of the full spectra during heating (Figure 2). The area of the amide III region remained reasonably constant throughout heating, whereas a reduction in the area of all TEG-related peaks was observed (Figure 3).

Triethylene glycol has a high boiling point (288°C) and a low vapor pressure, ideal for use as a plasticizer in thermoplastics as it is less likely to evaporate under standard temperatures used for thermoplastic processing of proteins. Thermogravimetric analysis of DBM and DBM containing TEG showed similar mass loss profiles between 25°C and 120°C, appearing to lose ~1.5–2.5 wt % between 80°C and 120°C, this is most likely in the form of water but may also contain TEG (Figure 4).

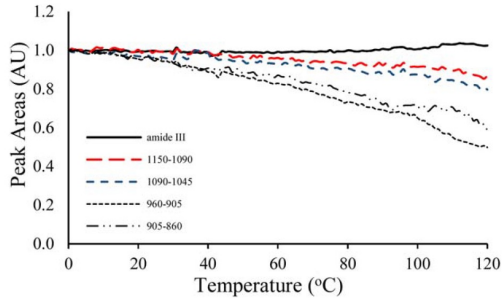

Figure 3. Normalized peak area of the amide III region and each of the TEG peaks with increasing temperature. [Color figure can be viewed in the online issue, which is available at wileyonlinelibrary.com.]

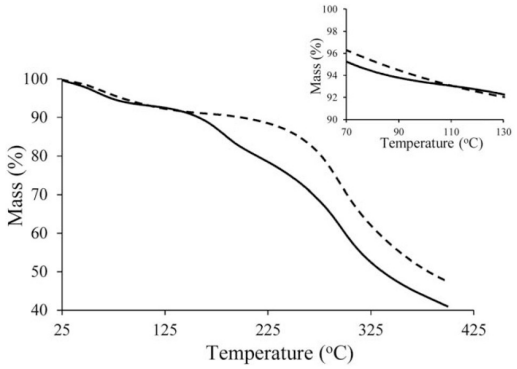

Figure 4. Thermogravimetric analysis of decolored bloodmeal (DBM) (---) and decolored bloodmeal containing sodium dodecyl sulfate and triethylene glycol (DBM TEG) (—) carried out at 10°C min^{-1}. Insert: Mass loss occurring between 70°C and 130°C.

The larger mass loss event occurred from ~150°C to 250°C could correspond with the evaporation of TEG, as it is not observed in its absence. While minor quantities of TEG may evaporate during heating, it is possible the change observed in Figure 3 is a result of the TEG migrating out of the 10 × 10 μm spot being scanned, and was further investigated by determining the spatial distribution of TEG prior to and after rapid heating.

Spatial Distribution of TEG

The relative TEG content was measured as a ratio of the area between 1150 and 1045 cm^{-1} to the amide III area between 1330 and 1180 cm^{-1} (TEG : amide III ratio). Prior to heating, TEG content across the particles appeared to be normally distributed (Figure 5), with no statistical difference in TEG content between the perimeter and the core of the particle. After heating, the TEG content is significantly reduced ($P < 0.01$)

Despite an apparent normal distribution of TEG throughout the DBM, the spatial distribution indicated the formation of plasticizer-rich (high ratio) and plasticizer-poor (low ratio) domains uniformly scattered throughout an otherwise homogenous matrix [Figure 6(A)]. Both the TEG-rich and TEG-poor domains were found to be statistically different to the average composition of the sample ($P < 0.01$).

The distribution of TEG-rich and TEG-poor domains may be a result of porosity in the DBM feedstock leading to adsorption of TEG in layers within the cavities and diffuses only partially into the protein. However, it is much more likely that the concentration of TEG in DBM exceeded the compatibility limit of the protein resulting in phase separation, often observed as plasticizer exclusion in biopolymer materials.[10]

TEG distribution was found not to correlate with secondary structure distribution,[5] indicating that TEG interacts with protein structures at a primary structure level indiscriminately. Therefore, the observed distribution of TEG is not caused by preferential localization in hydrophilic or hydrophobic areas of the protein.

After the application of the heat–cool cycle (simulating the residence time of an extruder), spatial maps indicated an approximate 14% loss in TEG, equivalent to 2.3 wt % total mass loss, along with a reduction in the variation of TEG content throughout the particle. The distribution of TEG was found to be more homogenous, evidenced by a reduction in standard deviation and range of the TEG : amide III peak area ratio [Figure 6(B)]. Improved homogeneity could be caused by both the evaporation of phase-separated TEG (from areas initially rich in TEG) as well as by the migration of TEG throughout the particles because of thermally induced diffusion.

An interesting observation is the small but statistically significant increase in the *v*C-OH to *v*C-O-C ratio upon heating and cooling ($P < 0.01$) (Figure 7). Their peak shape and their position are thought to be related to their hydrogen bonding environment, as discussed earlier. This was explored further using spatial mapping after isothermal holds at different temperatures to allow thermal equilibration.

The increase in the ratio of *v*C-OH to *v*C-O-C is caused by the increase in the area of the alcohol C-O stretch in TEG. After heating, the spatial variation is still heterogeneous, with approximately the same standard deviation and range. Despite this, the increase in the mean ratio (because of increase in *v*C-OH area) reflects the increased variety of hydrogen bonding interactions TEG is involved with after heating, which is a good indicator

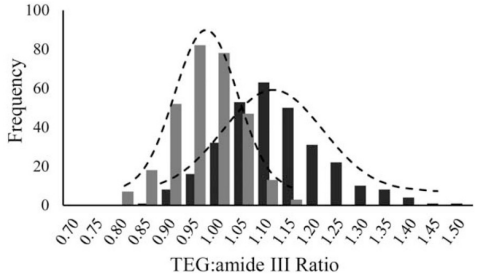

Figure 5. Histogram for distribution of TEG through decolored bloodmeal prior to heating (■) and after heat–cool cycle (■).

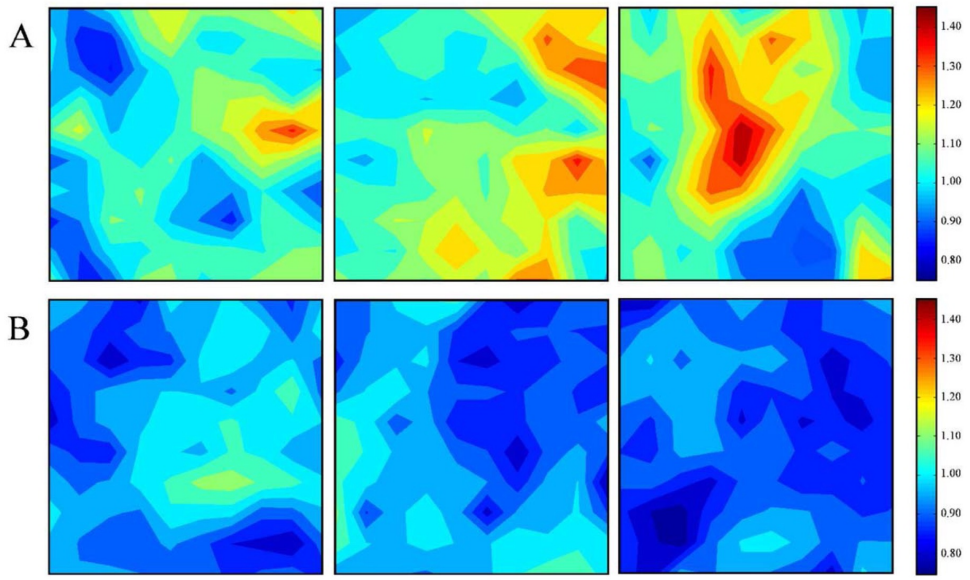

Figure 6. Spatial map of the ratio of triethylene glycol (TEG) to amide III region, showing the distribution of plasticizer throughout the decolored bloodmeal particle as three 10 × 10 μm grids, i.e. $N = 300$. (A) Distribution of TEG prior to heat cycle, (B) distribution of TEG after heat cycle and cooling to room temperature. [Color figure can be viewed in the online issue, which is available at wileyonlinelibrary.com.]

that TEG is interacting with more protein groups after heating. Furthermore, the *v*C-OH peak position that was shown to decrease during heating (Figure 2), reverts back to its original wavenumber (1076.2 cm^{-1}) upon cooling.

Spatial Mapping During Thermal Treatment Using Isothermal Holds

During preparation of the thermoplastic feedstock, TEG diffuses through the protein, forming heterogeneous regions of high and

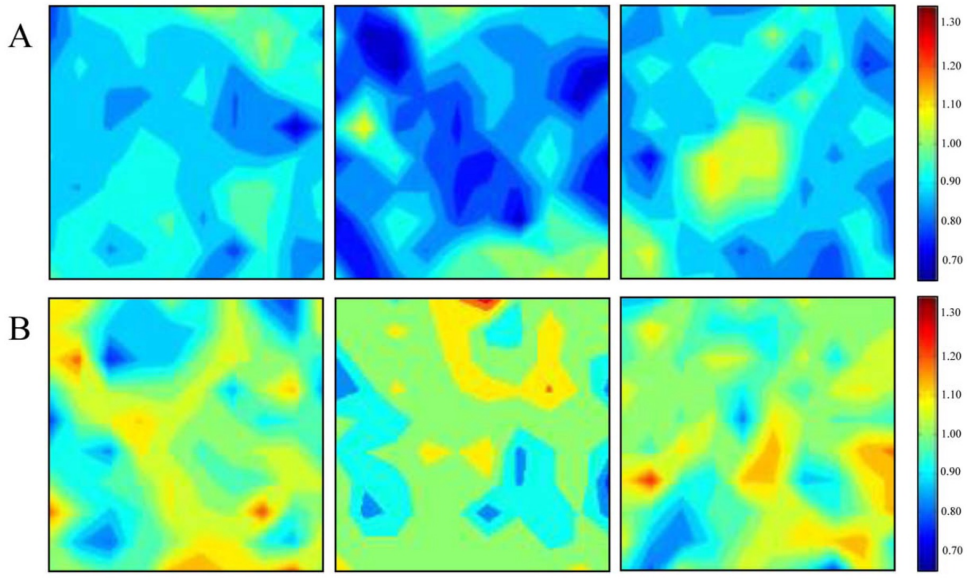

Figure 7. Spatial distribution of the *v*C-OH to *v*C-O-C peak area ratio for DBM containing sodium dodecyl sulfate and triethylene glycol (DBM TEG) at room temperature (A) before heating (mean = 0.88, $\sigma = 0.09$) and (B) after heat cycle and cooling to room temperature (mean = 1.02, $\sigma = 0.10$). [Color figure can be viewed in the online issue, which is available at wileyonlinelibrary.com.]

Table I. Summary of Statistics for the Peak Area Ratio of *v*C-OH to *v*C-O-C for Spatial Maps of DBM Containing SDS and TEG During Heating

	*v*C-OH:*v*C-O-C ratio		
	Total	Perimeter	Core
24°C			
Mean	0.99	0.95	1.01
Std. deviation	0.15	0.20	0.10
T-test *P* vs *C*		0.10	
45°C			
Mean	0.99	0.93	1.03
Std. deviation	0.16	0.21	0.14
T-test 24°C vs 45°C	0.92	0.60	0.50
T-test *P* vs *C*		0.00*	
55°C			
Mean	1.00	0.96	1.04
Std. deviation	0.13	0.17	0.08
T-test 45°C vs 55°C	0.59	0.45	0.60
T-test *P* vs *C*		0.00*	
75°C			
Mean	1.01	0.98	1.04
Std. deviation	0.13	0.16	0.09
T-test 55°C vs 75°C	0.49	0.49	0.76
T-test *P* vs *C*		0.00*	
100°C			
Mean	1.03	0.96	1.09
Std. deviation	0.20	0.24	0.14
T-test 75°C vs 100°C	0.49	0.70	0.05
T-test *P* vs *C*		0.00*	
120°C			
Mean	1.12	1.08	1.16
Std. deviation	0.22	0.24	0.21
T-test 100°C vs 120°C	0.00*	0.02*	0.06
T-test 24°C vs 120°C	0.00*	0.00*	0.02*
T-test *P* vs *C*		0.10	

Statistically significant results are marked * ($P < 0.05$)

low plasticizer content. A well-consolidated material requires uniform distribution of plasticizer, and relies on having overcome any immediate interactions to provide mobility allowing migration to new areas where new stabilizing interactions can form. The on-set of this phenomenon was determined during incremental increases in temperature, allowing enough time for thermal equilibration.

Below 100°C, the average relative peak area of *v*C-OH to *v*C-O-C showed no statistical difference before and after thermal treatment. No difference between maps obtained at 120°C, and those obtained upon cooling from 120°C was observed, indicating the change to *v*C-OH area was permanent. This suggests that the sample must surpass 100°C in order for the TEG to create new hydrogen bonding interactions in any significant amount (Table I), and that they remain upon cooling.

Prolonged heating at elevated temperature caused a small loss in TEG and an irreversible change in the types of intermolecular hydrogen bonding with which TEG is involved. However, there was no correlation between TEG content with secondary structure distribution.

FT-IR analysis indicated the occurrence of several important structural changes that take place during heating. Heating resulted in reduced stabilizing hydrogen bonding interactions within the protein, evidenced by the narrowing of the peak around 3290 cm^{-1}. The results from Figures 3 and 4 suggest evaporation accounts for ~14% of TEG, a total mass loss of 2.3 wt %. Finally, the TEG was shown to migrate, and partake in a larger variety of hydrogen bonding interactions, evidenced through improved distribution after heating, a larger *v*C-OH peak area which shifts back to its original wavenumber (1076.2 cm^{-1}) upon cooling.

Dynamical Mechanical Analysis

Upon cooling, FTIR showed a reduction in the variation of TEG content across the samples, with less extreme localized domains. Initially, these two domains were sufficiently different in material properties to give rise to what appeared to be two distinct glass transitions in DMA, which after heating were found to merge, reflecting improved homogeneity.

DBM and DBM with TEG containing ~8 wt % moisture were scanned from −60°C to 250°C before and after removing thermal history to investigate the effect of SDS and TEG and thermal treatment on material behavior. DBM showed two peaks in Tan δ, allocated to a *Tg* (75°C), and a transition owing to a *Tg* of dehydrated protein coupled with the onset of protein degradation (220°C) which is observed at the same temperature in both scans (Figure 8).

Preheating DBM to 120°C largely removed the peak around 75°C (smoothing it out), and may be attributed to the relaxation associated with aging of amorphous polymers, as a similar effect is observed during DSC.

The shift of glass transition temperature with frequency follows an Arrhenius relationship ($\log_{10} K \propto 1/T$) and is generally used to estimate the activation energy of the transition by plotting the log of the DMA frequency employed against the inverse of the absolute temperature at which the loss modulus peak occurs. The Arrhenius plot for DBM confirmed that the first transition around 75°C is a result of two overlapping events, as in the first scan it is not linearly proportional to the frequency applied, but becomes so if the thermal history is first removed by preheating to 120°C (Figure 9).

Upon addition of TEG, DMA showed three relaxation events, the first occurring below 0°C which may be because of frozen water melting as the sample was heated. The second and third peaks may both be glass transitions, caused by the TEG-rich and TEG-poor domains found in DBM with TEG. Thermal pre-treatment merges these peaks into one broader peak with the removal of the sub-zero transition. The Arrhenius plot confirmed this, indicating that both peaks occurring around 50°C and 115°C in the first scan are linear with respect to log frequency, strongly suggesting they are both the result of a glass

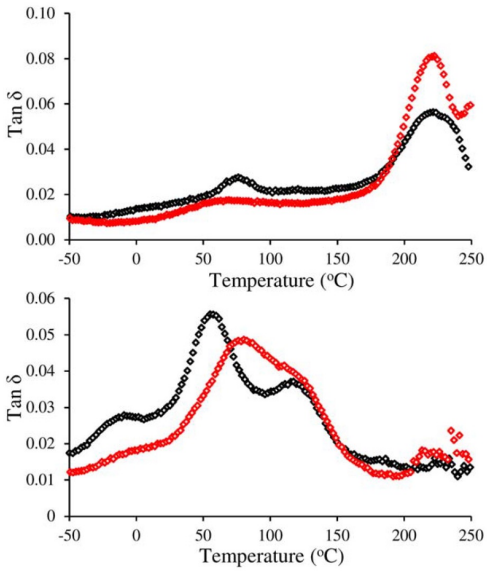

Figure 8. DMA of decolored bloodmeal: (A) DBM, (B) DBM with sodium dodecyl sulfate and triethylene glycol (DBM TEG). Without removing thermal history (◆) and after removing thermal history (◇) by preheating to 120°C. [Color figure can be viewed in the online issue, which is available at wileyonlinelibrary.com.]

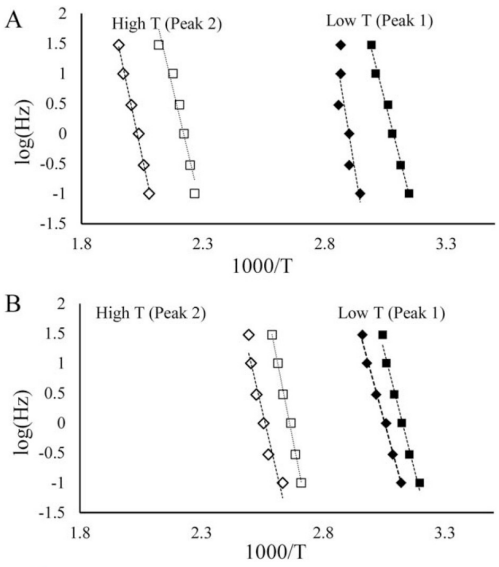

Figure 9. Arrhenius plot for A: DBM and B: DBM with SDS and TEG. Low temperature transition scan 1(◆) (R^2 values A = 0.7601, B = 0.9932) and Scan 2 (■) (R^2 values A = 0.9888, B = 0.9837) and high temperature transition scan 1(◇) (R^2 values A = 0.9931, B = 0.9368) and scan 2 (□) (R^2 values A = 0.9467, B = 0.9956). Plots are stacked for clarity.

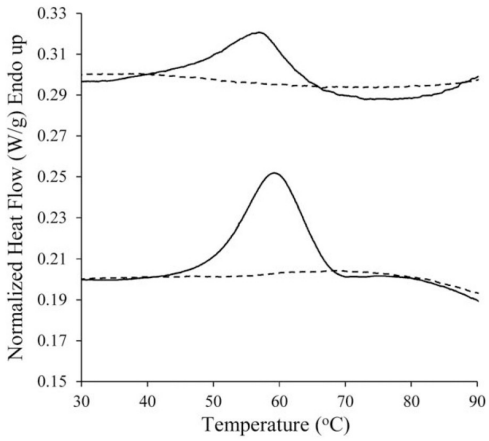

Figure 10. DSC thermograms of decolored bloodmeal (DBM) and DBM with sodium dodecyl sulfate and triethylene glycol (DBM TEG). Scans were carried out using a heating rate of 10°C min^{-1}. First scan solid line (—) and second scan dashed line (- -). Images have been stacked for clarity.

transition. Removing the thermal history (pre-heating to 120°C) also led to a linear response in the peak around 60°C and the position of the shoulder at around 115°C, indicating the lower temperature transition has increased in temperature as TEG has migrated slightly to become more homogeneously distributed after heating.

Physical Aging

DSC showed the presence of two overlapping thermal events occurring at 75°C. During heating to 120°C (to remove thermal history), the close packing that occurred during aging was lost. Physical aging is a phenomenon observed when an amorphous polymer is stored below its glass transition temperature,[20] under which material will have a free volume, enthalpy and entropy larger than it would have under equilibrium.[21] As a result, the nonequilibrium material undergoes slow chain rearrangement (through short-range, rotational reorientations) toward an equilibrium conformation, a process known as physical aging.[22]

When an aged polymer is heated above its *Tg*, it absorbs the heat lost during aging and recovers its lost free volume and this is accompanied by the development of an endothermic peak at its glass transition, observed during DSC.[20] This phenomenon has also been reported for numerous polymers and proteins.[20,23,24] The presence of this sub-*Tg* endothermic event was observed during DSC of DBM with and without TEG, Figure 10.

Initially the specific enthalpy for DBM was 2.8 J g^{-1} and decreased to 1.5 J g^{-1} after the addition of TEG. The addition of TEG reduced the degree to which aging can occur as observed as a reduction in the enthalpy of relaxation, also reducing the temperature at which it occurred. This may be because of TEG forming competing interactions with protein that reduce the ability of protein chains to form hydrogen bonds and other intermolecular interactions which facilitate close packing, increasing free volume. These endothermic peaks are no longer

observed upon reheating the material, suggesting that the event occurring during DSC is the same as the one which had occurred during DMA, where TEG is unable to evaporate.

CONCLUSION

Sorption of TEG into DBM protein led to two distinct domains: one plasticizer-rich and the other plasticizer-poor, distributed throughout an otherwise homogeneous blend. The two regions were found to be distinctly different in TEG concentration and also in their thermal behavior, resulting in two glass transitions.

Several important structural changes were found to take place during heating. First, heating resulted in reduced stabilizing hydrogen bonding interactions within the protein. Although a minor amount of evaporation occurred during FT-IR, the TEG was shown to migrate throughout the sample, and more importantly was shown to partake in a greater variety of hydrogen bonding interactions, evidenced by the permanent increase in the νC-OH peak area. An increase in the variety of TEG hydrogen bonding interactions was observed as the sample reached 100°C. These newly formed H-bonds were found to be just as strong as the original hydrogen bonding interactions, as the νC-OH stretch reverted to its original wavenumber upon cooling (1076 cm^{-1}). This suggests that noticeable migration of TEG begins around 100°C, and for the purpose of ensuring uniform dispersion of TEG, a processing temperature in excess of 100°C would be required.

Upon cooling, TEG content was more homogenously distributed across the samples, although some subtle localized domains remained. Initially the two domains were found to be sufficiently different in material properties such that two distinct glass transitions were observed. After heating and cooling, TEG was more homogeneously distributed in DBM, evident from its spatial distribution and the merging of glass transitions into one broader glass transition region.

DSC and DMA also indicated that physical aging occurred during the storage of DBM with and without TEG, but appeared to be less in the presence of TEG. This warrants further study to discern whether a plasticizer is able to inhibit aging, which is known to change the material properties of protein plastics.

ACKNOWLEDGMENTS

This research was undertaken on the infra-red microspectroscopy beamline at the Australian Synchrotron, Clayton, VIC, Australia. Proposal number AS132/IRMFI/6636. The authors would especially like to acknowledge the technical assistance of Dr. Mark Tobin and Dr. Danielle Martin. Travel funding support was received from the New Zealand Synchrotron Group.

REFERENCES

1. Verbeek, C. J. R.; Lay, M. C.; Low, A. W. K. Methods of manufacturing plastic materials from decolorized blood protein. US20130139725 A1. Application number 691,438, Waikatolink Limited: **2013**.
2. Barone, J. R.; Dangaran, K.; Schmidt, W. F. *J. Agric. Food Chem.* **2006**, *54*, 5393.
3. Hicks, T.; Verbeek, C. J. R.; Lay, M. C.; Bier, J. M. *RSC Adv.* **2014**, *4*, 31201.
4. Low, A.; Verbeek, C. J. R.; Lay, M. C. *Macromol. Mater. Eng.* **2014**, *299*, 75.
5. Hicks, T. M.; Verbeek, C. J. R.; Lay, M. C.; Bier, J. M. *Macromol. Mater. Eng.* **2014**, *300*, 3, 328.
6. Bier, J. M.; Verbeek, C. J. R.; Lay, M. C. *Macromol. Mater. Eng.* **2014**, *299*, 85.
7. Low, A. *Thesis*: Decoloured bloodmeal based bioplastic. In Materials and Process Engineering; University of Waikato: Hamilton, **2012**.
8. Bourtoom, T.; Chinnan, M. S.; Jantawat, P.; Sanguandeekul, R. *Food Sci. Technol. Int.* **2006**, *12*, 119.
9. di Gioia, L.; Guilbert, S. *J. Agric. Food Chem.* **1999**, *47*, 1254.
10. Vieira, M. G. A.; da Silva, M. A.; dos Santos, L. O.; Beppu, M. M. *Eur. Polym. J.* **2011**, *47*, 254.
11. Chen, P.; Zhang, L. *Macromol. Biosci.* **2005**, *5*, 237.
12. Bier, J. M.; Verbeek, C. J. R.; Lay, M. C. *J. Appl. Polym. Sci.* **2014**, 131.
13. Pal, S.; Kundu, T. K. *ISRN Phys. Chem.* **2013**, *2013*, 16.
14. Barth, A. *Biochim. Biophys. Acta* **2007**, *1767*, 1073.
15. Zeiss, H. H.; Tsutsui, M. *J. Am. Chem. Soc.* **1953**, *75*, 897.
16. Jeffrey, G. A. An Introduction to Hydrogen Bonding; Oxford University Press: New York, **1997**.
17. Singelenberg, F. A. J.; van der Maas, J. H.; Kroon-Batenburg, L. M. J. *J. Mol. Struct.* **1991**, *245*, 183.
18. Sun, C. L.; Wang, C. S. *Theochem. J. Mol. Struct.* **2010**, *956*, 38.
19. Ryu, S. R.; Noda, I.; Jung, Y. M. *Bull. Korean Chem. Soc.* **2011**, *32*, 4011.
20. Mo, X.; Sun, X. *J. Polym. Environ.* **2003**, *11*, 15.
21. Lawton, J. W.; Wu, Y. V. *Cereal Chem.* **1993**, *70*, 471.
22. Struik, L. C. E. Physical Aging in Amorphous Polymers and Other Materials; Elsevier: Amsterdam, **1978**, p 5.
23. Bengoechea, C.; Arrachid, A.; Guerrero, A.; Hill, S. E.; Mitchell, J. R. *J. Cereal Sci.* **2007**, *45*, 275.
24. Farahnaky, A.; Badii, F.; Farhat, I. A.; Mitchell, J. R.; Hill, S. E. *Biopolymers* **2005**, *78*, 69.

8

Thesis Summary

and Recommendations

Thesis Summary and Recommendations

Decoloured bloodmeal can be converted into a thermoplastic material using water, SDS and TEG. Although the chemical process is well established, until recently the mechanism of decolouring was not well understood. Furthermore, the decoloured product is expensive and understanding the mechanism may shed light on alternative strategies to reduce cost. A combination of chemical, spectroscopic, material and thermal analysis techniques were used to gain insight into the new physico-chemical properties of bloodmeal after oxidative decolouring and upon introduction of processing aids to improve polymer mobility. Using these techniques, a mechanism of decolouring was presented, the resulting modifications to protein structure and interactions and how these changes in the presence of processing aids affects final polymer mobility.

A mechanism for decolouring was proposed after measuring the consumption of peroxides during decolouring and establishing the role of each component present in peracetic acid solutions. Hydrogen peroxide, at any concentration, is incapable of fully decolouring BM due to its inability to oxidise haem present as methaemoglobin. Decolouring with PAA was facile, albeit at significant excess PAA (>3 wt% PAA). Excess PAA provides an adequate diffusion gradient and supplies enough reagent to overcome competing reactions. Based on literature, the efficacy of PAA has been attributed to its higher reduction potential (1.81 V) and the longevity of its radicals compared with those generated from hydrogen peroxide [1], allowing it to fully oxidise ferric haem in methaemoglobin. Comparison of PAA to similar aliphatic peroxycarboxylic acids indicated that although they are reactive, they do not result in adequate decolouring. Performic acid was thought to cause hydrolysis and encourage browning reactions whereas perpropionic acid may simply be too large to access the haem iron to form the necessary complex to initiate haem degradation.

Both water and acetic acid present were found to cause significant swelling of the proteins, but neither facilitated access of hydrogen peroxide to haem sites. In fact, pre-swelling with water had no more effect on decolouring efficacy than dilution of the hydrogen peroxide (HP) solution alone, and in the case of short chain aliphatic

carboxylic acids, pre-swelling the protein was found to inhibit both decolouring and the consumption of hydrogen peroxide.

Acetic acid in PAA solutions has a protective effect on the protein, presumably by inhibition of hydroxyl radical production through Fenton chemistry by the chelation of free iron. For this reason the presence of acetic acid results in lower decolouring efficacy of HP, but also results in higher protein recovery, an unchanged average molecular mass and a lesser degree of β-sheet aggregation.

Protein recovery during decolouring diminished with increasing concentration of oxidants. The presence of acetic acid was found to improve protein recovery, and result in a high solids yield, although co-precipitation of sodium acetate (formed during neutralisation) resulted in lower protein content by weight for PAA and HP/AA treated bloodmeal.

Oxidation at every concentration of PAA improved protein solubility, particularly bloodmeal decoloured with hydrogen peroxide (including HP with acetic acid). This change is primarily attributed to the increased hydrophilicity of the amino acids after oxidation, including the changes to aromatic side chains and degradation of cystine crosslinks. Overall, oxidation was found to result in a reduction to most aromatic amino acids, a significant reduction in lysine and cleavage of some of the cystine disulfide bonds.

Concepts from classical polymer physics explain why proteins have a particularly high glass transition temperature. This results predominantly from the large number and variety of chain interactions, along with bulky aromatic substituents and the occasional rigid structure such as proline or cystine, which all act to limit mobility. Thus it could be expected that protein oxidation would result in improved mobility; largely via the cleavage of the protein backbone and covalent crosslinks between adjacent protein chains, resulting in a larger number of chain ends and consequently increased free volume. Oxidation was also expected to reduce hydrophobic interactions and increase hydrophilicity, as well as result in cleavage of aliphatic amino acid side chains from the protein backbone (improving regularity), which would also influence the glass transition temperature to a certain degree.

The resulting changes in primary structure resulted in a lower glass transition temperature and an increased enthalpy of relaxation of the aging peak; this

improved mobility results from cystine oxidation, reduced hydrophobic interactions and improved chain regularity (a result of removing sterically hindering side chains).

Despite changes to the amino acids, minor changes to the overall molecular mass distribution of BM was observed after decolouring with 1 – 4 wt% PAA. This is a result of the many potential addition reactions which can take place, often in preference to hydrogen abstraction and protein fragmentation, for thermodynamic and steric reasons. However, treatment with 5 wt% PAA or HP led to significant fragmentation of the protein chains (inhibited to some extent by the presence of acetic acid) resulting in the formation of a peptide fragment of ~8.8 kDa mass.

Perhaps the most significant finding is the discovery of an obvious difference in the location of secondary structures throughout DBM particles. The distribution of disordered structures is consistent with a diffusion front which would be created by the two-phase reaction. The changes in secondary structure which occurred also confirmed that hydrogen peroxide (or a resultant hydroxyl radical) is easily able to diffuse through bloodmeal. Overall, after oxidation the protein contained a greater number of β-sheets concentrated at the core of the particle while α-helices and random coils were found in highest concentration at the periphery. The material behaviour of DBM would be defined by the chemical properties of the proteins located throughout the particles. Thus, at low PAA concentration (limited diffusion), the properties of DBM are more likely to be representative of the structures found at the core of the particle (representing the greater mass), whereas at higher PAA concentration the material is more likely to resemble the proteins located at the perimeter (beyond the diffusion front). Ideally, the material not only needs to be adequately decoloured and have a useful molecular mass, but also needs to be reasonably homogenous in order to easily process it.

The addition of SDS induced the formation of α-helices, reducing β-sheets and β-turns. However, simultaneous addition of TEG reduced α-helices and β-sheets, increasing random coils. Upon heating there was little change in the average structural composition of decoloured bloodmeal containing SDS, indicating that it was insufficient to promote mobility during heating, whereas heating DBM containing SDS and TEG combined resulted in the recovery of some ordered structures. The addition of sodium dodecyl sulfate and triethylene glycol to

decoloured bloodmeal as processing aids led to a more homogeneous distribution of secondary structures (becoming even more so after heating). This has important implications for extrusion, which requires quick homogenisation of crystalline and amorphous structures in the melt, to promote new interactions and prevent thermally induced protein degradation.

Despite TEG surpassing the compatibility limit of the DBM protein leading to phase separation (and the presence of two glass transition temperatures), heating was found to induce further diffusion of TEG throughout the particle, occurring as low as 55 – 75 ^{o}C. During heating, the migrating TEG began to form new hydrogen bonds with the protein. The overall strength of the hydrogen bonds in which both the protein and TEG participate, weaken during heating but strengthen again upon cooling, with TEG participating in a greater variety of hydrogen bonds after heating and cooling. It is then clear that to process proteins in general, these hydrogen bonds should be weakened for improved processing, but strengthened for optimal material properties.

Plasticisation with TEG allowed for sufficient chain mobility leading to random coils to be transformed into α-helices after a heat/cool cycle (simulating extrusion). Extended heating led to a gradual increase in β-sheets for all samples, however α-helices showed a dramatic increase around 55-75 ^{o}C for samples containing TEG as well as SDS (compared to 100 ^{o}C in the presence of SDS alone) suggesting that with sufficient chain mobility, α-helices will readily form from random coils, however β-sheet formation is a slower process.

Current literature suggests that while disordered regions provide elastomeric properties, ordered secondary structures impart resilience to proteinous materials. For example, β-sheets increase toughness and tensile strength, but depending on the extent of crystal structure, can also make the plastic brittle. Additionally, helical structures may be more beneficial in the preparation of protein films. Given that the formation of helices commences at lower temperature and prolonged time is required for sheet formation; film preparations from decoloured bloodmeal may require rapid low temperature processing with additional TEG (increased mobility, allowing quick processing at lower temperature) whereas to impart increased

toughness, longer residence times or multiple heating/cooling cycles may be required.

Prolonged heating caused structural changes that are largely irreversible for DBM and DBM treated with SDS, also reflected in an increase in crystallinity during heating (which did not change upon cooling). Such changes could have adverse effects on thermoplastic processing, as the material would become more difficult to extrude and injection mould if heated repetitively or for protracted periods. However, SDS and TEG treated DBM showed little or no change in total crystallinity upon heating, suggesting TEG provided sufficient chain mobility to prevent the onset of irreversible change, important for maintaining processability of the material during multiple heating and cooling cycles.

This shows that formulating a thermoplastic material from decoloured bloodmeal requires the same considerations, well known for other thermoplastic proteins. These are the requirements to overcome stabilising interactions to promote processing, typically via extrusion; allowing melt formation followed by allowing the formation of new interactions upon cooling to impart mechanical strength. For decoloured bloodmeal, many of the interactions present in bloodmeal have been overcome by oxidation and chains are therefore inherently more mobile (lower *Tg*).

The success of using PAA as oxidant is that, contrary to HP, it fulfils these requirements, by leading to an acceptable level of crosslink reduction without severe chain scission. Most importantly, chain architecture (including secondary structure) still allows for sufficient interactions to form a thermoplastic material, as shown by studies preceding this [2].

Recommendations for Future Work

Further work is being done to produce decoloured bloodmeal using a continuous-reactor (as opposed to batch reactions). Additionally, a substantial amount of peroxide remains once decolouring is complete. Optimisation of the decolouring process is currently underway at the University of Waikato, aimed at reducing the quantity of PAA solution used to contact the bloodmeal. Regardless of the decolouring method used, recovery of the wastewater for use elsewhere or as a return feed is sensible.

Future work regarding bleached bloodmeal should consider the generation of peroxyacids *in situ* or the application of peracetic acid containing lower levels of hydrogen peroxide in an effort to limit HP induced protein degradation. This could occur in conjunction with the use of a suitable chelating agent (ethylenediaminetetraacetic acid) or a hydroxyl radical scavenger (mannitol or isopropyl alcohol) further minimising damage to proteins due to the presence of HP. This might result in a decoloured bloodmeal which retains hydrophilicity, which may improve yield and result in a protein material with lower water permeability.

The extent of cystine oxidation and its effect on the preparation of extruded and injection moulded material should be investigated. This could be done by gaining access to a Raman spectrophotometer with a 1064 nm laser to characterise S-O bonds without the fluorescence experienced at 785 nm. Although oxidation of the disulfide linkage is useful, introduction of new sites for crosslinking to occur could be beneficial given the large decrease in lysine content. One example to consider is the addition of 2-iminothiolane hydrochloride to phenylalanine groups; this is a cross-linking agent used in wool and hair treatment to improve structural integrity.

References

1. Block, S.S. (2001). Peroxygen Compounds, in Disinfection, Sterilization and Preservation, Block, S.S., Editor. Lippincott Williams and Wilkins: Philadelphia. p. 185-204.

2. Low, A., Verbeek, C.J.R., Lay, M.C. (2014). Treating Bloodmeal with Peracetic Acid to Produce a Bioplastic Feedstock. Macromolecular Materials and Engineering. 299(1): p. 75-84.

Appendix 1

Protein Rich By-Products: Production Statistics, Legislative Restrictions and Management Options

An invited book chapter

By

TALIA M. HICKS AND C. J. R. VERBEEK

Published in

Elsevier B.V. Waste-derived Proteins: Transformation from Environmental Burden into Value-added Products

This chapter has been included to provide context for the restrictions regarding the use of protein by-products derived from the agricultural industry, along with potential management options. As first author, I prepared the initial draft manuscript, which was refined and edited in consultation with my supervisor, who has been credited as a co-author.

Protein Rich By-Products: Production Statistics, Legislative Restrictions and Management Options

*Talia. M. Hicks and #Casparus J.R. Verbeek

School of Engineering
University of Waikato
Private Bag 3105
Hamilton 3240
New Zealand
*tmh20@students.waikato.ac.nz; # jverbeek@waikato.ac.nz

1 Introduction

The majority of the world's food is derived from agricultural, horticultural and fishery processes. With a growing population, urbanization and increased income, the food industry has become increasingly market driven. As a result of globalization and reduced trade barriers, it has grown to account for approximately ten percent of the world's gross domestic product [1]. Fortunately, environmental protection and sustainability is currently better aligned with the worlds' consumption of natural resources. Over the past few decades, it has tried to adopted technologies to improve waste minimization and environmental performance. Although the most valuable elements are extracted from foods during harvest and processing, what remains in the product specific and non-specific wastes may also contain other potentially valuable components.

Predicting future food production and associated by-products is complicated and has to take into account not only changes in population size, dietary composition, land requirements and primary resources, but also climate and environmental aspects [2]. Overall, increased global demand for animal based products requires a substantially greater increase in plant and other feed resources, which will subsequently generate a much larger volume of protein-rich materials than currently produced.

The quantity of food materials wasted each year is exorbitant and urbanization and the increasing per capita income will see this quantity rise further, through increased consumption of staple foods as well as diversification into animal products such as

meat, fish and dairy. This will be most challenging for transitional countries, which are expected to undergo a much more rapid increase in per capita meat consumption compared to high-income countries (i.e. China will increase by ~50 %, from 49 kg in 2000 to 74 kg per capita per year in 2030 compared to an increase of ~ 9 %, from 86 kg to 95 kg per capita per year, in higher income countries) [3]. Such nutritional transitions result in a rapid increase in animal products, putting a significant amount more pressure on food supply chains within transitional countries than those in the developed world.

A major facet of the problem we face, is being able to source adequate quantities of high quality protein from which to feed both humans and animals, without intensifying the overall environmental impact [4]. Obviously, increasing production of animal based products will result in a much higher consumption of grain and protein feeds to feed livestock, which are estimated to require ~6 kg of plant protein for every kilogram of protein they produce [5]. However, this could be better perceived by the ~ 30 kg of grain required to produce 1 kg of edible boneless meat from grain-fed cattle [6]. On the other hand, while chicken and pork are more efficient converters of plant proteins, pasture fed cattle are able to convert nonfood material into usable protein.

The technology for recovering nutrients and usable materials from industry is often feasible but the regulations regarding what can be done with by-products of industry may not always allow for the technology to be adopted. Despite a concerted effort to better utilize by-products of the agricultural and food industry to improve the management of resources, sensible legislative incentives also need to be implemented.

This chapter identifies areas of food production and related industries generating waste and by-products with high levels of recoverable protein, in particular, those derived from agricultural production itself. Current and future management options for the transformation and/or disposal of these wastes and by-products are then considered in light of current legislation and technological restrictions.

2 Food production cycle and by-products

The modern food cycle is comprised of several stages, including agricultural production, post-harvest handling and storage, food processing and packaging,

distribution and retail, and finally consumption/end-of-life (Figure 1) [7]. Agricultural production, post-harvest handling and storage of food gives rise to unintended food losses and ancillary by-products, while processing and packaging, distribution and retail result in "food waste". Food loss, by-products and food waste are formed at every stage of the food production process. While the generation of by-products such as crop residues and animal by-products during agricultural production is considered unavoidable, food losses owing to a lack of market or degradation during handling or transportation could be avoided with care, but when considering statistics, it is often difficult to distinguish between the two.

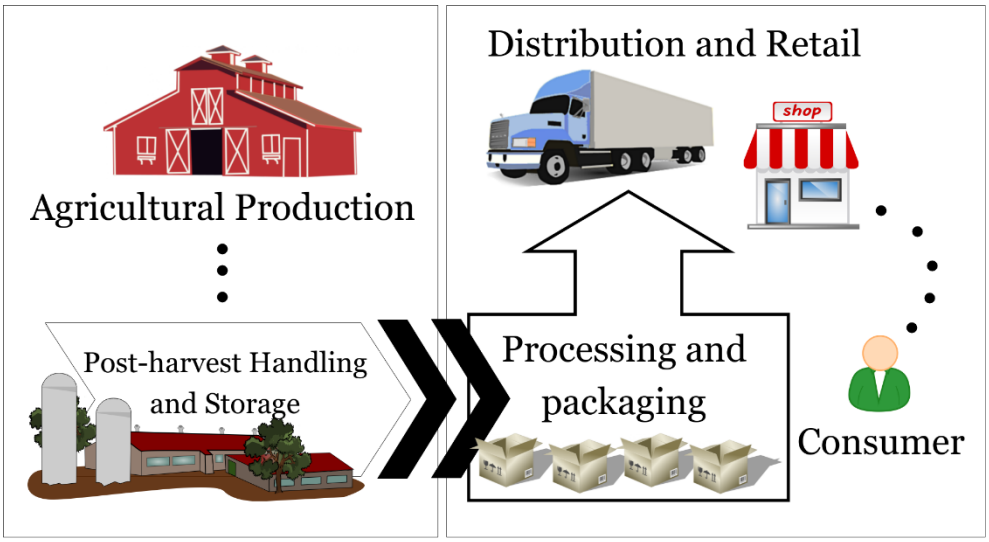

Figure 1: General food production stages starting from agricultural production and post-harvest handling and storage to processing and packaging, distribution, retail and consumption.

For various reasons, approximately one third of the food produced worldwide is wasted [2, 8]. These wastes (and possible by-products) are created during the manufacturing processes, and are often removed in order to give the product the desired sensory and nutritional qualities. Although, the magnitude of food losses, by-products and food waste varies depending on the product type (Table 1), the stage of production considered (Table 2), it is strongly influenced by the technology and infrastructure available to the region.

It has been estimated that around 60 million tonnes of animal by-products are produced worldwide every year [9], along with significantly higher quantities of crop residues [10]. Obviously, industrial processing of any food, whether it is intended for human or animal consumption (or other industrial processes such as biofuels) leads to a vast quantity of waste and by-products, typically ranging

between 30 – 60 % by weight (Table 1). In the case of crops only 60 % of global production is used for human consumption, mostly in the form of grains, pulses, oil plants, fruits and vegetables, leaving 35 % as by-products (used for animal fodder) and the remaining 5 % for conversion to biofuel and other industrial products [6].

Table 1: Percentage of by-products and waste generated during different production processes. Adapted from [11].

Production process	% converted to waste and by-products
Plant products	
Corn starch production	41-43
Fruit and vegetable processing	5-30
Potato starch production	80
Red wine production	20-30
Sugar production from sugar beet	86
Vegetable oil production	40-70
Wheat starch production	50
Animal products	
Beef slaughter	40-52
Crustacean processing	50-60
Fish canning	30-65
Fish filleting, curing, salting and smoking	50-75
Cheese production	85-90
Mollusk processing	20-50
Pig slaughter	35
Poultry slaughter	31-38
Yogurt production	2-6

In high income regions, most food waste occurs during distribution and consumption, with high losses also occurring during agricultural production of plant products and fish (Table 2). Harvesting of crops also results in an inedible portion of the biomass (including edible product lost during harvest) contributing to what is known as crop residues. For most common edible crops, the residue to crop production ratio is between 0.9 and 3 to 1 [12]. This mass is not accounted for in Table 2, however, typical quantities of some common food crops are given in Table 3. In lower income regions, losses occur at every stage, particularly post-harvest, to a much higher degree, but occur significantly less at the consumption stage. Higher losses throughout production in low income regions are an artefact of inadequate knowledge, skills, technologies and infrastructure to support the food supply chain compared to the industrialised world [13].

Table 2: Combined food losses and food waste for each stage of the food production chain, expressed as a weight percentage of the (edible only) incoming resource. Regions were grouped [14] into medium to high income regions (Europe, USA, Canada, Oceania and industrialised Asia) and low income regions (sub-Saharan Africa, North Africa, West and Central Asia, South and Southeast Asia and Latin America).

	Agricultural production	Post-harvest handling and storage	Processing and packaging	Distribution	Consumption
High income					
Cereals	2	2 – 10	0.5 – 10	2	20 – 27
Roots and Tubers	20	7 – 10	15	7 – 9	10 – 30
Oilseeds and Pulses	6 – 12	0 – 3	5	5	4
Fruits and Vegetables	10 – 20	4 – 8	2	8 – 12	15 – 28
Meat	2.9 – 3.5	0.6 – 1	5	4 – 6	8 – 11
Fish and Seafood	9.4 – 15	0.5 – 2	6	9 – 11	8 – 33
Milk and Dairy	3.5	0.5 – 1	1.2	0.5	5 – 15
Low income					
Cereals	6	4 – 8	2 – 7	2 – 4	1 – 12
Roots and Tubers	6 – 14	10 – 19	10 – 15	3 – 11	2 – 6
Oilseeds and Pulses	6 – 15	3 – 12	8	2	1 – 2
Fruits and Vegetables	10 – 20	9 – 10	20 – 25	10 – 17	5 – 12
Meat	5.1 – 15	0.2 - 1.1	5	5 – 7	2 – 8
Fish and Seafood	5.1 - 8.2	5 – 6	9	10 – 15	2 – 4
Milk and Dairy	3.5 – 6	6 – 11	0.1 – 2	8 – 10	0.1 – 4

Globally, billions of tonnes of agro-industrial residues and by-products are generated annually (Table 3). These include solid, liquid and gaseous residues and can be seen as one of the most abundant, cheap and renewable resources available [10]. Given that food waste has a typical composition of ~30 – 60 wt% starch, 10 – 40 wt% lipids and 5 – 10 wt% protein [15], millions of tonnes of protein, from plant and animal sources, could be better utilized. Further to this, agricultural production also has other unavoidable wastes associated with it, including manure and effluent, which also contain high levels of recoverable protein. These by-products and wastes find new life, often as animal feed ingredients.

Table 3: Estimates of production by-products and crop residues from commodity crops in million metric tonne (MMT) per annum [10]. Slaughterhouse by-products calculated from the proportion of liveweight in each rendering product for each species considered [16], using the 2013 estimate of livestock slaughtered globally [17]. Fishmeal estimate from 2002 [18].

Production process	Residue production (MMT/year)	Production process	Residue production (MMT/year)
Roots and tubers		Cereals	
Potato foliage, tops peels and pulps	116.7	Rice straw	457.0
Cassava peels, stalks, bagasse	82.6	Wheat straw	475.1
Fruits		Barley straw	105.0
Apple pomace	20.9	Maize straw and stalks	1266.6
Orange peels, pulps and membranes	34.7	Maize cobs	337.8
		Millet	88.9
Legumes		Banana leaves, stems/peels	183.8
Beans straw and pods	57.2	Grape pomace	20.5
Soybeans straw and pods	392.7	Slaughterhouse By-products	
Oil crops		*Cattle*	
Sunflower foliage/stems	15.3	Protein meal	6.9
Olive leaves and stems	10.3	Tallow	4.2
Coconut shells, husks/fronts	18.7	Bloodmeal	0.38
Palm oil shells, husks/fronts	13.5	*Sheep*	
Groundnuts stalks/shells	71.1	Protein meal	0.58
Rapeseed straw	73.8	Tallow	0.59
Cottonseed stalks	80.1	Bloodmeal	0.05
Treenuts		*Pigs*	
Almond hulls and shells	0.9	Protein meal	3.7
Walnut shells	1.70	Tallow	7.6
Industrial crops		Bloodmeal	0.34
Sugarcane leaves and tops	168.5	*Chicken*	
Cotton stalks	197.6	Protein meal	5.5
Fiber crops leaves/stalks	56.9	Tallow	2.6
Vegetables		Bloodmeal	0.18
Onion leaves and stems	35.0	*Fish*	
Tomatoes leaves and stems	72.9	Protein meal	6.2
Cucumber leaves and stems	25.9		

3 Protein-rich by-products

Waste materials generated during agricultural production, including inedible plant and animal parts, are removed during harvesting and post-harvest processing. Other unavoidable nutrient-rich wastes, such as manure and dead-stock, are also produced. Due to their high levels of recoverable protein, carbohydrate and fiber, many of the by-products and wastes of the agricultural industry currently find re-use as animal feeds, or animal feed ingredients.

Animal feed ingredients are blended in such a way as to create a more nutritious food for livestock. Plant derived ingredients include grains, such as maize, barley, sorghum, oats, and wheat (which can also be used for bioethanol production), from which the by-products are often diverted back to feed. These grain by-products include corn gluten meal, brewers and distiller's grains, malt sprouts, brewer's yeast and wheat mill feed [19, 20]. More importantly, it has been assumed that by 2020, up to 10% of transportation fuels will be derived from biofuels, generating up to 100 million tonnes of additional protein [21]. Higher value applications for inedible and non-essential amino acids derived from these by-products may eventually be commercialised, providing a feedstock for protein-based plastics, bio-pesticides or commodity organic compounds [20, 21].

Oil production by-products (oil meals and press-cakes) from processing oilseeds such as soybean, canola, sunflower seed, linseed, palm kernel and others are also important feed ingredients. Oil meals are obtained by solvent extraction of the oil cakes, which are obtained by pressing the seed. In 2013, 269 million metric tonnes of various oil meals were produced globally, of which 181 million tonnes was soymeal [22]. In the U.S. alone, 36 million metric tonnes of soymeal is produced annually [22], representing more than two-thirds of the proteinous animal feed in the U.S. [19]. Other oilseed meals are lower in protein and higher in fiber, and are often used for feeding ruminants. Cottonseed meal is also a high in protein, and is used mainly as cattle feed in the U.S.A, or as aquaculture feed. Unlike other seeds, the press cake obtained from castor seeds during castor oil production is inedible due to its high level of phytotoxins (ricin, a toxic protein), hydrocyanides and other allergens, however, this too has a high level of protein, ~20 -30 % (Table 4).

Other plant ingredients may include alfalfa by-products such as alfalfa meal, pellets and concentrated alfalfa solubles, which are typically fed to ruminants. Further, various nuts, seeds, and their by-products; hulls, seed screenings; legumes by-products such as bean straw meal and hulls and even dried roots and tubers such as sweet potatoes and chipped or pelletized cassava find use in animal feed.

Table 4: Typical protein content and U.S. and global production quantities of some protein meals produced from the agricultural industry.

Protein meal	Crude Protein (%)	Reference	US Production Million metric tonne	Global Production Million metric tonne
Plant products				
Alfalfa meal	19.2	[23]	0.513 – 1.91[a]	
Canola seed meal	37.8	[23]	1.07[c]	
Castor seed cake	31 – 36	[24, 25]		
Castor seed meal	20.8	[24]		
Corn gluten meal	53.9 – 65.0	[23, 26, 27]	5.9[a]	
Cottonseed cake	21.1 – 57.3	[28-30]		
Cottonseed meal	34.3 – 44.9	[23, 30, 31]	0.82 - 1.09[a,c]	10.3 – 15.5[a,b]
Cow pea seed meal	32.7	[32]		
Linseed cake	34.7	[28]		
Linseed meal	32.6 – 35.4	[23, 31]	0.142 – 0.147[a,c]	1.02[a]
Peanut meal	51.8	[23]	0.12 – 0.159[a,b]	4.32 – 6.83[a,b,c]
Rapeseed cake	35.6	[28]		
Rapeseed meal	34.1 – 37.9	[30, 33]		39.2[c]
Sesame seed cake	32.8	[28]		
Soybean cake	40.1 – 49.1	[27, 28]		
Soybean meal	44.4 – 53.8	[23, 31, 33]	39.1[c]	200.8[c]
Sunflower meal	28.4 – 42.0	[23, 31]	0.23 – 0.29[a, c]	16.0[c]
Animal products				
Bloodmeal	80.2 - 100.5	[34-37]		
Feather meal			0.63[f]	
Hydrolyzed feather meal	81.2 – 92	[23, 37, 38]		
Meat and bone meal	49.5 – 59.4	[23, 36-41]	1.8 – 2.1[d,f]	
Meat meal	51.7 – 58.4	[23, 41, 42]	2.4[a]	
Fish meal	59.0 – 68.5	[23, 42-44]	0.33[a]	4.1 – 6.2[a,c,e]
Poultry by-product meal	51.7 – 63	[37, 38, 41, 44]	1.2[f]	
Shrimp meal	22.8 – 50	[37, 45-48]		

A: Based on production statistics for 1989 – 1990 in Animal Feeds Compendium (1992) [49]. B: Based on production statistics for 2003 – 2012 in U.S.D.A Agricultural Statistics (2013) [50]. C: Based on a forecast for production quantities for 2014 in U.S.D.A Agricultural Statistics (2015) [51]. D: Based on U.S. manufacturing statistics from 1992 [52]. E: Fishmeal production statistics 2002 [18] F: Based on 2012 U.S. Rendering Market Report (2013) [53].

Agricultural production, specifically the production of animal-derived goods, also results in by-products. In fact, around 30 wt% of an animal produced for food is not used directly for human consumption, and further to this, downed or dead animals are another waste artefact of production. These waste materials are processed by the rendering industry, producing protein-rich products (Table 4).

Global production of animal by-product meals from rendering is in excess of 13 million metric tonnes per year (Figure 2). These products include meat meal, meat and bone meal, poultry by-product meal, poultry meal, blood meal, feather meal, hydrolyzed leather and leather meal, egg shell meal, hydrolyzed hair, unborn calf carcasses, ensiled paunch, bone marrow and dried plasma [19].

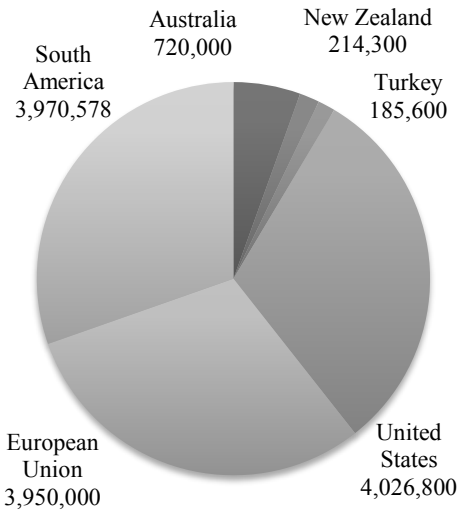

Figure 2: Global production estimate for animal by-product protein meals expressed in metric tonnes [54]. Total global production ~13 million metric tonne.

Other than the above, about 30 wt% of the fish caught globally each year is not used directly for human consumption; instead it is used to produce protein-rich marine by-products, in excess of 6 million metric tonnes per annum (Table 4). Typical animal feed ingredients derived from marine origin include fishmeal, dried fish solubles, crab meal, shrimp meal, fish protein concentrate, and other fish by-products [19].

Finally, animal waste has also been used as a feed ingredient, including dried ruminant waste (manure), dried poultry waste, dried poultry litter, dried swine waste, undried processed animal waste products, and processed animal waste derivatives [19]. According to the Association of American Feed Control Officials, in the U.S., these processed animal waste products must be treated appropriately to ensure a product which is free of harmful pathogens, pesticide residues, parasites, heavy metals, or drug residues [55]. Although recycled animal wastes have been knowingly incorporated into animal feed for almost 50 years, the Food and Drug Administration does not endorse the use of recycled animal waste [19]. Regardless, protein content in dried manure ranges from 12 – 18 wt% for cattle, 28 – 48 wt%

for poultry and 22 – 25 wt% for pigs [56], making it another source of valuable protein and nutrients.

Just as the sources of waste are diverse, so too are the wastes generated, each with a different chemical and physical make-up, directly impacting how they are best utilized (Table 5). Many studies focused on the valorization of these and other waste streams in a profitable way. Obviously, for protein meals which can be fed to livestock or fish, the price for which they are sold will generally cover the cost of producing them, and in the case of animal by-products, the revenue generates a reasonable profit. However, for inedible protein meals (including meals which either have no market, or limited market access) adding value through conversion into novel products is of greater necessity. The problems with imparting additional value to these products is not necessarily related to the scientific or technological feasibility or even cost, but are most commonly associated with the perceived risks and often restrictive supporting legislation.

Table 5: Residues of food processing and by-products. Adapted from [11, 57].

Industry	Food processed	Residues and by-products	Value addition of by-products
 Grain crops	Grain, flour, bread, biscuits, crackers, cakes, starch, bakery goods	Straw, stems, leaves, husks, cobs, hulls, fiber, bran, germ, gluten, steep liquor	Dietary fiber, biomass for ethanol production, biomass for other bio-processes
 Fruits and Vegetables	Tinned fruits and vegetables, juices, vegetable oils, starches, sugars	Rotten fruits and vegetables, stem waste, pits, seeds, peels, pulp	Pectin, pigments, sweeteners, antioxidants, essential oils, proteins, vitamins, sterols, ethanol, yeast, enzymes
 Seed oils	Oils, hydrogenated fats	Press cakes/oil seed cakes, oil water emulsions, rancid fats, shells of oil seeds	Bio-surfactants, growing media bio-char
 Seafood	Canned, filleted, smoked or salted fish, processed crustaceans and mollusks	Scales, fins, bones, guts, fish oil and shells	Fishmeal, fish oil, polyunsaturated fatty acids, fish protein concentrate, hydrolysate, collagen, gelatine, chitin, chitosan, calcium carbonate
 Meat and poultry	Processed meat and poultry products	Blood, hides, hair, heads, horns, hooves, offal, fat, meat trimmings, feathers, feet, giblets	Bloodmeal, Meat meal, fat, feather meal, hydrolysate, bone meal, plasma, red blood cells, collagen, gelatine
 Dairy products	Milk, butter, cream, yogurt, cheese, ice cream	Whey, wastewater	Whey protein, solids from wastewater treatment

4 Bio-security and risk governance

Every nation strives to maintain its bio-security to protect its ecological and economic resources from disease and invasive pests. The most effective means of governing the risks posed by the importation of dangerous or questionable materials, and the harm they may cause to animals or humans, is to impose legal restrictions. The importance to maintain biosecurity is most apparent when considering the risks of international trading. The introduction of invasive pests and disease through international trade could lead to adverse effects, on not only plant

and animal health, but biodiversity and food production as a whole, and should be appropriately managed [58].

These measures must consider not only the scientific evidence supporting such a restriction, but must also consider any reasonable precautions which can act to offset any deficiencies in a solely scientific approach. Hence, during the development of a new policy, a risk analysis is first performed, followed by evaluation of that risk through the lens of current legal, institutional, social and economic circumstances, all of which is undertaken by the stakeholders who represent them [59]. As such, risk governance deals with the management of both perceived and scientifically founded risks.

Although risk management implemented through public policy is focused at the national level, many food and natural resource policies operate at levels both below, and beyond the national level [59]. However, as a result of the discrepancies between each state's local policy making and a lack of cohesive global regulations, the intersection between risk and commerce continues to be a major challenge facing the international trading system.

A significant amount trade conflict experienced at the World Trade Organization has involved the US, Canada, and/or the EU [60]. Some topics which became the focus of either formal or informal disputes have included hormone-fed beef, bovine spongiform encephalopathy (BSE), raw milk cheese, genetically modified organisms, chlorine washed chicken and wood packing materials. Such disputes imply the presence of a transatlantic divide over what constitutes a legitimate risk regulation, however this is an over-simplification.

While the risk regulations set forth by the EU take a precautionary approach, acting in light of scientific uncertainty and taking into account public concerns, the US system is based upon a "sound science" approach, free from political influence, however, this has not always been the case. It has been argued that the US used to be more precautionary than the EU [60], but was pressured to limit the calculation of risk in public policy. The EU's regulatory failures during food safety crises served to undermine public trust in the EU institutions, resulting in the use of a precautionary approach [60]. Overall, it has also been proposed that both regions partake in 'occasional and selective application of precaution to different risks in

different places and time' [61]. Nevertheless, there are some consistencies around the world regarding the safe handling, distribution and disposal of food and animal wastes and by-products.

5 Policy regarding plant and animal by-products

The degree to which protein by-products, particularly animal by-products (ABPs) can be utilized is limited by the customs, religions and regulatory requirements of the region. All feedstuffs imported into a country must comply with general rules regarding hygiene, traceability, contaminants, labelling requirements and health issues given its expected use. The use of the product is then subject to more specific rules, largely limiting the use of those feedstuffs containing animal derived products. The first diagnosis of BSE in the United Kingdom in 1986, and the subsequent publication in 1996 that New Variant Creutzfeldt-Jakob disease in humans, had most probably arisen from exposure to BSE infected meat, sparked a global crisis with respect to food safety and risk management.

Up until the outbreak of BSE during the 1980s, almost all protein by-products were utilized as feed supplements for livestock. In 1989, the practice of feeding ruminant animal protein meals to other ruminants was banned, along with the use of specified bovine offal (brain, spinal cord, other organs potentially infected with BSE) [62]. More recent infectious disease outbreaks, such as Avian Influenza and Severe Acute Respiratory Syndrome, have further jeopardized diplomatic relations, frightened the public and caused massive economic losses by disrupting global commerce [63]. Since then, concern over the risks posed by animal by-products, including infectious diseases, such as swine fever, foot and mouth and other contaminants such as dioxins, to human and animal health, has resulted in strict regulations regarding their safe handling and disposal [64, 65]. As such, most countries now have local regulations put in place which are typically broad in scope and directly impacts any person or business that generates, uses, disposes, stores, handles or transports food waste containing animal products and animal by-products derived from the food processing industry.

Currently, most countries no longer allow animal by-product meals containing any amount of ruminant tissue to be fed to other ruminant animals, although meat and bone meals containing ruminant tissue are still able to be fed to non-ruminant

animals such as poultry, swine, pets, and aquaculture species in most countries, including New Zealand [39]. To the contrary, throughout the EU, meat and bone meals are banned from the feed of any animal which may become human food, and as a result, in the EU, meat meal and meat and bone meal are primarily incinerated or used as an ingredient in pet food [66].

In most countries legislation for waste disposal, disposal of dead animals and of slaughterhouse materials (animal rendering) is already in place. In Germany, the Animal Disease Act, the Meat Hygiene Act, the Poultry Meat Act and the Meat Hygiene Ordinance also regulate the disposal of slaughterhouse offal. To protect animal and human health, the Canadian Food Inspection Agency (CFIA) enforces federal regulations governing the production and use of rendered materials that may be used in animal feed. However, a policy established by the National Renderer's Association which prevented ovine material (sheep) from being used in meat and bone meals in the United States and Canada, and has recently been withdrawn [67].

Compared to Canadian and American policy, the framework of the EU regulations regarding animal by-products and derived products is complex, resulting from on-going reviews by the EU Commission. Each updated regulation is a result of the successive amendment to the initial Regulation (EC) 1774/2002, most recently amended with (EU) No. 749/2011. In addition to covering the safe disposal options available for all animal products including meat, fish, milk and eggs not intended for human consumption, and other products of animal origin including hides, feathers, wool, bones, horns, and hooves. It also prohibits catering waste being used as livestock feed, and covers disposal of fallen stock, companion animals and wild animals if they are suspected of being diseased. The regulations also control the use of animal by-products as feed, fertiliser and technical products with rules for their transformation via composting and biogas operations and their disposal via rendering and incineration [65].

6 Current management options

The existing options available for management of these by-products (and/or wastes) need to consider both legal regulations and the best ecological and economical solutions. Whether a material is deemed to be a valuable by-product (or a waste which needs to be disposed of) depends on the social, legal and technological

framework surrounding its origin. From there, the most sensible form of management becomes a compromise between what is viewed as acceptable based on legal requirements and local perceptions, and what is technologically and financially feasible (Figure 3).

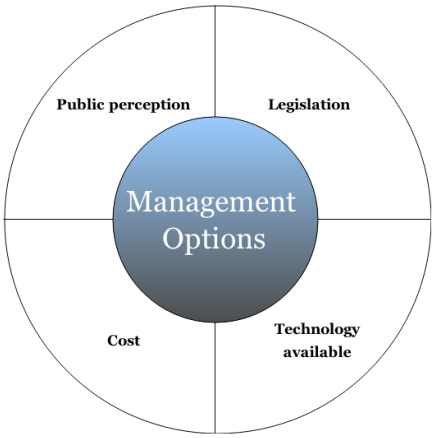

Figure 3: Forming a sensible waste management system relies on compromise between public perception, legislation, cost and technologies.

While it is most desirable to prevent waste and by-product formation, followed by re-use or recycling into other product lines, the formation of by-products and waste is inevitable and management options must be innovative and also meet local regulatory requirements. Waste management is then possible through several media; to use it in its current form, dispose of it through incineration or landfill or add value to it through bioprocessing or valorization technologies (Figure 4). The choice of media used will largely depend on the cost, customs and regulatory environment. For instance, converting the by-product to animal fodder (bio-reduction) may not be feasible in all countries.

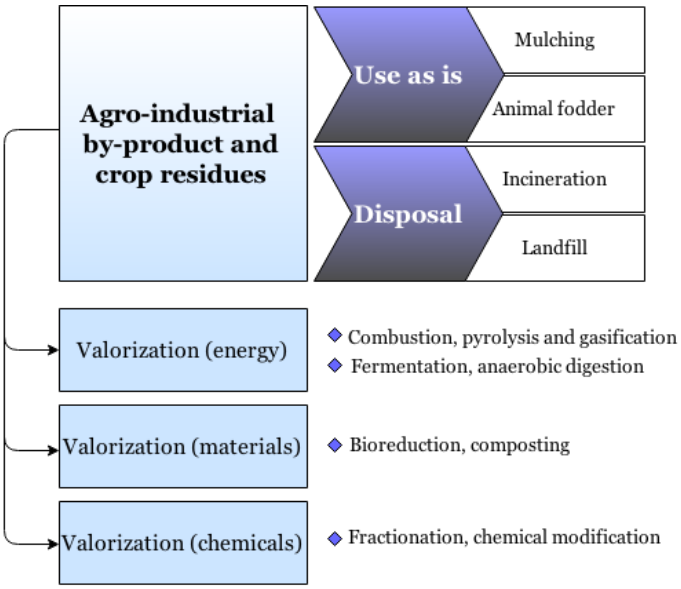

Figure 4: Flow diagram for conversion of agro-industrial by-products and crop resides.

6.1 Use in its current form

Excess and waste food has been used as animal fodder for centuries, and in many parts of the world, farmers still use waste food to feed their animals; primarily pigs and poultry. The practice of feeding waste material containing meat products to pigs was banned in the United Kingdom in 2001, (Statutory Instrument 2001, No. 1704 The Animal By-products Amendment) to prevent further spread of BSE, and soon after a new regulation was implemented throughout the Europe Union (The Animal By-Products Regulation, EC No: 1774/2002) prohibiting catering waste from being fed to farmed animals. This includes all waste food and used cooking oils, as well as waste from vegetarian restaurants and kitchens. Based on these laws, only certain types of waste food can be given to livestock, and must first be treated appropriately.

If the by-product cannot be immediately used as it is or treated appropriately for use as an animal feed, it must be safely disposed of. Due to the time and expense of treating these food wastes, most end up in landfill. Currently, landfilling and incineration account for the treatment of greater than 95% of food waste in most European countries [68]. In general, using the biomass waste in the form it is in, either as an animal feed or fertilizer or as a fuel to generate electricity, is the most simplistic approach and generates a value of ~$US 70 – 200 per tonne of biomass [69].

6.2 Incineration

Incineration is the simplest means of waste disposal, with its major advantage being the significant reduction in volume of the waste stream; up to 90 % for waste streams with high amounts of paper, cardboard, plastics and horticultural waste [70]. However, most food wastes aren't appropriate for incineration owing to their high moisture content. When properly equipped, an incinerator can be used as a means of energy recovery to generate electricity. Heat released from the combustion of waste can be used to produce steam, which can turn a steam turbine, generating electricity. However, due to the increased concentration of toxins in the ash, incinerators must be operated alongside landfill systems in order to dispose of them. Combustion destroys chemical compounds and disease causing bacteria, leaving it pathogen free, but causes serious environmental problems through the production of carbon dioxide, nitrogen oxides, sulfur dioxide, and trace quantities

of toxic pollutants, such as heavy metals and dioxins. The remaining residues are often landfilled owing to their high heavy metal content.

6.3 Pyrolysis and Gasification

Thermochemical conversion of food and industry wastes are an effective means of converting energy rich biomass into a more easily used liquid or gaseous intermediate. High temperatures can be used with minimal (gasification) or no oxygen present (pyrolysis) to break down hydrocarbon containing wastes, resulting in combustible syngas mixtures containing carbon monoxide and hydrogen (85%), with small amounts of carbon dioxide and methane. This syngas intermediate can be further processed to produce bio-based gasoline, diesel or jet fuel, or be used in a fuel cell to generate electricity or steam.

6.4 Landfilling

Landfills are a common final disposal site for waste and the residues remaining from other treatment options, and involves burying the material. At atmospheric pressure, one tonne of organic material generates approximately 200 – 500 m^3 of landfill gas over a 10 – 20 year timeframe [71], comprised of 60 – 65 % methane and 35 – 40 % carbon dioxide and represent around 8 % of the anthropogenic methane emitted worldwide [68]. Methane (CH_4), has 21 times the global warming potential of carbon dioxide, and can be recovered and burned (with or without energy recovery) to reduce greenhouse gas emissions [70]. Other serious environmental implications of landfilling include the risk of leachate (potential toxic liquid which drains from landfills) entering surrounding soils and groundwater.

Although the use of landfills is common, their use has been discouraged through the implementation of landfill taxes and directives such as the 'Landfill Tax' in the U.K. in 1996 and EU Landfill Directive established in 1999 [71]. Obviously, other disposal options are preferred to landfilling, which costs ~ $US 400 per tonne.

6.5 Bioprocessing

Around 60% of the municipal waste sent to landfill is biodegradable and mostly comprised of food waste [70]. This makes bioprocessing, such as composting and anaerobic digestion, sensible options for disposing of these organic waste streams.

A common means of obtaining a safe end product is achieved through composting. This involves a combination of chemical and microbiological processes occurring throughout three stages that convert organic materials to a stable, soil-like product called compost [72, 73]. Provided composting is carried out well, the volume and mass of the waste can be reduced by up to 40 %. For composting to occur efficiently, the conditions of the composting process must be maintained at an optimal level to encourage microbial growth. Due to changes in the composition of waste material with location and over time, the compost mixture needs optimization through regular adjustments. For instance, if the system becomes anaerobic, offensive odours can be produced, and if it becomes too wet or too dry the process will halt altogether. Some of these organic waste materials require specific pre-treatment before composting can occur. In the UK, EU standards must be implemented over and above UK standards if the site treats Category 2 ABPs which have first been pressure rendered, or Category 3 ABPs if they exclude catering waste. Exceptions apply for some types of ABPs in the UK which can be composted in closed reactors at 70 ^{o}C for > 1 hour or in housed windrows at 60 ^{o}C for > 8 days under strict operating parameters with a maximum particle size of 400 mm.

While compost is of limited value, it is still a more economic option compared to landfilling. Other bioprocesses can be employed which produce more valuable products. Biofuels can be produced using fermentation, valued at $US 200 – 400 per tonne more than the initial biomass-waste [69]. Anaerobic digestion is another means of disposing of organic waste materials, and is carried out in an enclosed vessel. The methane generated can either be flared or collected for combustion to generate heat and/or electricity which also adds value to the waste biomass.

The maximum value can be recovered from these waste materials by converting them into more purified streams, and using them in the manufacture of lubricants, surfactants, plastics, fibers and industrial solvents. Theoretically, all ABPs in the EU could be combusted as fuel for energy, provided the EU Commission formulates the appropriate rules and regulations, which as of yet has not been done.

Although there are many technologies currently available (or in developmental stages) which aim to valorize by-products of industry, legislation has yet to be passed which explicitly deals with higher technology outcomes. Most current law deals with the safe handling and disposal of animals, their products and by-products

and animal feeding. While it is necessary to contain health and environmental risks through appropriate legislation, it is becoming apparent that the use of animal by-products and food wastes (excluding crop residues and some agro-industrial by-products) for animal fodder and composting is not only obsolete, but in many nations, illegal.

7 Value addition

Many technologies exist which aim to valorize by-products of the agricultural industry. While the edible portion of these protein rich by-products could be used for recovery of essential amino acids for human consumption, or as is, for use in animal feeds, higher value applications for inedible and non-essential amino acids may include providing a feedstock for protein based materials such as plastics, and for the production of bio-pesticides and commodity organic compounds [20, 21].

Along with more obvious uses of protein hydrolysates, animal feeds and biomass for energy recovery, protein based meals from crop residues and agro-industrial by-products also find value addition through use in biological processes. An example is the use of various oil seed cakes which have been shown to be ideal mediums for many types of bacteria and fungi responsible for producing a variety of enzymes, anti-biotic and antimicrobial compounds and bioactive metabolites [57]. Protein based raw materials can be used for the production of 1,2-ethanediamine and 1,4-butanediamine from the amino acids serine and arginine respectively [74]. Furthermore, protein based surfactants are valuable mild surfactants, since the structure and properties of the amino acids in the surfactants are similar to the amino acids which make up the tissue of skin.

If valorization technologies are to be implemented on commercial scale, they must work within current legal constructs. However, this doesn't deal directly with the science involved and may inhibit progress if new legislation is not developed which more closely examines the evidence and whether risk regarding human and animal health is still an issue. In light of current legislation and potential markets for value added commodities, it is becoming apparent that the use of protein-rich agricultural by-products for lower value applications such as animal fodder, is no longer a sensible use of such a valuable resource.

References

1. Murray, S. The World's Biggest Industry. 2007 15/11/2007 [cited 2015 22/3/15]; Available from: http://www.forbes.com/2007/11/11/growth-agriculture-business-forbeslife-food07-cx_sm_1113bigfood.html.

2. Godfray, H.C.J., Beddington, J.R., Crute, I.R., Haddad, L., Lawrence, D., Muir, J.F., Pretty, J., Robinson, S., Thomas, S.M., Toulmin, C. (2010). Food Security: The Challenge of Feeding 9 Billion People. Science. 327(5967): p. 812-818.

3. Msangi, S., Rosegrant, M.W. (2011). Feeding the Future's Changing Diets: Implications for Agriculture Markets, Nutrition, and Policy, in 2020 Conference: Leveraging Agriculture for Improving Nutrition and Health. International Food Policy Research Institute: Washington, D.C., U.S..

4. van Huis, A. (2013). Potential of Insects as Food and Feed in Assuring Food Security. Annual Review of Entomology. 58(1): p. 563-583.

5. Pimentel, D., Pimentel, M. (2003). Sustainability of Meat-Based and Plant-Based Diets and the Environment. The American Journal of Clinical Nutrition. 78(3): p. 660-663.

6. Foley, J.A. (2011). Can We Feed the World and Sustain the Planet? A Five-Step Global Plan Could Double Food Production by 2050 While Greatly Reducing Environmental Damage. . Scientific American. 305: p. 60-65.

7. Kummu, M., de Moel, H., Porkka, M., Siebert, S., Varis, O., Ward, P.J. (2012). Lost Food, Wasted Resources: Global Food Supply Chain Losses and Their Impacts on Freshwater, Cropland, and Fertiliser Use. Science of The Total Environment. 438(0): p. 477-489.

8. Food and Agriculture Organization of the United Nations. (2011). Global Food Losses and Food Waste – Extent, Causes and Prevention. Food and Agriculture Organization of the United Nations: Rome, Italy.

9. Leoci, R. (2014). Animal By-Products (ABPs): Origins, Uses and European Regulations. Universitas Studiorum: Mantova, Italy. p. 15-21.

10. Santana-Méridas, O., González-Coloma, A., Sánchez-Vioque, R. (2012). Agricultural Residues as a Source of Bioactive Natural Products. Phytochemistry Reviews. 11(4): p. 447-466.

11. de las Fuentes, L., Sanders, B., Lorenzo, A., Alber, S. (2004). Awarenet: Agro-Food Wastes Minimisation and Reduction Network. in Total Foods. 2004. Institute of Food Research: Norwich, England.

12. Scarlat, N., Martinov, M., Dallemand, J. (2010). Assessment of the Availability of Agricultural Crop Residues in the European Union: Potential and Limitations for Bioenergy Use. Waste Management. 30(10): p. 1889-1897.

13. Godfray, H.C.J., Crute, I.R., Haddad, L., Lawrence, D., Muir, J.F., Nisbett, N., Pretty, J., Robinson, S., Toulmin, C., Whiteley, R. (2010). The Future

of the Global Food System. Philosophical Transactions of the Royal Society B: Biological Sciences. 365(1554): p. 2769-2777.

14. Gustavsson, J., Cederberg, C., Sonesson, U., van Otterdijk, R., Meybeck, A. (2011). Global Food Losses and Food Waste: Extent, Causes and Prevention. Food and Agriculture Organization of the United Nations: Rome, Italy.

15. Pleissner, D., Lin, C. (2013). Valorisation of Food Waste in Biotechnological Processes. Sustainable Chemical Processes. 1(1): p. 1-6.

16. Wiedemann, S., Yan, M. (2014). Livestock Meat Processing: Inventory Data and Methods for Handling Co-Production for Major Livestock Species and Meat Products, in Ninth International Life Cycle Assessment of Foods Conference: San Francisco, U.S..

17. Food and Agriculture Organization of the United Nations. (2013). Production Quantity 2013. Food and Agriculture Organization of the United Nations: Rome, Italy.

18. Hardy, R.W., Tacon, A.G.J. (2002). Fish Meal: Historical Uses, Production Trends and Future Outlook for Sustainable Supplies, in Responsible Marine Aquaculture, Stickney, R.R. and McVey, J.P., Editors. CABI: London.

19. Lefferts, L., Kucharski, M., McKenzie, S., Walker, P. (2006). Feed for Food Producing Animals: A Resource on Ingredients, the Industry, and Regulation. Vol. 115. Baltimore: Bloomberg School of Public Health, The Johns Hopkins Center for a Livable Future. 663-670.

20. Naik, S.N., Goud, V.V., Rout, P.K., Dalai, A.K. (2010). Production of First and Second Generation Biofuels: A Comprehensive Review. Renewable and Sustainable Energy Reviews. 14(2): p. 578-597.

21. Scott, E., Peter, F., Sanders, J. (2007). Biomass in the Manufacture of Industrial Products—the Use of Proteins and Amino Acids. Applied Microbiology and Biotechnology. 75(4): p. 751-762.

22. United States Department of Agriculture. (2015). World Agricultural Supply and Demand Estimates.

23. National Research Council. (2001). Nutrient Composition of Feeds, in Nutrient Requirements of Dairy Cattle: Seventh Revised Edition. The National Academies Press: Washington, D.C., U.S.. p. 281-314.

24. Annongu, A.A., Joseph, J.K. (2008). Proximate Analysis of Castor Seeds and Cake. Journal of Applied Sciences and Environmental Management. 12(1): p. 39-41.

25. Fuller, G., Walker, H.G., Jr., Mottola, A.C., Kuzmicky, D.D., Kohler, G.O., Vohra, P. (1971). Potential for Detoxified Castor Meal. Journal of the American Oil Chemists' Society. 48(10): p. 616-618.

26. Adeola, O. (2003). Energy Values of Feed Ingredients for White Pekin Ducks. International Journal of Poultry Science. 2(5): p. 318 -323.

27. Agunbiade, J.A., Susenbeth, A., Sudekum, K.H. (2004). Comparative Nutritive Value of Cassava Leaf Meal, Soya Beans, Fish Meal and Casein in Diets for Growing Pigs. Journal of Animal Physiology and Animal Nutrion. 88(1-2): p. 30-8.

28. Kassahun, A., Waidbacher, H., Zollitsch, W. (2012). Proximate Composition of Selected Potential Feedstuffs for Small-Scale Aquaculture in Ethiopia. Livestock Research for Rural Development. 24(6).

29. Pousga, S., Boly, H., Lindberg, J.E., Ogle, B. (2007). Evaluation of Traditional Sorghum (*Sorghum bicolor*) Beer Residue, Shea-Nut (*Vitellaria paradoxa*) Cake and Cottonseed (*Gossypium spp*) Cake for Poultry in Burkina Faso: Availability and Amino Acid Digestibility. International Journal of Poultry Science. 6(9): p. 666-672.

30. Khanum, S.A., Yaqoob, T., Sadaf, S., Hussain, M., Jabbar, M.A., Hussain, H.N., Kausar, R., Rehman, S. (2007). Nutritional Evaluation of Various Feedstuffs for Livestock Production Using in Vitro Gas Method. Pakistan Veterinary Journal. 27(3): p. 129-133.

31. El-Saidy, D.M.S.D., Gaber, M.M.A. (2003). Replacement of Fish Meal with a Mixture of Different Plant Protein Sources in Juvenile Nile Tilapia, *Oreochromis niloticus* (L.) Diets. Aquaculture Research. 34(13): p. 1119-1127.

32. El-Saidy, D.M.S.D., Saad, A.S. (2008). Evaluation of Cow Pea Seed Meal, Vigna Sinensis, as a Dietary Protein Replacer for Nile Tilapia, *Oreochromis niloticus* (*L.*), Fingerlings. Journal of the World Aquaculture Society. 39(5): p. 636-645.

33. Chu, Z.J., Yu, D.H., Yuan, Y.C., Qiao, Y., Cai, W.J., Shu, H., Lin, Y.C. (2014). Apparent Digestibility Coefficients of Selected Protein Feed Ingredients for Loach Misgurnus Anguillicaudatus. Aquaculture Nutrition.

34. Martínez-Llorens, S., Vidal, A.T., Moñino, A.V., Gómez Ader, J., Torres, M.P., Cerdá, M.J. (2008). Blood and Haemoglobin Meal as Protein Sources in Diets for Gilthead Sea Bream (*Sparus aurata*): Effects on Growth, Nutritive Efficiency and Fillet Sensory Differences. Aquaculture Research. 39(10): p. 1028-1037.

35. Haughey, D.P. (1976). Market Potential and Processing of Blood Products: Some Overseas Observations. MIRINZ, Hamilton.

36. National Research Council and Canadian Department of Agriculture (1971). Atlas of Nutritional Data on United States and Canadian Feeds. National Academy of Sciences: Washington, D.C., U.S..

37. Preston, R.L. (2014). 2014 Feed Composition Table, in Beef. Penton Media: Minneapolis, U.S.. p. 18-26.

38. Nengas, I., Alexis, M.N., Davies, S.J., Petichakis, G. (1995). Investigation to Determine Digestibility Coefficients of Various Raw Materials in Diets for Gilthead Sea Bream, *Sparus auratus L.* Aquaculture Research. 26(3): p. 185-194.

39. Garcia, R.A., Phillips, J.G. (2009). Physical Distribution and Characteristics of Meat and Bone Meal Protein. Journal of the Science of Food and Agriculture. 89(2): p. 329-336.

40. Howie, S.A., Calsamiglia, S., Stern, M.D. (1996). Variation in Ruminal Degradation and Intestinal Digestion of Animal By-Product Proteins. Animal Feed Science and Technology. 63(1–4): p. 1-7.

41. Kamalak, A., Canbolat, O., Gurbuz, Y., Ozay, O. (2005). In Situ Ruminal Dry Matter and Crude Protein Degradability of Plant- and Animal-Derived Protein Sources in Southern Turkey. Small Ruminant Research. 58(2): p. 135-141.

42. Qiao, S., Thacker, P.A. (2004). Use of the Mobile Nylon Bag Technique to Determine the Digestible Energy Content of Traditional and Non-Traditional Feeds for Swine. Archives of Animal Nutrition. 58(4): p. 287-294.

43. Bimbo, A.P. (2000). Fish Meal and Oil, in Marine and Freshwater Products Handbook, Martin, R.E., Carter, E.P., Flick, G.J.J., and Davis, L.M., Editors. Technomic Publishing Company: Pennsylvania, U.S.. p. 541-482.

44. Trushenski, J., Gause, B. (2013). Comparative Value of Fish Meal Alternatives as Protein Sources in Feeds for Hybrid Striped Bass. North American Journal of Aquaculture. 75(3): p. 329-341.

45. Okoye, F.C., Ojewola, G.S., Njoku-Onu, K. (2005). Evaluation of Shrimp Waste Meal as a Probable Animal Protein Source for Broiler Chickens. International Journal of Poultry Science. 4(7): p. 458-461.

46. Fanimo, A.O., Oduguwa, O.O., Onifade, A.O., Olutunde, T.O. (2000). Protein Quality of Shrimp-Waste Meal. Bioresource Technology. 72(2): p. 185-188.

47. Everts, H., Nguyen, L.Q., Beynen, A.C. (2003). Shrimp By-Product Feeding and Growth Performance of Growing Pigs Kept on Small Holdings in Central Vietnam. Asian-Australasian Journal of Animal Sciences. 16(7): p. 1025-1029.

48. Fanimo, A.O., Susenbeth, A., Südekum, K.H. (2006). Protein Utilisation, Lysine Bioavailability and Nutrient Digestibility of Shrimp Meal in Growing Pigs. Animal Feed Science and Technology. 129(3–4): p. 196-209.

49. Ash, M. S. (1992). Animal Feeds Compendium. United States Department of Agriculture. Washington, D.C., U.S..

50. United States Department of Agriculture. (2013). Agricultural Statistics. United States Department of Agriculture, Washington, D.C., U.S..

51. United States Department of Agriculture. (2015). Oil Crops Outlook, in Oil Crops Year Book Data Archive 2015. United States Department of Agriculture, Washington, D.C., U.S..

52. United States Department of Commerce. (1994). Current industrial reports: Manufacturing profiles 1992. Economics and Statistics Administration.

Bureau of the Census Editors. United States Department of Commerce: Washington, D.C., U.S..

53. Swisher, K. (2013). Market Report: US Rendering: A $10 Billion Industry. Rendering Magazine. April.

54. Kaluzny, D. (2013). World Renderers Organization: Rendered Products Worldwide. Global Feed & Food Congress, Sun City, South Africa.

55. Association of American Feed Control Officials. (2007). Official Publication: Association of American Feed Control Officials. 2007: Association of American Feed Control Officials.

56. Chen, S., Harrison, J.H., Liao, W., Elliot, D.C., Liu, C., Brown, M.D., Wen, Z., Solana, A.E., Kincaid, R.L., Stevens, D.J. (2003). Value-Added Chemicals from Animal Manure. Pacific Northwest National Laboratory, Editors. United States Department of Energy: Washington, D.C., U.S..

57. Ramachandran, S., Singh, S.K., Larroche, C., Soccol, C.R., Pandey, A. (2007). Oil Ccakes and their Biotechnological Applications – A Review. Bioresource Technology. 98(10): p. 2000-2009.

58. Maye, D., Dibden, J., Higgins, V., Potter, C. (2012). Governing Biosecurity in a Neoliberal World: Comparative Perspectives from Australia and the United Kingdom. Environment and Planning A. 44: p. 150-168.

59. Mills, P., Dehnen-Schmutz, K., Ilbery, B., Jeger, M., Jones, G., Little, R., MacLeod, A., Parker, S., Pautasso, M., Pietravalle, S., Maye, D. (2011). Integrating natural and social science perspectives on plant disease risk, management and policy formulation. Vol. 366. 2011. 2035-2044.

60. Hornsby, D. J. (2013). Risk Regulation, Science, and Interests in Transatlantic Trade Conflicts. International Political Economy Series. 2013: Palgrave Macmillan: London, U.K..

61. Wiener, J. (2011). The Real Pattern of Precaution, in The Reality of Precaution: Comparing Risk Regulation in the US and Europe, Wiener, J., Rogers, M., Hammitt, J., and Sand, P., Editors. Earthscan: New York, U.S..

62. Ockerman, H.W., Hansen, C.L. (2000). Rendering, in Animal By-Product Processing and Utilization. Ockerman, H.W., Hansen, C.L., Editors. CRC Press: Florida, U.S.. p. 87-126.

63. Karesh, W.B., Cook, R.A. (2005) The Human-Animal Link. [17 March 2015]; Available from: http://www.foreignaffairs.com/articles/60821/ william-b-karesh-and- robert-a-cook/the-human-animal-link.

64. Cunningham, E.P. (2003). After BSE: A Future for the European Livestock Sector. Wageningen Academic Publishers: Gelderland, Netherlands.

65. Department for Environment, Food and Rural Affairs, (2011). Controls on Animal By-Products: Guidance on Regulation (EC) 1069/2009 and Accompanying Implementing Regulation (EC) 142/2011, Enforced in England by the Animal By-Products (Enforcement) (England) Regulations 2011. Department for Environment, Food and Rural Affairs: London, U.K..

66. Kirchmayr, R., Resch, C., Mayer, M., Prechtl, S., Faulstich, M., Braun, R., Wimmer, J. (2007). Anaerobic Degradation of Animal By-Products, in Utilization of By-Products and Treatment of Waste in the Food Industry, Oreopoulou, V., Russ, W., Editors. Springer: New York, U.S.. p. 159-192.

67. Malone, J. (2005). NRA Rescinds Sheep Material Policy, in ASI Weekly Centennial. American Sheep Industry Association.

68. Melikoglu, M., Lin, C.S.K., Webb, C. (2013). Analysing Global Food Waste Problem: Pinpointing the Facts and Estimating the Energy Content. Central European Journal of Engineering. 3(2): p. 157-164.

69. Tuck, C.O., Pérez, E., Horváth, I.T., Sheldon, R.A., Poliakoff, M. (2012). Valorization of Biomass: Deriving More Value from Waste. Science. 337(6095): p. 695-699.

70. Hoornweg, D., Bhada-Tata, P. (2012). What a Waste: A Global Review of Solid Waste Management. Urban Development Series, ed. Urban Development & Local Government Unit. Vol. 12. 2012, World Bank: Washington, D.C., U.S..

71. Jardine, C.N., Boardman, B., Osman, A., Vowles, J., Palmer, J. (2004). Methane UK. Environmental Change Institute, Editors. University of Oxford: Oxford, U.K..

72. Som, M.-P., Lemée, L., Amblès, A. (2009). Stability and Maturity of a Green Waste and Biowaste Compost Assessed on the Basis of a Molecular Study using Spectroscopy, Thermal Analysis, Thermodesorption and Thermochemolysis. Bioresource Technology. 100(19): p. 4404-4416.

73. Verbeek, C.R., Hicks, T., Langdon, A. (2012). Biodegradation of Bloodmeal-Based Thermoplastics in Green-Waste Composting. Journal of Polymers and the Environment. 20(1): p. 53-62.

74. Sanders, J., Scott, E., Weusthuis, R., Mooibroek, H. (2007). Bio-refinery as the bio-inspired process to bulk chemicals. Macromolecular Bioscience. 7(2): p. 105-17.

Appendix 2

Meat Industry Protein By-Products:

Sources and Characteristics

An invited book chapter

By

TALIA M. HICKS AND C. J. R. VERBEEK

Published in

Elsevier B.V. Waste-derived Proteins: Transformation from Environmental Burden into Value-added Products

This chapter has been included to provide context for the use of protein by-products from the meat industry in value-added products. As first author, I prepared the initial draft manuscript, which was refined and edited in consultation with my supervisor, who has been credited as a co-author.

Meat industry Protein By-Products: Sources and Characteristics

Talia. M. Hicks and *Casparus J.R. Verbeek

School of Engineering
University of Waikato
Private Bag 3105
Hamilton 3240
New Zealand
jverbeek@waikato.ac.nz

Abstract

Global consumption of meat products established an enormous and constantly growing industry. By-products generated from this industry have a high biological oxygen demand and if not treated properly can have serious implications for the environment. Meat products, such as fish, chicken as well as beef, sheep and pork all result in similar waste products. These include carcasses, intestines, feathers, fish bones and scales as well as blood. Although these can be seen as waste from the meat producer they become much more valuable after rendering. A variety of products exist, such as gelatin from hooves, meat-and-bone meal from carcasses and intestines as well blood, feather and fish meal. These are mainly used as animal feed supplements due to their high protein content, but the nutritional properties vary dramatically, and in some cases further processing is required. In this chapter the sources and properties of animal-based proteins are discussed in terms of their biological composition as well as their physico-chemical properties.

1 Introduction

Domesticated livestock play a significant role in maintaining the modern human lifestyle. These animals are reared and slaughtered for meat as well as dairy and other animal products. Global demand will continue to rise along with population growth, and as more underdeveloped countries adopt westernized eating habits [1, 2].

The continual growth of this market has triggered some dramatic changes to what would now be considered traditional farming practice. Intensive breeding of livestock is aimed at maximizing product yield and has become commonplace in

developed countries [3, 4]. To keep up with the calorific demand of high production, pasture is often supplemented with grains, such as maize or wheat. Feed may also be fortified with protein meals, such as corn gluten meal, and in countries where there is no restriction, can include animal by-products, such as blood meal [5]. Pre- and pro-biotics, growth promoting factors, supplements and additives are often used in intensive farming practices to accelerate growth, boost production and improve animal condition.

No matter how rapid or big an animal grows, only 30 – 40 % of the animal is used for human consumption [6, 7] and what remains equates to a significant volume of solid and liquid waste. These are considered an aesthetic, environmental and economic burden, and their safe disposal can incur considerable cost to the meat processor.

With the expected rise in worldwide consumption of animal protein products, so too will there be an increase in associated waste. In a world with finite resources, the minimization, recovery and utilization of by-products becomes increasingly important [8].

This chapter evaluates various aspects of animal by-products obtained from commercial slaughterhouses which are then rendered to produce higher value products. Sources of raw materials are investigated, including emerging industry specific wastes, such as those from fisheries. The effect of some processing techniques and nuances of typical rendering processes on product quality, economic value and end-use are considered.

One limitation of this discussion is the intrinsic variability of meat processing. Although not covered extensively, it is important to realize that the following aspects of this industry directly influence the type of animal by-products and their final uses:

- Animal production and therefore by-product quantity and quality are subject to daily and seasonal variation.
- Animal market conditions vary between different locations and countries.
- Animal composition varies both between species and within a species depending on the animal's breed, age, gender, health and condition.

- Raw material obtained for rendering will depend on what is considered "edible", which is subject to the culture, customs, religion, regulations and market demand of the considered location.
- The collection process of the rendering plant and product handling also determines the quality and end-use.

Also, this chapter specifically deals with by-products from commercial slaughter of cattle, sheep/lamb, pork, poultry and seafood processing. Processing of animal wastes from farms, game meats, zoo animals and companion animals is outside the scope of this discussion.

2 The meat industry

Production and processing of animals for food results in ancillary animal by-products (ABP). Continuous research behind the technology and regulatory aspects of meat processing is aimed at improving hygienic meat collection and minimizing product loss. Slaughterhouse operations vary depending on the size and space limitations of the plant. Common operations, regardless of species, include holding, stunning, killing, bleeding, hide or hair removal, evisceration, carcass washing, trimming and dressing. Secondary operations may also occur on-site including cutting, deboning and processing into retail products.

A typical process flow for slaughter of livestock is described in Figure 1 where the principle commodity is meat, however other by-products obtained during the slaughter process are:

- edible by-products – offal, casings
- inedible by-products – hides, horn, wool
- low value by-products – protein meals for animal feed
- waste items, with no useful purpose to be disposed of.

While the most valuable materials have already been removed during processing, potentially useful components may remain in the low value products and waste [9]. These components need to be effectively utilized to cover the overheads of slaughtering, pollution control and disposal [6, 7]. Despite their associated environmental and health risks, these waste materials are now recognized for their potential to be recycled or converted into value-added products and now represent valuable economic commodities.

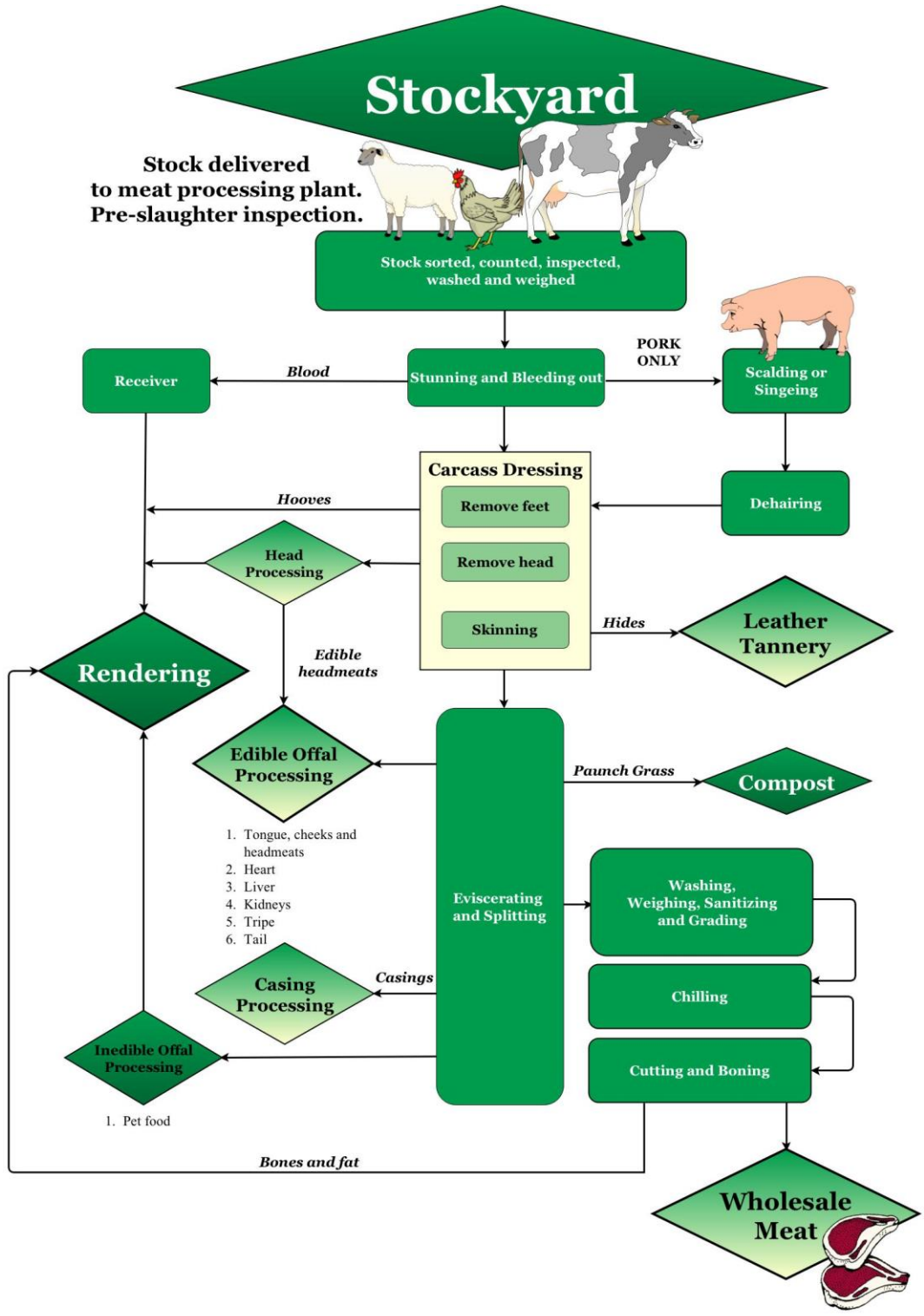

Figure 1: Process flow diagram for general meat processing.

1.1 Economics of by-product processing

Providing meat, milk and eggs for human consumption also results in the ancillary production of edible and inedible by-products. Approximately 49 % of the live weight of cattle, 44 % of pigs, 37 % of broilers, and 57 % of most fish species cannot be sold as meat or used in meat-products for human consumption and are classified as inedible by-products [10]. In the United States alone, this is estimated to correspond to the production of ~25 million metric ton of inedible animal tissue annually [11].

Animal by-products may represent up to 75% of an animal's live weight, but in their unprocessed state may be worth as little as 10-20% of the animal's total value [12]. However, with appropriate processing the revenue from the end-products may nearly equate to those of the meat. In some cases, the commercial value of these by-products is higher than the sum of the operating expenses and the margin required to operate profitably [7]. Rendering is the most economical method for safely handling these materials, salvaging billions of dollars of saleable product [11].

The edible products are considered to be the most valuable part of the slaughtered animal. Technologies have been developed to capitalize on the production of edible materials from normally inedible products, such as protein concentrates from horns and hooves for use as flavoring agents [12]. Classification of by-products depends on local culture, customs and regulations, and as a result, some products can be downgraded from edible to inedible [7]. Inedibles are then rendered into products, such as meat and bone meal (MBM), meat meal (MM), poultry meal, hydrolyzed feather meal, blood meal, fish meal, and animal fats.

1.2 Rendering

Rendering is a combination of mechanical, thermal and sometimes chemical processes to separate biological materials (the waste from the carcass of a dead animal) into its constituent components; fat, protein and water. More importantly, it can be seen as an integrated system to safely process raw material into a material that complies with environmental and disease control legislation. The purpose of rendering is to:

- Sterilize by-products for safety.
- Remove fat to prevent oxidation during storage.
- Drying to inhibit bacterial growth and facilitate transportation and storage.
- Create saleable products.

Rendering depends largely on the type and condition of raw material and directly influences production costs, product quality and financial success of the product [13]. Therefore, appropriate selection and operation is paramount for high quality.

1.2.1 Rendering sources

Biological raw material not only includes inedible offal, fat and animals classified as “condemned”, but also animals that died before slaughtering. Rearing animals leads to a large number of on-farm livestock mortalities. These deaths include stillbirths, the unwanted offspring of livestock, culled animals and animal deaths caused by disease or age. Rendering plants deals with the disposal of these animals, along with waste from slaughterhouses (Figure 2). Therefore rendering not only generates value-added products, it also provides a hygienic means of disposing of fallen and condemned animals.

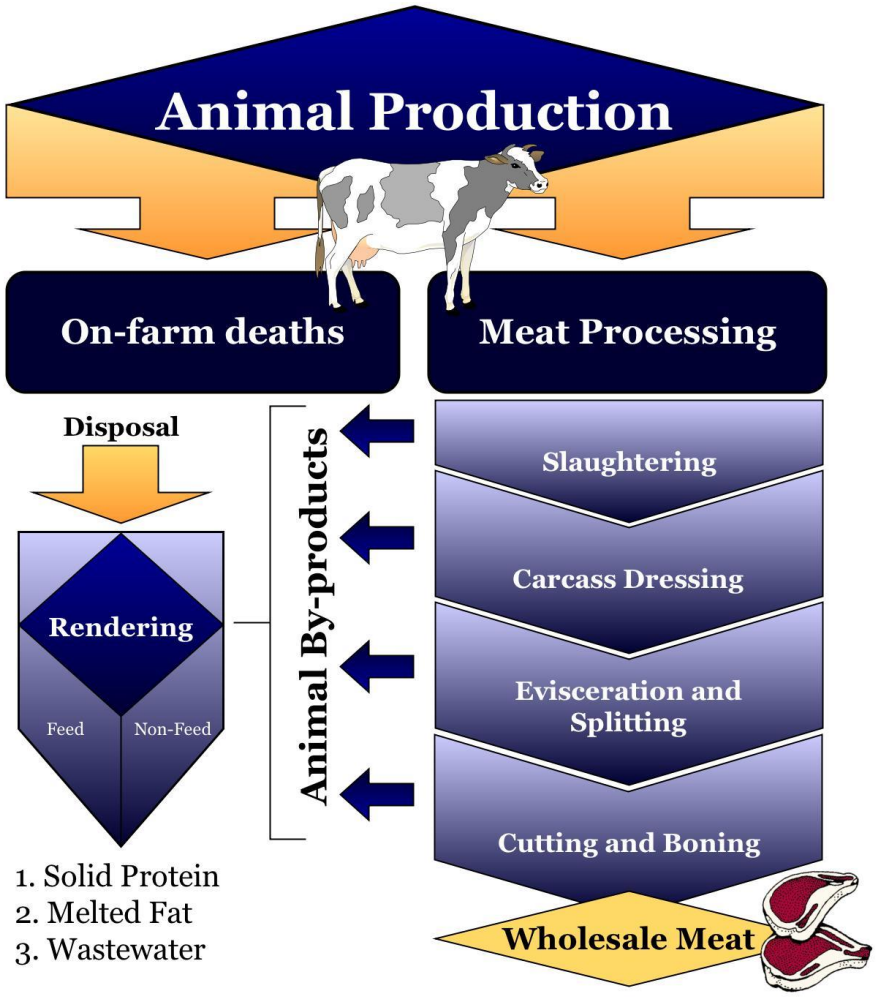

Figure 2: Sources of raw material for rendering from animal production.

1.2.2 Basic principles of rendering

The two basic processes occurring during rendering are the separation of fat and drying the remaining protein-rich residue. Rendering involves crushing the raw material and cooking at 110 – 120 °C for sterilization. The majority of the fat is decanted and the residual solids (~20 % fat) are then centrifuged. The solids are sometimes solvent extracted leaving degreased protein-meal (3 - 5% fat) as residue [8].

The main factors determining product quality are:

- pre-crushing and quantity of the raw material used
- steam pressure
- agitator speed and temperature
- cooking/drying temperature
- end-point moisture content

To obtain the highest quality products, material should be rendered as soon as possible after slaughtering to minimize bacterial degradation of proteins and fats. Where possible, processing should avoid introduction of additional air or moisture to minimize oxidation and hydrolysis.

Generally, rendering begins with the removal of undesirable parts from the raw materials. In particular, paunch content must be removed and viscera washed. Failure to do so results in a green-tinted product, degrades fat quality (higher free fatty acid content [14]) and increases moisture, impurity and unsaponifiable content [15]. Quality is also ensured by rapid cooking, allowed for by adequate heat transfer during cooking, achieved through size reduction of the raw material. The cooked mixture is separated into fat, water and protein by screening, pressing, centrifugation, solvent extraction, and drying [16].

Rendering can be categorized into either “edible” or “inedible”. Edible rendering only utilizes by-products obtained under sterile conditions. For example, fat trimming is ground and melted to release moisture and “edible” tallow. The three end-products (protein, fat, and water) are separated by screening and sequential centrifugation. The protein-rich solids are dried and sold for use as animal feed, water is treated for recycling or discharge, and the edible fat is stored for refinement. Other edible products are also produced, such as gelatin from bone collected hygienically.

By contrast, inedible rendering processes utilize the remaining protein, fat and keratin (hoof and horn). The rendering process also involves cooking, dewatering and separating fat, protein and water but often requires some pre-cooking processes. This includes the removal of skin and paunch and thorough washing of the entire carcass. The hide is not normally removed from hogs and small animals, but removal of their hair is carried out before washing and cleaning [16]. The cleaned carcasses are then crushed, weighed and passed through metal and non-metal detectors to remove nearly all of the magnetic and non-magnetic metal materials (tags, hardware and boluses).

Although edible and inedible rendering processes are similar, they differ in their raw materials, end products and sometimes equipment. Furthermore, different rendering systems work well for small (poultry), medium (swine, sheep, calves),

and large sized (cattle and horse) mortalities [16]. Typically all rendering systems can be classified as either wet or dry depending on whether the fat is removed before or after the drying operation; both can be carried out in a batch, semi-continuous or continuous mode. More recently, low-temperature rendering systems have become popular, as they prevent destruction of amino acids and maintain the biological activities of lysine, methionine and cystine [7, 16].

2 Animal products and by-products

2.1 Meat and poultry by-products

Rendered, inedible by-products are often divided into three categories:

1. tallows – the fats extracted during the rendering process.
2. degreased bones for use in the production of gelatin.
3. protein-meals such as meat meal, meat and bone meal, hoof and horn meal and blood meal.

Tallows are used in the manufacture of candles, soaps and cosmetics, paints, printing inks, water repellants and biodiesel production [8, 17]. In addition to gelatin production, degreased bone has been used in the manufacture of glues used in plywood and abrasive paper manufacture and bone flour in the production of fine china [8].

The by-product mass produced from four commercial meat species reared in Australia, relative to the supply of 1000 kg of retail portions is given and expressed as a percentage of the live-weight (Table 1) [18].

The most important and valuable use for the protein rich ABPs is as feed ingredient for livestock, poultry, aquaculture and companion animals. Although use of ABPs in feeds/fertilizers are technologically and economically viable, a growing market also exists for protein hydrolyzates [19], which may be used as flavor enhancers, functional ingredients or to boost the nutritional value of foods considered to have a low protein quality. Additionally, some inedible ABPs are transformed for use in pharmaceuticals and to recover amino acids for a feedstock for higher applications.

Table 1: Product mass for four commercial meat species relative to 1000 kilograms of retail edible product. Data retrieved from [18].

Description	Product	Beef	Sheep	Chicken	Pork
Farm-gate product	Live weight	2375	2255	1712	1618
Intermediate product	Hot standard carcass weight	1307	1060	1216	1229
Wholesale product	Cold carcass weight	1267	1017	1179	1177
Wholesale/retail product	Retail cuts	887	895	967	906
	Edible offal	113	105	33	94
Retail portions (retail cuts + edible offal)		1000	1000	1000	1000
	Hides	214	169	0	0
	Pet food	30	34	17	84
Rendering material	Unprocessed meat bone offal	989	800	593	372
Rendering products	Protein meal products	257	152	154	53
	Tallow	154	156	73	109
	Blood meal	14	14	5	5
Sum (%LW) material to rendering		41.6 %	35.5 %	34.6 %	23.0 %
	Protein meal (%LW)	10.8 %	6.7 %	9.0 %	3.3 %
	Tallow (%LW)	6.5 %	6.9 %	4.3 %	6.7 %
	Blood meal (%LW)	0.6 %	0.6 %	0.3 %	0.3 %
Total product from rendering (%LW)		17.9 %	14.3 %	13.6 %	10.3 %

In most countries, everything produced from the animal, other than the dressed carcass, is considered a by-product. These by-products include hides, skins, hair, feathers, heads, horns, hoofs, feet, toe nails, bones, tendons, glands, muscle and fat tissues, shells, and the contents of the gastro-intestinal tract, blood and internal organs (Table 2). This represents ~30 – 50 % of the live weight of the animal and equates to the production of ~60 million metric tons of ABPs globally every year [20]. These ABPs can be subdivided into two categories; edible and inedible, the allocation of which depends on the country of origin.

Table 2: Edible and inedible animal by-products [12] and estimated proportions as percentage live-weight (%LW) from commercially produced livestock [20] and [10].

Edible	Edible/Inedible	Inedible
Liver	Lungs	Horn
Heart	Spleen	Hooves
Tongue	Small intestine	Teeth
Kidneys	Large intestine	Bile liquid
Brain	Stomach	Hair
Oxtail	Urinary bladder	Wool
	Caecum	Bristles
	Oesophagus	Foetus
	Testicles	
	Uterus	
	Skin/Hide	
	Bone	
	Blood	
	Pancreas	
	Tallow	
	Lips	
	Snouts	
	Ears	

	Beef	Sheep	Chicken	Pork	Fish
Average %LW for human consumption [20]	55	50	70	60	
Average %LW edible and inedible ABPs [20]	45	50	30	40	
Average %LW not for human consumption [10]	49		37	44	57

The distribution of by-product yields varies for both species and different breeds of livestock, and is probably influenced by the age, gender, condition of the animal and slaughterhouse operation [6, 12, 21]. This variation is likely to be greater when the product yields of livestock from different countries are compared, as animals will be reared according to market demand, and disseminated and utilized according to the local cultural and regulatory environment. It is for this reason that factors such as the dressing percentage and retail yield should be determined based on data representative of the supply chain being investigated [18].

2.2 Seafood by-products

Over the past 20 years, global demand has driven a significant increase in aquaculture. The quota system for harvesting wild populations, along with changes in environmental and economic perception has been driving an increase in harvest utilization and like other meat processing industries, is also being pushed to maximize by-product recovery and utilization. Historically, only the most desirable portion of the fish was used, accounting for as little as ~20-30 wt% of the animal, and what remained was disposed of or processed into cheap animal feed [22]. While the quantity used for human consumption may have improved in recent years, fish

and shellfish processing results in more than 60 wt% by-products, including head, skin, trimmings, fins, scale, viscera, and bones [23].

In 2001, total global fishery production (excluding aquatic plants) was reported to exceed 130 million metric tons, with ~38 million tons obtained from aquaculture practices [24], and by 2012 total production had reached 158 million tons, with ~67 million tons from aquaculture [25]. Processing this seafood for consumption leads to the generation of a large volume of fish waste, most of which is used to create fish silage, fishmeal and fish sauce, along with approximately 8 wt% being discarded [26]. In addition to fish processing, a large quantity of wastes from other sources are processed, such as molluscs, crustaceans and cephalopods. A typical fish processing operation involves stunning, grading, removing slime, deheading, washing, scaling, gutting, cutting of fins, meat bone separation and preparing steaks and fillets (Figure 3) [27].

Many other valuable materials can be extracted from fish muscle, skin, oil, bone, viscera, shells of shellfish and crustaceans. These are all rich in bioactive components, such as water-soluble minerals, peptides, collagen, gelatin, enzymes, oligosaccharides and fatty acids [27, 28]. The value of these compounds is likely to increase due to growing evidence of their potential health benefits including antihypertensive, antioxidant, anti-microbial, anti-coagulant, anti-diabetic, anti-cancer, immunostimulatory, calcium-binding, hypocholesteremic properties and appetite suppression [29]. As such, marine by-products should be considered as valuable resources that show promise as functional food ingredients and potential as materials for use in biomedical and nutraceutical applications [30].

Fish meal and oil constitute the bulk of by-products generated from fisheries. In Iceland, these by-products comprise 63 wt% of the fish processed but only accounts for ~14 % of the total revenue of exported seafood products [23]. Like other ABPs, when appropriately processed, inedible portions are often equal to or exceed the value of the primary edible product [22]. However values tend to fluctuate depending on the availability of other animal feeds, particularly during pandemic events or disease outbreaks, such as bovine spongiform encephalopathy (BSE) or avian flu [23]. In the future, an increased understanding of proteins and fish oil chemistry may yield resources of greater value [23].

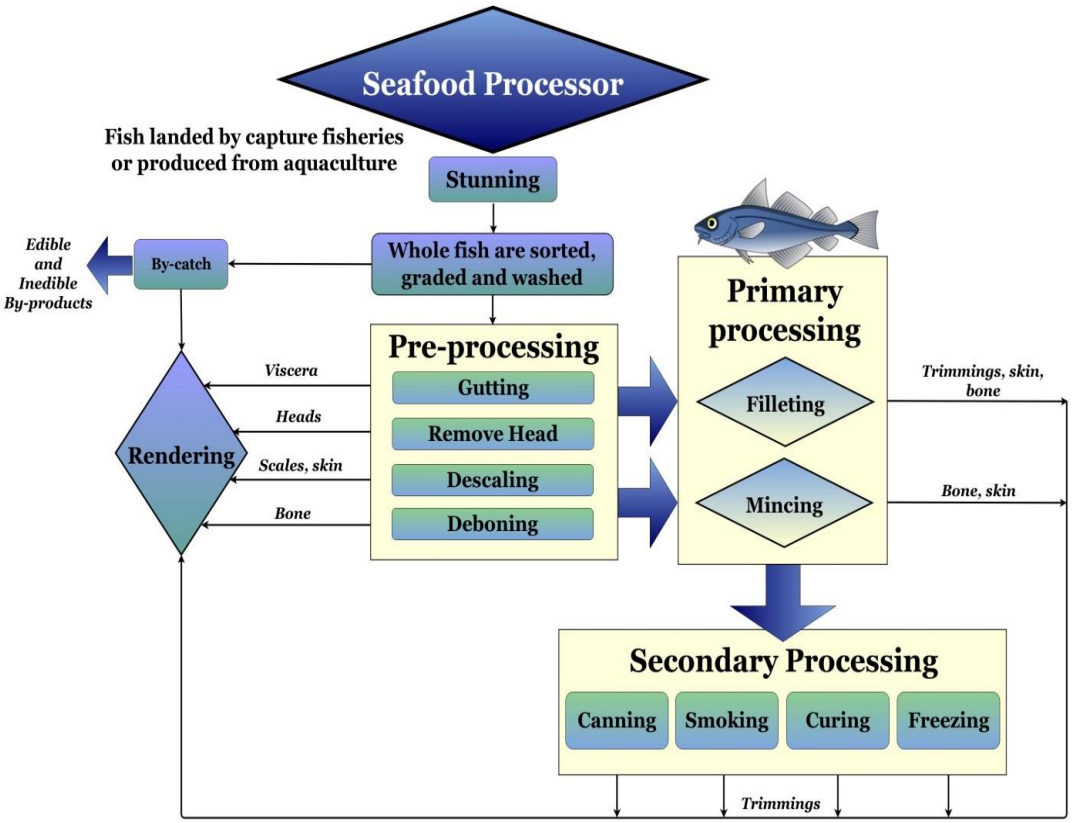

Figure 3: Generalized flow chart of fish processing operations and by-products.

2.3 Animal by-product meal quality

The quality of the final by-product meal is largely dependent on the extent of microbial degradation prior to rendering, the temperature, pressure and rendering time and any product refinement. The value of meals is reduced by microbial or thermal degradation reflected in sensory and aesthetic properties, often contributing a dark color and off-flavors and odors.

The extent of microbial degradation is determined by the type of material collected, its condition and the storage and handling techniques involved prior to rendering. To minimize the extent of degradation, the entire collection and rendering process is generally carried out as quickly as is possible.

Sensory attributes, such as color, texture, flavor, odor and physical qualities including solubility and particle size distribution are indicators of the overall quality of the protein meal [16]. These physical attributes are typically the controlling factors which dictate the overall taste and palatability of the product for use in animal feed supplements, and may also influence final digestibility. As such, poor

sensory qualities lower the value of the meal as it is more difficult to implement as a feed ingredient [31]. For instance, a product which is dark in color is often the result of browning reactions or oxidation between carbohydrates or lipids with proteins during heating [32] and is often accompanied by a burnt caramelized flavor and odor. Malodor is often an indication of poor storage and handling conditions that have resulted in putrefaction of proteins and auto-oxidation of lipids generating offensive volatile compounds [33, 34]. Other physical properties, such as the material's density and the overall uniformity of particle size may also become important depending on their intended final use.

The quantity and quality of the protein is what will decide the final value of the product. Animal protein meals are an important feed ingredient for poultry, fish and pigs in most parts of the world, although some limitations exist to prevent outbreaks of BSE (the US and Canada have banned specified risk material (SRM) from use in animal fodder or fertilizer applications, and no animal proteins can be used as feed ingredients for other farmed animals throughout Europe). Solubility can be a useful indicator of how denatured a protein source has become during rendering and drying. Proteins are generally denatured and undergo aggregation a result of the high temperatures, as a result they tend to become fairly insoluble.

In addition to physical properties, the chemical characteristics of the protein meal will also influence its value and final application. The quantity and bio-availability of both macro- and micro- nutrients is important for tailoring animal feed and are also indicators of quality, for example high calcium and phosphorus content in a meat meal may indicate the presence of bone.

Amino acid composition is also a good indicator of the quality, as heat labile amino acids, such as tyrosine, tryptophan, phenylalanine, histidine, cysteine, lysine and methionine tend to get damaged, oxidized or cross-linked during high temperature processing. Such changes in the primary structure of the proteins directly affects the solubility and nutritional value, and will also change the behavior of the material in higher end applications.

Product quality is generally improved by employing low temperature rendering operations, and is most notable for amino acid digestibility [6]. A study of New Zealand MBMs showed that on average, batch drying between 100 – 130 ^{o}C was

able to produce products of a similar nutritional quality to those produced at 60 – 90 ^{o}C [35]. While low temperature rendering could be used in countries which are free of BSE, such as New Zealand and Australia, it would not be recommended in countries with a known risk of BSE.

Current legislation in Canada, the US and the Europe Union acts to minimize the spread of BSE by prohibiting the use of SRM from cattle (such as the brain and spinal cord) in feeds or fertilizers. To ensure any BSE prions are inactivated in the final products, SRM is first segregated from the edible and inedible raw materials, which are then rendered under the EU guidelines of 133 ^{o}C at 300 kPa, for 20 minutes [36]. The SRM is subsequently treated using a method deemed sufficient to deactivate BSE prions within the material, such as hyperbaric thermal or alkaline hydrolysis [36], or is incinerated for disposal.

Slaughterhouses are the largest producer of animal by-products, and will often have processing operations on-site for some or all of the by-products produced. Blood may be processed on site, preserved, aged or refrigerated and transported by truck to a processing facility, while other materials from slaughterhouses, processors, wholesalers and retailers which cannot be processed on site are sent to rendering plants. The raw materials are usually first collected in large storage bins or silos and may have built in de-watering devices to drain excess water [14] prior to transport to a rendering plant by truck [37]. Most waste material contains a large number of microbes or is easily altered by microbial activity. Given a typical raw material composition (~ 60 % water, 20 % protein and minerals, and 20 % fat [10]), an ideal medium for microbial growth and enzymatic activity exists.

During storage and transportation, oxygen present in the blood and meat tissues is rapidly consumed by aerobic and facultative bacteria, and once consumed the proteins begin to undergo putrefaction as anaerobic bacteria decompose them. The formation of odorous amines, such as indole, skatole, putrescine and cadaverine during putrefaction lowers the quality and value of the final product. Putrefaction can be prevented through the addition of a suitable preservative, such as formic acid, sodium chloride and unslaked lime, 3 % sulfuric acid or potassium metabisulfite in the case of blood [14, 38].

Rendering of carcasses in advanced stages of decomposition is uncommon as both hide removal and carcass cleaning becomes difficult. Furthermore, the high water content increases transportation cost and separation can lead to other disposal problems due to the high levels of organic compounds in the water.

It is generally better to store the raw material as long as possible before size reduction as grinding of the material leads to an increase in free fatty acid (FFA) content. Preservatives such as sodium chlorite or dilute acids (reducing the pH to 3.5-4.0) can be added to delay the increase in FFAs but in general it is best practice to carry out rendering as soon after size reduction as is practical [14].

3 Characteristics of common protein by-products

3.1 Blood meal

Collectible blood makes up approximate 4-6 % of an animal's live weight. It is protein rich (~17 wt%) with a good balance of amino acids, is rich in lysine and is also high in iron [9]. During collection, whole blood begins to coagulate as fibrinogen proteins form insoluble complexes with free calcium ions. If necessary, coagulation can be inhibited through the addition of ethylenediaminetetraacetic acid disodium salt (EDTA), oxalic acid or anhydrous sodium citrate [39, 40]. However, it is not common practice as blood is typically coagulated to aid dewatering. Blood is often aged prior to drying to induce coagulation at lower temperature thereby minimizing thermal degradation [41], although low temperature coagulation can also be achieved by adding free calcium ions in the form of 1 % calcium chloride [42].

When stored in a dry condition, blood meal is a microbiologically stable material, relying on its low moisture content and water activity for preservation [40]. Blood can be dried in a number of ways to obtain a stable, highly nutritive product, free of contaminants, such as wool or hair. Whole blood is strained prior to dewatering to remove debris, followed by coagulation using direct steam injection (~90 ^{o}C) or being passed through a heated pipe [43, 44]. The coagulant is separated using a centrifuge decanter to remove up to 50 %, followed by thermal drying. Common drying operations include direct batch drying, batch coagulation followed by batch

drying, continuous coagulation prior to drying, continuous dryers, spray dryers or other novel systems [14].

Drying conditions have a significant impact on crude protein content, protein quality and bioavailability of amino acids. Ring drying typically produces a better quality product than a flash dryer as it uses warm air rather than a heated metal surface. Because direct contact with a hot surface is avoided, heat labile amino acids (e.g lysine) are not destroyed [43]. Typical commercial blood meals have a moisture content of 5-8 wt% and a water activity of 0.3-0.45 [45], typical characteristics of thermally dried blood meals are given (Table 3).

The amino acid composition of blood proteins vary between species. Notably, poultry blood has a significantly higher quantity of isoleucine compared to bovine or porcine blood; similarly, porcine blood has a significantly lower quantity of lysine [46]. The differences in amino acid composition between species has been observed in the meals produced from spray drying, where avian blood meals have higher arginine, cysteine, isoleucine and tyrosine content compared with porcine and bovine blood meals [47]. Variation in amino acid content not only influences the feed application, but also higher end applications, such as the manufacture of thermoplastics.

Table 3: Typical product characteristics and proximate analysis of blood meal [48-58], amino acid composition [57, 59, 60] and mineral content [48, 51, 57, 61].

Characteristic	Value
Dry material %	85.2 - 98.5
Crude protein %	80.2 - 100.5
Ether extract %	0.2 – 1.5
Crude fiber %	0 - 6.2
Gross energy kcal/kg	4844 – 5660
Ash	1 - 8.6 %
Moisture content	5 - 8 %
Water activity	0.30 - 0.45
Particle size	85 - 200 µm
Color	Dark, red-brown
CIE L*a*b* value	L* = 25.2
	a* = 14.4
	b* = -2.9

Amino acids		**Mineral content**	
Alanine	7.82 %CP	Ca	0.30 – 0.40 %
Arginine	4.38-4.91 %CP	P	0.23-0.30 %
Asparagine	4.67 %CP	Mg	0.03-0.24 %
Aspartic acid	6.20 %CP	K	0.09-0.33 %
Cystine	0.11-1.92 %CP	Na	0.31-0.40 %
Glutamine	4.32 %CP	Cl	0.26-0.33 %
Glutamic acid	6.38 %CP	S	0.32-0.77 %
Glycine	3.86-4.95 %CP	Cu	9.7-10.8 mg/kg
Histidine	5.57-6.61 %CP	Fe	2453-4110 mg/kg
Isoleucine	1.18-2.54 %CP	Mn	5.2-9 mg/kg
Leucine	11.4-14.8 %CP	Se	0.77 mg/kg
Lysine	8.25-10.7 %CP	Zn	22-33 mg/kg
Methionine	0.01-1.17 %CP	Mo	0.6 mg/kg
Phenylalanine	5.83-8.20 %CP		
Proline	6.29 %CP		
Serine	4.49 %CP		
Threonine	3.95—7.06 %CP		
Tryptophan	1.30-3.89 %CP		
Tyrosine	2.86 %CP		
Valine	8.21-10.45 %CP		

3.2 Meat by-product meals

Meat meal and meat and bone meal are both produced by rendering the inedible or unsold by-products from slaughterhouse operations. The majority of the raw materials present in MM and MBM come from cattle, swine, and poultry, with most of the literature available on MBM containing material sourced from more than one species. Meat meals often include the addition of dead stock (animals which died before slaughter) in some cases representing greater than 10% of the total raw material rendered [62]. It may also include expired meats from retailers and materials recovered from dissolved air floatation used for treating rendering effluent.

Until recently, a policy established by the National Renderer's Association prevented ovine material (sheep) from being used in MBMs in the United States and Canada, and has been withdrawn [63]. It is unlikely the exclusion or inclusion of sheep in MBM has any more effect on the variation of the product composition than the rendering processes itself.

The average MBM is dark red-brown in color, however, it is known to range from tan to dark brown in color, with an average CIE L*a*b* value indicated in Table 5. It is generally sold based on the quantity of crude protein, which although it is typically high, can be rather variable. MBM has a high mineral content (higher than MM) and is relatively low in fat [62]. Like most other thermally denatured proteins, those present in MBM have very low solubility in water (~5.4 % of the true protein, which is ~55 % of the dry mass). MBM is a heterogeneous mixture of particles; those derived from bone are high in ash, while those from soft tissues are high in protein. Lower temperature processing typically leads to greater amino acid bioavailability, but the phenomenon apparently is not due to improved protein solubility, as any correlation between processing parameters, such as 'peak cooking temperature' and protein solubility has not yet been found [62].

As a feedstuff, MM and MBM have been thoroughly characterized including the proximate composition, gross energy and amino acid profiles, which are more useful for designing non-feed applications. A compilation of typical values for general blends of MM and MBM meal are shown in Table 4 and Table 5.

Meat and bone meal can be distinguished from MM by its higher mineral content, containing much higher levels of phosphorus and calcium. More specific variations exist, indicative of the raw materials used, for example "poultry meat meal", "porcine meat and bone meal", or the raw materials composition, for example "meat meal" or "meat meal with blood after solvent extraction". In addition, mixed species meat and bone meals can be sold. The comprehensive catalogue of data from the U.S. and Canada has been published by the National Academy of Sciences and contains average values obtained for proximate analysis of these more specific animal by-products, along with nutritional information. This includes digestibility, mineral content and amino acid composition [48]. More regular, but less comprehensive updates are given as part of the NRC nutritional recommendations for livestock [57, 64].

Table 4: Typically reported range of product characteristics and proximate analysis of meat and bone meals [48, 51, 53, 54, 57, 58, 62], amino acid composition [57, 60] and mineral content reported by [48, 51, 57].

Characteristic	Typical values		
Dry material %	92.9 – 100		
Crude protein %	49.5 – 59.4		
Ether extract %	8.9 – 16.0		
Crude fiber %	1 – 5.13		
Ash	20.7 – 52.9 %		
Moisture content	1.9 – 5.7 %		
pH	5.89 – 7.19		
Protein solubility	2.2 – 7.2 %		
Particle size	25.6 – 800 µm		
Color	Light tan brown to dark brown		
CIE L*a*b* value	L* = 51.2		
	a* = 22.1		
	b* = 38.9		
Amino acids		**Mineral content**	
Alanine	9.19 %CP	Ca	10.60 – 13.50 %
Arginine	6.98 – 7.06 %CP	P	4.73 – 6.50 %
Aspartic acid	4.25 %CP	Mg	0.24 – 1.20 %
Cystine	0.94 – 1.01 %CP	K	1.02 – 1.56 %
Glutamine	5.40 %CP	Na	0.71 – 0.78 %
Glutamic acid	7.79 %CP	Cl	0.44 – 0.80 %
Glycine	16.67 %CP	S	0.39 %
Histidine	1.89 – 2.29 %CP	Cu	1.5 - 10 mg/kg
Isoleucine	2.76 – 3.69 %CP	Fe	500 - 602 mg/kg
Leucine	6.13 – 6.85 %CP	Mn	12.3 - 22 mg/kg
Lysine	5.18 – 6.08 %CP	Zn	94 mg/kg
Methionine	1.40 – 2.12 %CP	Mo	2.7 mg/kg
Phenylalanine	3.36 – 3.56 %CP		
Proline	11.3 %CP		
Serine	4.00 %CP		
Threonine	3.27 – 4.65 %CP		
Tryptophan	0.58 – 0.75 %CP		
Tyrosine	2.79 %CP		
Valine	4.20 – 4.29 %CP		

Table 5: Typically reported range of product characteristics and proximate analysis of meat meal [48, 51, 54, 57, 65, 66], amino acid composition [51, 57] and mineral content reported by [48, 51, 57, 66].

Characteristic	Typical values		
Dry material %	90.2 – 100		
Crude protein %	51.7 – 58.4		
Ether extract %	9.4 – 12.7		
Crude fiber %	2 – 2.7		
Gross energy kcal/kg	4294		
Ash	18.4 – 26.4 %		
Moisture content	5.4 %		
Color	Dark, red-brown		
Amino acids		**Mineral content**	
Alanine	8.11 %CP	Ca	8.49 – 9.01 %
Arginine	7.06 – 7.96 %CP	P	4.18 – 4.44 %
Aspartic acid	7.96 %CP	Mg	0.27 – 0.29 %
Cystine	0.93 – 1.12 %CP	K	0.49 – 0.58 %
Glutamic acid	12.46 %CP	Na	0.78 – 1.78 %
Glycine	16.38 %CP	Cl	0.44 – 1.39 %
Histidine	2.06 – 2.96 %CP	S	0.48 – 0.53 %
Isoleucine	2.81 – 2.96 %CP	Cu	9.7 - 21 mg/kg
Leucine	6.24 – 6.31 %CP	Fe	400 - 701 mg/kg
Lysine	5.38 – 5.46 %CP	Mn	9.5 - 26 mg/kg
Methionine	1.43 – 1.72 %CP	Se	0.45 mg/kg
Phenylalanine	3.43 – 3.57 %CP	Zn	114 - 190 mg/kg
Proline	10.45 %CP	Mo	2.4 mg/kg
Serine	4.05 %CP		
Threonine	3.12 – 3.38 %CP		
Tryptophan	0.67 – 0.93 %CP		
Tyrosine	2.34 %CP		
Valine	4.06 – 4.44 %CP		

As indicated in the tables, large variation can be expected for some properties of MM and MBM as they tend to vary in composition between different rendering facilities. In addition, variation of product characteristics also varies significantly within a rendering plant, indicating that obtaining MBM from the same plant does not guarantee a consistent quality [35]. To ensure better consistency, some renderers blend MBM from different sources, resulting in a product with less variation in ash and protein content [62].

Although, MBM has been recommended for use in animal feeds as a source of protein due to its high availability of essential amino acids, minerals and vitamin B12, MBM and other rendered protein meals have potential for use in other applications including as a fuel, phosphorus fertilizer, as a source of amino acids for chemical synthesis and for the production of bio-based plastics.

3.3 Poultry by-product meals

By-products of poultry processing include feathers, heads and feet, viscera and meat trimmings. Unlike the meat components, feathers are processed separately to produce feather meal. Keratin is the main protein in feathers and is virtually insoluble. To improve digestibility feathers are rendered using a batch or continuous hydrolyzer. The material first passes through a spreader to cut up any large components such as heads or feet. Hydrolysis is carried out under pressure (30-50 psi) for ~45-60 minutes to break peptide and disulfide bonds, as well as hydrogen bonding interactions between non-adjacent amino acids. After hydrolysis the material is dried to yield feather meal which can be ground to finer particle sizes, and is an excellent source of cysteine [10]. Hoof, horn and hair meal are produced via a similar process. The typical composition of hydrolyzed feather meal is given in Table 6.

Another means of improving the digestibility of feather meal includes inoculation with a feather degrading bacterium (*Bacillus licheniformis*), which excretes a strong keratinase enzyme capable of hydrolyzing collagen, elastin and feather keratin [9].

Poultry by-product meal is produced by rendering necks, feet, undeveloped eggs and viscera of poultry, excluding feathers. In contrast, poultry meal contains only skin, bone and trimmings and excludes feathers, heads, feet and entrails. As a result, poultry meal tends to have a lower fat and ash content than poultry by-product meal, but due to the large amount of variability within either type of meal it is unlikely that there is any real difference in the proximate composition despite the differences in the raw materials rendered. Further to this, there appears to be no difference in the digestibility of the protein or free amino acids present in the two meals [67]. The composition of poultry by-product meal is given in Table 7.

Table 6: Typically reported range of product characteristics and proximate analysis of hydrolyzed feather meal [51, 57, 58], amino acid composition [57, 60] and mineral content reported by [51, 57].

Characteristic	Typical values		
Dry material %	91.5 – 93.3		
Crude protein %	81.2 – 92		
Ether extract %	6.2 – 7.0		
Crude fiber %	1 – 1.1		
Ash	3 – 3.5 %		
Color	Off-white to brown		
Amino acids		**Mineral content**	
Alanine	5.09 %CP	Ca	0.33 – 0.48 %
Arginine	6.93 – 6.99 %CP	P	0.45 - 0.50 %
Asparagine	2.03 %CP	Mg	0.22 %
Aspartic acid	3.56 %CP	K	0.10 - 0.33 %
Cystine	5.07 – 5.09 %CP	Na	0.34 %
Glutamine	3.48 %CP	Cl	0.20 - 0.26 %
Glutamic acid	5.86 %CP	S	1.39 – 1.20 %
Glycine	10.90 %CP	Cu	10 mg/kg
Histidine	1.07 – 1.15 %CP	Fe	76 mg/kg
Isoleucine	4.62 – 4.85 %CP	Mn	10 mg/kg
Leucine	8.22- 8.51 %CP	Se	0.69 mg/kg
Lysine	2.57 – 2.63 %CP	Zn	90 - 111 mg/kg
Methionine	0.75 – 0.91 %CP	Mo	0.8 mg/kg
Phenylalanine	4.81 – 4.93 %CP		
Proline	14.37 %CP		
Serine	10.72 %CP		
Threonine	4.73 – 4.84 %CP		
Tryptophan	0.73 – 0.97 %CP		
Tyrosine	2.48 %CP		
Valine	7.02 – 7.52 %CP		

Table 7: Typically reported range of product characteristics and proximate analysis of poultry by-product meal [51, 54, 58, 68], amino acid composition [60, 69] and mineral content reported by [51, 57].

Characteristic	Typical values		
Dry material %	92.5 – 93.0		
Crude protein %	51.7 – 63		
Ether extract %	12.5 – 29.5		
Crude fiber %	1.2 – 2.5		
Ash	10.5 – 17 %		
Color	Tan to light brown		
Amino acids		**Mineral content**	
Alanine	7.64 %CP	Ca	0.33 – 0.48 %
Arginine	6.77 – 7.20 %CP	P	0.45 - 0.50 %
Asparagine	4.25 %CP	Mg	0.22 %
Aspartic acid	6.38 %CP	K	0.10 - 0.33 %
Cystine	1.63 %CP	Na	0.34 %
Glutamine	5.51 %CP	Cl	0.20 - 0.26 %
Glutamic acid	7.60 %CP	S	1.39 – 1.20 %
Glycine	14.65 %CP	Cu	10 mg/kg
Histidine	2.02 – 2.12 %CP	Fe	76 mg/kg
Isoleucine	3.61 – 3.64 %CP	Mn	10 mg/kg
Leucine	6.55 – 6.93 %CP	Se	0.69 mg/kg
Lysine	5.35 – 6.27 %CP	Zn	90 - 111 mg/kg
Methionine	2.03 – 2.16 %CP	Mo	0.8 mg/kg
Phenylalanine	3.67 – 3.74 %CP		
Proline	10.45 %CP		
Serine	4.15 %CP		
Threonine	3.55 – 4.43 %CP		
Tryptophan	0.76 – 0.84 %CP		
Tyrosine	2.86 %CP		
Valine	4.49 – 4.81 %CP		

3.4 Seafood by-product meals

Fish, bones and offal from processed fish are wet or dry rendered to produce a brown protein powder known as fish meal. Fish meal can be made from various mixed species, usually from the by-catch obtained during harvesting, but is also made from the by-products of dressing specific species, such as menhaden, anchovy and to a lesser extent, herring [10]. During a dry rendering process, fish oil generated during cooking is not removed. The oil is removed during wet rendering operations, and is the most common method used. Wet rendering is applied to fish which have a high oil content, as removal of the oil is necessary for producing a shelf-stable product [43]. After cooking and oil removal, the remaining material is hydraulically pressed to remove any liquor and the solids (presscake) are dried and ground to produce fish meal. The stickwater can be concentrated and added back to the presscake to form wholemeal, or can be sold as a separate products called fish solubles [43]. The typical composition of menhaden fish meal and shrimp meal are given in Table 8 and Table 9.

Table 8: Typically reported range of product characteristics and proximate analysis of menhaden fish meal [57, 65, 68, 70], amino acid composition [57, 70, 71] and mineral content reported by [57, 70].

Characteristic	Typical values		
Dry material %	91.2 – 92.0		
Crude protein %	59.0 – 68.5		
Ether extract %	9.1 – 10.4		
Crude fiber %	0.9		
Gross energy kcal/kg	3025 – 4440		
Ash	19.7 – 21.4		
Moisture content	4.8		
Color	Brown		
Amino acids		**Mineral content**	
Arginine	3.43 – 6.04 %CP	Ca	4.87 – 5.34 %
Cystine	0.58 – 0.97 %CP	P	2.93 – 3.05 %
Glycine	7.35 %CP	Mg	0.20 %
Histidine	2.45 – 2.83 %CP	K	0.74 %
Isoleucine	3.67 – 4.09 %CP	Na	0.68 %
Leucine	7.02 -7.22 %CP	Cl	0.80 %
Lysine	7.51 – 7.65 %CP	S	1.16 %
Methionine	2.61 – 2.81 %CP	Cu	7 mg/kg
Phenylalanine	3.59 – 3.99 %CP	Fe	562 mg/kg
Serine	4.08 %CP	Mn	32 mg/kg
Threonine	3.92 – 4.20 %CP	Se	2.26 mg/kg
Tryptophan	0.82 – 1.05 %CP	Zn	112 mg/kg
Tyrosine	1.87 – 2.94 %CP	Mo	1.8 mg/kg
Valine	4.57 – 4.82 %CP		

Table 9: Typically reported range of product characteristics and proximate analysis of shrimp meal [51, 72-75], amino acid composition and mineral content reported by [75].

Characteristic	Typical values		
Dry material %	89.6 – 99.7		
Crude protein %	22.8 – 50		
Ether extract %	2.5 – 7.5		
Crude fiber %	3.6 – 20		
Ash	14 – 56		
Color	Light tan brown		
Amino acids		**Mineral content**	
Alanine	4.47 %CP	Ca	15.6 %
Arginine	3.82 %CP	P	2.0 %
Aspartic acid	8.11 %CP	Mg	0.83 %
Cystine	0.96 %CP	K	0.23 %
Glutamic acid	10.18 %CP	Na	0.31 %
Glycine	4.56 %CP		
Histidine	1.58 %CP		
Isoleucine	3.58 %CP		
Leucine	5.00 %CP		
Lysine	3.86 %CP		
Methionine	1.75 %CP		
Phenylalanine	7.15 %CP		
Proline	3.25 %CP		
Serine	3.42 %CP		
Threonine	3.42 %CP		
Tryptophan	1.05 %CP		
Tyrosine	4.43 %CP		
Valine	4.34 %CP		

The meals made from oily fish, such as herring, tend to have much higher fat content (~ 8.5 %) [49] compared to other fish species, such as anchovy or sardine [55, 57]. Fish meals can be used in all types of animal feeds, usually where the fishy odor and flavors are beneficial, such as pet food [10]. Unlike other by-product meals, fish meals appear to have significantly higher calcium, phosphorus and selenium content, making it an ideal nitrogen and phosphorus rich fertilizer for application to selenium deficient soils, such as those found in New Zealand.

4 Innovations in by-product treatment and uses

Utilization of animal by-product meals as feed ingredients has become increasingly restricted, therefore growing attention has been focused on developing novel, non-feed applications which have a substantially higher economic value. Higher value applications of ABPs generally require the product to already be fit for, or made fit for, human consumption or medical use. For example, blood proteins collected under sterile conditions are typically employed as binders, natural color enhancers, emulsifiers, fat replacers and meat curing agents, and have also found use as egg replacers, protein and iron supplements and as a source of bioactive compounds [76].

The degree to which ABPs can be utilized is often limited not only by the customs, religions and regulatory requirements of the region they are processed in, but also by the biological and physicochemical properties of the materials. This is particularly true for red blood cells and whole blood, which despite their nutritional value, are generally not used as food ingredients due to their dark red color and the metallic flavor imparted by the high iron content [39]. As a result, the use of blood is generally restricted to products where the black color is acceptable, although the heme pigment and its chelated iron can be removed through extraction with acidified acetone or via bleaching with hydrogen peroxide to remove the color [77]. An alternative is to use plasma, which makes up 65 – 70 % of blood by volume and contains 7.9 % protein, (albumins, 3.3%, immunoglobulins and globulins, 4.2%, and fibrinogen, 0.4%), and is more commonly used in food applications due to its neutral flavor and color [39].

Blood components, which are currently isolated for medical uses, include fibrinogen, fibrinolysin, serotonin, immunoglobulins and plasminogen. Purified

bovine serum albumin is used during testing for the Rh factor in human beings, as a stabilizer for vaccines and in antibiotic sensitivity tests. Bovine thrombin is used to promote coagulation of blood and hold skin grafts in place and porcine plasmin enzyme is used to digest fibrin in the blood clots of heart attack patients [78].

Innovations have been made over the years to alter the apparent quality of rendered products and include various bleaching techniques, addition of antioxidants and adulterants. Although some of these treatments enhance the quality of the product, adulterants interfere with chemical detection methods used to classify the products, placing them higher on the quality and price scale than they should be.

Potential non-feed uses of ABP meals exploit their high protein concentration. All animal by-product meals have potential as a source of biomass for biofuel production. Poultry meal, feather meal and MBM have been used as alternative nitrogen sources to replace yeast extract during the fermentation of potato starch to produce bio-ethanol [79]. Feather meal has recently been shown to be a good source of fat for the production of biodiesel while subsequently improving the protein concentration of the feather meal [80].

The components of MBM could be separated to utilize the protein from particles derived from soft tissues or exploited for the high mineral concentration of the bone particles. Like other nitrogen rich organic products, MBM has demonstrated an ability to control plant pathogens [81], its protein concentrated to create an adhesive [82] and as the feedstock for the production of a plastic material designed to be a pet chew toy [83]. These and other applications have potential commercial value, but with the exception of fuel uses, most have only been implemented on a laboratory or demonstration scale [84].

Current high value applications of blood products include preparation of blood agar, providing a source of hydrolyzates for microbial use, producing commercial porphyrin derivatives and enzymes used in medical applications. Recent research has also shown promise for the recovery and extraction of bioactive compounds from hydrolyzed blood proteins. Some of the peptides studied have shown medical benefits including inhibition of the angiotensin I-converting enzyme (subsequently minimizing the formation of compounds which cause constriction of blood vessels raising blood pressure and creating an antihypertensive effect), antioxidant activity,

antimicrobial properties, antigenotoxic effects, mineral-binding ability and opioid activity [78, 85].

There are still challenges that need to be overcome in order to adopt animal by-product meals as a feedstock for bio-based products. Many potential applications for blood meal and MBM are ruled out by the potential for prion contamination of the material [62]. Most of the higher end applications require sterile conditions for the collection of the raw material and often, subsequent thermal or chemical treatment to ensure its integrity. In cases where it is impractical to collect and generate the protein meal under sterile conditions, or where it is considered an SRM, other novel applications can be created. Recent examples include extrudable thermoplastic materials produced from blood meal and its decolored derivative, compression molding of defatted feather meal and whey blends [86] and the incorporation of hydrolyzate from SRM as a curing agent to create a thermosetting epoxy resin [87]. Protein hydrolyzates have also been shown to have flocculant activity, such as those from enzyme hydrolyzed MBM [88, 89]. In the future, amino acids derived from animal protein meals may even be used to synthesize commodity chemicals, such as acetonitrile [90].

While there is a significant volume of literature available regarding the physical, chemical and nutritive characteristics of ABP meals, including licensed software AminoDat®4.0, containing data compiled over decades by the U.S. National Research Council, very little data exists which is relevant to the material properties and handling of such products. Furthermore, there is limited industry-wide information on the sources of raw material used to produce animal by-product meals, the rendering treatment used, or geographic availability [62] making economic analysis for the pilot scale and start-up phases of novel technologies difficult.

This chapter has shown that differences in the sources of raw material, how they are handled and the rendering processes used result in significant variation in the physical, chemical and nutritive properties of the animal by-product meals produced. As such, innovative technologies designed to utilize these protein meals will have to account for this, particularly if the technology is taken to the global stage.

List of abbreviations

ABP Animal by-product

BSE Bovine spongiform encephalopathy

EDTA Ethylenediaminetetraacetic acid disodium salt

FFA Free fatty acid

LW Live weight

MBM Meat and bone meal

MM Meat meal

3 References

1. Horrigan, L., Lawrence, R.S., Walker, P. (2002). How Sustainable Agriculture Can Address the Environmental and Human Health Harms of Industrial Agriculture. Environmental Health Perspectives, 110(5): 445-456.
2. Thornton, P.K. (2010). Livestock Production: Recent Trends, Future Prospects. Philosophical Transactions of the Royal Society of London B: Biological Sciences, 365(1554): 2853-2867.
3. Hazell, P., Wood, S. (2008). Drivers of Change in Global Agriculture. Philosophical Transactions of the Royal Society of London B: Biological Sciences, 363(1491): 495-515.
4. Pretty, J. (2008). Agricultural Sustainability: Concepts, Principles and Evidence. Philosophical Transactions of the Royal Society of London B: Biological Sciences, 363(1491): 447-465.
5. Bocquier, F., González-García, E. (2010). Sustainability of Ruminant Agriculture in the New Context: Feeding Strategies and Features of Animal Adaptability into the Necessary Holistic Approach. Animal, 4 (Special Issue 07): 1258-1273.
6. Ockerman, H.W., Hansen, C.L. (2000). Introduction and History of Processing Animal By-products, in Animal By-Product Processing and Utilization. Ockerman, H.W. and Hansen, C.L., Editors. CRC Press: Florida, U.S.. p. 1-22.
7. Swan, J.E. (1999). Animal By-Product Processing, in Wiley Encyclopedia of Food Science and Technology. Francis, F.J., Editor. John Wiley & Sons Inc.: New York, U.S.. p. 35-43.
8. Fallows, S.J., Wheelock, J.V. (1982). By-Products from the U.K. Food System 2. The Meat Industry. Conservation & Recycling, 5(4): 173-182.
9. Jayathilakan, K., Sultana, K., Radhakrishna K., Bawa, A.S. (2012). Utilization of By-Products and Waste Materials from Meat, Poultry and Fish Processing Industries: A Review. Journal of Food Science and Technology, 49(3): 278-293.
10. Meeker, D.L., Hamilton, C.R. (2006). An Overview of the Rendering Industry, in Essential Rendering: All About The Animal By-Products Industry. Meeker, D.L., Editor. National Renderers Association: Virginia, U.S,. p. 1-16.

11. Bisplinghoff, F.D. (2006). A History of North American Rendering, in Essential Rendering: All About The Animal By-Products Industry. Meeker, D.L., Editor. National Renderers Association: Virginia, U.S.. p. 17-30.
12. Scaria, K.J. (1989). Economics of Animal By-Products Utilization. Issue 77. Food and Agriculture Organization of the United Nations. Rome, Italy. p. 1-68.
13. Anderson, D.P. (2006). Rendering Operations, in Essential Rendering: All About The Animal By-Products Industry. Meeker, D.L., Editor. National Renderers Association: Virginia, U.S.. p. 31-52.
14. Fernando, T. (1992). Blood Meal, Meat and Bone Meal and Tallow, in Inedible Meat By-Products, Pearson, A.M. and Dutson, T.R., Editors. Springer Netherlands. p. 81-112.
15. Bennett, R.P. (1927). Dry rendering of animal products. Oil and Fat Industries., 4: 275-83.
16. Auvermann, B., Kalbasi, A., Ahmed, A. (2004). Rendering, in Carcass Disposal: A Comprehensive Review. National Agricultural Biosecurity Center: Kansas State University, Kansas, U.S.. p. 1-76.
17. Bhatti, H.N., Hanif, M.A., Qasim, M., ur Rehman, A. (2008). Biodiesel Production from Waste Tallow. Fuel, 87(13–14): 2961-2966.
18. Wiedemann, S., Yan, M. (2014). Livestock Meat Processing: Inventory Data and Methods for Handling Co-production for Major Livestock Species and Meat Products, in Ninth International Life Cycle Assessment of Foods Conference: San Francisco, U.S..
19. Bhaskar, N., Modi, V.K., Govindaraju, K., Radha, C., Lalitha, R.G. (2007). Utilization of Meat Industry By-Products: Protein Hydrolysate from Sheep Visceral Mass. Bioresource Technology, 98(2): 388-394.
20. Leoci, R. (2014). Animal By-Products (ABPs): Origins, Uses and European Regulations. Universitas Studiorum: Mantova, Italy. p. 15-21.
21. Ockerman, H.W., Basu, L. (2014). By-Products: Edible, for Human Consumption, in Encyclopedia of Meat Sciences. Devine, C. and Dikeman, M., Editors. Elsevier: London, U.K.. p. 104-111.
22. Pigott, G.M. (2007). Fish and Shellfish Products, in Kirk-Othmer Encyclopedia of Chemical Technology. John Wiley & Sons, Inc: New York, U.S.. p. 1-44.
23. Kristbergsson, K., Arason, S. (2007). Utilization of By-Products in the Fish Industry, in Utilization of By-Products and Treatment of Waste in the Food Industry. Oreopoulou, V. and Russ, W., Editors. Springer: New York, U.S.. p. 233-258.
24. Vannuccini, S. (2004). Overview of Fish Production, Utilization, Consumption and Trade: Based on 2001 Data: Rome, Italy.
25. Food and Agriculture Organization (2014). 2012/FAO Yearbook.. Fishery and Aquaculture Statistics. United Nations: Rome, Italy.
26. Kelleher, K. (2005). Discards in the World's Marine Fisheries: An Update. FAO Fisheries Technical Paper. Vol. 470. Food and Agriculture Organization of the United Nations: Rome, Italy.
27. Ghaly, A.E., Ramakrishnan, V.V., Brooks, M.S., Budge, S.M., Dave, D. (2013). Fish Processing Wastes as a Potential Source of Proteins, Amino

Acids and Oils: A Critical Review. Journal of Microbial and Biochemical Technology, 5: 107-129.

28. Kim, S., Mendis, E. (2006). Bioactive Compounds from Marine Processing By-Products: A Review. Food Research International, 39(4): 383-393.
29. Harnedy, P.A., FitzGerald, R.J. (2012). Bioactive Peptides from Marine Processing Waste and Shellfish: A Review. Journal of Functional Foods, 4(1): 6-24.
30. Senevirathne, M., Kim, S. (2012). Utilization of Seafood Processing By-Products: Medicinal Applications, in Advances in Food and Nutrition Research. Vol 65. Se-Kwon, K., Editor. Academic Press: San Diego, U.S. p. 495-512.
31. Baumont, R., Prache, S. Meuret, M., Morand-Fehr, P. (2000). How Forage Characteristics Influence Behaviour and Intake in Small Ruminants: A Review. Livestock Production Science, 64(1): 15-28.
32. Papadopoulos, M.C. (1989). Effect of Processing on High-Protein Feedstuffs: A Review. Biological Wastes, 29(2): 123-138.
33. den Brinker, C.A., Rayner, C.J., Kerr, M.G. Bryden, W.L. (2003). Biogenic Amines in Australian Animal By-Product Meals. Australian Journal of Experimental Agriculture, 43(2): 113-119.
34. Verbeek, C.R., Hicks, T., Langdon, A. (2012). Odorous Compounds in Bioplastics Derived from Bloodmeal. Journal of the American Oil Chemists' Society, 89(3): 529-540.
35. Hendriks, W., Cottam, Y.H., Morel, P.C.H., Thomas, D.V. (2004). Source of the Variation in Meat and Bone Meal Nutritional Quality. Asian-Australasian Journal of Animal Sciences, 17(1): 94-101.
36. Taylor, D.M., Woodgate, S.L. (2003). Rendering practices and inactivation of transmissible spongiform encephalopathy agents. Revue scientifique et technique (International Office of Epizootics), 22(1): 297-310.
37. Goldstrand, R.E. (1992). An Overview of Inedible Meat, Poultry and Fishery By-Products, in Inedible Meat By-Products. Pearson, A.M. and Dutson, T.R., Editors. Springer: Netherlands. p. 1-17.
38. Hertrampf, J., Piedad-Pascual, F. (2000). Blood Products, in Handbook on Ingredients for Aquaculture Feeds. Springer: Netherlands. p. 69-79.
39. Duarte, R.T., Carvalho Simões, M.C., Sgarbieri, V.C. (1999). Bovine Blood Components: Fractionation, Composition and Nutritive Value. Journal of Agricultural and Food Chemistry 47(1): 231-236.
40. Ockerman, H.W. Hansen, C.L. (1988). Animal By-Product Processing. Ellis Horwood: Chinchester, England.
41. van Oostrom, A.J. (2001). Waste Management, in Meat Science and Applications. Hui, Y.H., Nip, W., Rogers, R.W., Young, O.A. Editors. Marcel Dekker: New York, U.S.. p. 635-672.
42. MIRINZ (1985). Bulletin No. 10: Maximizing Yields from Conventional Blood Processing - Guidelines to Improve Production: Hamilton, New Zealand.
43. Bimbo, A.P. (2005). Rendering, in Bailey's Industrial Oil and Fat Products. John Wiley & Sons, Inc: New York, U.S..

44. Macy, C.D., Butler, H.B. (1969). Process and Apparatus for Coagulating and Drying Blood, Office, U.S.Patent 3431118. Assignee. Macy, L.G. and Hormel & Co Geo A.

45. Roberts, T.A., Cordier, J.L., Gram, L., Tompkin, R.B., Pitt, J.I., Gorris, L.G.M., Swanson, K.M.J. (2005). Feeds and Pet Foods, in Micro-Organisms in Foods 6. Roberts, T.A., Cordier, J.L., Gram, L., Tompkin, R.B., Pitt, J.I., Gorris, L.G.M., Swanson, K.M.J. Editors. Springer: New York, U.S.. p. 250-276.

46. Márquez, E., Bracho, M., Archile, A., Rangel, L., Benítez, B. (2005). Proteins, Isoleucine, Lysine and Methionine Content of Bovine, Porcine and Poultry Blood and Their Fractions. Food Chemistry, 93(3): 503-505.

47. Kats, L.J., Nelssen, J.L., Tokach, M.D., Goodband, R.D., Weeden, T.L., Dritz, S.S., Hansen, J.A., Friesen, K. G. (1994). The Effects of Spray-dried Blood Meal on Growth Performance of the Early-weaned Pig. Journal of Animal Science, 72(11): 2860-9.

48. National Research Council and Canadian Department of Agriculture (1971). Atlas of Nutritional Data on United States and Canadian Feeds. National Academy of Sciences: Washington, D.C., U.S.

49. Martínez-Llorens, S., Vidal, A.T., Moñino, A.V., Gómez Ader, J., Torres, M.P. Cerdá, M.J. (2008). Blood and Haemoglobin Meal as Protein Sources in Diets for Gilthead Sea Bream (*Sparus aurata*): Effects on Growth, Nutritive Efficiency and Fillet Sensory Differences. Aquaculture Research, 39(10): 1028-1037.

50. Haughey, D.P. (1976). Market Potential and Processing of Blood Products: Some Overseas Observations. MIRINZ: Hamilton, New Zealand. p. 1-55.

51. Preston, R.L. (2014). 2014 Feed Composition Table, in Beef. Penton Media: Minneapolis, U.S.. p. 18-26.

52. Hicks, T.M., Verbeek, C.J.R., Lay, M.C., Manley-Harris, M. (2013). The Role of Peracetic Acid in Bloodmeal Decoloring. Journal of the American Oil Chemists' Society, 90(10): 1577-1587.

53. Howie, S.A., Calsamiglia, S., Stern, M.D. (1996). Variation in Ruminal Degradation and Intestinal Digestion of Animal By-Product Proteins. Animal Feed Science and Technology, 63(1–4): 1-7.

54. Kamalak, A., Canbolat, O., Gurbuz, Y., Ozay, O. (2005). In situ Ruminal Dry Matter and Crude Protein Degradability of Plant- and Animal-derived Protein Sources in Southern Turkey. Small Ruminant Research, 58(2): 135-141.

55. Laining, A., Rachmansyah, Ahmad, T., Williams, K. (2003). Apparent Digestibility of Selected Feed Ingredients for Humpback Grouper, *Cromileptes altivelis*. Aquaculture, 218(1–4): 529-538.

56. Marichal, M. d.J., Carriquiry, M., Pereda, R., San Martín, R. (2000). Protein Degradability and Intestinal Digestibility of Blood Meals: Comparison of Two Processing Methods. Animal Feed Science and Technology, 88(1–2): 91-101.

57. National Research Council (2001). Nutrient Composition of Feeds, in Nutrient Requirements of Dairy Cattle: Seventh Revised Edition. The National Academies Press: Washington, D.C.,U.S.. p. 281-314.

58. Nengas, I., Alexis, M.N., Davies, S.J., Petichakis, G. (1995). Investigation to Determine Digestibility Coefficients of Various Raw Materials in Diets for Gilthead Sea Bream, *Sparus auratus L.* Aquaculture Research, 26(3): 185-194.

59. Knaus, W.F., Beermann, D.H., Robinson, T.F., Fox, D.G., Finnerty, K.D. (1998). Effects of a Dietary Mixture of Meat and Bone Meal, Feather Meal, Blood Meal, and Fish Meal on Nitrogen Utilization in Finishing Holstein Steers. Journal of Animal Science, 76(5): 1481-7.

60. Li, X., Rezaei, R., Li, P., Wu, G. (2011). Composition of Amino Acids in Feed Ingredients for Animal Diets. Amino Acids, 40(4): 1159-1168.

61. Pearl, G.G. (2004). Rendering 101: Raw Material, Rendering Process, and Animal By-Products. Rendering Magazine, August.

62. Garcia, R.A., Phillips, J.G. (2009). Physical Distribution and Characteristics of Meat and Bone Meal Protein. Journal of the Science of Food and Agriculture, 89(2): 329-336.

63. Malone, J. (2005). NRA Rescinds Sheep Material Policy, in ASI Weekly Centennial. American Sheep Industry Association.

64. National Research Council (1982). United States-Canadian Tables of Feed Composition: Nutritional Data for United States and Canadian Feeds, Third Revision. The National Academies Press: Washington, D.C., U.S.

65. Qiao, S., Thacker, P.A. (2004). Use of the Mobile Nylon Bag Technique to Determine the Digestible Energy Content of Traditional and Non-traditional Feeds for Swine. Archives of Animal Nutrition, 58(4): 287-294.

66. Kong, C., Kang, H.G., Kim, B.G., Kim, K.H. (2014). Ileal Digestibility of Amino Acids in Meat Meal and Soybean Meal Fed to Growing Pigs. Asian-Australasian Journal of Animal Sciences, 27(7): 990-995.

67. Watson, H. (2006). Poultry Meal Versus Poultry By-Product Meal in Dogs in Canada Magazine. Apex Publishing Ltd: Etobicoke, Canada

68. Trushenski, J., Gause, B. (2013). Comparative Value of Fish Meal Alternatives as Protein Sources in Feeds for Hybrid Striped Bass. North American Journal of Aquaculture, 75(3): 329-341.

69. Dust, J.M., Grieshop, C.M., Parsons, C.M., Karr-Lilienthal, L.K., Schasteen, C.S., Quigley, J.D., Merchen, N.R., Fahey, G.C. (2005). Chemical Composition, Protein Quality, Palatability, and Digestibility of Alternative Protein Sources for Dogs. Journal of Animal Science, 83(10): 2414-22.

70. Bimbo, A.P. (2000). Fish Meal and Oil, in Marine and Freshwater Products Handbook, Martin, R.E., Carter, E.P., Flick, G.J., Davis, M.L., Editors. Technomic Publishing Company: Lancaster, Pennsylvania. p. 541-482.

71. Kerr, C.A., Goodband, R.D, Smith, J.W., Musser, R.E., Bergström, J.R., Nessmith, W.B., Tokach, M.D., Nelssen, J.L. (1998). Evaluation of Potato Proteins on the Growth Performance of Early-weaned Pigs. Journal of Animal Science, 76(12): 3024-33.

72. Okoye, F.C., Ojewola, G.S., Njoku-Onu, K. (2005). Evaluation of Shrimp Waste Meal as a Probable Animal Protein Source for Broiler Chickens. International Journal of Poultry Science, 4(7): 458-461.

73. Fanimo, A.O., Oduguwa, O.O., Onifade, A.O., Olutunde, T.O. (2000). Protein Quality of Shrimp-waste Meal. Bioresource Technology, 72(2): 185-188.

74. Everts, H., Nguyen, L.Q., Beynen, A.C. (2003). Shrimp By-Product Feeding and Growth Performance of Growing Pigs Kept on Small Holdings in Central Vietnam. Asian-Australasian Journal of Animal Sciences, 16(7): 1025-1029.

75. Fanimo, A.O., Susenbeth, A., Südekum, K.H. (2006). Protein Utilisation, Lysine Bioavailability and Nutrient Digestibility of Shrimp Meal in Growing Pigs. Animal Feed Science and Technology, 129(3–4): 196-209.

76. Ofori, J.A., Hsieh , Y.P. (2012). The Use of Blood and Derived Products as Food Additives, in Food Additive, El-Samragy, Y., Editor. InTech. p. 229-256.

77. Wismer-Pedersen, J. (1988). Use of Haemoglobin in Foods: A Review. Meat Science, 24(1): 31-45.

78. Bah, C.S.F., Bekhit, A.E.A., Carne, A., McConnell, M.A. (2013). Slaughterhouse Blood: An Emerging Source of Bioactive Compounds. Comprehensive Reviews in Food Science and Food Safety, 12(3): 314-331.

79. Izmirlioglu, G., Demirci, A. (2012). Ethanol Production from Waste Potato Mash by Using Saccharomyces Cerevisiae. Applied Sciences, 2(4): 738-753.

80. Kondamudi, N., Strull, J., Misra, M., Mohapatra, S.K. (2009). A Green Process for Producing Biodiesel from Feather Meal. Journal of Agricultural and Food Chemistry, 57(14): 6163-6166.

81. Lazarovits, G. (2001). Management of Soil-borne Plant Pathogens with Organic Soil Amendments: A Disease Control Strategy Salvaged from the Past. Canadian Journal of Plant Pathology-Revue Canadienne De Phytopathologie, 23(1): 1-7.

82. Park, S., Bae, D.H., Hettiarachchy, N.S. (2000). Protein Concentrate and Adhesives from Meat and Bone Meal. Journal of the American Oil Chemists' Society, 77(11): 1223-1227.

83. Garcia, R.A., Onwulata, C.I., Ashby, R.D. (2004). Water Plasticization of Extruded Material Made from Meat and Bone Meal and Sodium Caseinate. Journal of Agricultural and Food Chemistry, 52(12): 3776-9.

84. Garcia, R.A., Flores, R.A., Phillips, J.G. (2005). Use of an Aspirator to Separate Meat and Bone Meal into High-ash and High-protein Streams. American Society of Agricultural Engineers 48(2): 703-708.

85. Toldrá, F., Aristoy, M.C., Mora, L., Reig, M. (2012). Innovations in Value-addition of Edible Meat By-Products. Meat Science, 92(3): 290-296.

86. Sharma, S., Hodges, J.N., Luzinov, I. (2008). Biodegradable Plastics from Animal Protein Coproducts: Feathermeal. Journal of Applied Polymer Science, 110(1): 459-467.

87. Mekonnen, T., Mussone, P., El-Thaher, N., Choi, P.Y.K., Bressler, D.C. (2013). Thermosetting Proteinaceous Plastics from Hydrolyzed Specified Risk Material. Macromolecular Materials and Engineering, 298(12): 1294-1303.

88. Piazza, G.J., Garcia, R.A. (2010). Meat and Bone Meal Extract and Gelatin as Renewable Flocculants. Bioresource Technology, 101(2): 781-787.

89. Piazza, G.J., Garcia, R.A. (2014). Proteolysis of Meat and Bone Meal to Increase Utilisation. Animal Production Science, 54: 200-206.

90. Lammens, T.M., Franssen, M.C.R., Scott, E.L., Sanders, J.P.M. (2012). Availability of Protein-derived Amino Acids as Feedstock for the Production of Bio-based Chemicals. Biomass and Bioenergy, 44(0): 168-181.